FINAL TECHNICAL REPORT - MARCH 1988

Investigation of Chemical Durability Mechanisms

and Structure of Fluoride Glasses

by

Joseph H. Simmons and Catherine J. Simmons
Department of Materials Science and Engineering
University of Florida
Gainesville, Florida 32611

ABSTRACT

The research conducted under this grant consisted of three major thrusts: (1) the development of an understanding of the chemical dissolution behavior of fluoride glasses, (2) the development of guidelines for the formation of structural models for binary fluoride glasses and (3) the investigation of fabrication conditions and the resulting structures for binary fluoride films.

The research was conducted over a span of $4\frac{1}{2}$ years. The results include the development of a comprehensive data base and model for the corrosion of the three principal fluoride glass composition systems, and the development of a theoretical framework for the analysis of the structural stability of fluoride glass systems based upon microscopic considerations. The work has yielded nine publications, with three more in preparation, and has contributed to two MS theses and two PhD dissertations.

Accession For	
NTIS GRA&I	☑
DTIC TAB	☐
Unannounced	☐
Justification	
By per letter	
Distribution/	
Availability Codes	
Dist	Avail and/or Special
A-1	

SUMMARY OF RESEARCH PROGRAM

A. **Scientific Goals**

1. Develop a comprehensive understanding of the mechanisms which control the chemical corrosion behavior of fluoride glasses.

2. Determine and assess the corrosion behavior of fluoride glasses in a variety of aqueous environments in order to make valid in-use lifetime predictions and in order to develop corrosion-resistant compositions.

3. Fabricate single and multi-component fluoride thin films for applications in integrated optical circuits and in structural studies.

4. Investigate the structure of fluoride glasses by molecular dynamics and develop a simple research approach for testing the glass-forming tendency of combinations of components.

B. **Significant Results**

Thus far, this work has yielded 9 publications, with 3 more currently in preparation and 8 lectures given in 1987, alone. This work has also contributed to 2 MS theses with 2 PhD dissertations.

(a) **Chemical Corrosion Studies**

In our research under this contract, we succeeded in developing a fundamental understanding of the chemical processes which control the aqueous corrosion of fluoride glasses. Our past research led to the development of test methods for the contemplated studies and to the collection of a sizeable data base on the leaching characteristics of fluoride glasses. The results were classified into 3 families of behavior distinguished by the compositions of the glasses: (a) Fluorozirconates, (b) Barium-thorium based glasses, and (c) Uranium-based glasses. The work culminated in a comprehensive paper, published in September 1986[*], which described the corrosion behavior of fluorozirconate glasses, and presented an analytical model of the major controlling mechanisms, followed by an additional 4 papers on a more detailed study of corrosion emphasizing the other systems.

We continued to analyze the data gathered on the leaching processes of fluoride glasses and found that the model presented in the fluorozirconate paper was consistent with the behavior of the other families of glasses. In addition, studies of corrosion in different pH buffered solutions led to a comprehensive understanding of the kinetics of the corrosion process in all the fluoride-based glasses studied. Four additional papers, listed in the

---

[*]C. J. Simmons and J. H. Simmons, "Chemical Durability of Fluoride Glasses--I, Reaction of Fluorozirconate Glasses with Water," J. Am. Ceram. Soc. 69 [9] 661-669 (1986).

Appendix were then published covering the leaching behavior of Th-Ba fluoride glasses, UF_4 glasses and the effect of solution pH.

In our research under this contract, we were successful in validating our test conditions in order to (1) separate results associated with the fundamental behavior of the glasses from results associated with test conditions, and (2) to carefully monitor and/or control solution pH to understand how corrosion products in solution and reactions in the glass influence the ambient pH and how this pH environment affects glass corrosion.

We have measured the chemical corrosion behavior, in both deionized water and various pH buffered solutions, of three major families of fluoride glasses, consisting of fluorozirconates, Ba-Th-based fluorides and UF_4-based fluorides. The measurements consisted of leachate solution analysis by plasma emission spectroscopy, of degree of hydration by infrared absorption, of layer thickness and structure by scanning electron microscopy, and of crystal precipitate compositions by x-ray diffraction and electron microprobe analysis.

We have determined the corrosion behavior of these glasses and analyzed the chemical mechanisms which take place in the glass and in the solution during corrosion. Briefly, we have found that fluoride glasses corrode in aqueous solution though the dissolution of their components and that the leach rate is pretty well determined by the component dissolution rate and solubility. However, the corrosion products can and do affect the process of corrosion. These products when liberated into the water (1) act to reduce the pH, (2) precipitate as fluoride and hydrate crystals on the surface and (3) form colloidal suspensions which deposit back on the glass surface. Figure 1 (attached) shows a comparison of the leach rates of these fluoride glasses and a few common silicates.

Measurements in pH buffered solutions show that all three families of fluoride glasses behave similarly. The corrosion rate is high in acidic solutions, reaches a minimum in neutral solutions and increases moderately in basic solutions. Fig. 2 shows the combined pH dependence of the glasses tested. Fluorozirconate glasses exhibit the greatest variation in corrosion rate with solution pH. They undergo rapid corrosion at acidic pH values. At neutral solution pH values, however, they exhibit the lowest corrosion rate of all fluoride glasses tested. This unexpected result points the direction in which composition and solution modifications may go in an attempt to improve the chemical durability of fluorozirconate glasses. In fact, tests conducted by exposing the glass surface to a basic solution and then to deionized water showed that, indeed, the corrosion can be temporarily arrested by the modified surface.

When considering the change in solution pH with time in deionized water, the measured corrosion rates are consistent with the buffered solution measurements. Effectively, as fluorozirconate glasses dissolve and ZrF_4 hydrolyzes in solution to push the pH into the acidic region, this pH drop leads to an accelerated leach rate which is only moderated by the formation of thick crystal deposits on the surface. If these were not formed, the leach rate would continue to increase with time. In stagnant solutions, however, saturated solution layers evidently form near the glass surface, so that the corrosion rate is then determined by the rate of precipitation of components
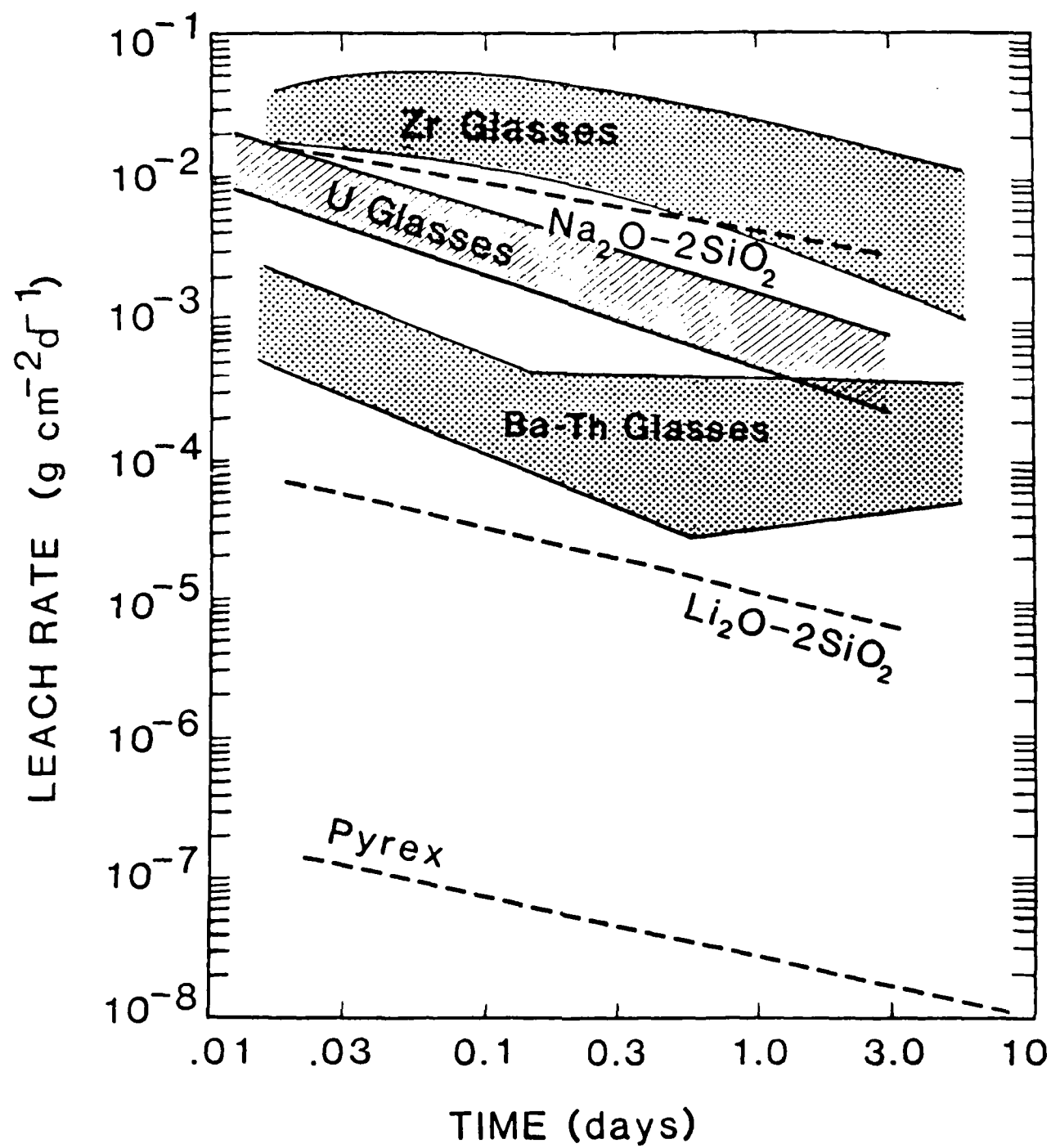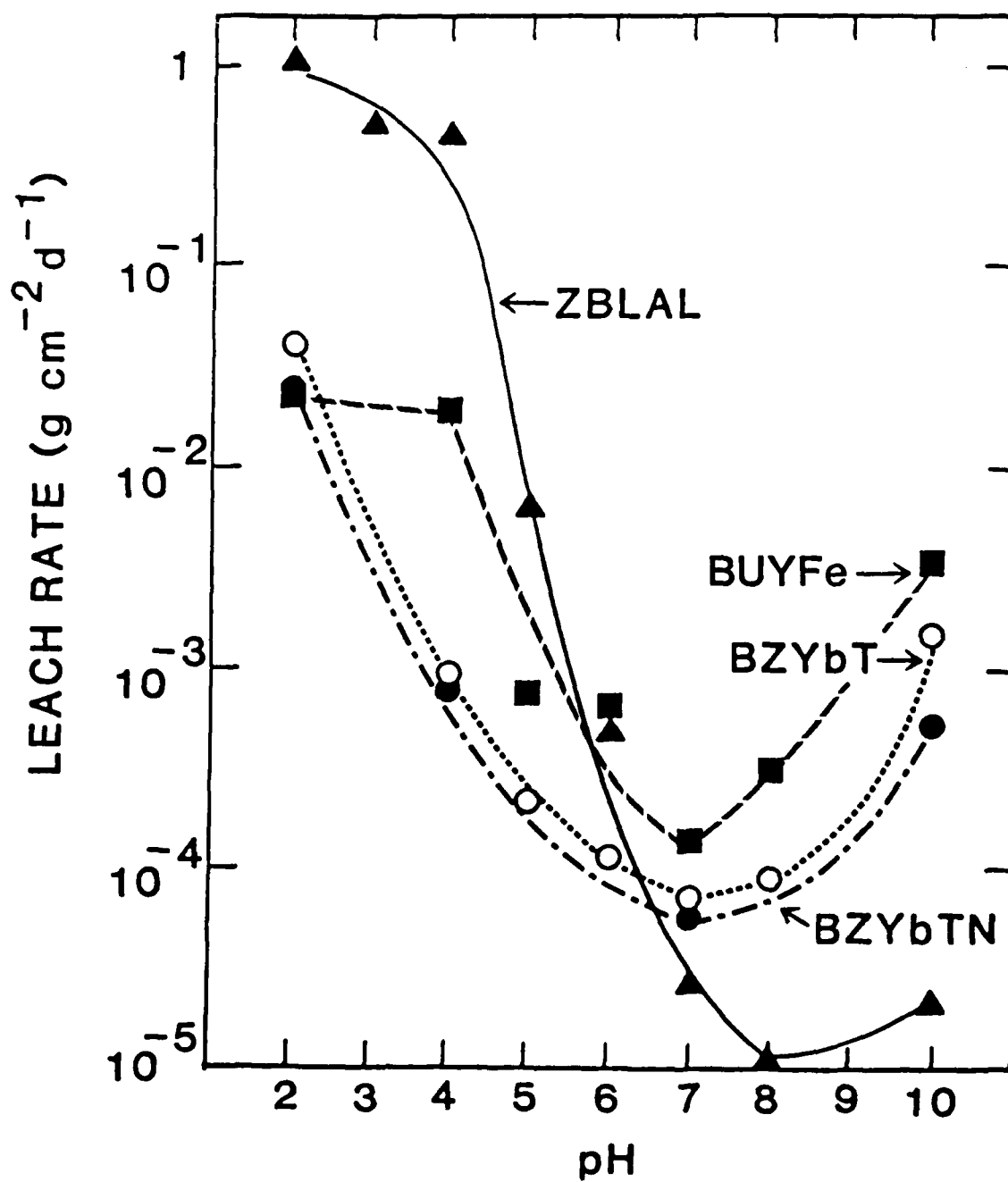
FIGURE 1

FIGURE 2

from solution and the rate at which the bulk solution can diffuse to the glass surface.

In order to model typical in-use conditions, we conducted studies of the chemical corrosion of fluorozirconate glasses under different conditions of exposure to water. These divided into exposure to stagnant low volume solutions, stagnant high-volume solutions and flowing solutions. Through these tests, we identified additional features of the mechanisms proposed in our earlier work, but the concepts remained the same. The results of the analysis clearly show that hermetic coatings are necessary for fluoride glasses which are to be exposed to ambient moisture. Ba-Th fluorides have the best resistance to aqueous corrosion, but even they require protection. The protection afforded by the moderately porous organic coatings typically used with silicate glass fibers are unacceptable here. The results of the stagnant, low-solution volume tests which model the effect of an incomplete barrier to aqueous diffusion, clearly show that corrosion under this condition is severe and that the presence of corrosion products in the solution acts to accelerate leaching of the glass. Low solution volume conditions thus lead to a major modification of the glass.

Studies were conducted to reduce the susceptibility of fluoride glasses to aqueous corrosion. The major thrust, was to balance the initial solution pH drop near the glass with free hydroxyls resulting from the addition of oxides to the glass composition. So far the results are encouraging. Additions of a few percent oxide to the bulk composition of fluoride-based glasses, appear to have improved their glass-forming tendency, as well.

Based upon our limited experience, at present, with protective coatings on fluoride glasses, it is possible to state the following conclusions:

(1) Coatings are necessary for both bulk and fiber optics to avoid major degradation of the optical properties.

(2) Organic coatings are not impervious to water, and thus, while retarding the rate of penetration to various degrees, they cannot arrest it.

(3) Preliminary studies at our laboratories have shown that Diamond-Like-Carbon coatings have promise, but we have been unable to find a regular source for coated fluoride glasses.

Resulting from the collection of data achieved over the past four years, we have been able to unambiguously interpret the results and model the corrosion process. Therefore, we have prepared major papers for publication, reporting our results on the corrosion processes for fluorozirconates,[3] barium-thorium fluorides,[4] and uranium fluorides,[8] in water and in solutions buffered at various pH values.[7]

The significance of our research is two-fold. First, we have now developed a basic understanding of the corrosion process in fluoride glasses. We know some of the factors which influence the corrosion rate and know the mechanisms which control the corrosion rate. Secondly, we have determined the primary reason for observed major differences in corrosion rate for glasses soaked in solutions of different pH. While fluoride glasses corrode rapidly

in water, they exhibit a much smaller reaction in moist air, and resist corrosion relatively well in neutral solutions. This knowledge can be used to make more resistant glass compositions, and to control the leaching environment by external agents to minimize corrosion behavior.

(b) Structure and Thin Film Studies

Amorphous ZrF_4 films were prepared by thermal evaporation Fig. (3) and from sublimed ZrF_4 vapor quenched at rates above several hundred degrees per second. The amorphous films were obtained by deposition onto room temperature and cooled substrates. Their structure was determined by x-ray diffraction (Fig. 4). Their composition was determined by XPS measurements for Zr^{4+} and F^- (Fig. 5) showing the appropriate bonding for ZrF_4.

Thin films of the entire range of compositions in the binaries ZrF_4-PbF_2, ZrF_4-CdF_2 and PbF_2-CdF_2 were also successfully produced. The amorphous ZrF_4 films proved to be very sensitive to moisture attack from the air and crystallized rapidly within several hours. This result was used to advantage to study the effect of coatings on the rate of crystallization of the amorphous ZrF_4 films and thus test the effectiveness of the coating as a barrier to aqueous diffusion. Extensive studies with very thin gold coatings (less than 10) have shown an unexpected ability to protect the surface of the amorphous ZrF_4 films from attack by ambient atmospheric moisture. The oldest films are over 6 months old and show no deterioration. We anticipate that this test may offer a rapid, inexpensive screening test of the coatings on fluoride glasses.

The amorphous single component and binary fluoride films were measured with x-ray photoelectron spectroscopy to reveal their bonding distributions. the results show clearly that an enhanced formation of mixed bonds, such as Zr-F-Pb or Zr-F-Cd, is present in these glasses. This increased distribution of bonds is far greater than predicted either by molecular dynamics calculations or by random selection analysis. It indicates that both PbF_2 and CdF_2 components have a strong attractive exchange interaction with ZrF_4 and that they should form glasses stable against immiscibility phase transitions. This work offers an inexpensive and rapid test of the compatibility of fluoride components, to be used for the development of new glass compositions.

In conjunction with the thin film studies, we conducted molecular dynamics modeling studies of the ZrF_4-BaF_2 and ZrF_4-PbF_2 binary systems. The results were compared to the distributions found in the XPS measurements, to show the anomalous increase in cross-species bonds. The calculations showed that on the scale of the nearest neighbor cell, MD can fit very well the behavior of fluoride glasses. The results are:

(1) Pair correlation functions calculated by MD match well the available neutron data.

(2) Densities are accurately reproduced at low ambient pressures.

(3) The ZrF_4 based binaries are made up of $[ZrF_8]$ cages which remain unaltered by additives.

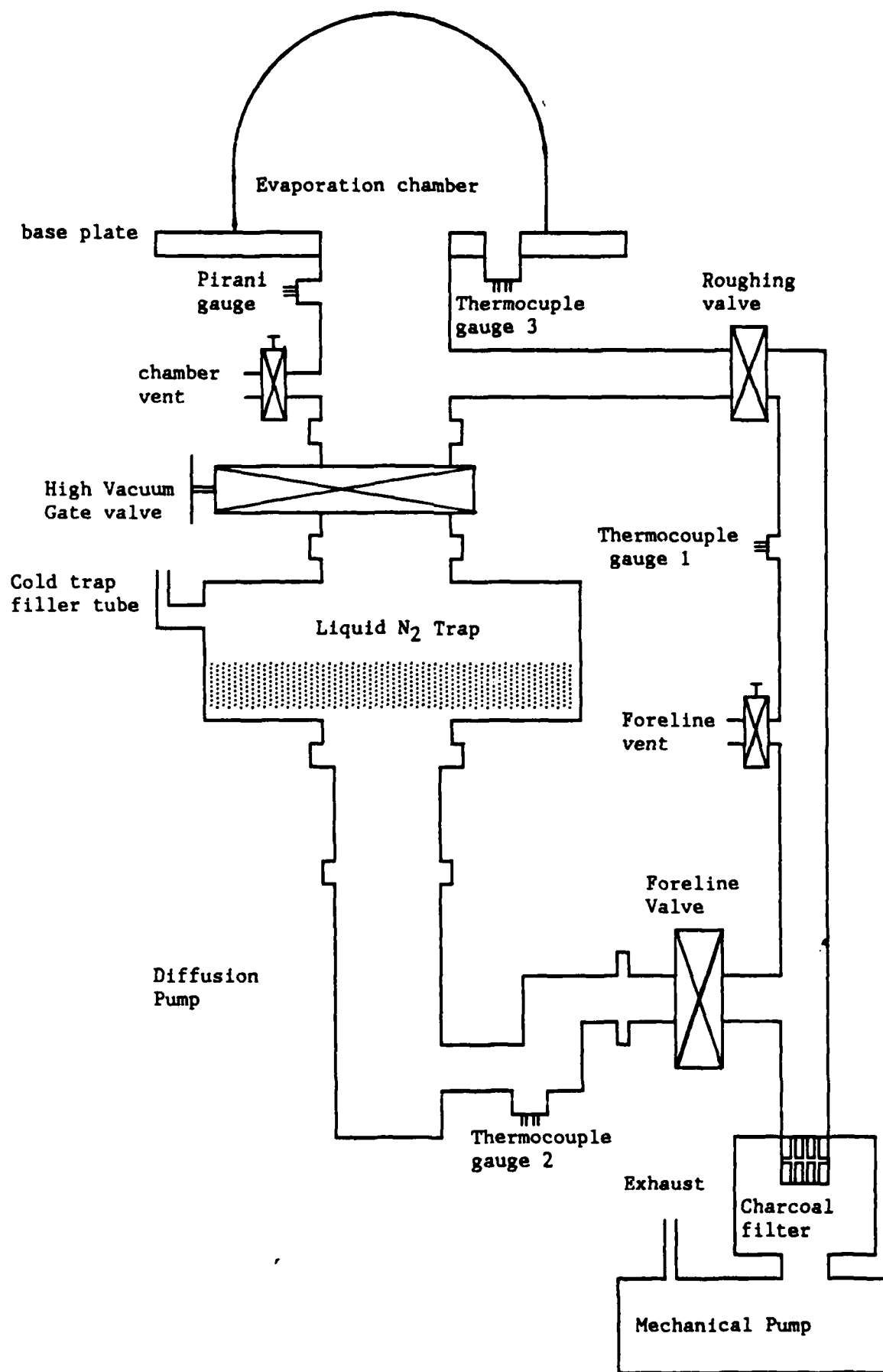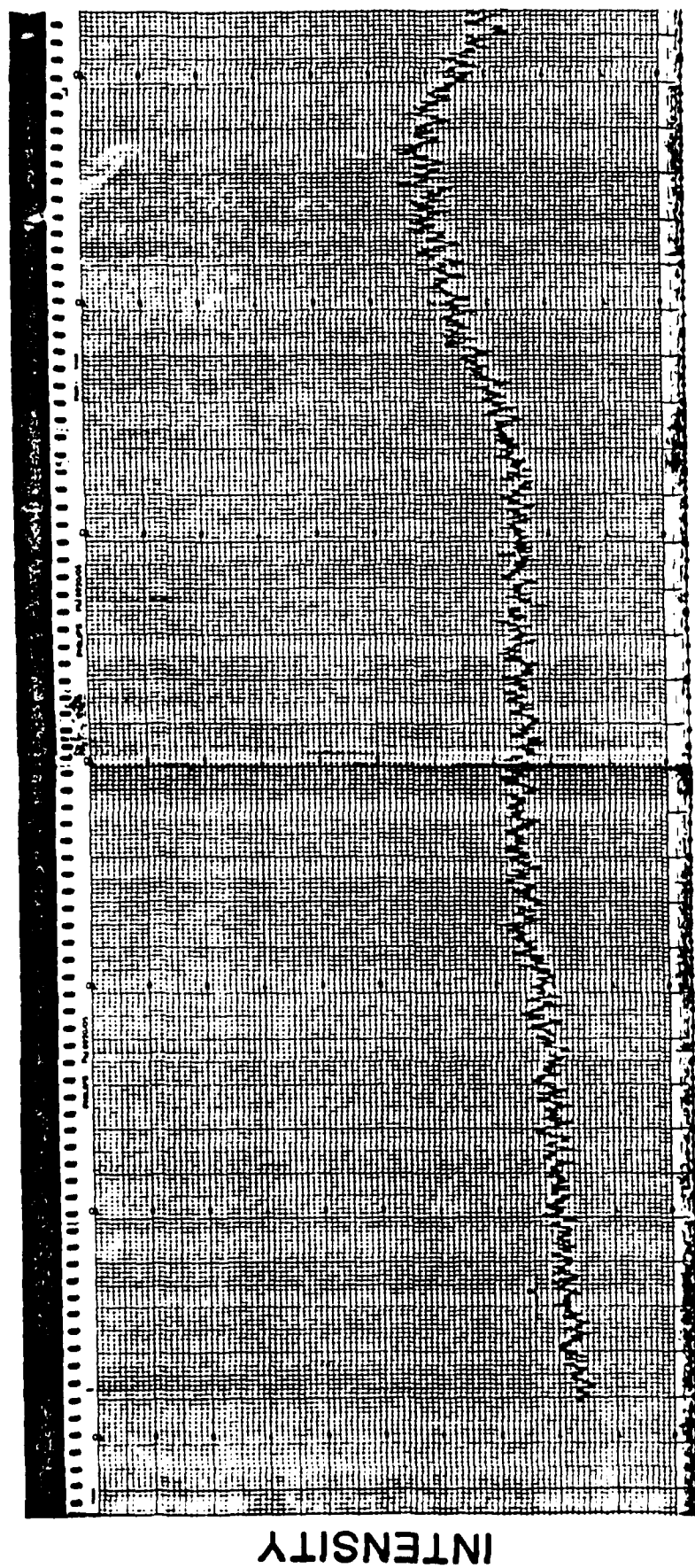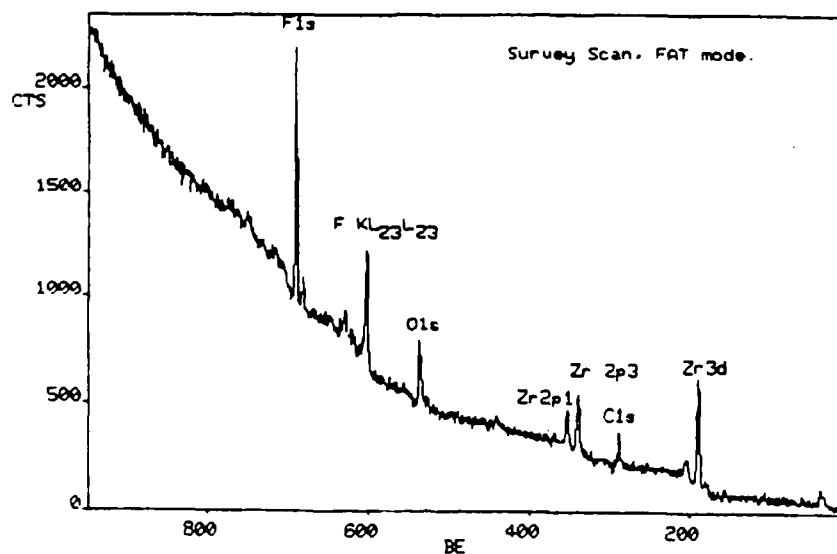(4) The Ba and Pb additives fit into the holes of the structure until they reach foreign atom concentration of 80%.

Evaporation chamber

base plate

Pirani gauge

chamber vent

Thermocuple gauge 3

Roughing valve

High Vacuum Gate valve

Cold trap filler tube

Liquid N_2 Trap

Thermocouple gauge 1

Foreline vent

Foreline Valve

Diffusion Pump

Thermocouple gauge 2

Exhaust

Charcoal filter

Mechanical Pump

FIGURE 3

DIFFRACTION ANGLE 2θ

INTENSITY

FIGURE 4

RUN: ZR2   REG: 3 SCAN: 1 BACKGROUND: 227 MAX CTS/SEC: 3236

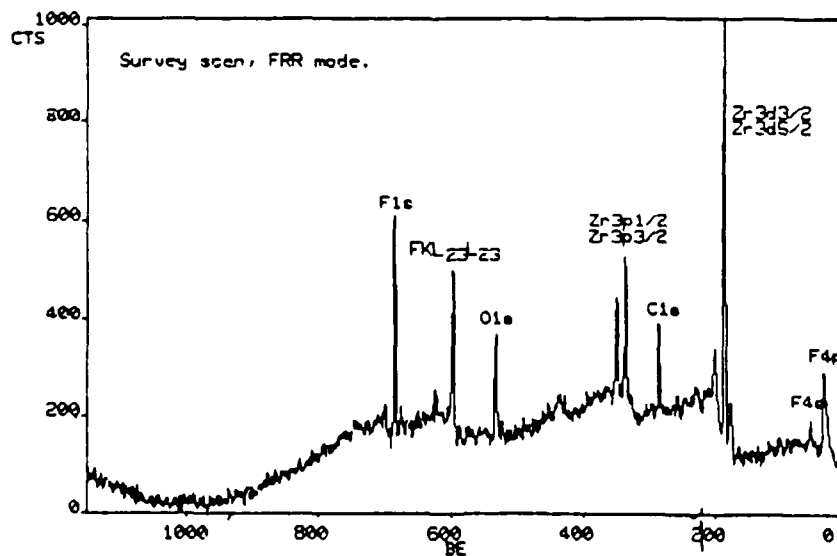RUN: ZR1   REG: 3 SCAN: 1 BACKGROUND: 367 MAX CTS/SEC: 1763

FIGURE 5

(5) The fluorine structure remains fixed by the $[ZrF_8]$ cages until 80% additive concentrations.

(6) The bond distribution which shows the stacking structure of nearest neighbor cells, is not accurately predicted by MD. This discrepancy results from the lack of 3-body forces in the modeling work.

(c) Personnel

We had the following personnel on the program.

Graduate Students

- Saied Azali completed MS in Chemical Engineering (spring 1984), studied corrosion.
- Din Guo Chen has completed his MS thesis in Materials Science (summer 1987), studied corrosion.
- Greg O'Rear is working on an MS thesis in Computer Sciences, studying structure by MD.
- Temel Buyuklimanli is working on a PhD dissertation in Physics, studying thin films.
- Brigitte Boulard (PhD candidate from the Universite du Maine in Lemans, France) studied the PbF_2-ZrF_4 system.

Post Docs

- Joelle Guery - 9/84-10/85 - graduated from University du Maine, LeMans, France, (with partial support from the French Foreign Office), studied corrosion of UF_4-based fluorides.
- Michel Le Toullec - 10/86-10/87 - graduated from the University of Rennes, Rennes, France (with partial support from the French Foreign Office), studied hydrolysis reactions of fluorides..

Visiting Professor

- Professor Adrian Wright, Physics Department, University of Reading, Reading, U.K. (expert in structure modeling and neutron diffraction measurements).

Minority Summer High School Student

- 1986 - Gloria Dennis, ONR minority student summer fellowship.
- 1986 - Adrian McCoy, ONR minority student summer fellowship.
- 1987 - Kelvin Howard, ONR summer fellowship provided through the Florida Foundation for Future Scientists.

LIST OF PAPERS AND PRESENTATIONS

1. Publications

   1. "Chemical Durability Studies of Heavy Metal Fluoride Glasses," C. J. Simmons, S. Azali and J. H. Simmons, Proceedings from the 2nd International Symposium on Halide Glasses, Troy, NY, August 1983.

   2. "Leaching Behavior of Heavy Metal Fluoride Glasses," C. J. Simmons, J. Guery, D. G. Chen, and C. Jacoboni, Materials Science Forum, 5, 329-334 (1985).

   3. "Chemical Durability of Fluoride Glasses: I, Reaction of Fluorozirconate Glasses with Water," C. J. Simmons and J. H. Simmons, J. Amer. Ceram. Soc., 69 (9), 661-669 (1986).

   4. "Chemical Durability of Fluoride Glasses: II, Reaction of Barium-Thorium-Based Glasses with Water," C. J. Simmons, J. Amer. Ceram. Soc., 70 (4), 295-300 (1987).

   5. "Molecular Dynamics Simulations of Fluoride Glass Structures," J. H. Simmons, R. Faith and G. O'Rear, Materials Science Forum, 19, 121-126 (1987).

   6. "Corrosion Layer Formation of ZrF_4-Based Fluoride Glasses," Ibid, 315-320 (1987).

   7. "Chemical Durability of Fluoride Glasses: III, the Effect of Solution pH," C. J. Simmons, J. Amer. Ceram. Soc., 70 (9), 654-661 (1987).

   8. "Corrosion of Uranium IV Fluoride Glasses in Aqueous Solutions," J. Guery, D. G. Chen, C. J. Simmons, J. H. Simmons and C. Jacoboni, Physics and Chemistry of Glasses, 29 (1), 30-36 (1988).

   9. "Infrared Spectroscopic Studies of the Hydrolysis Reaction During Leaching of Heavy Metal Fluoride Glasses," M. Le Toullec, C. J. Simmons and J. H. Simmons, J. Amer. Ceram. Soc., 71 (4), 219-224 (1988).

2. Technical Reports: FY87

   1. "Corrosion Layer Formation of ZrF_4-based Fluoride Glasses," D. G. Chen, C. J. Simmons and J. H. Simmons, Proceedings for the 4th Int. Symp. on Halide Glasses, 414-419, Monterey, CA , Jan. 26-29, 1987.

   2. "Molecular Dynamics Simulations of Fluoride Glass Structures," J. H. Simmons, R. Faith and G. O'Rear, Ibid, 101-105.

   3. "Master's Thesis, "Glass/Water Interactions During the Corrosion of Fluorozirconate Glasses," D. G. Chen, University of Florida, August, 1987.

3. Presentations

   (a) Invited

   "Molecular Dynamics Simulations of Glass Structure and Properties," J.
   H. Simmons, Amer. Ceram. Soc., 89th Annual Meeting, Pittsburgh, PA,
   April 26-29, 1987.

   "Leaching Process in Fluoride Glasses," C. J. Simmons, University of
   Rennes, Rennes, France, October 1986.

   "Corrosion Mechanisms in Fluoride Glasses," Workshop on Strength,
   Durability and Coating of Heavy Metal Fluoride Glasses, San Diego, CA,
   Jan. 27-28, 1986.

   (b) Contributed: FY87

   4th International Symposium on Halide Glasses, January 26-29, 1987,
   Monterey, CA.

   "Molecular Dynamics Simulations of Fluoride Glass Structures," J. H.
   Simmons, R. Faith and G. O'Rear.

   "Corrosion Layer Formation on ZrF_4-Based Glasses," D. G. Chen, C. J.
   Simmons and J. H. Simmons.

   American Ceramic Society, Glass Division Meeting, Sept. 30 - Oct. 2,
   1987, Bedford Springs, PA.

   "Reaction of Fluorozirconate Glass with Water," D. G. Chen, C. J.
   Simmons and J. H. Simmons, Amer. Ceram. Soc. Bul. 66, 1220 (1987).

   "Infrared Spectroscopic Studies of the Hydrolysis Reactions during
   Leaching of Heavy-Metal Fluoride Glasses," M. Le Toullec and C. J.
   Simmons, Amer. Ceram. Soc. Bul. 66, 1222 (1987).

   "Thin Films of Amorphous Zirconium Fluoride," T. Buyuklimanli and J.
   H. Simmons, Amer. Ceram. Soc. Bul. 66, 1222 (1987).

   "Investigation of the Structure of Fluoride Films," T. Buyuklimanli
   and J. H. Simmons, Amer. Ceram. Soc. Bul. 66, 1222 (1987).

   "Molecular Dynamics Modeling of the BaF_2-ZrF_4 Glass Structure," J. H.
   Simmons and G. O'Rear, Amer. Ceram. Soc. Bul. 66, 1222 (1987).

4. Publications in Preparation

   1. "Amorphous ZrF_4 Films," T. Buyuklimanli and J. H. Simmons.

   2. "Molecular Dynamics Modeling of the Structure of the ZrF_4-BaF_2
      Binary," G. O'Rear and J. H. Simmons.

   3. "Structure of ZrF_4-PbF_2 Binary," T. Buyuklimanli and J. H. Simmons.

APPENDIX

The appendices contain copies of the published papers.

A. Chemical Durability Studies of Heavy Metal Fluoride Glasses

B. Leaching Behavior of Heavy Metal Fluoride Glasses

C. Chemical Durability of Fluoride Glasses: I, Reaction of Fluorozirconate Glasses with Water

D. Chemical Durability of Fluoride Glasses: II, Reaction of Barium-Thorium-Based Glasses with Water

E. Molecular Dynamics Simulations of Fluoride Glass Structures

F. Corrosion Layer Formation of ZrF_4-Based Fluoride Glasses

G. Chemical Durability of Fluoride Glasses: III, The Effect of Solution pH

H. Corrosion of Uranium IV Fluoride Glasses in Aqueous Solutions

I. Infrared Spectroscopic Studies of the Hydrolysis Reaction During Leaching of Heavy Metal Fluoride Glasses

J. Glass/Water Interactions During the Corrosion of Fluorozirconate Glasses

Appendix A

CHEMICAL DURABILITY STUDIES

OF HEAVY METAL FLUORIDE GLASSES

by

Catherine J. Simmons, Saied Azali and Joseph H. Simmons

Catholic University of America

Washington, D. C. 20064

This presentation covers several studies related to the chemical durability (ie. corrosion resistance) of a variety of fluoride glasses, shown in Table 1.

Table 1: **COMPOSITION (mole %)**

GROUP I

	ZrF_4	BaF_2	LaF_3	AlF_3	LiF	NaF	PbF_2	Source
ZBL	62	33	5	......	......	......	......	R.P.I.
ZBLA	58	33	5	4	......	......	......	R.P.I.
ZBLAN	54.0	15.0	6.0	4.0	......	21.0	......	R.P.I.
ZBLAL	51.8	20.0	5.3	3.3	19.6	......	......	N.R.L.
ZBLALP-1	50.2	19.3	5.1	3.1	18.9	......	3.4	N.R.L.
ZBLALP-2	50.4	15.5	4.9	3.1	20.2	......	4.9	N.R.L.

GROUP II

	BaF_2	ZnF_2	LuF_3	YbF_3	ThF_4	NaF	Source
BZLT	19	27	27	......	27	......	R.A.D.C.
BZYbT	19	27	......	27	27	......	R.P.I.
BZYbTN	10	27	......	27	27	9	R.P.I.

I. Resistance to Aqueous Attack:

A. Composition Study

All glasses were immersed in deionized water at 25 C to determine their leach rates as a function of time. Chemical analyses of the leaching solutions showed that, within each family of glasses, the leach rates observed were virtually identical, regardless of variations in composition. However, the results show a distinct difference between the Zr/Hf based glasses and those based on Th-Ba, with the latter exhibiting an improvement in leach resistance of 50-100 times. (See Figs. 1 and 2 for leach data of individual components of BZYbT and BZYbTN glasses, Fig. 3 for leach data of individual components of ZBLAL, and Fig. 4 for a general comparison between the 2 families of halide glasses with well-known silicate glasses.) Whereas the Zr/Hf glasses had developed a thick, hydrated surface layer, overlayed by a crystalline crust, and were quite opaque after 5 days of exposure, the Th-Ba glasses appeared to have suffered much less damage and were still fairly transparent. The thickness of these crusts was determined by SEM to be > 150 μm for the Group I glasses and ~ 2-3 μm for the Group II glasses. This ratio is in good agreement with the leach rate data (Table 2).

Weight loss was measured for all samples and, when compared with solution analysis, proved to be up to 15% too low in estimating the leach rates due to hydration during leaching.

B. pH Effects

One composition (ZBLAL) was selected for study in a variety of solutions at different pH values. Results show an increase in leach rate of approximately 10 times at pH 2 as compared with deionized water at pH 5.7. In more alkaline solutions (pH 10-11) the Zr leach rate drops due to the formation of insoluble hydroxides and, although the other components continue to leach, the rate decreases sharply with time. This appears to be caused by the formation of a protective $Zr(OH)_4$ barrier on the surface.

C. Powdered-vs-Bulk Samples

Two samples of ZBLAL glass, one powdered and one in the form of a polished rectangular parallelpiped, were leached to determine the validity of powder test results. The surface areas were calculated to be identical initially. Leach rates were comparable for the first 4 hours. However, this was followed by a steady decline in powder sample rates as the surface area decreased. At the end of 4 days, the leach rates for the powder samples were 1/10 those of the bulk sample. The results of this study strongly suggest that powder samples should be used only for very short term testing (ie. < 4hrs.) when leaching non-durable glasses such as these.

II. Humidity Effects:

Infrared transmittance spectra were obtained from a ZBLAL polished sample before, midway through, and after exposure to 100% relative humidity at 80 C for 7 days. Care was taken to maintain the sample at the same temperature in order to avoid condensation of water vapor. There was no visible damage to the

glass over the period of the test, and the IR spectra only showed a loss in transmittance of ~5% centered at 2.85 μm due to OH⁻ presence.

III. SEM Surface Studies:

The surface topography of leached samples was examined by scanning electron microscopy. Once again, samples within Group I or II were very similar to one another in the extent of attack and type of surfaces formed. Group II (Th-Ba) glasses were found to be far less damaged by aqueous leaching. Elements contained in the crystal deposits on the surfaces were identified by x-ray analysis using a wavelength dispersive spectrometer and are listed in Table 2.

Table 2: Summary of Observations in Composition Study

Type	Leach Rate g/cm^2 day	Sample Surface	Crust Thickness	Crystals Identified
Group I	10^{-2}	Opaque	150 μm	Zr, Ba, La
Group II	10^{-4}	Frosted	3 μm	Ba, Yb, Th

Acknowledgements:

Fig.1: Leach rates, normalized to composition, show nearly congruent dissolution except for Th, which was found in high concentration in the crystalline crust.
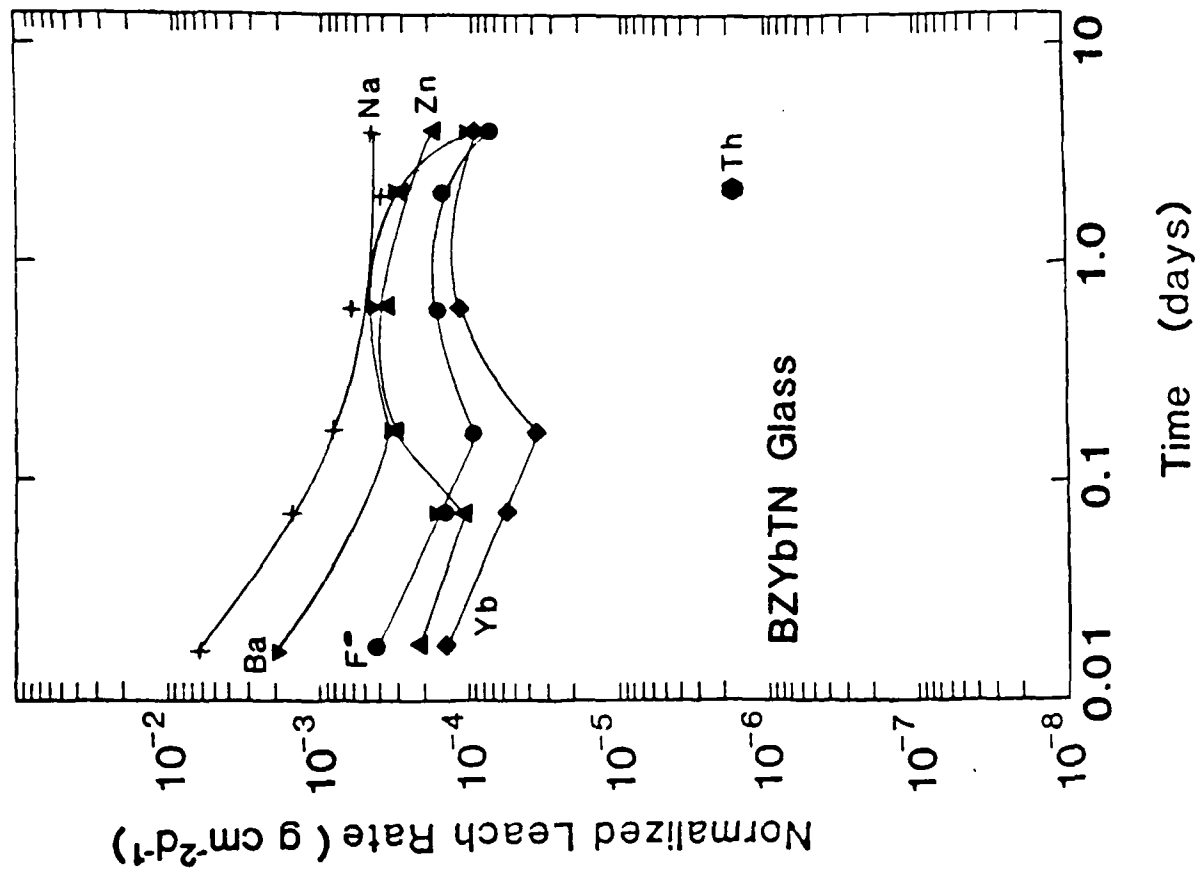
Fig.2: Addition of Na accelerates Ba and Zn dissolution slightly.
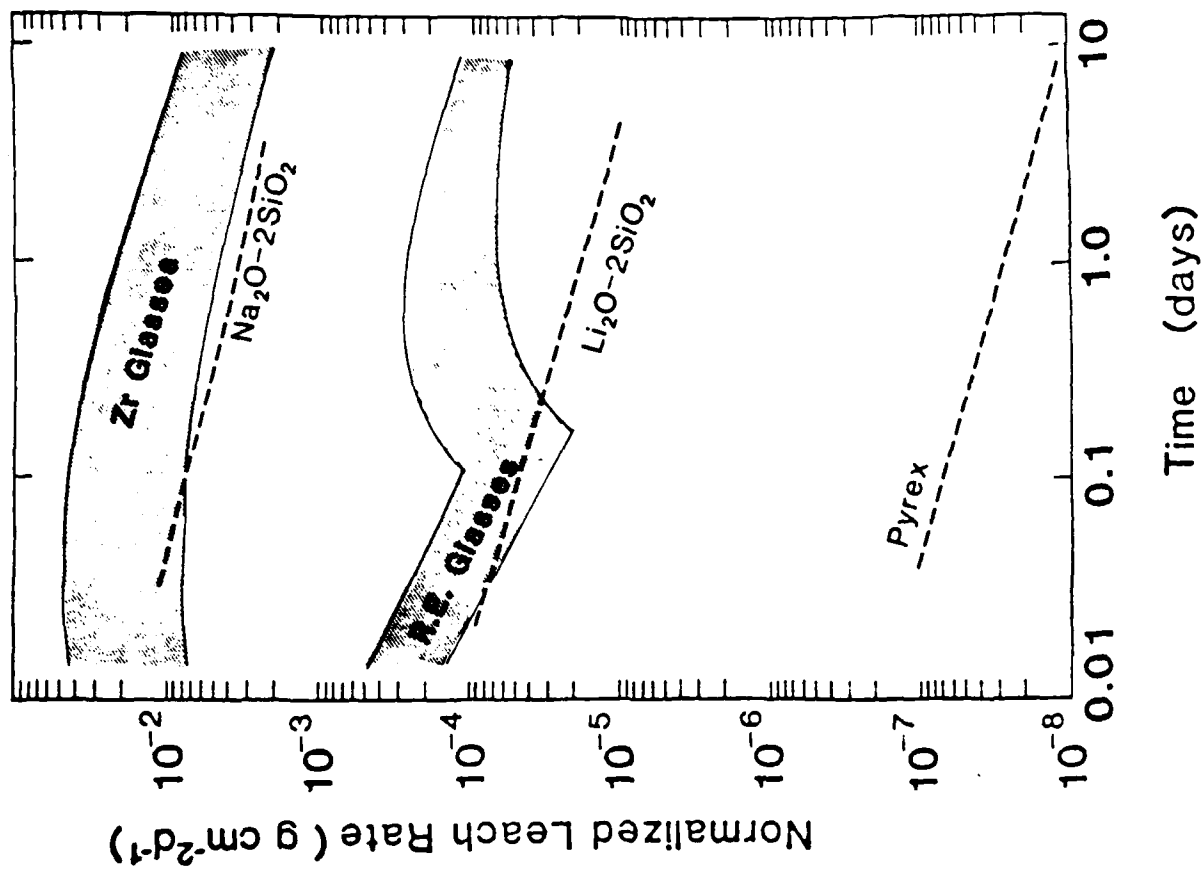
Fig.4: Leach rate comparison of Group I (Zr Glasses) and Group II (R.E. Glasses) with some well known silicate glasses.
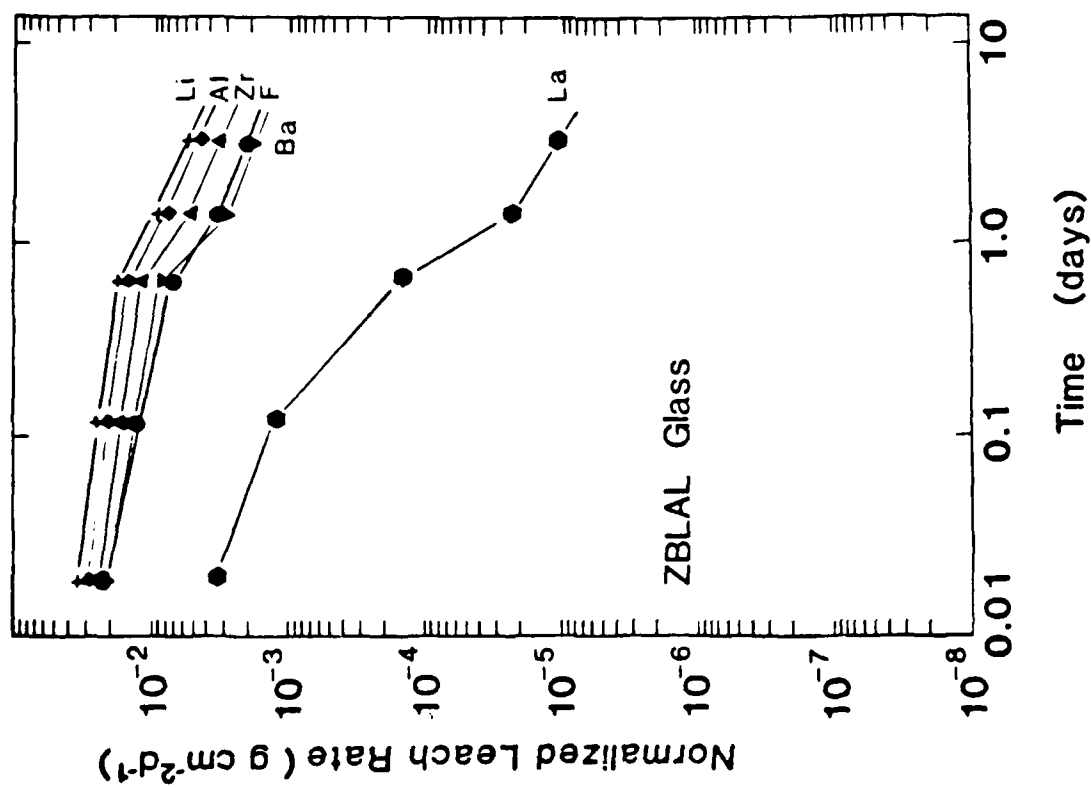

Fig.3: Typical of all Group I compositions, this shows nearly congruent leaching except for La which deposits in the crust.

Appendix B

LEACHING BEHAVIOR OF HEAVY METAL FLUORIDE GLASSES*

C. J. Simmons, J. Guery and D. G. Chen
University of Florida
Gainesville, Florida 32611

C. Jacoboni
Université du Maine
72017 Le Mans, France

INTRODUCTION

The aqueous corrosion of fluoride glasses has received increasing attention since the onset of studies of these non-oxide glasses. In 1982 the first results of aqueous leach tests on a fluorozirconate glass (generally denoted as ZBLAL) were reported.[1] The corrosion rate reported, obtained by solution analysis, showed that the major components of the glass, including Zr, Ba, Al, Li, and F, were leached at comparable rates (differing by less than a factor of 5), while the rare-earth, La, was leached at a rate 2 orders of magnitude lower (see Fig. 1, Ref. 1). Scanning electron microscope studies showed that the surface was covered by crystalline deposits (Fig. 3A, Ref. 1) and that a thick (> 100 μm/5 days) hydrated, transformed layer lay beneath the crystals (Fig. 3B, Ref. 1). This layer was cracked due to dehydration during drying in vacuum. IR absorption measurements of the leached glass showed high absorption due to the stretching OH and bending HOH vibrations, which increased with time and layer thickness. These absorption bands remained, even after drying in vacuum, indicating that a large water content was present in the hydrated layer. It was also noted that the pH of the solution drifted rapidly from 5.8 to 3.4 within 18 hours.

Leach rate studies of thorium-based glasses (Zn-Ba-Y-Th, Zn-Ba-Yb-Th, Zn-Ba-Yb-Th-Na) were later reported[2] and showed that these glasses were 50-100 times more resistant to corrosion by deionized water than the zirconium-based series. Leach rates for individual elements in the non-alkali composition were observed to be similar for all except Yb, which followed the same behavior as La in the Zr glasses. In the alkali-containing glass, the Na release rate was much higher at short times, presumably due to bulk diffusion, and was seen to decrease with time as the Na was depleted from the surface. Little, if any, drift of solution pH was observed during these tests.

Reports by Guery et al.[3] indicated that some uranium fluoride glasses could be even more resistant to corrosion than Zr- or Th-based glasses. Soak tests conducted at pH of 1 and 10 for 100 hours showed no visible evidence of the formation of crystals or a hydrated surface layer.

It has been reported[2,4] that the leach rate of ZrF_4-based glasses increases dramatically with decreasing solution pH, yielding a vital clue to understanding the controlling mechanisms of aqueous corrosion in fluoride glasses. This data led to the proposal that, unlike silcates, whose leaching behavior is dominated by alkali-proton ion exchange at acidic pH, the major factor in determining the leach rate of zirconium-based fluorides in water is the dissolution of ZrF_4.[5]

In this paper, we report a comparison between the aqueous corrosion processes in Zr-, Th- and U-based fluoride glasses. This comparison is not based solely on their leach rates in deionized water. Instead, it combines this data with leaching data obtained in buffered solutions at a variety of pH values to study the mechanisms dominating aqueous corrosion in these glasses and the reasons for their apparent differences in resistance to aqueous attack.

RESULTS

Measurements of aqueous leach rates were conducted on zirconium-, thorium-, and uranium-based fluoride glasses (Table 1) as a function of time in deionized water. The curves of Fig. 1 show the relative leach rates of the three types of glass. From this data, it is clear that the ZrF_4-based glass appears to be far less durable than the others. However, it has been noted previously that the solution pH drift is far more severe in the case of the Zr glasses due to the dissolution of ZrF_4.[5] From an initial pH of 5.8, the

solutions drifted to 4.5, at short times, and 3.2 at longer times for ZrF_4 glasses, 5.6 for ThF_4 glasses, and 4.0 for UF_4 glasses.

In order to determine how the degree of pH drift and the resulting change in solubility of ZrF_4, ThF_4, and UF_4 contribute to these differences, measurements were conducted in buffered aqueous solutions at pH values from 2 to 10. The results are shown in Fig. 2.

While all glasses tested exhibit similar behavior, with a minimum near neutral pH, there are several interesting differences worth noting. First, we find that, at low pH, the ZrF_4 glass has the highest leach rate. Second, we find that, at basic pH, all the glasses show an increase in leaching, with the ZrF_4 glass showing the smallest rise. Finally, and most surprising, we find that, at neutral pH, the ZrF_4 glass exhibits a lower minimum than either the ThF_4 or UF_4 glasses.

Clearly, the combination of pH drift and the acid leaching behavior of these glasses explains the differences in durability observed in earlier tests in unbuffered deionized water. Comparing the leach rate at short times in Fig. 1 with the measured leach rates in Fig. 2, it can be seen that the ZrF_4 glass, leaching at 3×10^{-2} g cm^{-2} d^{-1}, should be in a solution at pH = 4.7, in good agreement with the value of 4.5 measured in the leaching solution; while the ThF_4 glass leaches at a rate of 2×10^{-4} g cm^{-2} d^{-1} at a pH of 5.6, and the UF_4 glass leaches at a rate of 2.1×10^{-3} g cm^{-2} d^{-1} at pH = 4.0.

In basic solutions, hydroxides are formed and the glass leach rates are controlled by the dissolution rates of these species.[2] These results support our earlier conclusions[2,5] that matrix dissolution is the major factor controlling the corrosion behavior of these glasses.

REFERENCES

1. C. J. Simmons, H. Sutter, J. H. Simmons and D. C. Tran, "Aqueous Corrosion Studies of a Fluorozirconate Glass," Mat. Res. Bull., Vol. 17, 1203-10, 1982.

2. C. J. Simmons, S. Azali and J. H. Simmons, "Chemical Durability Studies of Heavy Metal Fluoride Glasses," Extended Abstract #47, Second International Symposium on Halide Glasses, Troy, NY, 1983.

3. J. Guery, G. Courbain, C. Jacoboni and R. de Pape, "Fluoride Glasses of Uranium IV and 3rd Transition Metals," Extended Abstract #14, 2nd Symposium on Halide Glasses, Troy, NY, 1983.

4. T. A. McCarthy and C. G. Pentano, "Dissolution of Fluorzirconate Glasses,"
    Extended Abstract #30, 2nd International Symposium on Halide Glasses,
    Troy, NY, 1983.

5. C. J. Simmons and S. Azali, "Effect of Solution pH on Leaching of Fluoride
    Glass," (paper 8-G-84) 86th Annual Meeting of the American Ceramic
    Society, Pittsburgh, PA, April 10, 1984; Amer. Ceram. Soc. Bull., 63, 491
    (1984).

TABLE 1

COMPOSITION
(mole %)

Group I

	ZrF_4	BaF_2	LaF_3	AlF_3	LiF
ZBLAL	51.8	20.0	5.3	3.3	19.6

Group II

	BaF_2	ZnF_2	YbF_3	ThF_4	NaF
BZYbT	19.0	27.0	27.0	27.0	---
BZYbTN	10.0	27.0	27.0	27.0	9.0

Group III

	BaF_2	UF_4	AlF_3	YF_3	ZnF_2	MnF_2	FeF_3
BUYAZ	30.4	30.4	2.0	4.8	32.4	---	---
BUYAM	30.4	30.4	2.0	4.8	---	32.4	---
BUYFe	20.0	40.0	---	20.0	---	---	20.0

Fig. 2: Leach rates vs. pH for representative
         compositions from the three fluoride
         glass families.

The value corresponding to
U glasses should be x by factor
of ten.
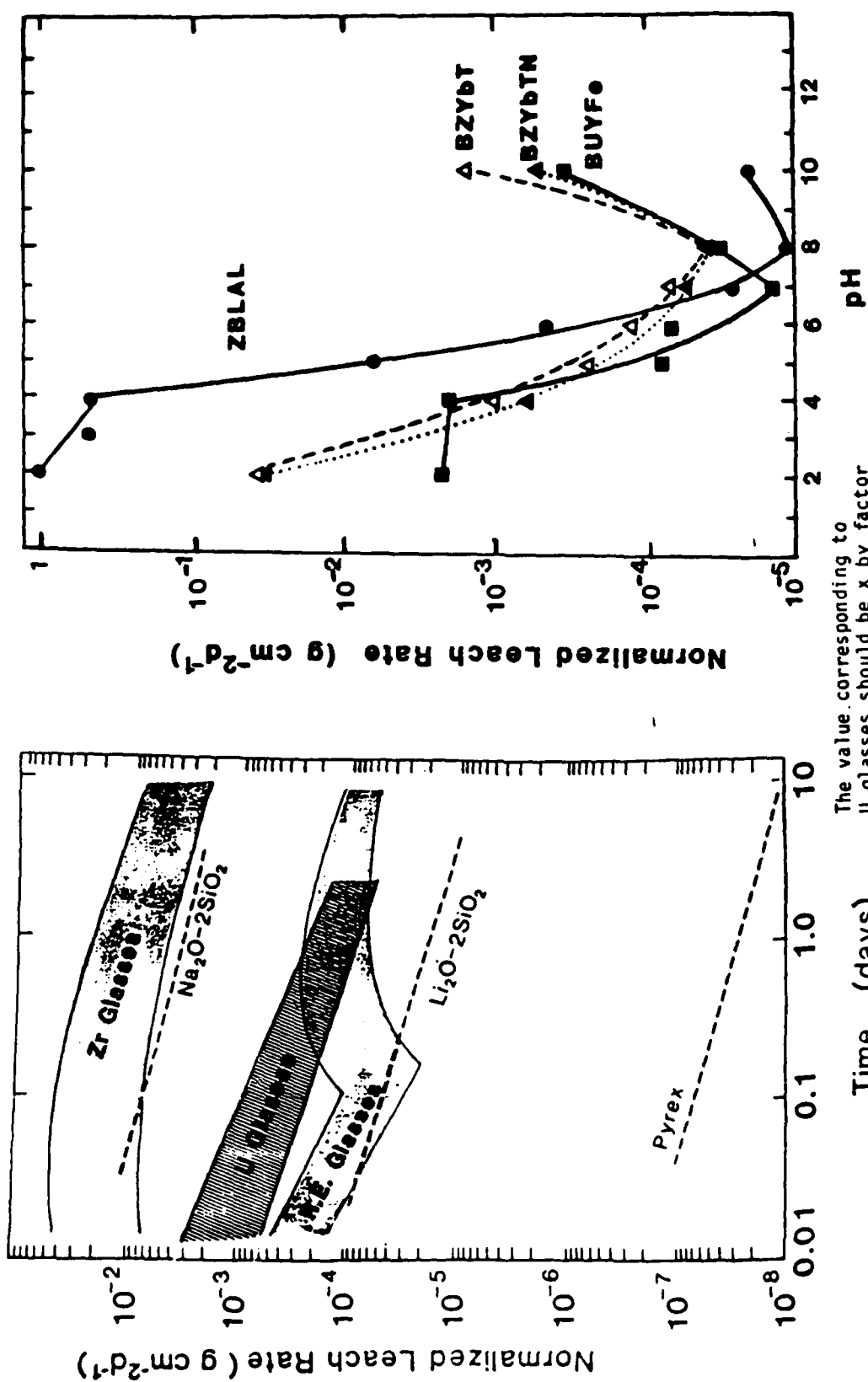
Fig. 1: Comparison of Normalized Leach Rates
         in deionized water for the three types
         of fluoride glasses studied with those
         of several common silicates.

Appendix C

Chemical Durability of Fluoride Glasses: I, Reaction of Fluorozirconate Glasses with Water

CATHERINE J. SIMMONS and JOSEPH H. SIMMONS

Chemical Durability of Fluoride Glasses: I, Reaction of Fluorozirconate Glasses with Water

CATHERINE J. SIMMONS* and JOSEPH H. SIMMONS*

Department of Materials Science and Engineering, University of Florida, Gainesville, Florida 32611

The chemical durability of five fluorozirconate glass compositions was studied. Measurements of leachant composition and solution chemistry by plasma emission spectroscopy, pH, and fluoride analysis are reported. Changes in surface structure were monitored by scanning electron microscopy, electron-probe X-ray analysis, and X-ray diffraction. The modifer additives with high aqueous solubility (AlF_3, NaF, LiF, PbF_2) exhibited the highest leach rates with ZrF_4, BaF_2, and LaF_3 exhibiting lower rates. The leaching order of $Zr > Ba > La$ was maintained for all samples. The leaching process consists of the dissolution of the glass matrix, leaving a thick and porous layer containing Zr, Ba, La, and molecular water. Hydroxylation of the Zr species to form a hydroxy-fluoride complex in solution dominated a decrease in pH to moderately acidic values. The resulting increase in component solubility (particularly zirconium fluoride) in the acidic solutions accelerated the glass dissolution rate and demonstrated that, if no buffer is present to avert the pH drift, the chemical durability of these glasses in aqueous environments is extremely poor, being roughly equivalent to that of $Na_2O \cdot 2SiO_2$.

I. Introduction

$\mathbf{F}$LUOROZIRCONATE glasses are under study for a variety of IR transmitting applications; therefore, their optical properties and phase stability behavior have received intense scrutiny. We have found these glasses of great interest in studies of chemical corrosion behavior because of the large constrast in behavior with silicate glasses. Our initial studies of the chemical behavior of a Zr-Ba-La-Al-Li fluoride glass in water[1] suggested far different processes from the known typical silicate leaching processes which are characterized by alkali-ion exchange for protons in solution followed by matrix dissolution as the solution pH drifts into the basic range.[2]

In this paper, we examine the leaching behavior of a series of fluorozirconate glasses whose added components are well-known for producing changes in the leaching behavior of silicates. The behaviors of these glasses are compared to one another and compared to established silicate glass leaching mechanisms. A sample containing PbF_2 was selected because it represents a composition of current interest for fiber optics applications.[3] The chemical durability behavior of fluoride glasses not containing zirconium will be reported in later publications.

II. Experimental Procedure

Fluorozirconate glasses melted at various laboratories were obtained for the chemical durability study. Table I shows the glass compositions selected, the commonly used mnemonics for them,

Table I. Composition (mol%)

Mnemonic	ZrF_4	BaF_2	LaF_3	AlF_3	LiF	NaF	PbF_2	Source*
ZBL	62.0	33.0	5.0					RPI[4]
ZBLA	57.5	34.5	4.0	4.0				RPI,[4] RADC[4]
ZBLAL	51.8	20.0	5.3	3.3	19.6			NRL[1]
ZBLAN	54.0	15.0	6.0	4.0		21.0		RPI[5]
ZBLALPb	50.4	15.5	4.9	3.1	20.2		4.9	NRL[1]

*NRL = D C Tran, Naval Research Laboratory, Washington, DC RPI = C T Moynihan, A J Bruce, and K H Chung, Rensselaer Polytechnic Institute, Troy, NY RADC = M G Drexhage and O H El-Bayoumi, Rome Air Development Center, Hanscom Air Force Base, MA
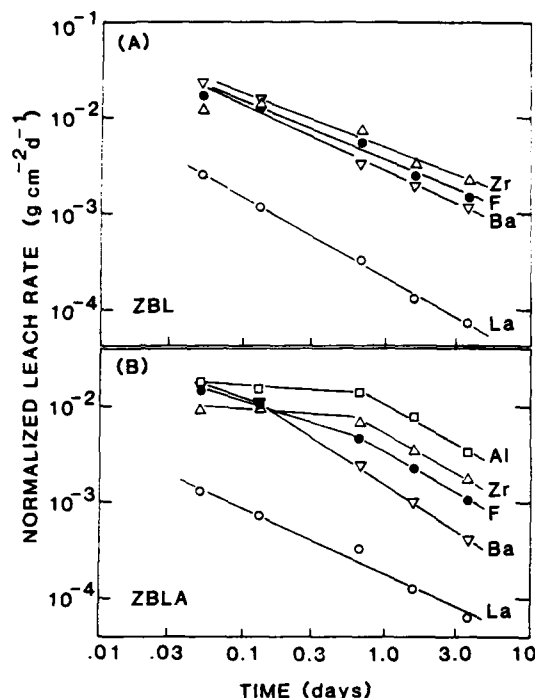
Fig. 1. Normalized leach rates vs. time from leachate analysis for individual elements of glasses: (A) ZBL; (B) ZBLA.

Fig. 2. Normalized leach rates vs. time from leachate analysis for individual elements of glasses: (A) ZBLAL; (B) ZBLALPb; (C) ZBLAN.

and the sources of the glasses. These glasses were melted under a variety of conditions varying from the use of oxide raw materials with added ammonium bifluoride[4] to the direct use of anhydrous fluoride raw materials, melted under an Ar or CCl_4 atmosphere.[6,7] In the case of ZBLA, samples melted by both techniques were studied. In all cases the glasses showed low water and low oxide content, as determined spectroscopically.

Corrosion tests were conducted with deionized, pH 5.6, water at 25°C. The tests, except where noted, were conducted on solid samples polished under halocarbon oil, which is oxygen and water free, in order to remove the aged surface layer and obtain a reproducible surface finish without aqueous contact. Samples were rinsed in toluene to remove the oil. Solution analysis was conducted by removing the soaking solution and analyzing duplicate samples using a dc plasma spectrometer, a fluoride-selective electrode, and an ion chromatograph. Static tests were conducted in PMP containers with the samples supported by prewashed Teflon* baskets, following the test procedures recommended by MCC.[8] The solution volume to sample surface area was maintained at a constant ratio of 100:1 for all tests in order to minimize saturation effects. Normalized leach rates were calculated from Eq. (1):

$$\frac{XV}{S \cdot \Delta t} wt = \mu g \cdot cm^{-2} \cdot d^{-1} \tag{1}$$

where X = ppm in solution, V = solution volume (mL), S = surface area (cm^2), Δt = soak time (days), and wt = weight fraction of element in the original glass.

III. Results

Leach rates in solution for the fluorozirconate glasses are plotted as function of time in Figs. 1 and 2. These rates are normalized by the concent ations of ions in the glass for easy comparison between different elements, as well as different compositions. As shown in Fig. 1(A), zirconium leaches at the fastest rate in the ZBL glass, followed by barium, with lanthanum appearing at a much slower
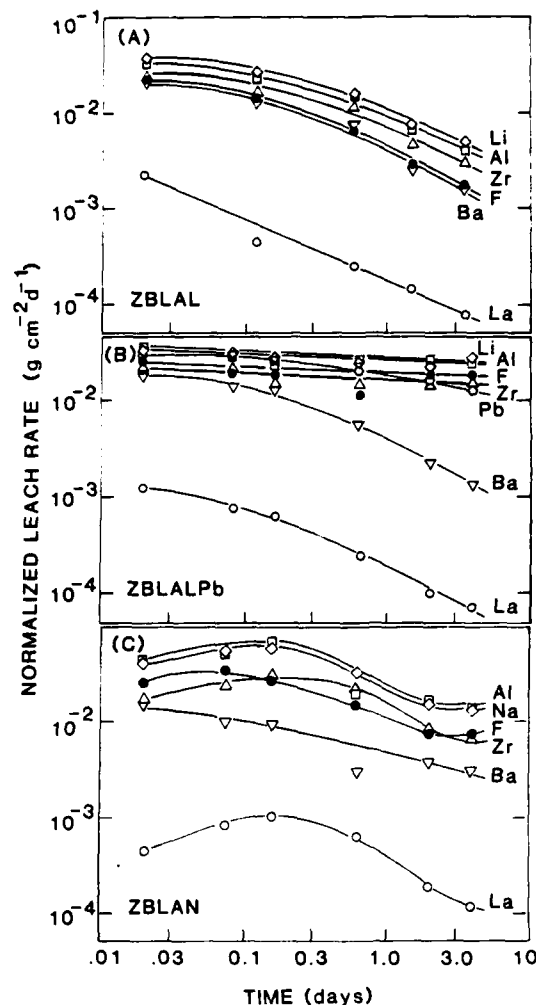
rate. This Zr/Ba/La order appears for all the compositions studied. The addition of Al to the glass (ZBLA) (Fig. 1(B)) induces little change in the leach rates of Zr and La, but reduces the Ba leach rate by a factor of ≈3, while the Al additive exhibits the highest normalized leach rate. The addition of Al and Li to the glass (ZBLAL) (Fig. 2(A)) appears to cause little change in the leach rate of the ZBL components with both Li and Al exhibiting the higher normalized leach rates. The addition of Na and Al to form the ZBLAN glass (Fig. 2(C)) increases the corrosion rate of all of the components with again Na and Al providing the higher leach rates. The highest leach rate observed for zirconium, however, is found in the fiber optics glass containing the base ZBL composition with additives of Al, Li, and Pb (Fig. 2(B)). Initially, lead enters the solution at the same rate as Al and Li, decreasing only slightly at longer times. The major difference between this glass and its predecessors is that it does not exhibit the marked decrease with time in component leach rate observed for the other compositions. After 5 d of soaking, the Li and Al leach rates are 5 to 6 times higher in the ZBLALPb glass than the ZBLAL glass. In general, the tests were stopped after 5 d because of the thick surface corrosion layer (≥150 μm), which developed in that time.

IV. Discussion

A composite curve of the average weighted leach rates of all five glasses (Fig. 3) shows the curious result that, within a factor of 10
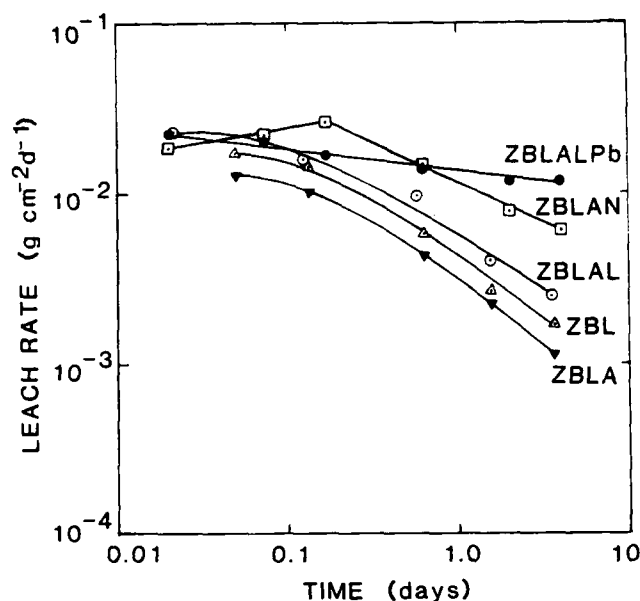
Fig. 3. Compositionally weighted average leach rates for all five glasses (La neglected).

Fig. 4. Temporal variation of solution pH for all five glasses.

in leach rates. all the glasses behave in a similar manner with equivalent rates. closely following the behavior of ZBL and relatively unaffected either by the addition of modifiers or by varying the preparation conditions. This result contradicts that reported recently by Barkatt and Boehm,[9] who claim to see a large melting history effect due to the presence of residual ammonium bifluoride in the glass. However. Moynihan *et al.* [10,14] have shown that there is little. if any, effect on durability in samples melted with and without ammonium bifluoride. In general. therefore. it appears that in deionized water the leach rate of fluorozirconate glasses is controlled both by the behavior of the zirconium and barium components. as shown here, and by the pH drift of the soaking solution during the test. as described in detail below and elsewhere.[11,12] Additives of matrix modifiers such as the fluorides of Al. Pb. Li. and Na have only a limited effect on the leach rate of fluorozirconate glasses. In contrast. the oxides of these elements normally have a profound effect on the balance between ion exchange and matrix dissolution of silicate glasses. For example. the addition of 10% to 20% alkali to a silicate glass produces a decrease in durability of several orders of magnitude. The lower leach rate of La appears to come from the lower solubility of LaF$_3$. In subsequent papers. we will show that composition-dependent differences do appear in the aqueous leach rates of glasses containing the thorium,[11] rare-earth. and uranium fluorides.[12] but that these differences arise from the pH dependence of the respective solubilities.

(1) pH Drift Behavior

A clue to the major difference between fluorozirconate and silicate glasses lies in the measurement of solution pH during the leaching process. Silicates containing alkali oxides exhibit a solution pH drift to basic values generally above 10. This results from a dominating ion-exchange process between alkali ions in the glass with protons (H$^+$) or hydronium ions (H$_3$O$^+$) in solution. Figure 4 shows the temporal variation of solution pH for the five fluoride glasses. All show a marked decrease in pH to between 3.6 and 4.5 within the first few hours. A test was conducted to determine the equilibrium solution pH of ZBLAL glass by soaking an excess of fine powder in deionized water at a pH of 5.6 while stirring in a rotating cylindrical bottle. After an initial rapid drop in pH. the solution maintained a constant value of 2.46 over several days. This decrease in pH could result either from an ion exchange of OH$^-$ in the solution for F$^-$ in the glass corroded layer or from the OH$^-$/F$^-$ exchange of dissolved species in solution.
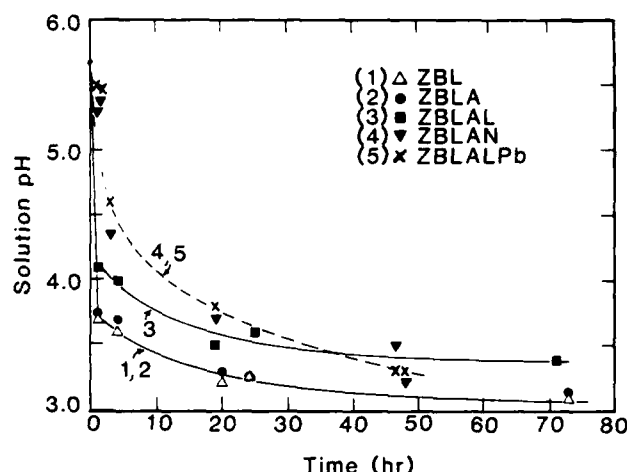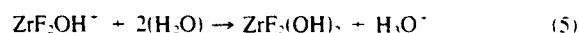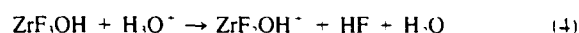
In order to determine the effect of the individual glass components on pH. we conducted a test where the crystalline form of each component fluoride (ZrF$_4$, BaF$_2$, AlF$_3$, PbF$_2$, NaF. and LiF) was dissolved separately in deionized water. The results showed that as little as 12 ppm of ZrF$_4$ produced a significant decrease in the solution pH from 5.45 to a value of 3.95. Subsequent additions of ZrF$_4$ to solution. above 30 ppm. caused an increasingly smaller drop in pH. indicating that the dissociation of fluoride and subsequent hydrolysis of zirconium decrease with increasing concentrations of fluoride ions in solution. None of the other components affected a significant decrease in pH when dissolved individually. It appears. therefore. that it is the hydrolysis of zirconium fluoride which is responsible for the majority of the pH drop during leaching of fluorozirconate glasses. The species formed appears to be [ZrF$_x$(OH)$_y$]$^{-4-x-y}$ [H$_2$O]$_n$. The reaction may be written as

$$ZrF_4(aq) + H_3O^+ \rightarrow ZrF_3^+ + HF + H_2O \qquad (2)$$

$$ZrF_3^+ + 2(H_2O) \rightarrow ZrF_3OH + H_3O^+ \qquad (3)$$

$$ZrF_3OH + H_3O^+ \rightarrow ZrF_2OH^+ + HF + H_2O \qquad (4)$$

$$ZrF_2OH^+ + 2(H_2O) \rightarrow ZrF_2(OH)_2 + H_3O^+ \qquad (5)$$

A chemical analysis of the supernatant solutions for metal and fluoride ion concentration indicated that. on the average. each Zr and Ba ion retains a fluoride ion despite the addition of a strong complexing agent (TISAB). One of every six atoms of Al at low concentrations and one of every three Al atoms at higher concentrations also retain a fluoride ion. This indicates that. in the pH ranges covered by the test. and particularly for Zr. the metal does not release all its fluoride ions. These results also explain the lower than anticipated values obtained in fluoride ion concentration measurements of the leachate solutions using electrode analysis.

Since the major pH drift occurs during the first hour. a titration experiment was performed to determine the rate and degree of hydrolysis occurring during that time in a solution of constant pH. A freshly powdered sample of ZBLAL was placed in water whose pH was adjusted to 5.0 using dilute HCl. The solution was stirred constantly and the pH was monitored throughout the test. A dilute NaOH (10^{-3} M) solution was added by means of a buret in order to maintain the solution at pH 5.0. The amount of additional OH$^-$ necessary to maintain the pH was monitored as a function of time and is shown in Fig. 5. After a brief induction period. the hydrolysis reaction is seen to follow $t^{1/2}$ behavior. The induction period may be due to a short delay in ZrF$_4$ dissolution and hydrolysis following the preferential leaching of Li and Al. Table II summarizes the data obtained through solution analysis. It is clear from the results of individual component dissolution. above. that none of the dissolving species. except ZrF$_4$, undergoes hydrolysis to any significant degree. B: comparing the concentration of Zr in
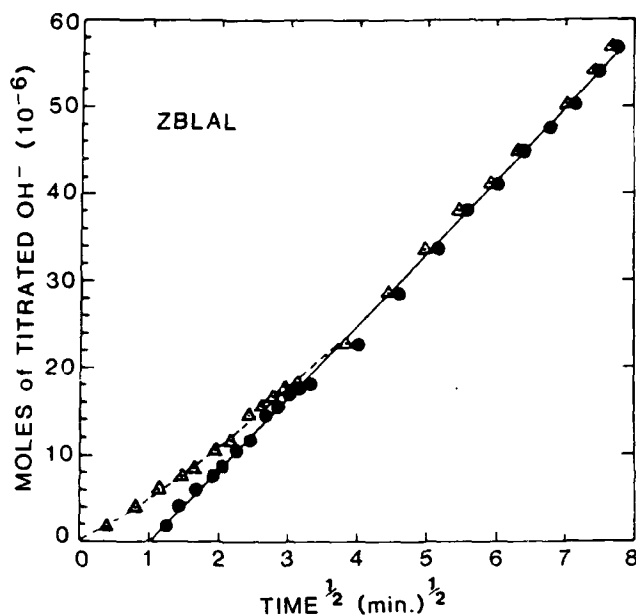
Fig. 5. Moles of titrated hydroxyls plotted vs. time$^{1/2}$ (solid circles) and $(t - t_0)^{1/2}$ (open triangles), showing the rate of hydrolysis of $[ZrF_x]^{-4-x}$ from ZBLAL glass in a solution maintained at constant pH.

Fig. 6. Relative $[ZrF_x]^{-4-x}$ species concentrations as calculated from association constants.

solution (27.6 μmol) to the titrated hydroxyl concentration (58.2 μmol), we obtain the result that the dominant zirconium hydroxyfluoride complex discussed above contains two hydroxyl ions (i.e., $y = 2$).

A calculation of the dependence of the relative concentrations of the various dissociated $[ZrF_x]^{-4-x}$ species was conducted based on published values of association constants.[13] The results are plotted in Fig. 6 and show that, over the range of solution fluoride concentrations encountered in these tests, the dominant species are $[ZrF_2]^{+2}$, $[ZrF_3]^+$, and $[ZrF_4]$. Most of the test results obtained after 1 h of corrosion were at concentrations between 1 and 10 ppm F, showing a dominance of $[ZrF_4]$ with between 50% and 20% of $[ZrF_3]^+$. The more highly dissociated species are only expected in appreciable relative concentrations in the very early stages of corrosion.

In conclusion, the pH behavior of the solution and the zirconium fluoride species formed are strongly dependent on the concentration of dissociated F and the availability of hydroxyls; therefore, the most probable zirconium species in solution are the hydrated forms of $[ZrF(OH)_2]^+$ and $[ZrF_2(OH)_2]$, with the neutral species favored at higher fluoride concentrations (>10 ppm).

(2) Surface Water Content

Infrared absorption measurements showed, for all glasses, the same OH stretching (2.9 μm) and HOH bending (6.1 μm) vibrations seen in our previous studies,[1] with increasing absorption for longer corrosion times. This obviously indicates that the for-

mation of a hydration layer occurs by a complementary mechanism to the leaching process. Loehr et al.[14] have measured the intensity of both vibrations in short-term leach tests for the first four glasses reported here: the time dependence closely follows our leaching behavior. Their measurement also shows the same relative differences and ordering of the hydration rates between the various glasses that we report in Fig. 3. The time dependence of the growth of the water and hydroxyl bands appears to follow a t^1 power law for times up to 20 to 30 min and then a $t^{1/2}$ law for longer times. These authors were not able to separate, in the hydroxyl vibration, the contributions due to molecular water from that due to metal hydroxides. However, by comparing the rate of growth of the two peaks and calculating a constant ratio, they concluded that only molecular water is present in the hydrated layer of the glass. On the basis of these results and some solution analysis, Doremus et al.[15] have suggested that only matrix dissolution occurs in these glasses and that leaching occurs congruently. Since only one composition was studied, the consistent difference in leach rates between the glass components reported here was not observed. This difference becomes important in determining the mechanism of formation of the porous leach layer. Furthermore, Loehr and Moynihan deduced a lack of OH formation in this leached layer from a comparison of the time dependence of the ratio of absorption peak heights of the water bending to OH stretching motions. The peaks, however, broaden considerably, particularly for the OH stretching motion, and our preliminary results indicate that if one calculates the integrated peak area instead, the OH vibration peak grows slightly faster than the HOH bending peak. This would indicate the formation of some hydroxides in the layer and would be more consistent with the development of an oxide peak during drying as seen in Ref. 1.

Table II. Equivalent F⁻ Calculated from DCP Cation Analysis

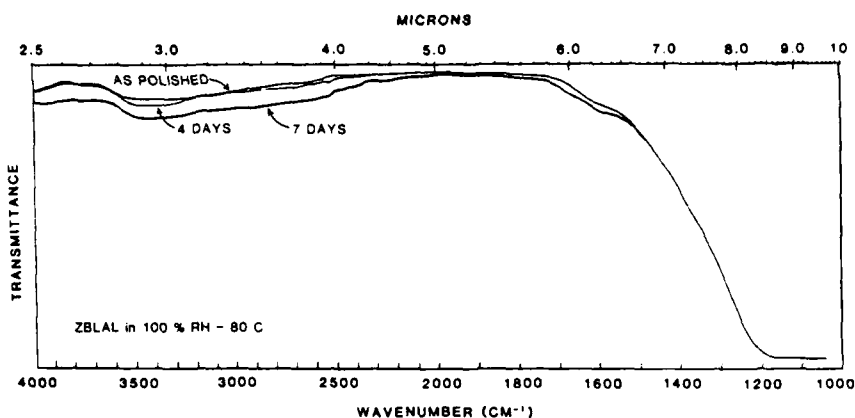| Cation	Analyzed [M⁻] (10⁻⁶ mol)	Equivalent F (10⁻⁶ mol)	% of total F	Normalized leach rate (g·cm⁻²·d⁻¹)
Zr⁴⁺	27.6	110.4	72	3.57×10^{-2}
Ba²⁺	10.0	20.0	13	3.36×10^{-2}
La³⁺	0.08	0.24	0.1	1.03×10^{-3}
Al³⁺	3.2	9.7	6	6.56×10^{-2}
Li⁺	14.0	14.0	9	4.80×10^{-2}
		154.34	100	
Titrated moles OH (10⁻⁶)		58.20	38	

Fig. 7. IR transmission spectra of ZBLAL glass exposed to 100% relative humidity for 4 and 7 d at 80°C.

The series of glasses studied in Ref. 14 exhibits an order of hydration rate with respect to composition (ZBLAN > ZBLAL > ZBL > ZBLA) which is the same as that observed in our leach tests based on solution analysis. The combination of these results suggests that the layer forms as a result of the selective leaching of the more soluble glass species (NaF, LiF, AlF₃, PbF₂) and that the leach rate is controlled both by solubility and by the diffusion of molecular water through the layer to the unreacted glass surface and the counterdiffusion of dissolved species into the solution. Thickening of the layer with time is expected to lead to an increase in diffusion time and a decrease in leach rate. Since the steepest decrease in leach rate is observed in the ZBLA glass, and this glass has the thinnest layer, the porosity of the layer must play a major role in the diffusion process. The more durable glasses evidently develop the less porous and thinner layers, while the less durable glasses, such as ZBLALPb, develop a thick layer with a sufficiently high porosity to maintain a nearly constant leach rate with time. In the case of ZBLALPb, the rapidly dissolved species (LiF, AlF₃, PbF₂) constitute 28 mol% of the glass composition, while ZBLA contains only 4% ALF₃.

(3) Effects of Atmospheric Moisture

Most nondurable silicates are highly susceptible to corrosion in humid environments, frequently exhibiting visible surface damage within hours of exposure. Tests were conducted on ZBLAL glass samples exposed to an environment of 100% relative humidity at 80°C for up to 7 d. Care was taken to avoid temperature cycling and moisture condensation on the sample surface during the tests. The samples showed no visible evidence of corrosion. Figure 7 shows the infrared transmittance spectra of the as-polished sample as compared with a 4- and 7-d exposure period. A 2% to 3% increase in absorbance at 2.85 μm is evident after 4 d, increasing slightly at 7 d. This may be due to the formation of an extremely thin reaction layer or to the presence of a small amount of atmospheric water adhering to the surface. This result demonstrates that, in spite of their poor durability in aqueous environments, Zr-based fluoride glasses are relatively unreactive in the presence of atmospheric moisture. Similar results were reported by Robinson *et al.*,[16] who noted that no corrosion was observed up to 200°C for a variety of fluoride glasses containing ThF₄, and by Gbogi *et al.*,[17] who noted no increase in surface-OH absorbance for a ZBL sample exposed to ambient laboratory atmosphere for 30 d.

(4) Microscopic Appearance of Surface

Scanning electron microscopic observations of the corroded surface gave essentially the same results as our previous study of ZBLAL.[1] All glasses exhibited precipitated crystal deposits over the entire surface with a highly porous, thick, hydrated layer of material beneath the crystals and above the uncorroded glass surface. Figure 8 shows the corroded surface of a ZBLA glass after 2 d in solution. Figure 9 shows various aspects of the corroded surface of the same glass after 5 d in solution, with Fig. 9(B)

Fig. 8. Typical crystal deposits on the surface of ZBLA glass following 2 d in stagnant, deionized water. Letters correspond to EDS analysis in Fig. 10; bar = 100 μm.

showing the surface with crystals removed and Fig. 9(C) showing a cross section of the crust of ZBL glass. The results of EDS analysis of the surface pictured in Fig. 8 are shown in Figs. 10(A) to (D). The most significant change observed, when comparing the spectrum of the uncorroded glass (A) with that of the leach layer or crust (B), is the appearance of a measurable amount of La concentrated in the layer. This is in good agreement with our solution analysis, showing a much lower leach rate for La. The crystals consist of two distinct structures: long parallelepipeds shown by EDS analysis to contain a high concentration of Zr (Fig. 10(D)) and spherical shapes made up from a multitude of thin platelets containing Zr and Ba (Fig. 10(C)). The long crystals were identified by X-ray diffraction to be ZrF₄. They comprise the majority of the surface deposits seen. Doremus[18] has also reported that the needlelike crystals are ZrF₄, while Pantano[19] has recently suggested that they are a hydrate form [ZrF₄(H₂O)₂]. X-ray diffraction measurements also tentatively identify the thin Ba-rich platelet crystals making up the spherulites of Figs. 8, 9(A), and 9(D) as ZrBaF₆. In several tests where the Ba concentration in solution was observed to become independent of corrosion time due to solution saturation, the spherical crystals became more abundant with no appearance of new crystal types, indicating that those crystals resulted from precipitation from solution near the surface of the sample undergoing corrosion. Since the ZrF₄ crystals were mixed with the Zr-Ba crystals, occasionally becoming surrounded by them (for example, see Fig. 9(D)), it is clear that they also form by continuous precipitation from solution. Nearly all tests reported here, and in Refs. 18 and 19, were conducted under static
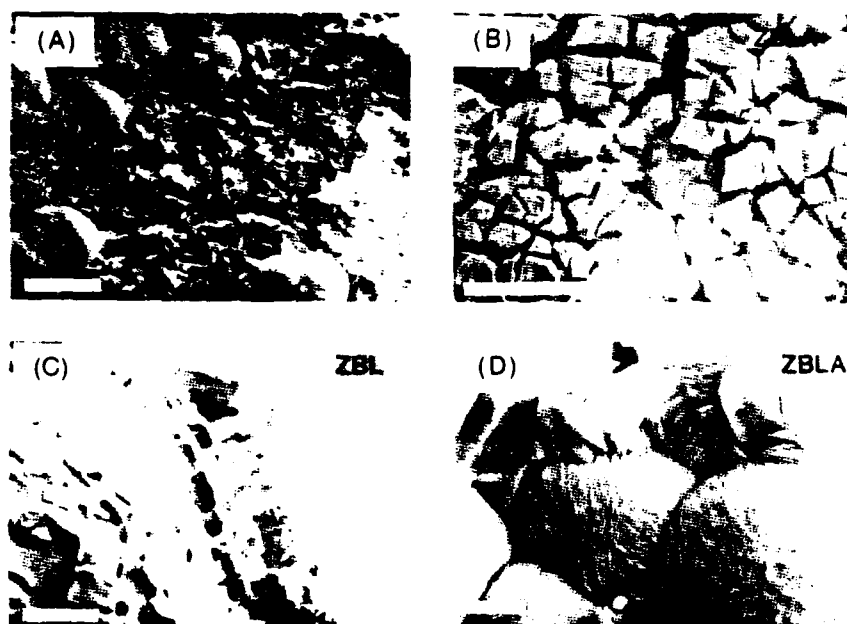
Fig. 9. SEM micrographs of surface structure after leaching 5 d at 25°C: (*A*) surface crystal deposits (bar = 100 μm), (*B*) corrosion layer with crystals removed (bar = 100 μm), (*C*) cross section of corrosion layer (bar = 100 μm), (*D*) magnified crystal deposits (bar = 10 μm).

conditions. These results strongly suggest the formation of a rapidly saturated static diffusion layer in the solution surrounding the glass. This conclusion is supported by results of our studies comparing the leach rates of stirred powders with those of static solids,[20] which show an increase in leach rate in stirred solutions, and by the results of Houser and Pantano,[21] who stirred the solution around solid samples and observed an increase in the hydration depth. Our SEM comparison of the corroded surfaces of bulk samples leached under static and stirred conditions showed a complete absence of crystal deposits in the latter. These results, therefore, lead to the conclusion that a major step in the static leaching of these glasses is the dissolution and subsequent saturation and precipitation of fluorides at the glass/solution interface.

The formation of a static diffusion layer in the solution surrounding the glass apparently leads to the saturation of ZrF_4- and Ba-containing fluoride compounds in solution, which is then followed by precipitation of the crystals. It is, therefore, the combination of the interdiffusion of water and the dissolving species through the porous layer and the rate of crystal precipitation which controls the temporal evolution of the leach rate of the glass. This could explain the $t^{1/2}$ time law observed without the requirement of involving an F diffusion process through the glass or the hydrated cyrstalline layer, which is seen beneath the precipitated crystals. The hydrated corrosion layer attained a thickness of ⩾150 μm within 5 d (Fig. 9(*C*)) and, under microscopic examination, appeared severely cracked due to dehydration under vacuum. Where pieces of the layer had peeled off, further chemical attack and mild cracking were observed extending into the glass (Ref. 1, Fig. 3(*B*)).

(5) Corrosion Mechanism

These results, when combined with the work of others, begin to form a composite understanding of the leaching process in fluorozirconate glasses. This model is best examined in the context of and in comparison with known leaching processes in silicate glasses.

Briefly described, silicate glasses leach by the competing mechanisms of ion exchange and matrix dissolution. While both processes are always occurring, their rates can be drastically affected by the composition of the glass and by the events occurring during leaching, such as the formation of a protective, dealkalized

layer. Generally, it is the porosity and the chemical composition of the dealkalized layer which control the temporal evolution of the leach rate characteristic of a silicate glass. The dealkalization process involves the exchange of alkali-metal cations for either protons or hydronium ions. The behavior of the dealkalized layer and its effectiveness in protecting the glass matrix from further dealkalization and matrix dissolution are dependent upon alkali diffusion through the layer, layer porosity, layer thickness, precipitated or adsorbed species, and the pH of the solution before and during corrosion. Under static conditions the rapid dealkalization process drives the pH to basic values whose limit is determined either by the other glass components, such as the dissociation of boric and silicic acids, or by buffers in the soaking solution. Since the solubility of silica is greatly increased in basic solutions, the increase in pH accelerates the matrix dissolution rate. In well-mixed or flowing solutions, the concentration of silica from durable silicate glasses generally increases, first with a $t^{1/2}$ law, due to the rate-controlling interdiffusion of alkali-metal ions and H$^+$ or H_3O^+ ions, and then as t^1, due to matrix dissolution through a steady-state dealkalized layer. With time, the silica concentration in solution reaches a saturation level for the ambient pH. This can drastically lower the leach rate, but often complexes are formed with silica which precipitate in the form of crystals or colloids. Frequently, other effects may complicate the observed behavior, such as inadequate solution exchange or stirring, the appearance of other buffers, the reprecipitation into the layer of selected components from the glass (such as the alkaline earths and the transition metals), and possible mechanical damage to the layer. But, in silicate glasses, the underlying principles are clear.

Our data suggest that fluorozirconate glasses undergo little, if any, ion exchange and that the corrosion process occurs primarily by selective extraction followed by matrix dissolution. The high leach rates of the alkali fluorides and AlF_3 also suggest that they have a high solubility and, as demonstrated by our results, they precede ZrF_4 dissolution. Only the Ba and La components are removed from the layer at a lower rate than Zr. The drop in pH, which results from the dissolution and hydrolysis of ZrF_4, increases the solubility of all of the fluoride components and accelerates dissolution, thus leading to a severe attack on the glass in a manner similar to that exhibited by silicates at high pH (nucleophilic attack).
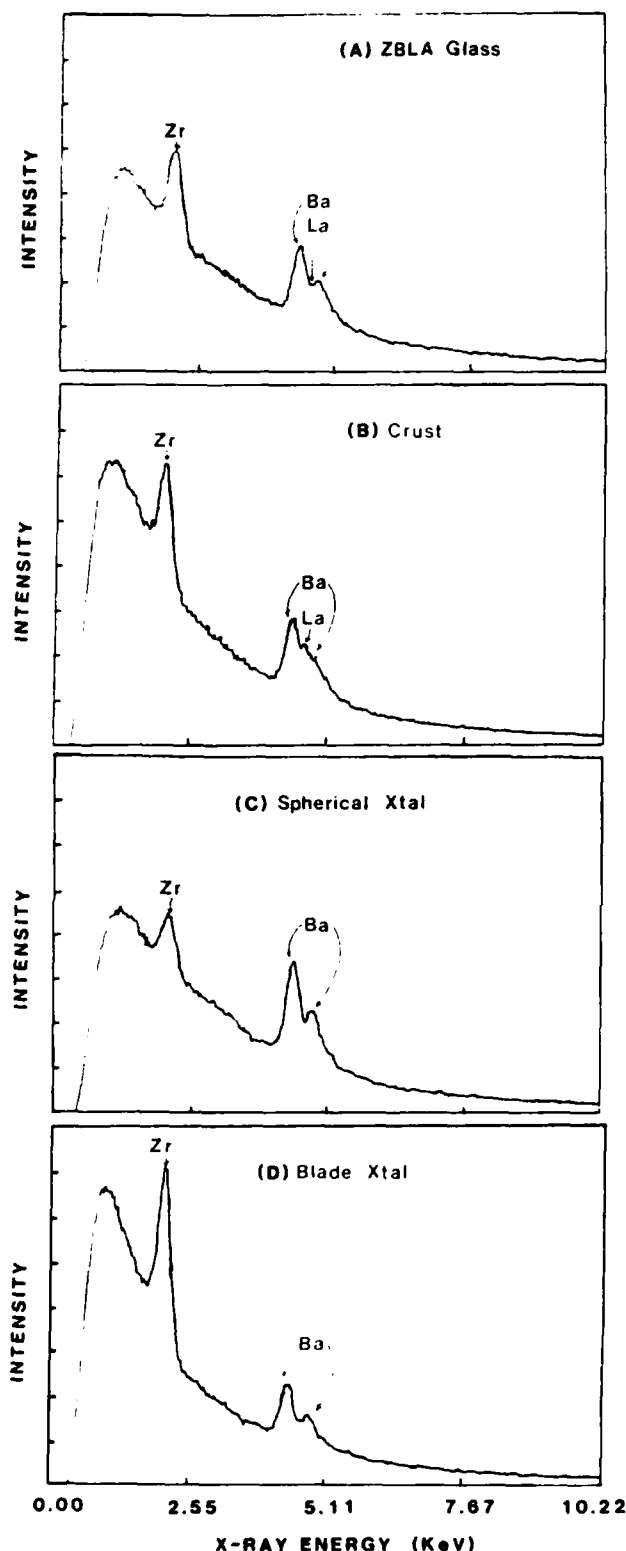
Fig. 10. EDS analysis of a ZBLA sample from Fig. 8 showing (*A*) uncorroded, as-polished surface; (*B*) dehydrated corrosion layer (crust); (*C*) spherical crystal deposits; (*D*) blade-shaped crystal deposits.

There are numerous additional complications in the corrosion process which must be carefully analyzed. For example, the presence of a liquid diffusion layer allows saturation of the Zr, La, and Ba components and is responsible for the presence of precipitated crystals on the surface of samples corroded in static solutions. The

formation of the nonprotective, yet very thick, hydrated layer results from the selective leaching process and its porosity influences the temporal behavior of the leach rate. Therefore, studies of the thickness or water content of the layer, while reflecting the surface hydration which occurs during the leaching process, do not investigate the controlling corrosion mechanisms, which appear to be matrix dissolution with a subsequent formation of zirconium hydroxyfluoride complexes. The latter process, because it leads to a reduction in solution pH and an increase in the leaching process, is most responsible for the comparatively poor durability of fluorozirconate glasses in water.

(6) Coatings

In order to take full advantage of the unique optical properties of these fluoride glasses, it is imperative that hermetic coatings be developed to shield them from severe attack in aqueous environments. In some cases, particularly for use with lenses and laser windows, these coatings must also be transparent in the IR. One promising coating material currently under study is diamond-like carbon.[22] Results of infrared transmission spectroscopy for short-term (4 h) aqueous corrosion tests on identical ZBLA samples,[23] coated (*A*) and uncoated (*B*), are plotted in Fig. 11. The differences in degree of corrosion are evident from a comparison of the before and after spectra of the two samples. Whereas very little change is seen to have occurred in the coated sample, fairly extensive surface hydration is observed in the uncoated ZBLA. This observation was confirmed by SEM; the surface of the uncoated sample was covered with the typical dehydration cracking discussed above, while the coated surface showed only isolated pit corrosion and no cracking or spalling of the surface was observed. The pit corrosion is thought to have resulted from pinholes in the experimental coating and it is believed that with improved deposition techniques this problem can be overcome.

V. Conclusions

The static leaching of fluorozirconate glasses appears to be a complex process involving component solubility, matrix dissolution, ion exchange, hydration, species saturation, and re-precipitation. For this reason, weight loss measurements cannot be relied upon to determine either the controlling mechanisms or the comparative resistance of various fluoride glasses to leaching.

As shown in this study, fluorozirconates leach rapidly in water, their solution pH becomes acidic quickly, a thick hydrated layer forms which absorbs a large amount of water, and crystal precipitates form on the hydrated layer surface. Measurements of solution composition by plasma emission spectroscopy, of degree of hydration by infrared absorption, of layer thickness and structure by scanning electron microscopy, and of crystal precipitate compositions by X-ray diffraction and electron microprobe analysis were conducted on a series of fluorozirconate samples. These measurements have now led to the evolution of a comprehensive model of the corrosion process.

The corrosion mechanism which emerges from these conclusions can be recapitulated as follows:

(1) The zirconium-based fluoride glasses corrode primarily by matrix dissolution. However, unlike silicates which go into solution as hydroxides, the components of these glasses go into solution as fluorides without a prior hydroxylation step.

(2) LiF, NaF, AlF$_3$, and, in some cases, BaF$_2$ dissolve at faster rates than either ZrF$_4$ or LaF$_3$. This difference in extraction rates, coupled with the rapid penetration of water into the glass, leads to the formation of a porous, hydrated corrosion layer at the glass surface.

(3) With time, the leach rates of LiF, NaF, and AlF$_3$ remain high, while that of BaF$_2$ decreases significantly as a possible result of (i) an increase in [F$^-$] ion concentration, which can interfere with BaF$_2$ solubility, and (ii) the depletion of BaF$_2$ from the glass surface.

(4) LaF$_3$ is highly insoluble in aqueous solutions and, therefore, remains in the surface layer.

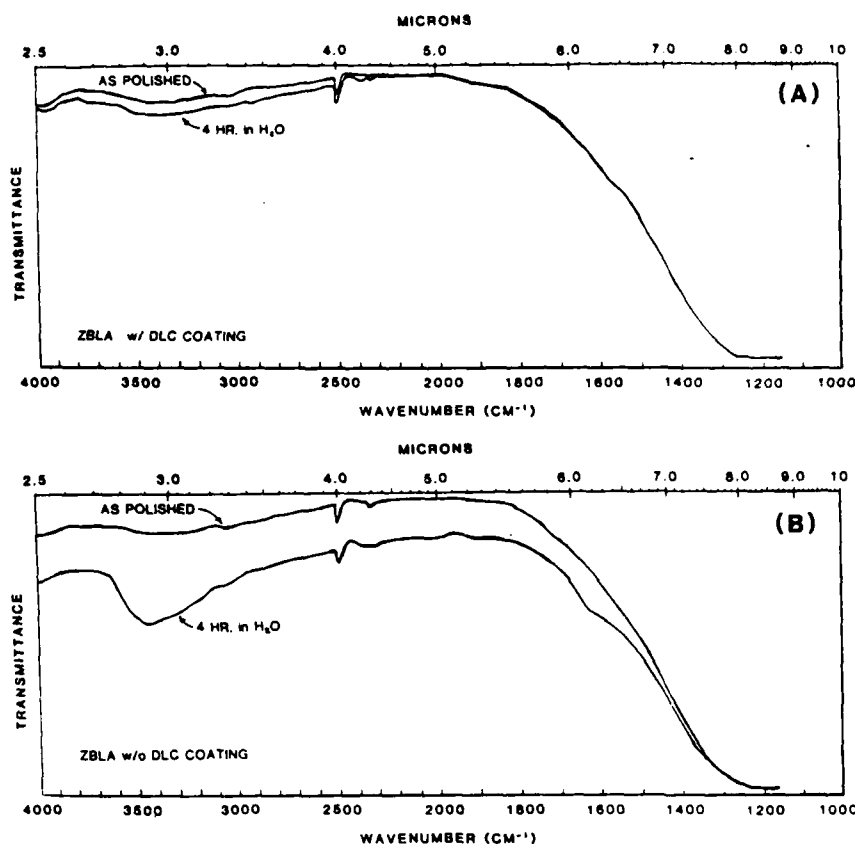(5) Zirconium fluoride dissolves into solution as ZrF$_4$. Evi-

Fig. 11. IR transmission spectra of ZBLA samples before and after corrosion: (A) surface coated with diamond-like carbon; (B) without coating.
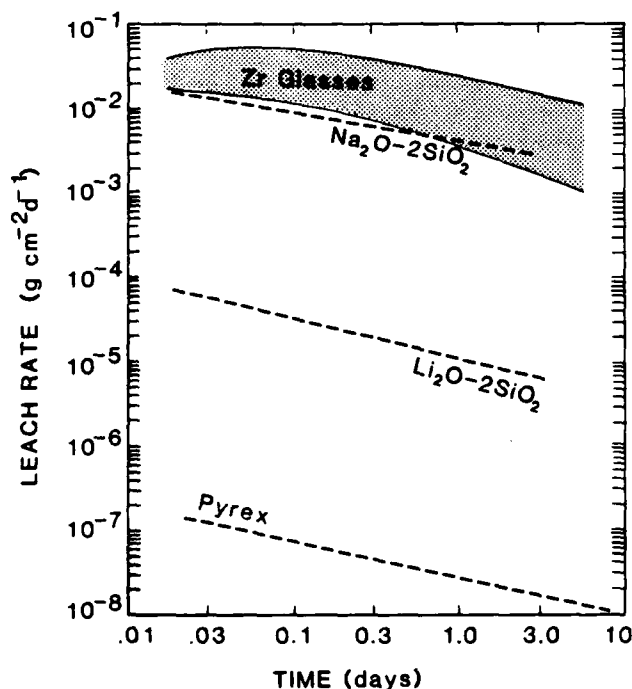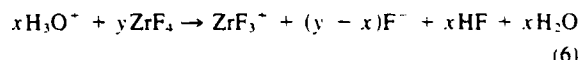

Fig. 12. Comparison of the collective leaching behavior of fluoro-zirconate glasses with three well-studies silicate glasses $Na_2O \cdot 2SiO_2$,[24] $Li_2O \cdot SiO_2$,[24] Pyrex (Corning Glass Works, Corning, NY).[25]

dence of the dissolution of ZrF_4 is supported by its appearance as a precipitated surface crystal. In addition, there is a partitioning:

$$xH_3O^+ + yZrF_4 \rightarrow ZrF_3^+ + (y - x)F^- + xHF + xH_2O \quad (6)$$

This partitioning favors $[ZrF_3]^+$ over $[ZrF_4]$ at low $[F^-]$ concentrations; the two species are equal at ≈ 3 ppm of $[F^-]$ and the $[ZrF_3]^+$ concentration drops to only 20% when 10 ppm $[F^-]$ is present in solution. Since the fluoride ion concentration rapidly increases to >3 ppm during corrosion, it appears that, while the $[ZrF_3]^+$ ion dominates in the early stages, it makes up a relatively small percentage of the leachate after several hours, when the fluoride ion concentration increases above 10 ppm.

(6) A decrease in solution pH with time is observed which results from successive hydrolysis of the zirconium fluoride species [Eqs. (1) to (4)]. Measurements of the equivalent hydroxyl concentrations exchanged, as described in the titration tests, indicate that two hydroxyls are exchanged per Zr in solution:

$$2[OH]^- + [ZrF_4] \rightarrow [ZrF_2(OH)_2] + 2F \quad (7)$$

$$2[OH]^- + [ZrF_3]^+ \rightarrow [ZrF(OH)_2]^+ + 2F \quad (8)$$
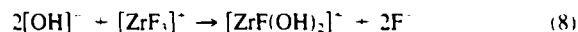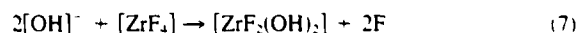
(7) Under static conditions, the outer layer of the corroded glass is porous and hydrated and is covered by precipitated crystals of two distinct types. These are long, needlelike crystals identified by X-ray diffraction as ZrF_4 and spherical assemblages of thin platelike crystals tentatively identified as $ZrBaF_6$. These crystals form by precipitation due to saturation at the glass-solution interface. The two crystal types appear to form simultaneously, since they are seen to form around one another. Under dilute, well-stirred conditions, the corrosion layer appears to be similar in character; however, no crystals are formed, even after leaching for 10 d.[18]

(8) The thick, porous layer plays a minor role in protecting the unreacted bulk glass and acts as an ineffective diffusion barrier to reduce the leach rate. The porosity of the layer reflects the molar

volume of highly soluble species (NaF, LiF, AlF₃, PbF₂) in the glass composition and can be related to the comparative leach rates of different glasses. For example, the less durable glasses form a thick and highly porous layer.

(9) The pH drift of the solution into an acidic region during leaching raises the solubility of zirconium fluoride, which accelerates the glass dissolution by several orders of magnitude, causing it to be comparable in durability to the poorer silicates (Fig. 12). The addition of any buffer to the solution can have a profound effect on the leach rate if it eliminates or retards the pH drift. The results of varying the pH of the solution on the leach rate of fluorozirconate glasses will be presented in a subsequent publication.

References

[1]C. J. Simmons, H. Sutter, J. H. Simmons, and D. C. Tran, "Aqueous Corrosion Studies of a Fluorozirconate Glass," *Mater. Res. Bull.*, **17**, 1203-10 (1982).

[2]J. H. Simmons, A. Barkatt, and P. B. Macedo, "Mechanisms That Control Aqueous Leaching of Nuclear Waste Glass," *Nucl. Technol.*, **56**, 265-70 (1982).

[3]D. C. Tran, C. F. Fisher, and G. H. Sigel, Jr., "Fluoride Glass Preforms Prepared by a Rotational Casting Process," *Electron. Lett.*, **18**, 657-58 (1982).

[4]R. N. Brown, B. Bendow, M. G. Drexhage, and C. T. Moynihan, "Ultraviolet Absorption Edge Studies of Fluorozirconate and Fluorohafnate Glass," *Appl. Opt.*, **21**, 361-63 (1982).

[5]M. G. Drexhage, O. H. El-Bayoumi, C. T. Moynihan, A. J. Bruce, K. H. Chung, D. L. Gavin, and T. J. Loretz, "Preparation and Properties of Heavy-Metal Fluoride Glass Containing Ytterbium or Lutetium," *J. Am. Ceram. Soc.*, **65** [10] C-168-C-171 (1982).

[6]M. Robinson, R. C. Pastor, R. R. Turk, D. P. Devor, and M. Braunstein, "Infrared-Transparent Glasses Derived from the Fluorides of Zirconium, Thorium, and Barium," *Mater. Res. Bull.*, **15**, 735-42 (1980).

M. G. Drexhage, C. T. Moynihan, B. Bendow, E. Ghoji, K. H. Chung, and M. Boulos, "Influence of Processing Conditions on IR Edge Absorption in Fluorohafnate and Fluorozirconate Glasses," *Mater. Res. Bull.*, **16**, 943-47 (1981).

Materials Characterization Center (MCC) Test Methods, PNL 3990, Pacific Northwest Lab, Richland, WA, 1981.

[9]A. Barkatt and L. Boehm, "The Corrosion Process of Fluoride Glass in Water and the Effects of Re-melting and of Glass Composition," *Mater. Lett.*, **3** (1,2) (1984).

C. T. Moynihan, private communication.

[11]C. J. Simmons, S. Azali, and J. H. Simmons, "Chemical Durability Studies of Heavy Metal Fluoride Glasses," Paper No. 47 in Proceedings, 2nd International Symposium on Halide Glasses, Troy, NY, 1983.

[12]C. J. Simmons, J. Guery, D. G. Chen, and C. Jacoboni, "Leaching Behavior of Heavy Metal Fluoride Glasses," pp. 329-34 in Proceedings of the 3rd International Symposium on Halide Glasses, Rennes, France, June 1985. Edited by J. Lucas and C. T. Moynihan. TransTech Publications, Switzerland, 1986.

[13]Lange's Handbook of Chemistry, 13th ed. Edited by John A. Dean. McGraw-Hill, New York, 1985.

[14]S. R. Loehr, A. J. Bruce, R. Mossadegh, R. H. Doremus, and C. T. Moynihan, "IR Spectroscopy Studies of Attack of Liquid Water on ZrF₄-Based Glasses," pp. 311-22 in Proceedings of the 3rd International Symposium on Halide Glasses, Rennes, France, June 1985. Edited by J. Lucas and C. T. Moynihan. TransTech Publications, Switzerland, 1986.

[15]R. H. Doremus, D. Murphy, N. P. Bansal, C. T. Moynihan, and W. A. Lanford, "Reaction of Water with Zirconium Fluoride Glasses," pp. 291-98 in Proceedings of the 3rd International Symposium on Halide Glasses, Rennes, France, June 1985. Edited by J. Lucas and C. T. Moynihan. TransTech Publications, Switzerland, 1986.

[16]M. Robinson and M. G. Drexhage, "A Phenomenological Comparison of Some Heavy Metal Fluoride Glasses in Water Environments," *Mater. Res. Bull.*, **18**, 1101-12 (1983).

[17]E. O. Ghogi, K. -H. Chung, C. T. Moynihan, and M. G. Drexhage, "Surface and Bulk -OH Infrared Absorption in ZrF₄- and HfF₄-Based Glasses," *J. Am. Ceram. Soc.*, **64**, C-51-C-53 (1981).

[18]R. H. Doremus, N. P. Bansal, and D. M. Murphy, "Kinetics of the Reaction of Fluorozirconate Glasses with Water," see *Am. Ceram. Soc. Bull.*, **64** [3] 476 (1985) (Paper No. 100-G-85).

[19]C. G. Pantano, "Surface Chemistry and Fracture of Fluoride Glasses," pp. 285-90 in Proceedings of the 3rd International Symposium on Halide Glasses, Rennes, France, June 1985. Edited by J. Lucas and C. T. Moynihan. TransTech Publications, Switzerland, 1986.

[20]C. J. Simmons and S. Azali, "Effect of Solution pH on Leaching of Fluoride Glasses"; for abstract see *Am. Ceram. Soc. Bull.*, **63** [3] 491 (1984).

[21]C. A. Houser and C. G. Pantano, "Surface Studies of Fluorozirconate Glasses," Paper No. 15 in Proceedings, 2nd International Symposium on Halide Glasses, Troy, New York, 1983.

[22]Proceedings of the Workshop on Diamond-Like Carbon Coatings. Edited by B. Bendow. BDM Corp., Albuquerque, NM, 1982.

[23]M. L. Stein, A. Green, B. Bendow, O. H. El-Bayoumi, and M. D. Drexhage, "Diamond-Like Carbon Coatings for Protection of Halide Glass Surfaces," Paper No. 48 in 2nd International Symposium on Halide Glasses, Troy, NY, 1983.

[24]L. L. Hench and D. E. Clark, "Surface Properties and Performance Prediction of Alternative Waste Forms," Annual Rept. to Nuclear Regulatory Commission on Contract No. NRC-04-78-252, 1981.

[25]A. Barkatt, J. H. Simmons, and P. B. Macedo, "Evaluation of Chemical Stability of Vitrification Media for Radioactive Waste Products," *Phys. Chem. Glasses*, **22** [4] 73-85 (1981).

Appendix D

Chemical Durability of Fluoride Glasses: II, Reaction of Barium-Thorium-Based Glasses with Water

CATHERINE J. SIMMONS

Chemical Durability of Fluoride Glasses: II, Reaction of Barium-Thorium-Based Glasses with Water

CATHERINE J. SIMMONS*

Department of Materials Science and Engineering, University of Florida, Gainesville, Florida 32611

The aqueous leaching behavior of three Ba-Th-based fluoride glasses was studied. Results of solution analysis, SEM, and IR spectroscopy are reported and compared with earlier studies on fluorozirconate-based glasses. Leaching appears to be by matrix dissolution dominated by component solubility. No hydrated leach layer was seen to form on the surface. Only a mild drift in solution pH, resulting from a limited hydrolysis of dissolved thorium fluoride, was observed. The reduced pH drift away from neutral, coupled with lower component solubilities, is credited with the 100-fold improvement in chemical durability of the Ba-Th-based fluoride glasses over the fluorozirconate-based glasses reported previously.

I. Introduction

BARIUM-thorium-based fluoride glasses in general have pushed the multiphonon absorption edge to longer IR wavelengths (near 10 μm) without a significant loss of transparency at the UV edge.[1] In addition to an improved transmission window, these glasses exhibit higher melting temperatures and, in some cases, a wider working range below the crystallization temperature and, therefore, a greater resistance to devitrification. Fabrication problems and raw material costs (due to their high rare-earth content) have decreased their popularity; however, they promise to make a major contribution to technological applications of IR-transmitting materials in the future.

A major obstacle to wide technological use of fluoride glasses has been the poor chemical durability exhibited by ZrF₄-based glasses. In this paper, we will examine the aqueous corrosion behavior of Ba-Th-based fluoride glasses and compare it to that of fluorozirconate glasses. In our previous research,[2] we have found that fluorozirconate glasses corrode in aqueous solutions primarily by component dissolution, accompanied by ion exchange and hydrolysis of solution species to drastically reduce the solution pH. This leads to increases in component solubility and, therefore, increases in dissolution rates. The results have shown that ZrF₄-based glasses have very poor chemical resistance to unbuffered deionized water, especially if the solution volume is limited or the solution is unstirred.

It was noted that, of the components which make up the ZrF₄-based glasses studied,[2,3] LaF₃ exhibits the best resistance to chemical dissolution and shows a strong tendency to concentrate on the glass surface. Since it is the solubility of the major components which controls the chemical durability of fluoride glasses, and since the Ba-Th glasses contain a much greater concentration of rare-earth and actinide components, these glasses promise to show better resistance to corrosion if the leaching mechanisms are similar.

Below, we report results of studies conducted on three Ba-Th fluoride glasses. The tests were conducted in a fashion identical with that of fluorozirconate studies previously reported.[2,3] The results show that Ba-Th glasses can further outperform ZrF₄

glasses by adding chemical durability to the list of improved characteristics.

II. Experimental Procedure

Three glass compositions, melted at two laboratories, were obtained for the chemical durability study. Table I shows the glass compositions selected, the commonly used mnemonics for them, and the sources of the glasses. These glasses were all prepared using oxide raw materials with added ammonium bifluoride.[1,4] In all cases they showed low water and low oxide content, as determined spectroscopically.

Stagnant corrosion tests were conducted at 25°C as previously described.[2,3,5] The solution volume to sample surface area was maintained at a ratio of 100:1 for all tests in order to minimize saturation effects. Solution analysis was conducted using a DC plasma spectrometer* to measure the solution cation concentrations and using a selective electrode to determine fluoride ion concentrations. All data points represent the analysis of at least two samples with error bars falling within the symbols. Normalized leach rates were calculated from Eq. (1):

$$\frac{XV}{S \cdot \Delta t \cdot wt} = \mu g \cdot cm^{-2} \cdot d^{-1} \tag{1}$$

where X is the ppm in solution, V the solution volume (mL), S the surface area (cm²), Δt the soak time (days), and wt the weight fraction of element in the original glass.

III. Results

Leach rates in solution for the three Ba-Th-based glasses are plotted as a function of time in Fig. 1. These rates are normalized by the concentration of ions in the glass (Eq. (1)) for easy comparison between different elements, as well as different compositions. Filled symbols represent actual measurements. In some cases, where the concentration of cation measured in solution was at, or slightly below, reliable detection limits, highest leach rates were calculated based on those detection limits and are represented by open symbols. As shown in Figs. 1(A), (B), and (C), in all cases there is an initial decrease in leach rate during the first 5 to 10 h, followed by a slight rise which levels off or drops again by the fifth day. Also, it is interesting to note that although the majority of the data lie within a factor of 2 or 3 of each other, there is a consistent order maintained of Zn ≳ Ba > Lu/Yb ≳ F ≫ Th. Not surprisingly, the substitution of Yb (Fig. 1(B)) for Lu (Fig. 1(A)) appears to cause little difference in the leaching behavior of the two glasses. With the addition of 9 mol% NaF several

Table I. Glass Compositions

| Mnemonic | Composition (mol%) | | | | | | Source* |
	BaF₂	ZnF₂	LuF₃	YbF₃	ThF₄	NaF	
BZLT	19	27	27		27		RADC
BZYbT	19	27		27	27		RPI
BZYbTN	10	27		27	27	9	RPI

*RADC, O. H. El-Bayoumi and M. G. Drexhage. Rome Air Development Center, Hanscom Air Force Base, MA. RPI, C. T. Moynihan, A. J. Bruce, D. Gavin, and K.-H. Chung, Rensselaer Polytechnic Institute, Troy, NY

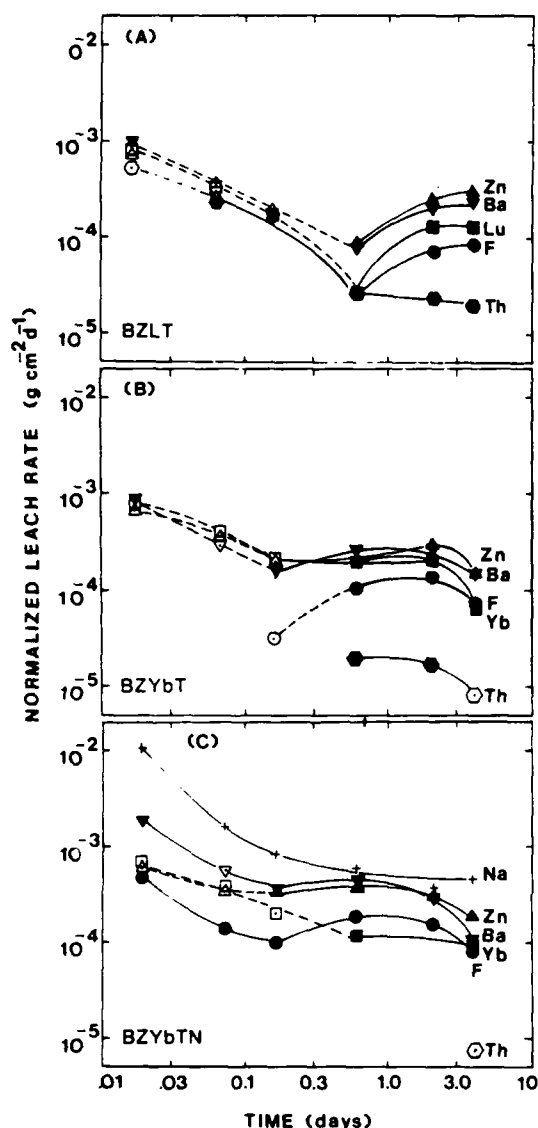**Fig. 1.** Normalized leach rate vs. time from leachate analysis for individual elements of the glasses: (A) BZLT, (B) BZYbT. (C) BZYbTN.

Fig. 2. Average leach rates for all three glasses (Th neglected).

differences occur at short times. First. Na is extracted from the glass at a rate 10 times that of the other glass components, rapidly decreasing by 25 times within the first day. This behavior is similar to that observed for silicate glasses containing Na and leads to the formation of a dealkalized surface layer. Ba appears to leach from the surface twice as fast as in the other glasses, and the fluoride concentrations in solution are measurably higher. Finally. no Th at all could be detected in any of the leaching solutions from the BZYbTN samples.

IV. Discussion

A composite curve of the average leach rates of all three glasses is shown in Fig. 2. Within a small scatter, all of the data fit comfortably on a single curve. Despite a substantial addition of NaF to the base glass, the overall leaching behaviors appear, from solution analysis. to be nearly identical. These results agree well with those previously reported[2] for the Zr-Ba-La system, where the addition of 20 mol% LiF did not substantially affect the leach rate. This tends to support the notion that alkali, added to these predominately ionic glasses, does not alter the structure as drastically as

do similar additions to covalent silicate glasses. In addition, the average leach rates of these glasses, which include a major proportion of the fluorides of Lu/Yb and Th, coincide exactly with the La rates observed for glasses in the Zr-Ba-La series.[2] This would seem to support the conclusion that individual component solubility in solution is the controlling factor and that where large quantities of low-solubility materials are included. the chemical durability may be expected to improve.

(1) pH Drift Behavior

As noted previously.[2] solution pH drift was of major concern in studying the leaching behavior of ZrF_4-based glasses. In that study the solution pH was observed to decrease to values below 4.0 within the first 12 h (Ref. 2. Fig. 4), while liquid at the glass solution interface was estimated to be at $\approx$pH 2.5. This drift was attributed primarily to hydrolysis reactions involving ZrF_4. Solutions monitored during the current study showed no such pronounced drift. Over the 5-d test period the leach solutions remained at fairly constant pH, varying less than 0.2 unit.

In order to determine the equilibrium pH value of BZYbT glass with water an excess of fine powder ($\leq$250 μm) was placed in deionized water for several days in a sealed polymethylpentene (PMP) jar.[12] After 24 h of agitation the pH was observed to have drifted from the initial value of 5 7 to 4.8. No further change in pH occurred, indicating that. when compared with data obtained for ZrF_4-based glass (pH 5.8 → 2.46),[2] the hydrolysis of leach products in solution. and/or ion exchange at the glass surface. is minimal. Further. this reaction must involve the ThF_4 solely. since none of the other constituents present undergo hydrolysis at the pH values measured.[6] Under the high dilution conditions of these stagnant leach tests. 100 mL/cm^{2} surface area, it is not expected that the solution pH measured in the bulk solution is representative of the conditions which exist at the glass/solution interface. Lack of solution agitation leads to the formation of a very thin liquid layer rapidly becoming saturated with the leach products. and more closely resembling the equilibrium conditions described above. A gradual drift toward pH 4.8 would increase the component solubilities and could help to account for the increase in leach rate observed after about 5 h (Fig. 1). Also. as dissolution occurs. surface roughness is seen to increase. providing additional surface area not included in the leach rate calculation (Eq. (1)).

(2) Surface Water Content

Infrared transmission measurements (Fig. 3), for the BZYbTN glass showed the same OH stretching (2.9 μm) and HOH bending (6.1 μm) vibrations seen in our previous studies.[3,5] with increasing absorption for longer corrosion times. Additional bands are noted at 6.55 and 7.15 μm and may be due to impurities or to the formation of oxides.[5] At present, the source of these modes has not been determined conclusively for these glasses. Spectra for the

Fig. 3. IR transmission spectra of BZ-YbTN glass before and after exposure to deionized water for 5 d.
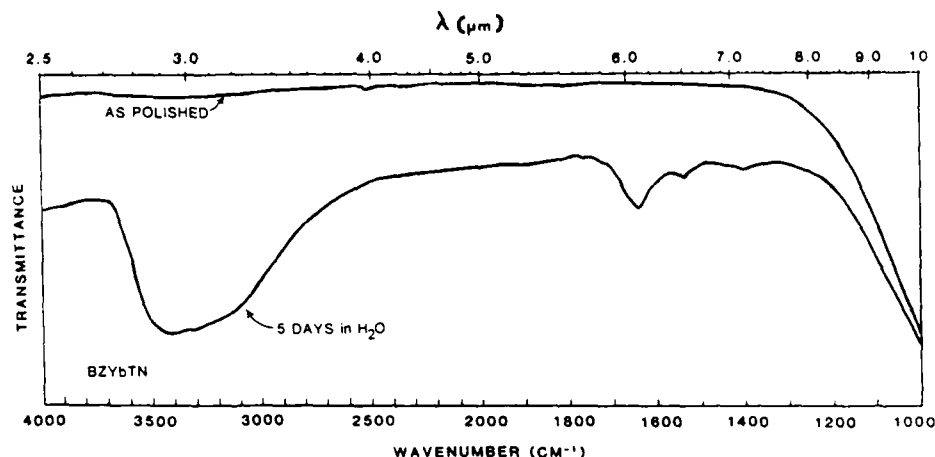
BZLT and BZYbT samples showed the same features although the intensity of the band was marginally less severe. Transmittance through the sample is decreased across the entire spectrum because of scattering from increased surface roughness. The degree of surface hydration is much less severe than that noted for fluorozirconate glasses in our earlier studies. The surfaces appeared lightly frosted and the samples were translucent, while the corroded fluorozirconate samples had a thick white surface film and were nearly opaque, both in the visible and in the IR, after the same exposure time.

As with the fluorozirconates, exposure of the Ba-Th glasses to high levels of atmospheric moisture at temperatures above the dew point produced no visible signs of surface degradation. This result

is in agreement with those reported earlier by Robinson *et al.*,[ ] who noted that no corrosion was observed up to 200°C for a variety of fluoride glasses containing ThF_4.

(3) Microscopic Appearance of Surface

Scanning electron microscope observation of these corroded samples yielded several interesting results, especially when contrasted with those obtained for the corroded fluorozirconate glasses. In our earlier study (see Ref. 2, Figs. 8 and 9) we described the formation of several layers seen on the corroded surface: (1) surface crystal deposits formed by supersaturation of a thin liquid layer immediately surrounding the sample, (2) a severely cracked, dehydrated layer of transformed material, formerly
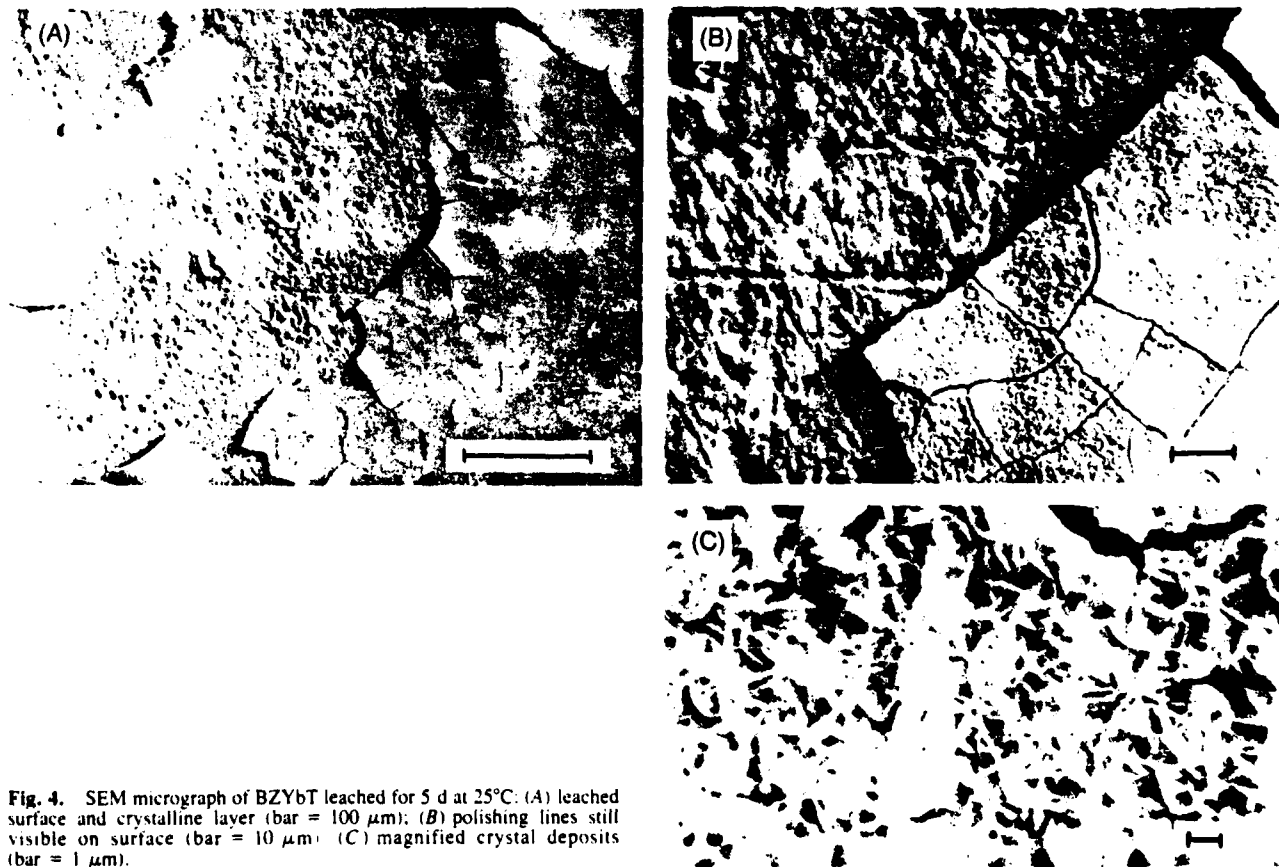
Fig. 4. SEM micrograph of BZYbT leached for 5 d at 25°C: (*A*) leached surface and crystalline layer (bar = 100 μm); (*B*) polishing lines still visible on surface (bar = 10 μm) (*C*) magnified crystal deposits (bar = 1 μm).

glass, and (3) further signs of hydration and mild corrosion extending into the bulk material. The combined thickness of (1) and (2) was estimated at approximately 20 μm + 130 μm = 150 μm for samples leached 5 d. In the current study, Figs. 4 and 5 show the surfaces of the leached BZYbT and BZYbTN samples, respectively. The surface is seen to be covered with a thin crystalline layer which is cracked (due to dehydration during vacuum drying) and peels off easily. Below this layer is the leached glass surface. Polishing lines are still clearly visible on the BZYbT sample (Figs. 4(A) and (B)), although they are considerably broader than on the freshly polished sample, and small corrosion pits, ranging in sizes up to 6-μm diameter, can be seen. For the sample BZYbTN, containing 9 mol% NaF, corrosion appears to be more

extensive (Figs. 5(A) and (B)) since the polishing lines are no longer discernible and the surface roughness is greater, with many corrosion pits $\geqq$ 10 μm in diameter. The most remarkable characteristic of these samples, when compared with the fluorozirconates, is the total absence of hydration/dehydration cracking on the glass surface. Whereas, in the previous work, severe cracking was seen to extend down into an altered leach layer $\approx$ 130 μm deep, in the samples currently under study there is no visible evidence of the penetration of water into the surface. This would seem to indicate that the water bands seen in the IR spectra for these Ba-Th samples are due entirely to water adsorbed in the crystalline layer or trapped between the layer and the glass surface. In this case, the intensity of the absorption band may simply reflect

Crystals : Th, Yb, Ba
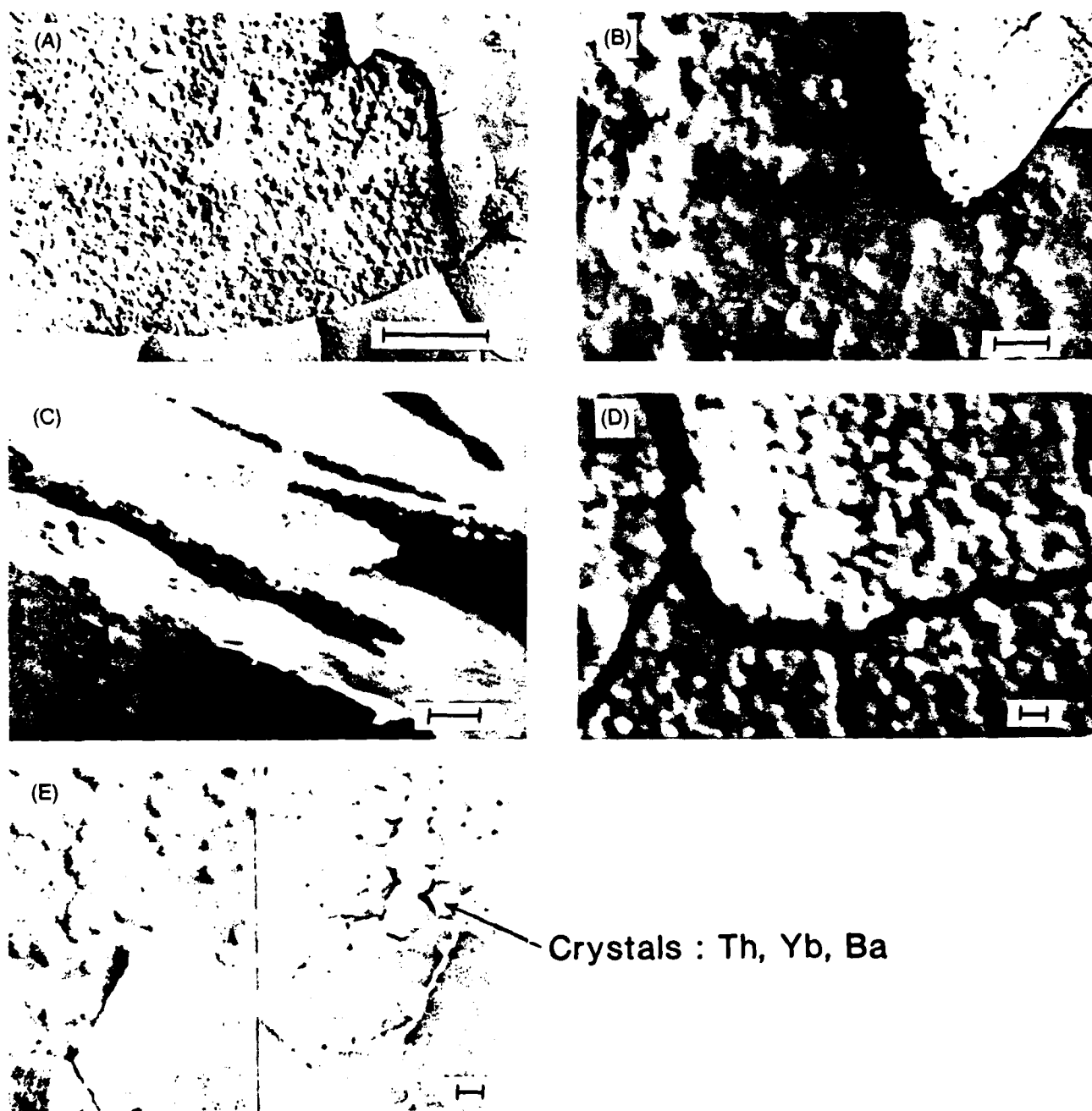
Fig. 5. SEM micrograph of BZYbTN leached for 5 d at 25°C: (A) leached surface and crystalline layer (bar = 100 μm); (B) pitted surface, no polishing lines visible (bar = 10 μm); (C) crystal layer peeling from surface (bar = 10 μm); (D) magnified crystal deposits (bar = 1 μm); (E) SEI showing topography (left) and BEI showing compositional differences (right) (bar = 10 μm). Crystal analysis by WDS.

the thickness and porosity of this crystal layer.

Differences can also be noted between the shapes of crystals which formed on the BZYbT (identical with BZLT) and those seen on the BZYbTN samples. In the first case, the crystals appear to be of a single type, formed by several vertical plates arranged in a star pattern, ≈10 to 20 μm across. In the latter sample, crystals of two distinct types can be seen on the surface: (1) Those which make up the continuous film (≈3 μm thick) are roughly spherical and ≤1 μm in diameter (Figs. 5(C) and (D)), and (2) those which adhere to the glass surface in localized areas beneath the layer (Fig. 5(E)) and appear to be similar in size and shape to the BZYbT/BZLT type. X-ray analysis of the larger crystals, using a wavelength dispersive spectrometer attached to the SEM, showed higher concentrations of Yb and Ba and a much higher Th reading than for the bulk glass. The size of the smaller crystals was insufficient for reliable analysis. However, from the results of solution analysis it can be assumed that they at least contain a high percentage of Th.

V. Conclusions

Static leach tests were performed on a series of Ba-Th-based fluoride glasses. Measurements of solution composition by plasma emission spectroscopy, of degree of hydration by IR absorption, of layer thickness and surface structure by SEM, and of crystal composition by WDS were conducted to determine the mechanisms involved in the aqueous corrosion of this family of glasses. Although the process appears to involve most of the same mechanisms observed for the fluorozirconates, it would also appear to be somewhat less complex.

Initially, component solubility is the rate-controlling mechanism. This leads to selective leaching of some of the glass components (i.e., ZnF_2, BaF_2, and especially NaF). As the matrix dissolves, a crystal layer deposits on the glass surface. This layer formation complicates the dissolution process.

The mechanism by which the crystal layer forms can be deduced from a combination of leachate analysis, IR spectral data, and SEM observations. Shortly after the sample is immersed in the deionized water and begins to dissolve, a very thin stagnant boundary layer is established at the glass/solution interface. This layer quickly becomes saturated with respect to the less-soluble species, whereupon crystals begin to precipitate on the glass surface. Increased surface roughness augments the stagnation of the liquid boundary layer and dissolution/precipitation reactions continue until the entire surface is covered with a crystalline layer. The evidence for the existence of a liquid boundary layer is clear since, if the solution immediately surrounding the sample were not at saturation with respect to the crystals, they would simply dissolve into the unsaturated liquid or would not form in the first place. This conclusion was also noted for ZrF_4-based glasses and is more fully described in Ref. 2. Necessarily, there must exist a gradient in pH matching the gradient in dissolved ion concentration, from the bulk solution at 5.7 to the glass/solution interface at ≈4.8 (saturation equilibrium). This lower pH near the glass surface, resulting from hydrolysis and/or ion exchange of dissolved ThF_4, enhances the solubilities of all of the components. However, the dissolution will be hampered somewhat by the presence of high concentrations of F in the solution, and will be strongly influenced by the kinetics of crystallization of the less-soluble species as well as the rate of diffusion of dissolved species away from the surface through the highly concentrated solution permeating the porous crystalline layer.

The mechanisms governing dissolution of Ba-Th-based fluoride glasses can be summarized as follows:

(1) Corrosion occurs primarily through matrix dissolution of glass components as fluorides.

(2) Apparent selective leaching of some fluorides (ZnF_2, BaF_2) reflects the higher solubility of these materials in solution.

(3) NaF is selectively extracted from the surface, as evidenced by the initially high leach rate followed by a particularly steep drop over the first 24 h; this decrease being the result of dealkalization of the glass surface.
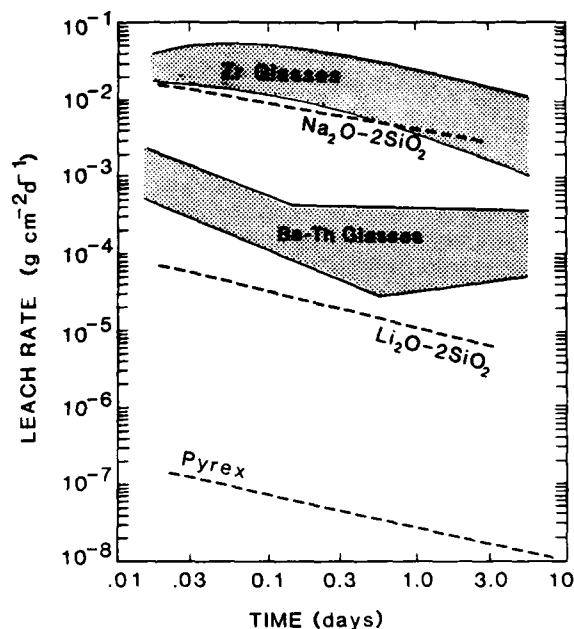
Fig. 6. Comparison of leach rates of Ba-Th-based fluoride glasses with those measured for the Zr-based fluoride glasses.[2] Durable (Pyrex)[9] and nondurable[8] silicates included for reference.

(4) Thorium fluoride is only slightly soluble in water at neutral pH. For this reason, the cation concentration of Th was seldom above the detection limit in the test solutions. Small amounts of dissolved $ThF_5^{(4-x)}$ quickly precipitate as Th_xF_y or $Th_xF_x(OH)_{4y-x}$, alone or in combination with BaF_2 and/or YbF_3 to form a layer of crystals on the surface.

(5) The comparatively small drop in the pH of saturated solutions results from hydrolysis of dissolved $ThF_5^{(4-x)}$, i.e.

$$ThF_4(s) + H_2O \rightarrow ThF_5^-(aq) + F^-(aq) + H_2O$$
$$\rightarrow ThF_3OH(s) + HF(aq) \quad (2)$$
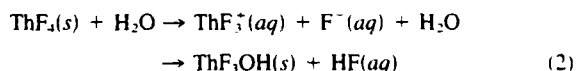
(6) Under stagnant conditions a stationary liquid boundary layer develops at the glass/solution interface. As this layer approaches saturation, there is a drift in pH toward 4.8 increasing solubility limits and, therefore, the leach rate. Concurrently, as the [F] in solution increases, this enhanced dissolution is inhibited.

(7) Crystals form on the glass surface by precipitation from the saturated liquid layer immediately surrounding the sample. As the crystals spread to form a thin blanket covering the glass surface, water is trapped within and beneath this layer. This helps to maintain saturation conditions at the glass surface while acting as an ineffective diffusion barrier to reduce the leach rate. It also creates an environment leading to a steady-state dissolution/precipitation process for the less-soluble components, while the more-soluble components will continue to diffuse through the very porous crystalline layer.

Table II summarizes the differences noted in the leaching behavior of the ZBL series[2] and the Ba-Th series presented here.

In contrast to the severely cracked hydrated layer seen to form

Table II.   Summary of Observations

Type	Leach rate (g/(cm²·d))	Surface appearance	Crystal layer thickness (μm)	Leach layer thickness (μm)	Crystal components
ZBL	10^{-2}	Opaque	20	130	Zr, Ba, La
Ba-Th	10^{-4}	Frosted	3	0	Th, Ba, Yb

below the crystals on ZBL-type glasses, there was no sign of surface hydration or of water having penetrated into the glass in any of the Ba-Th glasses. The surface was roughened and pitted, but with a total absence of surface cracks. This was the most surprising difference observed in leaching behavior between these two fluoride families. The most technologically significant difference between these two groups of glasses is the 100-fold improvement in chemical durability exhibited by the Ba-Th-based fluorides (Fig. 6), although they are still 1000 times less resistant to attack than durable silicates (i.e., Pyrex[*]).

This improvement is attributed to lower component solubility and to the much less severe drift in solution pH observed for these samples. It will be shown in a subsequent publication that large increases in leach rate do occur in acidic and basic environments.

---

[*]Corning Glass Works, Corning, NY.

References

[1]M. G. Drexhage, B. Bendow, R. N. Brown, P. K. Banerjee, H. G. Lipson, G. Fonteneau, J. Lucas, and C. T. Moynihan, "Extended IR Absorption of Multi-component Glasses Based on the Fluorides of Thorium, Barium and Other Metals," *Appl. Opt.*, **21** [6] 971–72 (1982).

[2]C. J. Simmons and J. H. Simmons, "Chemical Durability of Fluoride Glasses: I. Reaction of Fluorozirconate Glasses with Water," *J. Am. Ceram. Soc.*, **69** [9] 661–69 (1986).

[3]C. J. Simmons, H. Sutter, J. H. Simmons, and D. C. Tran, "Aqueous Corrosion Studies of a Fluorozirconate Glass," *Mater. Res. Bull.*, **17**, 1203–10 (1982).

[4]G. Fontaneau, F. Lahaie, and J. Lucas, "A New Family of Infrared Transmitting Fluoride Glasses: Vitreous Fluorides in the System ThF_4-BaF_2-MF_2 (M = Mn, Zn)" (in Fr.), *Mater. Res. Bull.*, **15**, 1143–47 (1980).

[5]Materials Characterization Center (MCC) Test Methods PNL 3990. Pacific Northwest Laboratory, Richland, WA, 1981.

[6]Charles F. Baes, Jr., and Robert E. Mesmer, *The Hydrolysis of Cations*. Krieger, Malabar, FL, 1986.

[7]M. Robinson and M. G. Drexhage, "A Phenomenological Comparison of Some Heavy Metal Fluoride Glasses in Water Environments," *Mater. Res. Bull.*, **18**, 1101–12 (1983).

[8]L. L. Hench and D. E. Clark, "Surface Properties and Performance Prediction of Alternate Waste Forms," Annual Report to Nuclear Regulatory Commission, Contract No. NRC-04-78-252, 1981.

[9]A. Barkatt, J. H. Simmons, and P. B. Macedo, "Evaluation of Chemical Stability of Vitrification Media for Radioactive Waste Products," *Phys. Chem. Glasses*, **22** [4] 73–85 (1981).

Appendix E

MOLECULAR DYNAMICS SIMULATIONS OF FLUORIDE GLASS STRUCTURES

J.H. Simmons, R. Faith and G. O'Rear
Department of Materials Science and Engineering
University of Florida
Gainesville, FL 32611 (USA)

INTRODUCTION

Fluoride glasses are of great interest for molecular dynamics (MD) simulations because of the high ionicity of the bonding of these materials.[1] This allows modeling the interatomic forces with a spherically symmetric expression. The function most widely used in modeling inorganic glasses has been the Born-Mayer Pair Potential:[2]

$$V_{ij}(r) = A_{ij} \exp{-(\sigma_{ij}r)} + q_i q_j/r$$

All simulations conducted to date on silicate and fluoride glasses have used either this function or a variety of minor modifications which include a truncation term.[3] While this function has appeared to yield a good simulation of many static and most dynamic properties of silicate glasses, the lack of angular-dependent terms has posed an uncertainty about the relevance of structural models of silicates. Recent studies conducted by A. Wright and one of these authors have shown that the lack of angular-dependent forces indeed causes deviations between the radial distribution function modeled for silica glass and the results of neutron diffraction measurements.[4]

In principle, fluorides with their highly ionic F$^-$ ion do not seem to be subject to angular dependent forces. Consequently, the radius ratio concept of crystal chemistry gives a very accurate guide to the crystal structures of simple fluoride compounds.[5] Their highly ionic interatomic force should therefore be adequately well modeled with the spherically symmetric Born-Mayer function.

Several investigators have studied the structure of fluoride glasses, and, in particular, heavy-metal fluorides, using molecular dynamics modeling.[6-11] Glasses in the family ZrF_4-BaF_2 have received the most attention. In this paper, we report the results of yet another MD study of the structure of ZrF_4-BaF_2 glasses. However, we show that despite central forces and the strong radius-ratio induced geometrical character of fluoride structures, the glass phase has not yet been adequately modeled.

SUMMARY OF PREVIOUS WORK

The pioneer work in this area was conducted in Angell's group, in collaboration with Lucas.[6] In their paper, MD studies were reported on a $Zr_7Ba_4F_{36}$ glass which was formed by randomizing the liquid at 1500K and quenching it to 300K. The Zr-Zr radial distribution function yielded 2 distinct peaks at 3.85 and 4.3A. The short distance peak was attributed to edge-sharing polyhedra in relatively good agreement with the structure of crystals of comparable compositions. The fluorine coordination of Zr was found to be 7.5. Subsequent studies [7] conducted at the same laboratory on Zr_2BaF_{10} glass, randomized at 3000K, then quenched in 2 steps to 2000K and 300K followed the behavior of this edge-sharing peak as a function of density, Ba ionic size and Ba ion content. The results show that the edge-sharing peak is reduced by decreasing density, increasing Ba concentration and decreasing Ba ion size.

Subsequent publications by other groups supported these results. Kawamoto et. al.[8] studied $BaZrF_6$ with 108 particles by forming a random structure at 1673K, then quenching to 300K and to 133K. The Zr-Zr pair correlation function exhibited similar features to Angell's work with a broad peak at 300K which breaks up into a distinct double peak at 133K. Hamill and Parker [9] modeling 200 atoms at 6000K and 300K looked at a number of fluoride compositions, including ZrF_4, $30\%BaF_2-70\%ZrF_4$ and $40\%BaF_2-60\%ZrF_4$. Their ZrF_4 model shows a distribution of fluorine ions into 1% non-bridging, 90% corner-sharing and 9% edge sharing. The Zr coordination by fluorine is 8. Yasui and Inoue [10] added to this by observing edge-sharing connections usually surrounded by Ba ions, as had been previously postulated by Angell.[7]

RESULTS OF PRESENT WORK

In reviewing the past work, one generally finds that the distribution of fluorine ions between non-bridging, corner-sharing and edge-sharing in the glass is reasonable, since these reflect structures also found in the crystals. The difference in coordination numbers is puzzling and the split in the Zr-Zr pair correlation function is very surprising. The molecular dynamics glasses are purely ionic, due to the exclusive use of the Born-Mayer potential. Under this condition, the radius-ratio concept models very well the crystal structures found in nature. There is no reason to believe that this concept should fail in the glass structure. The radius-ratio concept results from the well-known tendency of Coulomb forces to maximize coordination of the heavily-charged cations (Zr^{+4} in this case). The size parameters used for the Zr^{+4} and F^- ions were selected to yield the proper Zr-F and Zr-Zr distances. They do so admirably, as found when comparing EXAFS and X-RAY data to MD calculations. In fact, all investigators use about the same size for Zr, F and Ba using Angell's calculations [6] and those of Tosi and Fumi.[12] The large sizes chosen for Zr^{+4} compared to F^-, however favor Zr coordination numbers greater than 8.

The second puzzle is presented by the split in the peak of the Zr-Zr pair correlation function. The minimum observed in the split of the peak indicates a very low probability of finding Zr atoms separated by the corresponding distance (about 4A). This result is difficult to understand since purely ionic forces cannot exclude Zr ions, from any space outside the first coordination shell. Only the translational invariance of crystal structures can lead to such

an exclusion. The ionic amorphous structures are solely determined by charge balance and the geometrical accomodation of each Zr ion with its first coordination shell. Therefore, while the reported minimum is expected in crystalline structures, it should be very unlikely in amorphous structures, particularly those made by MD techniques modeling pure ionic forces in a solid rapidly quenched from some equilibrium liquid structure where randomization dominates.

We conducted MD studies of ZrF_4, $Zr_{3.25}BaF_{15}$ and Zr_2BaF_{10} glasses to investigate these puzzles. Calculations were conducted with 600 F^- ions, and the appropriate number of Zr^{+4} and Ba^{+2} ions (150, 130/40 and 120/60). Our samples were equilibrated at 5000K for 4000 time steps, then quenched to 1500K for another 4000 time steps. The glasses were made by further quenching these samples to 300K and 133K. Analyses were conducted after 1000; 2000, 3000 and 4000 time steps. The interatomic pair force used was a screened Born-Mayer function:[3,13]

$$F_{ij}(r) = [B_{ij} \exp(\sigma_i + \sigma_j - r)/\rho + Z_i Z_j e^2/r^2] [1 - (r/R_{max})^6]$$

The size parameters used were those of Ref. 6 [$\sigma_i(Zr) = 1.35A$, $\sigma_i(Ba) = 1.65A$ and $\sigma_i(F) = 1.237A$].

The first problem encountered was in the selection of the screening distance, R_{max}. Prior studies by numerous investigators had shown that, for silicate glasses, an R_{max} value of 5.6A was sufficient to yield an accurate set of pair correlation functions. This was found not to be the case here. Figure 1 shows, in ZrF_4 glass, a comparison of the Zr-Zr pair correlation function obtained from calculations with R_{max} = 5.6A (Fig 1(a)) and that obtained with R_{max} = 9A (Fig 2(a)). The latter was the minimum size beyond which no further change was observed. The fluorine coordination number around Zr was also affected, varying from between 7 and 8 for the short R_{max} to between 8 and 9 for the long R_{max}. All subsequent calculations were conducted with R_{max} = 9A.

The Zr-Zr pair correlation function of Fig. 1(b) shows no split peak. However, it is broad enough to include both the edge-sharing and the corner-sharing distances. No split peaks were observed in the other glasses containing BaF_2. An examination of the glass structure revealed the existence of numerous edge-sharing structures. In fact, a few face-sharing structures were observed in the ZrF_4 glass, where 3 fluorines were bonded to the same 2 Zr ions. The distributions of edge-sharing, corner-sharing and face-sharing structures were calculated and will be reported. The coordination of fluorine ions shows that there are 3 Zr-coordinated fluorine ions as well. The fluorine coordination about Zr has a very broad peak as should be expected for amorphous structures.

We found little difference between the 300K and the 133K data, as expected, since mass transport and defect motion are not possible at these temperatures in the experimental times. The reduction in the span of thermal vibrations has a slight effect of sharpening some of the features, but the major characteristics of the structure are present at both temperatures. As will be seen by photographs of the structure, the presence of different fluorine and zirconium environments was best investigated through a visual analysis of the structure. The pair correlation functions did not show distinct features corresponding to particular structural arrangements. This, we feel, is more consistent with the characteristics of amorphous structures.

An examination of the Zr-Zr and Zr-F correlation functions revealed that both the Zr-F and the Zr-Zr distances are smaller in the Ba-free glass indicating a possibly tighter structure. For example, the Zr-F nearest neighbor peak was narrower and shifted to shorter distances in the ZrF_4 glass. Also, the distribution of coordination numbers of F about Zr is noticeably narrower in the ZrF_4 glass. Both these results lead to the expected conclusion that the addition of Ba loosens the Zr coordination sphere, adds more F^- ions to it and generally increases disorder in the structure. Further studies of the specific effect of Ba on the glass structure and the glass formation tendency in this system are on-going.

CONCLUSIONS

Unlike real experimental studies, MD calculations should generally not vary between investigators if the calculation methods are sufficiently alike. The differences reported therefore should result from differences in the calculation algorithms.

We immediately see 3 possible sources of differences, although more may arise from discussions between the authors, which this paper hopes to encourage. These are: (1) the number of particles used, (2) the force algorithm and (3) the fictive temperature of the glasses modeled. Our studies, reported here, have used between 750 and 780 particles. Calculations with up to 2000 particles showed the same reults. However, most investigators have used a dangerously small number of particles (particularly in view of the presence of 3 kinds of ions) with fewer than 200 particles, and some as low as 108.[8] When the number of particles is low, one must be concerned with conducting calculations at constant volume, instead of constant pressure, [14] and in boxes with fixed flat sides instead of allowing the structures to determine the shape of the periodic boundaries.[15] Under the condition of a small number of particles, crystallization or the formation of a more ordered state are more likely and could explain the splitting. This and the thermal history of the sample could also affect the fictive temperature and thus lead to different structures. Finally, as we have shown, the force calculation algorithm can have a strong effect on the structure developed. How is the force truncated? How are the Ewald sums conducted?

REFERENCES

1. L. Pauling, The Nature of the Chemical Bond, Cornell Univ. Press, Ithica, NY (1960).
2. F. G. Fumi and M. P. Tosi, J. Chem. Sol. 25, 31 (1964).
3. T. F. Soules, J. Non-Crystalline Solids 49, 29 (1982).
4. A. Wright, private discussion.
5. R. C. Evans, Introduction to Structural Inorganic Chemistry, 2nd Ed. Cambridge Univ. Press, London, UK (1966).
6. J. Lucas, C. A. Angell and S. Tamaddon, Mat. Res. Bull. 19, 945 (1984).
7. C. C. Phifert and C. A. Angell, Bull. Amer. Ceram. Soc. 65, 533 (1986).
8. Y. Kawamoto, T. Horisaka, K. Hirao and N. Soga, J. Chem. Phys. 83, 2398 (1985).
9. L. T. Hamill and J. M. Parker, Mat. Science Forum 6, 437 (1985).

10. I. Yasui and H. Inoue, J. Non-Crystalline Solids 71, 39 (1985).
11. S. A. Brawer and M. J. Weber, J.Chem. Phys. 75, 3522 (1981).
12. M. P. Tosi and F. G. Fumi, J. Phys. Chem. Solids 25, 45 (1964).
13. R. Ochoa and J. H. Simmons, J. Non-Crystalline Solids 75, 413 (1985).
14. H. C. Andersen, J. Chem. Phys. 72, 2384 (1980).
15. M. Parrinello and A. Rahman, Phys. Rev. Letters 45, 1196 (1980).

FIGURE 1 - Zr-Zr Radial Distribution Function

Fig. 1(a) R_{max}=5.6A

Fig. 1(b) R_{max}=9A
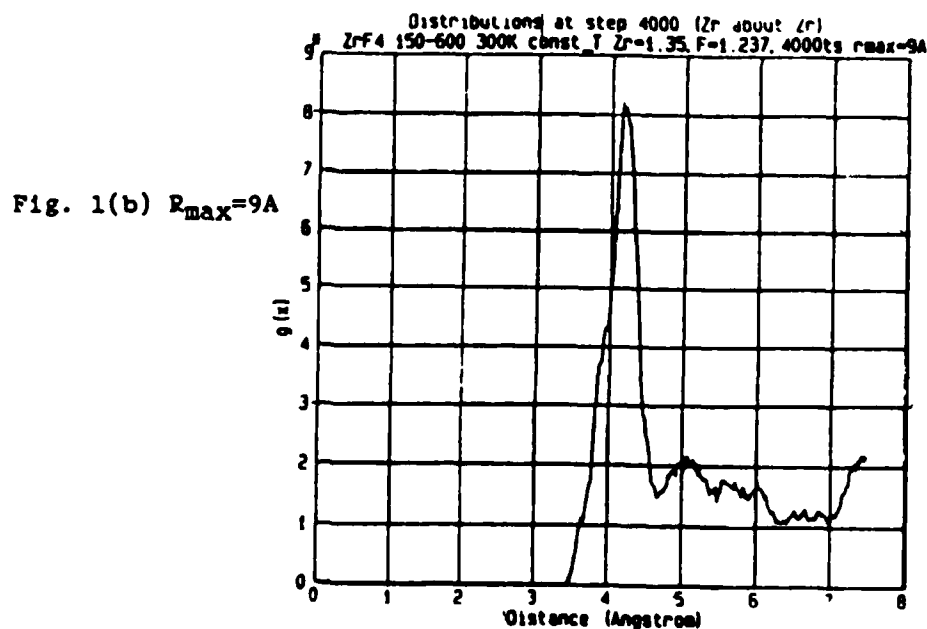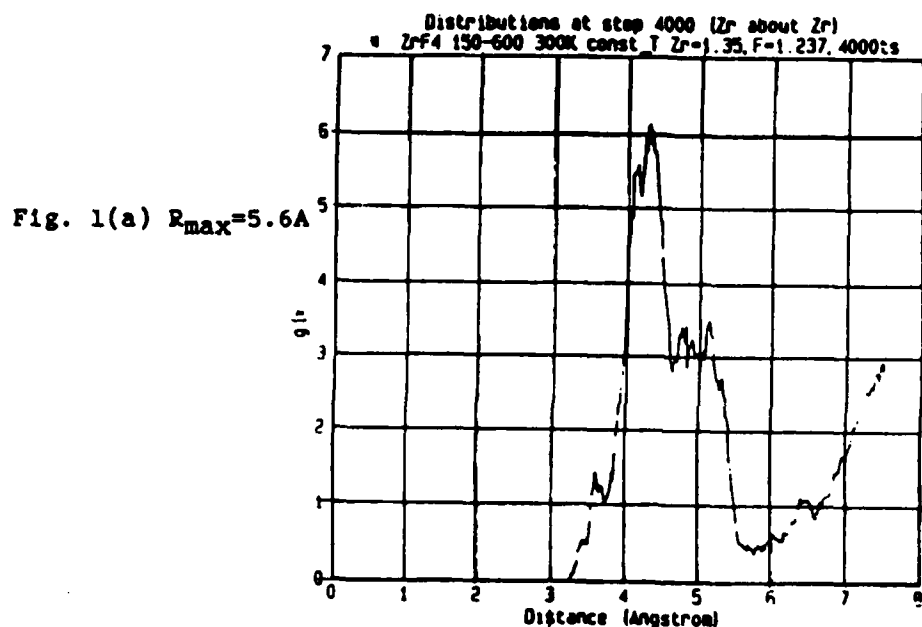
Appendix F

CORROSION LAYER FORMATION OF ZrF$_4$ - BASED FLUORIDE GLASSES

D.G. Chen, C.J. Simmons and J.H. Simmons
Department of Materials Science & Engineering
University of Florida
Gainesville, FL 32611 (USA)

INTRODUCTION

Fluoride glasses offer excellent transmission characteristics at visible and infrared wavelengths. Therefore they have great promise for applications as optical components and fibers. However, their poor chemical durability appears to be a crucial limiting factor for their practical applications. ZrF$_4$-based heavy metal fluoride glasses appear relatively stable in the presence of water vapor [1] but degrade rapidly when contacted by either condensed or liquid water [2]. Early studies of aqueous corrosion of these materials done by Simmons, et al [2] found a) dissolution of the glass into the aqueous phase, b) development of a hydrated surface layer manifested by the appearance of a 3440 cm^{-1} (2.9 μm) - OH stretching band and a 1630 cm^{-1} (6.1 μm) H$_2$O bending band in the IR spectra and c) precipitation of crystal-line dissolution products on the surface. This work also suggested that the hydrated surface layer was not protective. Subsequent studies of the hydrated surface layer via IR spectroscopy [3] and SIMS [4] showed that its thickness increased with increasing time and temperature of exposure to liquid water. A number of other studies have been conducted on the aqueous corrosion of ZrF$_4$ glasses. [5-11] These show that fluorozirconates leach rapidly with crystal precipitates appearing on a highly damaged surface. Recent work by Simmons and Simmons [6] has developed a corrosion model for the attack of fluoro-zirconates by water. This work suggests that these glasses corrode primarily by the dissolution of ZrF$_4$ and other fluoride components. The hydrolysis of the dissolved fluorides (mainly ZrF$_4$) leads to a rapid drop in solution pH to very acidic values and to a dramatic increase in leach rates due to an increase in the solubility of the glass components [11].

The objective of the present study was to examine the corrosion behavior of ZrF$_4$-based glasses under different corrosion conditions i.e., temperature, time, surface area to solution volume ratio (s/v) stagnant versus stirred and solution pH value. The mechanism of dissolution and surface layer formation is discussed.

RESULTS

ZrF$_4$-based glass samples were corroded under different corrosion conditions including very low dilution static tests (s/v = 40), intermediate dilution static tests (s/v = 1), and very high dilution dynamic tests (s/v∗Time = 10^{-5}/cm∗hr). The corroded samples were removed from the solution, rinsed in methanol and then in toluene to remove adhering liquid. The layer formation was observed by scanning electron microscopy on both the surface and the fractured cross-section of each sample.

The micrographs in Fig. 1 show the formation of corrosion layers on ZBLA glass during static tests in DI water for different times. We can see clearly the formation of a transform layer due to the reaction between glass and water as water penetrates into the glass starting from the original glass-water interface. Above this layer, a crystalline layer can form containing several different crystal types owing to the supersaturation of the water film adjacent to the glass surface. Under this corrosion condition, at the beginning, as shown in the 0.5 day picture, the main crystal precipitates are blade-shape ZrF$_4$ crystals [6]. Another hemispherical crystal usually forms afterward and covers the ZrF$_4$ crystals. Additional types of crystals can precipitate out when the concentration of corrosion species reaches the corresponding solubility limit. The depth of water penetration, plotted as the thickness of the transform layer, varies with the length of exposure as shown in Fig. 2. The measured thickness of the transform layer varies spatially over the sample as indicated by the error bars in Fig. 2. Within the experimental time no steady state was reached. The thickness of the transform layer increases rapidly at first and much more slowly at longer times.

The TGA weight loss measurement of the corrosion layer containing both the precipitation and transform layers of a seven day static test sample, shown in Fig. 3, shows an 18% weight loss due to water and suggests that these layers are very porous.

Flow tests were conducted in order to maintain a stable solution pH value and prevent corrosion species build-up in the near glass surface water film. ZBLA was corroded under stirred flow conditions, where approximately 7.5 liter/hr of DI water flowed through the corrosion vessel, the solution was stirred and the solution pH remained above 5.2. In this case, no local super-saturation near the glass-water interface could develop.

A transform layer enriched with water formed on the flow samples. Its appearance is different from that of the stagnant test samples. The layer thickness increases with time almost linearly as shown in Fig. 4 and no steady state was reached. Corrosion in flow tests is less severe than that in stagnant tests, (compare Fig. 4 with Fig. 3), because at this solution pH value the rate of aqueous attack is much slower than that seen for more acidic environments [11].

Crystals were observed to precipitate from solution onto the glass surface even in very high dilution conditions due to local supersaturation of the near glass surface water film when the solution was not agitated enough to carry away the corrosion species.

For samples corroded at different temperatures in stirred flow tests a surprising result was found, as indicated in Fig. 5. The transform layer thickness increases much more rapidly at higher temperatures, i.e. above 45C, when compared with the samples corroded at temperatures below 45C. This abrupt change in slope suggests two different corrosion mechanisms, each one being dominant over a different temperature range.

REFERENCES

1. E. O. Gbogi, K. H. Chung, C. T. Moynihan and M. G. Drexhage, "Surface and Bulk OH Infrared Absorption in ZrF_4- and H_fF_4-Based Glasses," J. Amer. Ceram. Soc. 64, C-51 (1981).

2. C. J. Simmons, H. Sutter, J. H. Simmons and D. C. Tran, "Aqueous Corrosion Studies of a Fluorozirconate Glass," Mat. Res. Bull. 17, 1203 (1982).

3. A. J. Bruce, S. R. Loehr, N. P. Bansel, D. M. Murphy, C. T. Moynihan and R. H. Doremus, "I.R. Measurement of the Rate of Surface Layer Development on ZrF_4-BaF_2-LaF_3 Glass in Aqueous Solution," Paper No. P5, Extended Abstracts, 2nd Int. Sym. on Halide Glasses, Troy, New York (1983).

4. C. A. Houser and C. G. Pantano, "Surface Studies of Fluorozirconate Glasses," Paper No. 15, Extended Abstracts, 2nd Int. Sym. on Halide Glasses, Troy, New York (1983).

5. G. H. Frischat and I. Overbeck, "Chemical Durability of Fluorozirconate Glasses," J. Amer. Ceram. Soc. 67 [11], C-238 (1984).

6. C. J. Simmons and J. H. Simmons, "Chemical Durability of Fluoride Glasses - I Reaction of Fluorozirconate Glasses with Water," J. Amer. Ceram. Soc. 69 [9], 661 (1986).

7. T. A. McCarthy and C. G. Pantano, "Dissolution of Fluorozirconate Glasses," Extended Abstract No. 30, 2nd Int. Sym. on Halide Glasses, Troy, New York (1983).

8. C. J. Simmons, J. Guery, D. G. Chen and C. Jacoboni, "Leaching Behavior of Heavy Metal Fluoride Glasses," Mater. Sci. Forum, 5, 329 (1985).

9. C. J. Simmons and S. Azali, "Effect of Solution pH on Leaching of Fluoride Glass," Paper (8-G-84) 86th Annual Meeting of the Amer. Ceram. Soc., Pittsburgh, PA, April 10, 1984; Bull. Amer. Ceram. Soc. 63, 491 (1984).

10. R. H. Doremus, N. P. Bansal, T. Bradner and D. Murphy, "Zirconium Fluoride Glass Surface Crystals Formed by Reaction with Water," J. Mat. Sci.Lett. 3, 484-488 (1984).

11. C. J. Simmons, "Chemical Durability of Fluoride Glasses - III, The Effect of Solution pH," J. Amer. Ceram. Soc., submitted.

ZBLA GLASS–STAGNANT TEST, S/V:1
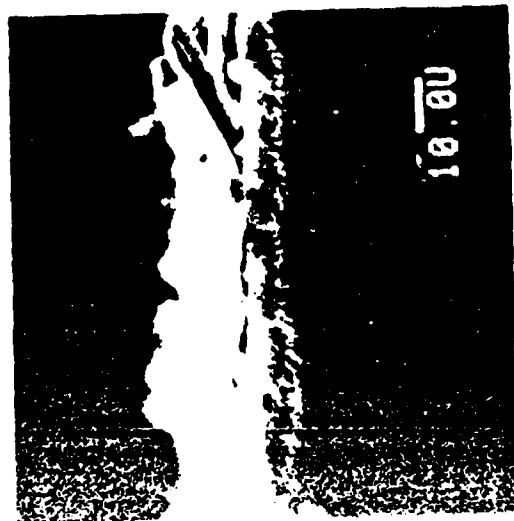
0.5 Day

2 Days
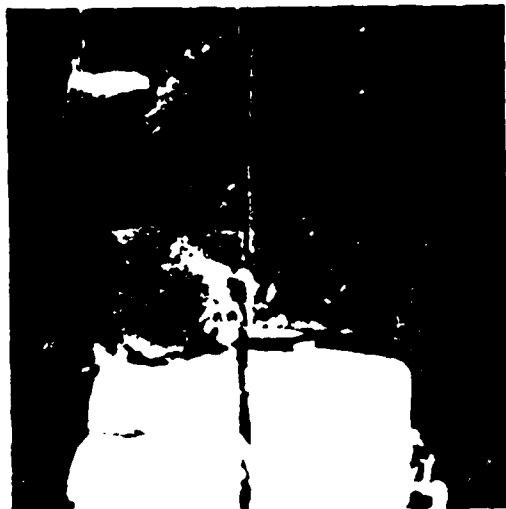
8 Days

Fig.1 Corrosion layer formation of ZBLA glass in stagnant test, in D.l. water, S/V:1, for different times.
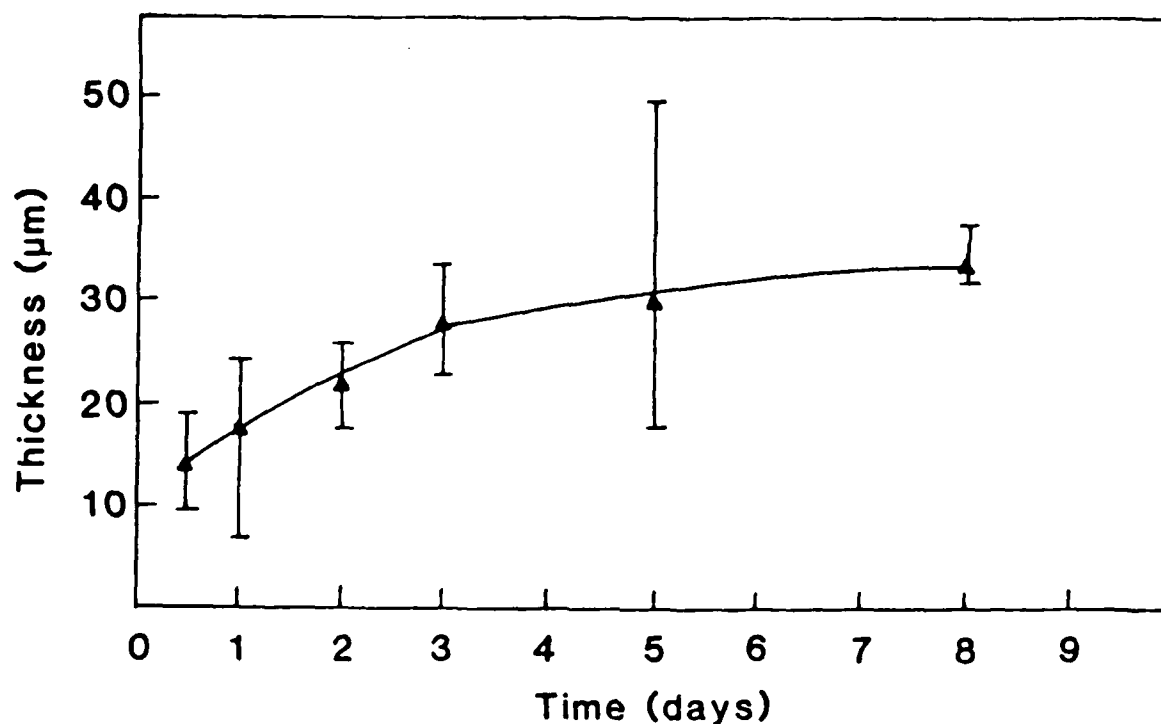
Fig.2   Thickness of the transform layer of stagnant
        samples versus corrosion time. ZBLA glass
        corroded in D.I. water, S/V:1.
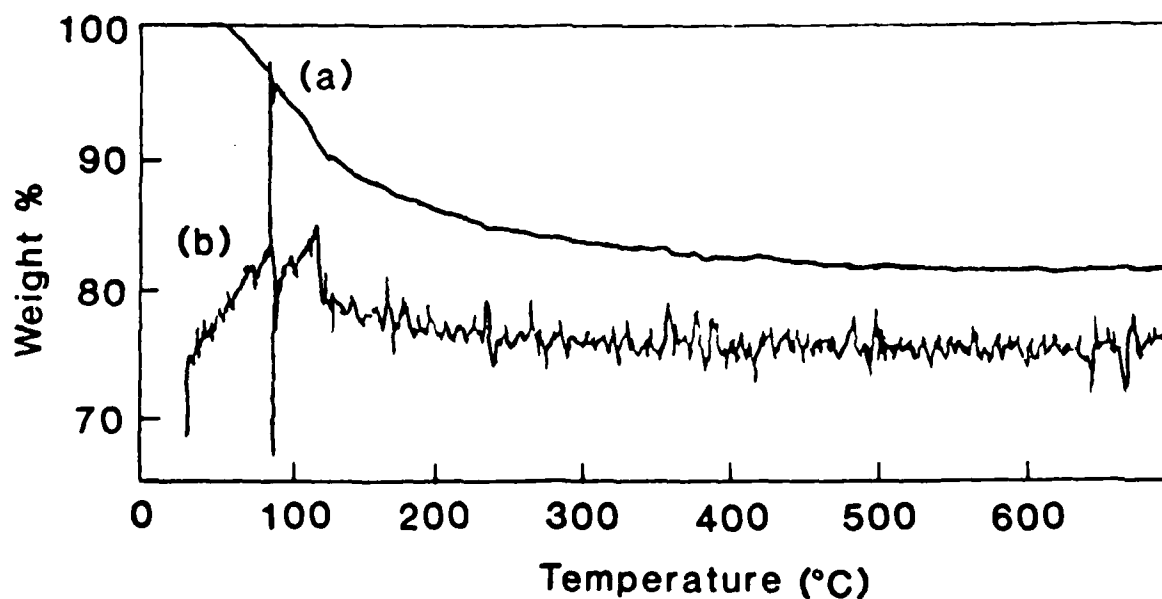
Fig.3   (a) TGA weight loss measurement of corrosion
        layers of the 7 days ZBLA stagnant test sample,
        corroded in D.I. water, S/V:1.
        (b) Differential curve of (a).
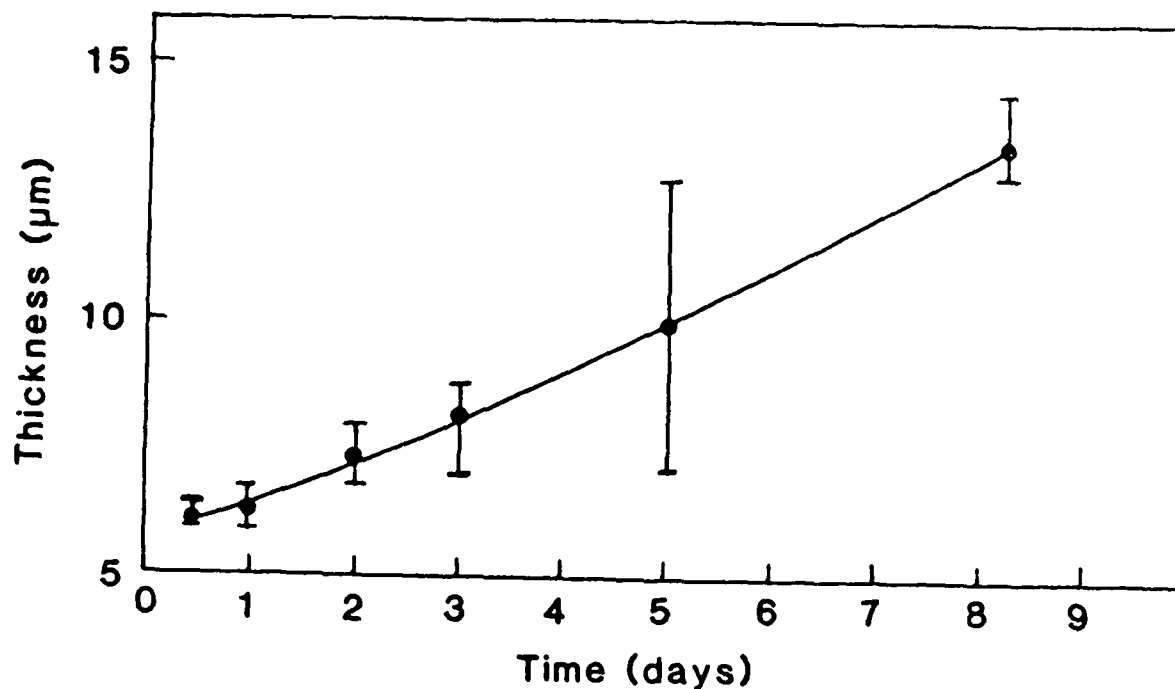
Fig.4   Transform layer thickness versus corrosion time.
ZBLA glass corroded in stirred flow condition.
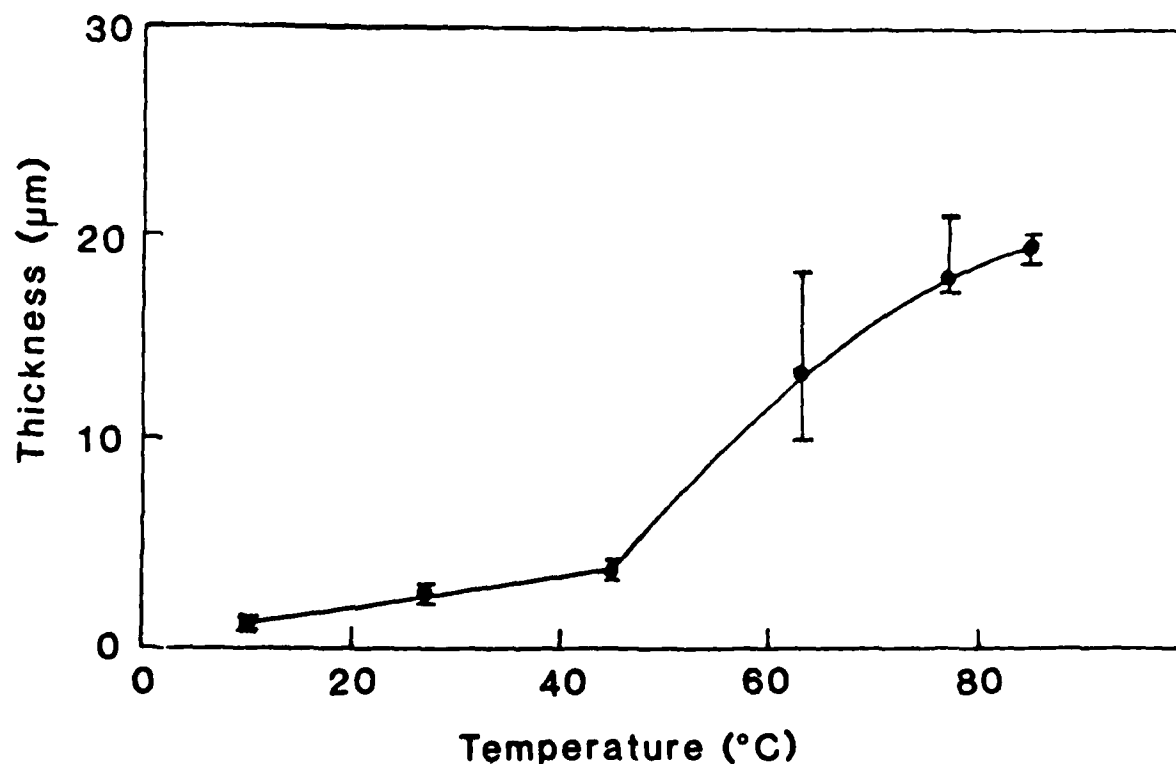
Fig.5   Transform layer thickness versus temperature.
ZBLA glass corroded in stirred flow condition for
6 hours at different temperatures.

Appendix G

Chemical Durability of Fluoride Glasses: III, The Effect of Solution pH

Catherine J. Simmons[*]

J. Am. Ceram. Soc., 70 [9] 654-61 (1987)

Chemical Durability of Fluoride Glasses: III, The Effect of Solution pH

CATHERINE J. SIMMONS*

Department of Materials Science and Engineering. University of Florida. Gainesville. Florida   32611

The aqueous corrosion behavior of glasses from two heavy-metal fluoride families (ZrF_4-based and BaF_2-ThF_4-based) was studied as a function of controlled solution pH and of glass composition. Leach test results demonstrate a profound pH dependence of corrosion over the range pH 2 to 13. Whereas the glasses readily undergo congruent matrix dissolution in acidic media, they exhibit a marked increase in chemical durability in neutral and basic solutions, with the optimum aqueous environment occurring near pH 7. Results of this study are discussed and compared with results reported earlier for leach tests of these two compositional families in unbuffered deionized water. In addition, several testing methods, both static and dynamic, are described and point to the importance of appropriate test selection in predicting the corrosion resistance of these glasses over prolonged periods.

I. Introduction

SINCE the discovery of the first infrared-transparent heavy-metal fluoride (HMF) glasses more than a decade ago,[1] the physical and optical properties of a vast array of stable compositions have been studied. One property which is particularly important to con-

sider when selecting a material for any purpose is its ability to resist corrosion during normal use. Since both gaseous and liquid water exist in great abundance in our environment, and since water is known to react with and cause the deterioration of glass over a period of time, it is essential to study these reactions in order to attempt predictions of the long-term effects of environment on the glass, its vitreous stability, optical properties, and mechanical strength.

Several authors have studied the effects of gaseous water on fluoride glasses. Early studies of vitreous BeF_2 found it to be very hygroscopic,[2] rapidly showing signs of surface degradation on exposure to air, while multicomponent fluoroberyllate glasses containing substantial amounts of the alkaline earths were found to be more resistant.[3] Although a recent study[4] of BaF_2-ZnF_2-YbF_3-ThF_4 (BZYbT) glass heat-treated in air at a temperature near the glass transition showed a diffusion-controlled –OH uptake at the glass surface (penetrating to a depth of ~10 μm in 1 d), in general, heavy-metal fluoride glasses, such as those studied here, have been found to be remarkably unreactive to high levels of atmospheric moisture over prolonged periods at temperatures below the transition range (i.e., 25° to 200°C).[5-10]

On the other hand, chemical durability studies of two major families of fluorides, ZrF_4-based[5,8,9,11-13] and BaF_2-ThF_4-based[10] glasses, have shown them to be highly susceptible to corrosion in liquid water. It was demonstrated through leach tests that the Ba-Th-based glasses were 50 to 100 times less prone to attack in deionized water than glasses based on ZrF_4, but that they were still ~1000 times less durable than some commonly used silicates.[10] It was also noted that the pH of the solutions underwent drastic changes, rapidly moving from the neutral into the acidic range.

Table I.   Glass Compositions

| | Composition (mol%) | | |
	ZBLAL*	BZYbT†	BZYbTN†
ZrF4	51.8		
BaF2	20.0	19	10
LaF3	5.3		
AlF3	3.3		
LiF	19.6		
ZnF2		27	27
YbF3		27	27
ThF4		27	27
NaF			9

*Source: D. C. Tran, U.S. Naval Research Lab, Washington, D.C. †Source: C. T. Moynihan, A. J. Bruce, D. Gavin, and K. -H. Chung, Rensselaer Polytechnic Institute, Troy, NY.

during leaching of ZrF4-containing glasses.[5,9,11] This acidic shift in solution pH was much less severe in the case of Ba-Th glasses. The contrast in leach rates observed for these two compositional families was believed to be due, primarily, to increased solubility of fluorides in the more acidic solution.[10] The following study was undertaken in order to compare these glasses under equivalent conditions by eliminating the variable of solution pH drift. It is hoped that, through gaining a better understanding of the basic mechanisms for dissolution in these HMF systems, predictions of corrosion behavior can be made for a variety of use conditions and that the most favorable aqueous environment can be determined.

II.   Experimental Procedure

Leach tests were conducted on the three fluoride glass compositions listed in Table I. The effect of solution pH on glass corrosion rates was determined by chemical analysis of the leachate solution from glass samples immersed in a series of standard buffers ranging from pH 2 to 10. Additional solutions were prepared over the range pH 2 to 5 using HCl, and over the range pH 10 to 12.4 using either NaOH or NH4OH, to compare with results obtained for the commercial buffered solutions. In the case of acid solutions, the use of HF or H_2SO_4 was avoided because, in the case of HF, large concentrations of F^- in solution would be expected to inhibit dissolution of fluoride species from the glass (see Ref. 9, Fig. 6) and, in the case of H_2SO_4, the formation of insoluble sulfate complexes might lead to a difficult or erroneous analysis of the leachate. All tests were carried out in sealed polymethylpentene (PMP)[5] containers in solutions maintained at 25°C. Solution cation analysis was conducted by use of a dc plasma spectrometer.

Normalized leach rates (NLRs) for individual elements were calculated using Eq. (1) with all elements normalized to composition:

$$\frac{X(10^6)V}{S \cdot \Delta t \cdot wt} = \text{NLR (g/(cm}^2\text{·d))} \qquad (1)$$

where X is the concentration of cation in solution (ppm), V is the solution volume (mL), S is the surface area (cm²), Δt is the soak time (d), and wt is the weight fraction of element in the original glass.

All glass leach rate samples were freshly powdered and sieved to −45, +60 mesh (250 to 355 μm), except as noted in Fig. 1. Powders were used to maximize surface area in order to maintain ion concentrations well above detection limits while minimizing the quantity of glass used. Soak times were 15 min in acidic solutions and 30 to 60 min in neutral and basic solutions. The precise test method used for this study and the reasons for its selection are described in the following sections.

The effect of solution pH on the infrared transmission characteristics of these glasses was monitored through the use of polished" rectangular plates (1 cm by 1 cm by 0.3 cm) exposed to the same solutions described above.
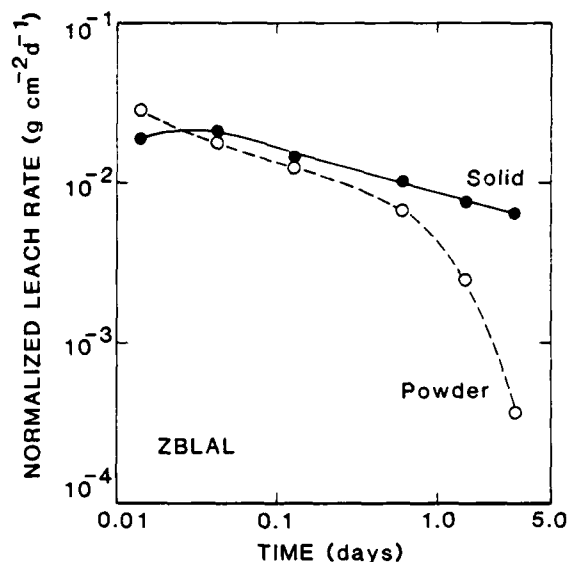
Fig. 1. Comparison of NLR for a rectangular bulk sample and a powdered sample with the same calculated surface area.

(1)   Powder vs Bulk Samples

In order to verify the equation used to calculate the surface area of the powders used in this study (−45, −60 mesh), measurements of leach rates in deionized water were performed for a bulk sample of known surface area and compared to a powder sample whose surface area was calculated to be identical from the following equation:

$$\frac{250 \text{ cm}^{-1}}{\rho} = \text{cm}^2/\text{g} \qquad (2)$$

where ρ is the glass density. The comparison is plotted in Fig. 1 and shows good agreement between the two types of samples for times up to several hours. It is thought that the slight difference noted at the shortest time (15 min) is due to the difference between the surfaces of the polished bulk sample and the freshly fractured powder sample. The dissolution rate of ZBLAL glass is sufficiently high that a notable reduction in powder surface area occurs after 3 to 5 h in deionized water and the data no longer agree. At the end of 4 d, the leach rate for the powder sample was ¹⁄₅ that of the bulk sample. These results show that Eq. (2) yields a correct value for the surface area of the powders used in the study and that, when using powder samples, it is important to continually monitor the solution to ensure that the test is stopped before extensive leaching, and consequent surface area reduction, has occurred (≤1 to 5 wt%).

(2)   Selection of Test Conditions

The results obtained from leach rate measurements have been shown to be strongly influenced by test conditions.[14,15] Fluoride glasses are particularly susceptible to this problem because, under stagnant conditions, a thin, static liquid boundary forms around the glass as it leaches.[8-10,13] This liquid film rapidly becomes saturated with respect to the less soluble glass components and leads to precipitation, crystallization, a local solution pH drop (near pH 2.5 for ZBLAL and near pH 4.8 for Ba-Th-based glasses), and an apparent noncongruent leaching of the glass surface. These complications tend to mask the ultimate mechanisms of dissolution.

A number of experiments were performed to determine the method of testing that would yield the most reproducible results with the fewest variables. The results are shown in Fig. 2.

All tests in Fig. 2 were conducted using small amounts of freshly powdered ZBLAL glass (−45, −60 mesh) immersed in a standard buffer solution at pH 2.0 for 15 min at 25°C in a sealed PMP jar. The ratio of solution volume to surface area (V/S) was
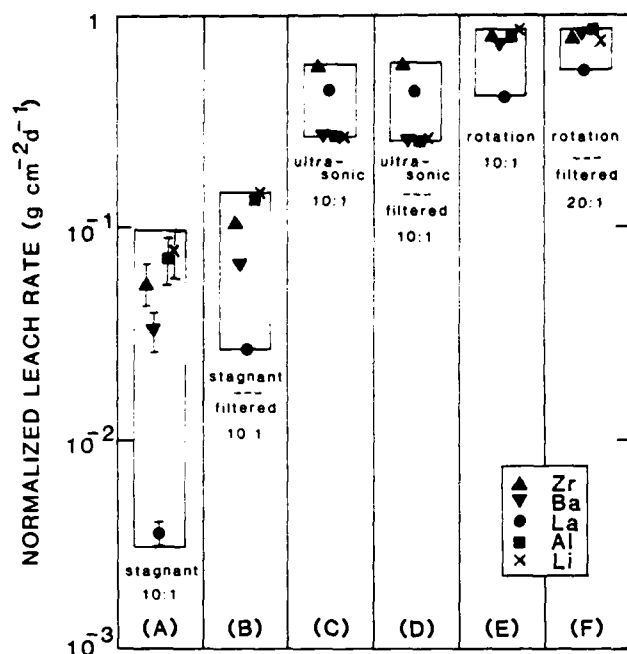
Fig. 2. NLR vs testing method for ZBLAL glass leached at pH 2.0. Symbols for individual elements in each test are displaced horizontally to improve clarity.

Fig. 3. NLR vs solution pH from leachate analysis for individual elements of ZBLAL.

maintained at 10 mL/cm⁻ for all except the last test (*F*), as noted. Duplicate analyses were run on the solutions collected after each experiment.

Column (*A*) shows the results of a stagnant leach test in which the solution was decanted gently into the two sample vials in order to avoid disturbing the powder and/or the concentrated liquid film adhering to each grain. The error bars represent the differences in the two leach rates calculated from analysis results of the two solution samples, while the symbols represent the average. The differences shown could arise from two sources: (1) a small glass grain may have been introduced into one sample, or (2) an ion concentration gradient may have existed in the stagnant solution so that a liquid sample poured from the top of the leach container might have a lower ion concentration than one collected from the bottom near the powder. An identical stagnant test (*B*) was performed: however, the container was gently agitated just before the contents were passed through a filter membrane. In this case both solution analyses yielded nearly identical results, falling within the data points, and indicate a well mixed solution. Also, the ion concentrations in solution were found to be somewhat higher in (*B*) than in (*A*), leading to a higher calculated leach rate. This result stems from the disturbance of the concentrated liquid film during agitation and filtering.

The data shown in Figs. 2(*C*) and (*D*) resulted from tests in which the samples underwent brief (30 s) ultrasonic agitation at the beginning and end of the 15-min testing period. The initial agitation was designed to ensure that none of the glass grains would remain floating on the surface and the final agitation was carried out in order to disperse, evenly and completely, the concentrated liquid film which formed around each grain during the intervening 14 min of stagnant leaching. Two conclusions can be drawn from the identical results. First, ultrasonic agitation at the end of the test period was effective in dispersing pockets of highly concentrated solution, leading to an overall increase in measuring leach rates, and second, no further homogenizing of the solution is necessary through a filtration step when using this technique. There are, however, disadvantages associated with using ultrasonic mixing. Although it is desirable to avoid the complications associated with local saturation during stagnant leaching, severe agitation over a more extended period of time may cause additional fracturing of
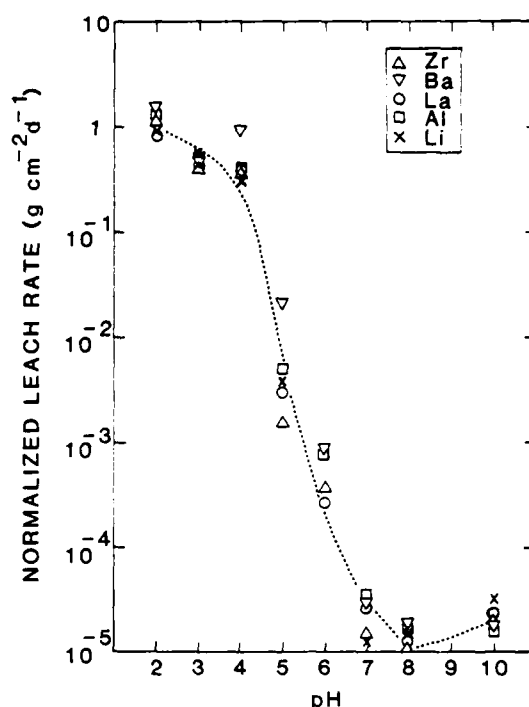
the glass grains through collisions with other grains or with the floor of the container.

In order to achieve constant and more gentle agitation, the glass powder was dispersed in solution and the container was placed in a horizontal rotating cylinder at 50 rpm. This exposed the powders to linear flow velocities of 10 to 15 cm/s. It was found that this speed was fast enough to maintain the powders in suspension without causing them to pulverize. The resulting leach rates are plotted in column (*E*) of Fig. 2 and show an increase in solution cation concentration for all elements except La. Since the La values were consistent for (*C*), (*D*), and (*E*), it was suspected that saturation may have occurred. Therefore, the solution volume was doubled for (*F*) with the results that the La concentration increased by a factor of 1.4. The sample can now be seen to be dissolving congruently in this pH 2.0 solution, no longer inhibited by species saturation and inhomogeneous solution conditions.

It is evident from Fig. 2 that vastly different results can be obtained by varying the test method. Although in some instances it is necessary to select a particular method in order to mimic and understand specific in-use conditions, it is preferable, when investigating basic mechanisms, to select a method which avoids extraneous complications. For this reason all subsequent NLR results discussed in this study were obtained using the method described in Fig. 2(*F*) at a ratio *V/S* = 20 cm for acidic solutions and *V/S* = 10 cm for neutral and basic solutions in which the glasses dissolve more slowly.

III. Results

Leach rates based on solution analysis and calculated from Eq. (1) are plotted as a function of solution pH in Figs. 3 to 5 for the three glasses listed in Table I. All data are based on duplicate solution analyses of at least three test samples for each pH value. Reproducibility was quite good, usually within 20%, and the data points represent the average of the values measured for each solution set.

Figure 3 shows the behavior exhibited by individual elements of the ZBLAL glass when exposed to solutions over the pH range 2 to 10. There is a profound improvement in corrosion resistance, by
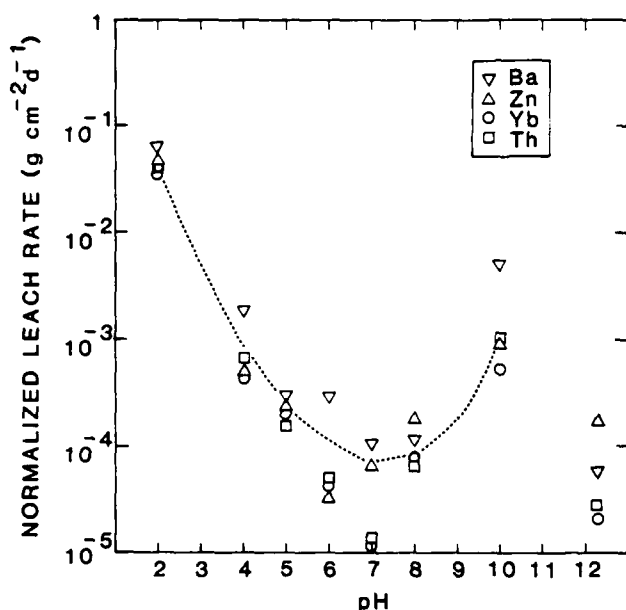
Fig. 4. NLR vs solution pH from leachate analysis for individual elements of BZYbT.
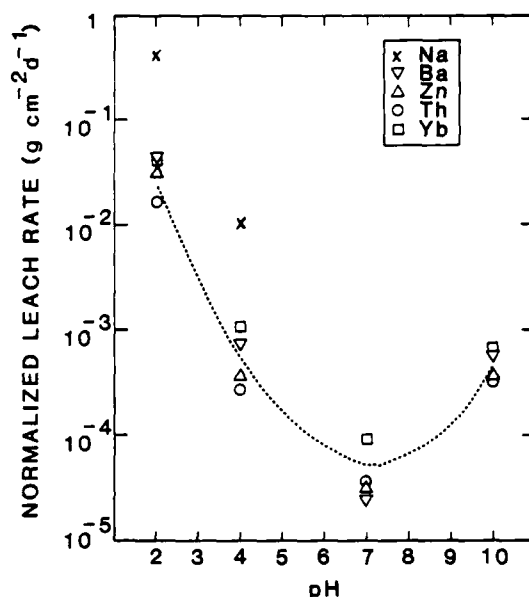
Fig. 5. NLR vs solution pH from leachate analysis for individual elements of BZYbTN.

a factor of nearly 100 000. for samples maintained at neutral pH. with the minimum occurring near pH 8. The pH 4 and 5 commercial buffers contained an organic acid. potassium biphthalate. which we felt might cause some interference in the leaching process or in analysis. Therefore. additional tests were performed using dilute HCl added to deionized water to produce solutions over the range of pH 2 to 5. Because of the strong tendency of dissolved ZrF_x^{4-x} to hydrolyze. thereby causing a reduction in solution pH. it was necessary to continually add small quantities of $0.001N$ NaOH to the unbuffered. stirred pH 5 solution during the test in order to maintain a pH of 4.8 to 5.0. The other solutions (pH 2. 3. and 4) remained at a stable pH over the 15-min test period. The results of these tests showed good agreement with those obtained for the commercial buffers.

In addition to the marked decrease in leach rates observed when going from acidic to neutral solutions. the data show the dissolution process to be nearly congruent. within a factor of 2 or 3. in all solutions except pH 5.0. In the latter case the V/S ratio of 10 cm may have been sufficiently low to cause some species to approach saturation and interfere with the normal dissolution process. In moving from neutral to basic solutions a slight increase in the solubility of some components occurs. causing an attendant increase in the normalized leach rates.

The leaching behavior of the Ba-Th-based fluoride glasses. BZYbT (Fig. 4) and BZYbTN (Fig. 5). follows the same general trend as that seen for the fluorozirconates. There is a steady improvement in durability as the solutions go from the acidic (pH 2) to the neutral (pH 6 to 8) range. followed by a marked decrease in durability at pH 10. Data collected at pH 12.4 (Fig. 4) do not follow the same trend. falling well below the expected values. This unexpectedly low leach rate may be due to the nature of the solution in which the samples were tested. Since no commercial buffers were available in this range. the solution was prepared by mixing 1 part concentrated NH_4OH with 3 parts deionized water. It is thought that the presence of such high concentrations of NH_4OH (3.7M) in solution caused the formation of insoluble complexes. both in solution and on the glass surface. and led to the lower NLR measured. For this reason. further use of NH_4OH was avoided.

Figure 5 demonstrates that the addition of 9 mol% NaF to the base glass does not appreciably alter the overall durability of the glass. although Na is leached at a rate ~10 times higher than the other components. This observation agrees with previously reported leach test results for this glass in deionized water.[11] Na data
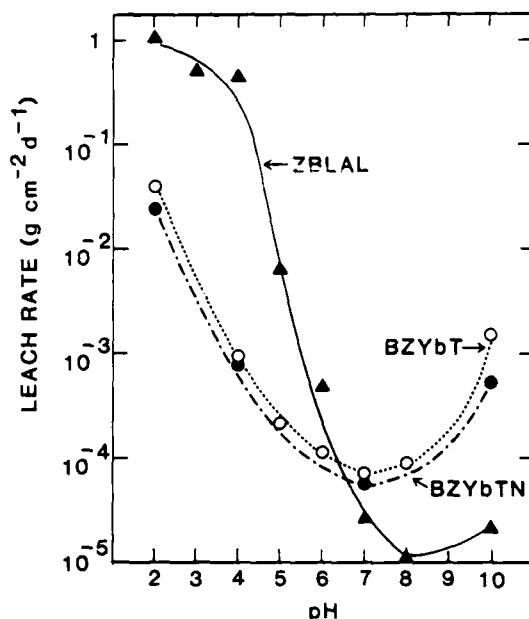
Fig. 6. Overall leach rates vs solution pH for all three compositions: ZBLAL ($\triangle$); BZYbT ($\bigcirc$); BZYbTN ($\bullet$).

were not available for pH 7 and 10 since both solutions initially contained Na and the analysis was considered to be unreliable. However. in these short-term tests (30 to 60 min). it is reasonable to assume that the Na extraction rates will remain consistently higher.

IV. Discussion

Overall corrosion rates for the three glasses under investigation were calculated for each pH value by summing the individual dissolved cation concentrations. and by assuming a stoichiometric dissolution for F. before applying Eq. (1). The results are plotted in Fig. 6.
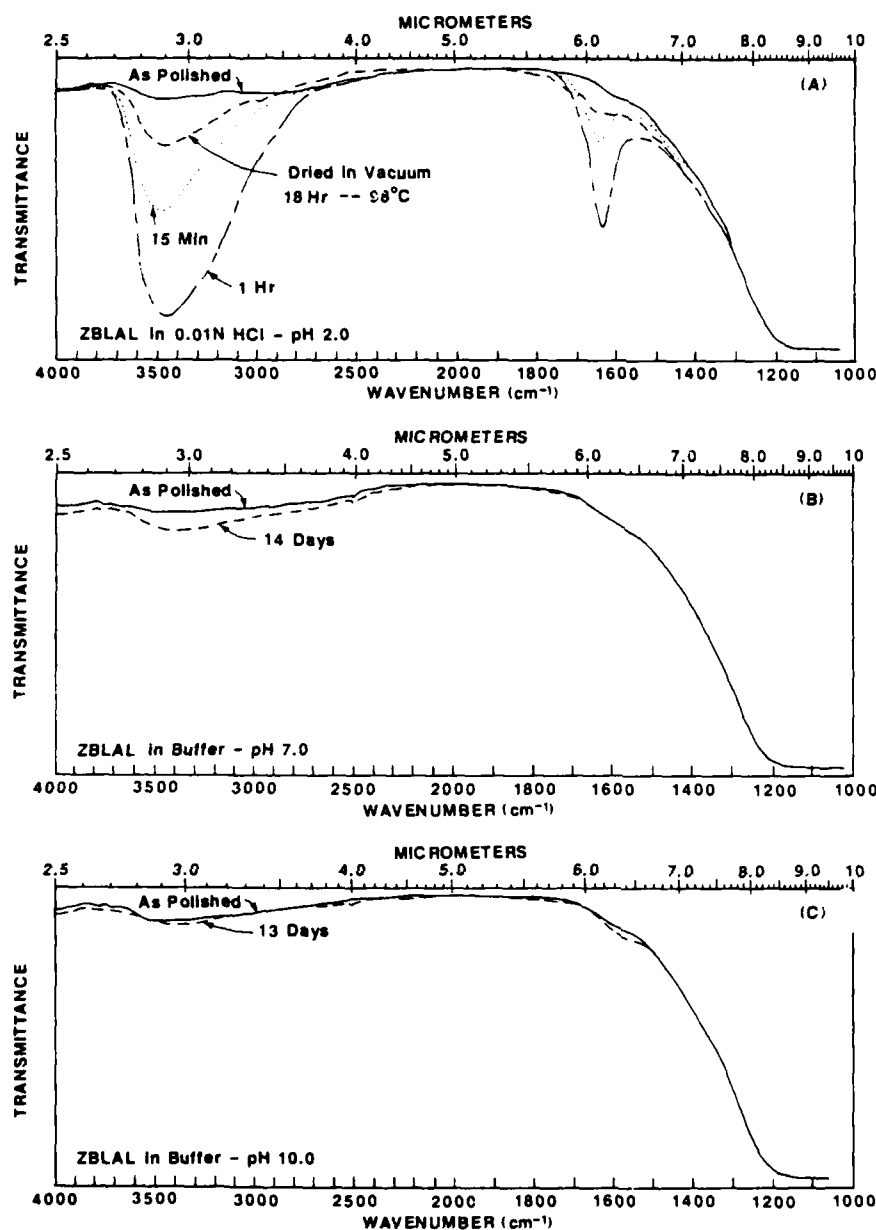
Fig. 7. Infrared transmission spectra for ZBLAL plates before and after exposure to (A) pH 2.0, (B) pH 7.0, and (C) pH 10.0 solutions.

(1) Fluorozirconate Glasses

It has been shown in previous work[9] that a wide variety of fluorozirconate glass compositions dissolve at a nearly identical rate during the early stages (≤ 2 h) and that the ZBLAL glass selected for this study is representative of this group. In Ref. 9 (Fig. 4) solution pH drift was monitored as a function of leaching time in deionized water. The pH drop over the first hour, from an initial value of 5.8 to a final value of 4.2, was attributed to hydrolysis of dissolved zirconium fluoride. It was also suggested that a static liquid film surrounding the glass was rapidly becoming saturated with respect to the less soluble species (particularly Zr and Ba compounds) and was likely to be much more acidic than the bulk solution. With time the acidity of this film may approach pH 2.5, the equilibrium for ZBLAL dissolved in H_2O. Through the study of the leaching behavior of this glass in solutions of controlled pH we can determine whether the rates previously measured for ZBLAL correspond to the bulk solution pH (i.e., >4.2) or whether a more acidic environment is indicated.

In the present work, Fig. 2 demonstrates that ZBLAL leach rates measured in constantly mixed solutions by the powder rotation method, (E) and (F), are typically a factor of 10 higher than those obtained from short-term stagnant tests, (A) and (B); therefore, in order to compare the results from our earlier study with those described here, the previously reported stagnant test results should be multiplied by 10. This allows us to estimate the drift in pH at the glass/solution interface. The average (corrected) leach rate over the first hour becomes 3×10^{-1} g/(cm²·d) for ZBLAL, which corresponds to leaching at a constant pH of 3 to 4. Remembering that the initial rate must correspond to pH 5.8 (deionized water) and that the solution was found to be 4.2 at the end of the 1-h test, it is clear that the average rate corresponding to pH 3 to 4 could not be achieved unless the environment surrounding the sample is much more acidic than the solution as a whole. These results, added to the evidence that crystals of zirconium fluoride and barium fluoride are seen to precipitate on the glass surface after a few hours, even when concentrations in the bulk solution are well below saturation, seem to support the conclusion that a thin, concentrated static liquid film develops around the sample under stagnant conditions.

In addition to demonstrating the large detrimental effect of solution pH drift on the chemical durability of fluorozirconate glasses, the data in Fig. 6 are also very useful in determining the most
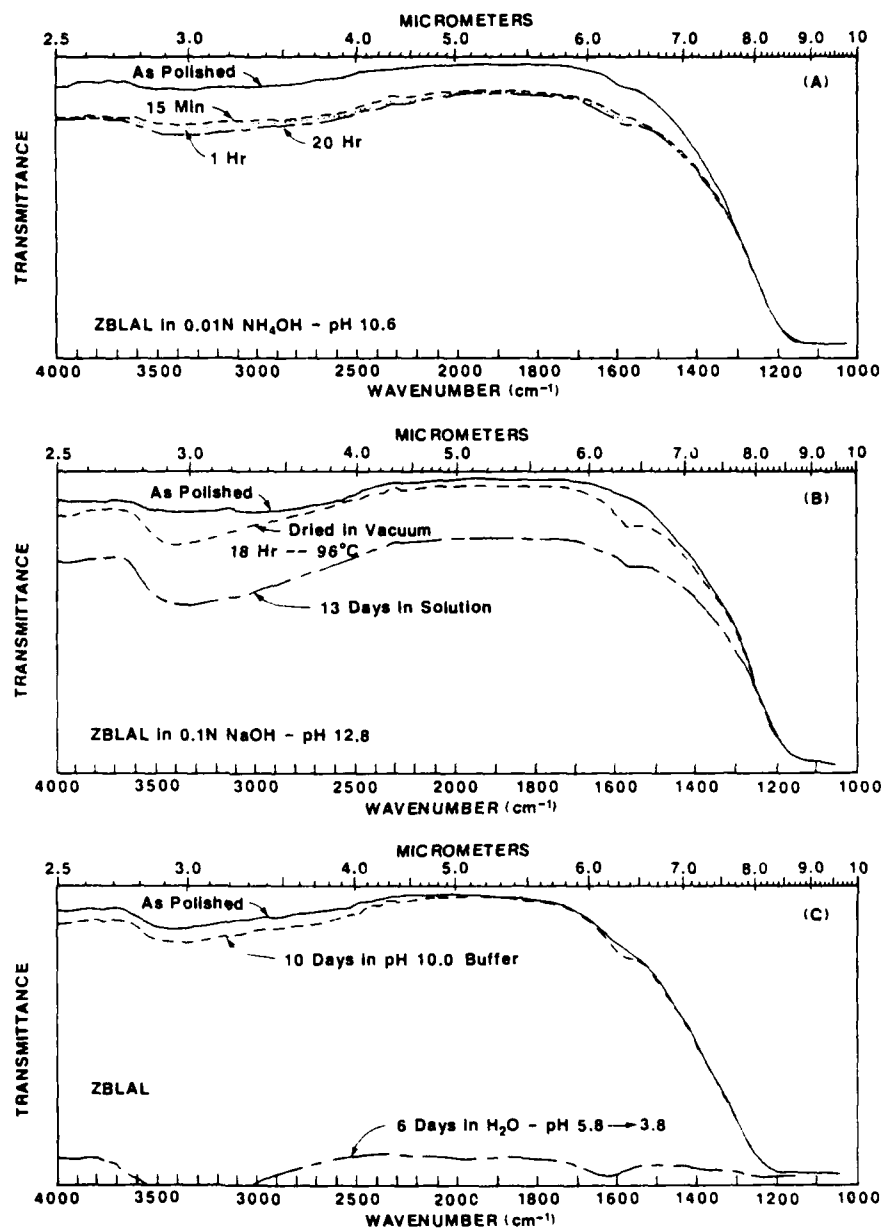
Fig. 8. Infrared transmission spectra for ZBLAL plates before and after exposure to solutions containing: (A) NH₄OH, pH 10.6, (B) NaOH, pH 13, and (C) pH 10.0 buffer, followed by immersion in deionized water.

advantageous aqueous environment. Although in acidic solutions these ionic glasses dissolve very rapidly, in a solution maintained near pH 8.0, they are only ~50 times less resistant to corrosion than durable silicates (i.e., Pyrex.* Ref. 10, Fig. 6). This large change in dissolution rates reflects the change in solubility of the fluoride components in acidic, neutral, and basic solutions.

(2) Infrared Effects in ZBLAL

Changes in the infrared spectra arising from exposure of polished ZBLAL specimen to pH 2, 7, and 10 solutions are shown in Figs. 7(A), (B), and (C), respectively. Immersion in 0.01N HCl (pH 2.0) for only 15 min (the normal test period for powder samples) produces unmistakable evidence of surface hydration in the form of the typical –OH stretching (2.9 μm) and HOH bending (6.1 μm) vibrations seen here (Fig. 7(A)) and elsewhere.[8-10,16] At 1 h these bands are even more pronounced although the sample surface remained fairly clear. By comparison, a 1-h soak in

deionized water produces a peak intensity somewhat less than is seen for 15 min at pH 2.0, but the sample has developed a surface film, making the glass appear cloudy. The hydration noted in Fig. 7(A) appears to be nearly, and perhaps completely, reversible as shown by the dashed curve representing the transmission spectrum obtained after overnight drying at 98°C under vacuum. The same drying behavior has been noted for samples soaked in deionized water.

The leach rate at pH 7 (buffered) is nearly 10⁵ times lower than at pH 2. Therefore, the soak time was increased to 14 d (Fig. 7(B)), long enough to allow ~3% of the extent of corrosion in (A). A small band can be seen in the –OH stretch region but, as yet, there is no sign of the bending vibration. This may indicate the formation of a thin hydroxyl layer on the surface or may simply result from too short an exposure time, since the 6.1-μm band is weaker and is sometimes difficult to distinguish at the early stages of corrosion.

Figure 7(C) shows the results of a 13-d soak in the pH 10.0 buffer solution followed by vacuum drying for 15 min. There is virtually no change in the spectrum even though the corrosion rate is approximately the same as for pH 7.0 and, according to solution
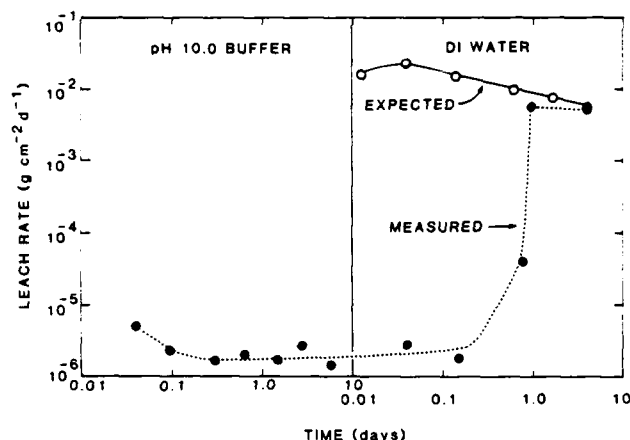
Fig. 9. NLR vs time for ZBLAL during pretreatment in pH 10 buffer for 10 d. followed by leaching in deionized water for 6 d (solid circles). Open circles represent values obtained for ZBLAL without pretreatment (Fig. 1), leached under identical conditions.

Table II. Solution pH Drift (ZBLAL)

Time (h)	Solution pH	
	Without pretreatment	With pretreatment
0	5.8	5.8
1	4.2	5.8
4	4.0	5.7
19	3.5	5.6
24	3.6	4.2
72	3.4	
96		3.8

analysis. the surface has dissolved to a depth of 0.3 to 0.5 μm during the 13-d test. Absence of the usual 2.9- and 6.1-μm features indicates a complete lack of surface hydration in this solution. The only notable feature is an unidentified band at 6.3 μm which could be due to the formation of a hydroxide species on the surface or to an impurity.

Figure 8 shows a comparison of the effect of solution composition and pH on leached ZBLAL samples. Within 15 min after immersion in 0.01N NH$_4$OH (pH 10.6) the IR transmission is seen to decrease by ~15% because of increased light scattering, probably from surface roughness. with only minor changes occurring over the next 20 h (Fig. 8(A)). In contrast. no such losses are evident in the sample immersed in the pH 10.0 buffer for a period of 13 d (Fig. 7(C)). This would seem to indicate that the surface reaction of ZBLAL exposed to NH$_4$OH is quite different and that it may involve the formation of NH$_3$ complexes on the surface. In Fig. 8(B). exposure of the glass to a solution of 0.1N NaOH (pH 12.8) for 13 d produces the same type of scattering losses seen in Fig. 8(A) in addition to the broad band centered at 2.9 μm (–OH stretching) but does not exhibit the 6.1-μm (HOH bending) vibration seen at low pH. Total absence of the bending mode in the presence of a strong hydroxyl peak. even after drying for 18 h at 96°C. leads to the conclusion that hydroxyl ions are chemically reacted with the glass. but that there has been no penetration of molecular water into the surface. SEM studies confirmed the absence of the hydration/dehydration cracking commonly seen for samples leached in water.

Finally. an experiment was conducted to determine whether pretreatment in a basic solution would produce a protective surface film. ZBLAL was soaked in a stagnant pH 10.0 buffer solution (V/S = 50 cm) for 10 d and then dried under vacuum for 2 h before recording the IR spectrum (Fig. 8(C)). The sample was then placed in stagnant deionized water (V/S = 50 cm) for 6 more days. Samples from each solution were analyzed for cation concentration periodically over the 16-d test to keep track of the leach rates as a function of time. At the end of 6 d in water the sample was almost entirely opaque (Fig. 8(C)). The leach rates. first in the buffer and then in water. are plotted in Fig. 9. along with the expected stagnant leach rate for bulk ZBLAL in water (from Fig. 1). It can be seen that the leach rate remains nearly constant during the 10 d at pH 10 and that there is no rate increase during the first 5 h in water. After 5 h there is a rapid increase with the leach rate reaching its expected value only after 24 h in water. Bulk solution pH drift also gives an indication of whether or not ZBLAL is leaching. Table II lists the solution pH values normally obtained for polished ZBLAL in water as compared with the values measured for the pretreated sample in water (Fig. 9) and lends support

to the conclusion that. although less soluble species may occupy the surface temporarily. after several hours in water they dissolve and the corrosion rate returns to normal.

(3) Ba-Th-Based Glasses

As in the case of fluorozirconates. the Ba-Th-based fluoride glasses exhibit a significant change in leach rate as a function of solution pH; however. this change is not nearly so pronounced. At pH 2 these glasses are seen to be 20 to 50 times less soluble than ZBLAL. but at pH 6 to 8 they leach at a rate 10 times higher than Zr-based fluoride glasses. In our earlier studies[8–10] it was shown that the overall resistance to corrosion in deionized water was much better for the Ba-Th family of glasses than for the fluorozirconate family. This was thought to be due to the difference in solubility of the major fluoride glass components (Zr. Ba. Li vs Th. Yb) and. in particular, to the difference in the solution pH drift behavior for the two systems. Whereas extensive hydrolysis of zirconium fluoride in solution led to a very large drop in solution pH for the Zr-containing glasses. no such pronounced effect was seen in this system where hydrolysis of thorium fluoride was observed to be very limited. The solution at the glass interface drifts very slowly toward 5 and never drops below 4.8,[10] the equilibrium pH for BZYbT in water. Because these glasses leach much more slowly in water. as compared with Zr-based compositions. saturation of the static liquid film occurs much later and extensive precipitation of surface crystals is rarely observed during the first 24 h of leaching

These results clearly show the effect of solution buffering on the observed dissolution rates. so that tests conducted in tap water from different sources and containing different amounts of natural buffers could easily give quite different leach rates and may even reverse the order of corrosion resistance between the fluorozirconate and the mixed barium-thorium fluoride glasses.

V. Conclusions

The mechanisms controlling aqueous corrosion of heavy-metal fluoride glasses are complex and vary widely depending on the test environment. In stagnant unbuffered water. particularly at low V/S ratios. accumulation of corrosion products can lead to severe modifications in the leaching process. Hydrolysis of certain fluoride species (i.e.. ZrF$_6^{4-}$ ...). consuming solution –OH. causes a rapid decrease in pH of the liquid in contact with the glass surface which. in turn. results in increased solubility and an accelerated dissolution rate. Ultimately. saturation of the less soluble species occurs. causing precipitation. crystallization. and the formation of an altered surface layer due to preferential leaching of the more soluble species. These complications to the leaching process. arising from the accumulation of corrosion products in solution. can be largely eliminated through the use of high V/S ratios (or short-term tests) in a well-mixed or flowing bath at constant pH.

Dynamic leach tests were performed on representative compositions from two HMF (ZrF$_4$-based[1] and BaF$_2$-ThF$_4$-based) glass families. Dissolution rates were studied as a function of solution pH and glass composition by means of solution cation analysis. The results demonstrate a dramatic change in corrosion rate when going from neutral to acidic solutions: a factor of 10^5 for ZBLAL and a factor of 250 for BZYbT. When these results were

compared with results from tests performed on the same glasses in deionized water, it was found that solution pH drift acts as a serious liability, especially in the case of the Zr-based fluoride glasses.

In the absence of complicating factors such as corrosion product buildup, precipitation, and solution pH drift, the corrosion of HMF glasses appears to be governed by matrix dissolution, the spread in the leach rates being dictated by the individual component solubilities at a given pH. Below pH 6.5 Ba-Th-based glasses exhibit a better resistance to corrosion, but above that value the Zr-based glass is clearly superior. In all cases the best chemical durability for a given system can be obtained near neutral pH (6 to 8).

Infrared spectral studies of polished bulk ZBLAL specimen exposed to solutions over the range pH 2 to 13 demonstrated distinct differences in the reactions of the glass to acidic, neutral, and basic solutions. In acid, as in deionized water, penetration into the glass surface by molecular water was clearly evident in the form of the typical 2.9- and 6.1-μm absorption bands. This adsorbed H_2O could be largely removed by heating the sample under vacuum. Leaching in the buffered pH 7.0 solution caused only a weak –OH band; however, because of the relatively short test duration, the absence of any HOH bending vibration is considered indicative of, but no conclusive proof of, hydroxyl reactions at the surface. A systematic study of the time dependence for growth of these absorption bands is needed to clarify the leaching mechanisms at neutral pH.

Surface reactions in the basic environments varied with solution composition and pH. Soaking in the pH 10.0 buffer for 13 d produced only a minimal surface –OH concentration, while a short exposure (15 min) to NH$_4$OH at pH 10.6 caused a general loss in transparency due to scattering. In addition, surface –OH can be seen to increase noticeably over the next 20 h, much faster than in the buffer solution at similar pH. In the NaOH solution near pH 13 the surface undergoes a distinct hydroxyl reaction with little or no molecular water being evident in the spectrum.

The conclusions arising from this study can be summarized as follows:

(1) In dynamic, high-dilution environments corrosion occurs primarily by matrix dissolution.

(2) Solubility of fluorides is greatly enhanced in acidic media; environments below pH 6 should be avoided.

(3) Glasses whose fluoride components readily undergo hydrolysis reactions create their own acidic environment on exposure to water and will, generally, exhibit higher corrosion rates.

(4) Chemical attack in basic solutions appears to occur through an –OH reaction of the surface followed by dissolution.

(5) General predictions concerning leaching behavior can be made using models developed through "ideal" tests; however, in order to make specific predictions of in-use durability, appropriate tests designed to mimic actual conditions should be evaluated, since we have demonstrated that results can vary widely depending upon the test method employed.

Finally, an attempt was made to improve the corrosion resistance of ZBLAL to water through pretreatment in the pH 10.0 buffer solution. The results show that it is possible to produce a passivating surface layer which is effective in reducing the leach rate. Although the benefit of this particular treatment was seen to be temporary, it is expected that further studies in this area will produce a surface with improved chemical durability without substantial losses of IR optical transparency.

References

[1]M. Poulain, M. Poulain, and J. Lucas, "Optical Properties of Zirconium Tetrafluoride Glass Doped with Nd^{3+}" (in Fr.), *Mater. Res. Bull.*, **10**, 243–46 (1975).

[2]G. Heyne, *Angew. Chem.*, **46**, 473 (1933).

[3]C. F. Cline, D. D. Kingman, and M. J. Weber, "Durability of Beryllium Fluoride Glasses in Water: Comparison with Other Glasses and Crystals," *J. Non-Cryst. Solids*, **33**, 417–21 (1979).

[4]D. Tregoat, G. Fonteneau, C. T. Moynihan, and J. Lucas, "Surface –OH Profile from Reaction of a Heavy-Metal Fluoride Glass with Atmospheric Water," *J. Am. Ceram. Soc.*, **68** [7] C-171–C-173 (1985).

[5]C. J. Simmons, H. Sutter, J. H. Simmons, and D. C. Tran, "Aqueous Corrosion Studies of a Fluorozirconate Glass," *Mater. Res. Bull.*, **17**, 1203–10 (1982).

[6]E. O. Gbogi, K.-H. Chung, and C. T. Moynihan, "Surface and Bulk –OH Infrared Absorption in ZrF$_4$- and HfF$_4$-Based Glasses," *J. Am. Ceram. Soc.*, **64** [3] C-51–C-53 (1981).

[7]M. Robinson and M. G. Drexhage, "A Phenomenological Comparison of Some Heavy-Metal Fluoride Glasses in Water Environments," *Mater. Res. Bull.*, **18**, 1101–12 (1983).

[8]C. J. Simmons, S. Azali, and J. H. Simmons, "Chemical Durability Studies of Heavy-Metal Fluoride Glasses," Proceedings, 2nd International Symposium on Halide Glasses, Troy, NY, 1983, Paper No. 47.

[9]C. J. Simmons and J. H. Simmons, "Chemical Durability of Fluoride Glasses: I. Reaction of Fluorozirconate Glasses with Water," *J. Am. Ceram. Soc.*, **69** [9] 661–69 (1986).

[10]C. J. Simmons, "Chemical Durability of Fluoride Glasses: II. Reaction of Barium-Thorium-Based Glasses with Water," *J. Am. Ceram. Soc.*, **70** [4] 295–300 (1987).

[11]G. H. Frischat and I. Overbeck, "Chemical Durability of Fluorozirconate Glasses," *J. Am. Ceram. Soc.*, **67** [11] C-238–C-239 (1984).

[12]C. A. Houser and C. G. Pantano, "Surface Studies of Fluorozirconate Glasses," Proceedings, 2nd International Symposium on Halide Glasses, Troy, NY, 1983, Paper No. 15.

[13]T. A. McCarthy and C. G. Pantano, "Dissolution of Fluorozirconate Glasses," Proceedings, 2nd International Symposium on Halide Glasses, Troy, NY, 1983, Paper No. 30.

[14]J. H. Simmons, A. Barkatt, and P. B. Macedo, "Mechanisms that Control Aqueous Leaching of Nuclear Waste Glass," *Nucl. Technol.*, **56**, 265–70 (1982).

[15]E. C. Ethridge, D. E. Clark, and L. L. Hench, "Effects of Glass Surface Area to Solution Volume Ratio on Glass Corrosion," *Phys. Chem. Glasses*, **20**, 35–40 (1979).

[16]S. R. Loehr, A. J. Bruce, R. Mossadegh, R. H. Doremus, and C. T. Moynihan, "IR Spectroscopy Studies of Attack of Liquid Water on ZrF$_4$-Based Glasses"; pp. 311–22 in Materials Science Forum, Vol. 5, Halide Glasses: I. Proceedings of the 3rd International Symposium on Halide Glasses, Rennes, France, June 1985. Edited by J. Lucas and C. T. Moynihan. TransTech Publications, Aedermannsdorf, Switzerland, 1986.

[17]C. J. Simmons and S. Azali, "Effect of Solution pH on Leaching of Fluoride Glasses"; presented at the 86th Annual Meeting of the American Ceramic Society, Pittsburgh, PA, April 30, 1984 (Glass Division, Paper No. 8-G-84).

Appendix H

Corrosion of uranium IV fluoride glasses in aqueous solutions

J. Guery, D. G. Chen, C. J. Simmons, J. H. Simmons

Department of Materials Science and Engineering, University of Florida, Gainesville, Florida 32611, USA

C. Jacoboni

Laboratoire des Fluorures UA 449, Faculté des Sciences, Université du Maine, 72017 Le Mans, Cédex, France

Three compositions, with the major components $BaF_2-UF_4-YF_3-MF_x$ ($MF_x = FeF_3$, MnF_2, ZnF_2), were leached in deionised water and a variety of buffer solutions (pH 2–10) to determine the effect of composition and environment. Although it was noted that increasing the concentration of less soluble YF_3 improved the durability somewhat, all the glasses leached at nearly equivalent rates. These data are compared with the results of two previous studies of zirconium based and thorium based glasses.

Investigations of the corrosion of fluoride glasses have been motivated by the high potential of these materials for infrared transmission applications. Studies have been conducted on the corrosion of fluorozirconate,[1–6] fluorohafnate,[2] and mixed barium–thorium glasses.[7,8] These measurements showed that fluoride glasses leach by a mechanism which is very different from that of silicate glasses. Simmons & Simmons[4] developed a model for the observed behaviour of fluorozirconate and fluorohafnate glasses which showed that when these glasses are exposed to deionised water the reactions of the solution with the corrosion products lead to a large decrease in the pH of the solution. In a subsequent paper, Simmons[9] showed that the dissolution rate of fluorozirconate glasses increases drastically in acidic solutions so that once the pH of the corroding solution begins to drop, the corrosion rate increases and the increased concentration of corrosion products rapidly leads to a further drop in pH. In solutions with limited volumes, the steady state value of pH 2·5 is rapidly reached and the glass dissolution rate is extremely high. Similar studies conducted on the mixed barium–thorium glasses[7,9] showed that they follow a somewhat similar behaviour but have a lower dependence of corrosion rate on solution pH than fluorozirconates and their corrosion products tend to acidify an unbuffered solution only to pH 4·8. These two effects combined explain why barium–thorium

fluoride glasses exhibit a lower leaching rate than fluorozirconates in deionised water.[7] Additions of Li, Na, Al, or Pb to the zirconium–barium–lanthanum fluoride base composition had a much smaller effect on the corrosion rate[4] than expected from studies of silicate glasses.

Similar compositions replacing zirconium fluoride with tetravalent uranium fluoride, while heavily coloured, have shown a good glass forming tendency and appear to be very interesting in their corrosion resistance, possibly exhibiting an improved leaching rate.[10] In this study, a comparison of the corrosion rates of glasses based on uranium fluoride compositions will be presented.

Following the experimental conditions described by Simmons[9] we have established a corrosion mechanism for some glasses in the systems $BaF_2-UF_4-YF_3$ + MnF_2, ZnF_2, or FeF_3 on the basis of the leaching rate and surface analysis of the samples.

Experimental procedures

Glass preparation

The glass compositions studied are listed in Table 1. The samples were prepared in the Laboratoire des Fluorures, Le Mans, by a method previously described:[10–12] a melt was formed from the mixture of the fluoride compounds in a platinium crucible at 800 C then cast into a brass mould heated to 280 C to produce pieces of glass $10 \times 10 \times 2$ mm. These steps were conducted in a dry air glove box.

Table 1. *Composition of the glasses (mol%)*

Glass	BaF_2	UF_4	YF_3	AlF_3	FeF_3	MnF_2	ZnF_2
BUYFe	20·0	40·0	20·0		20·0		
BUYAMn	30·4	30·4	4·8	2·0		32·4	
BUYAZn	30·4	30·4	4·8	2·0			32·4

Analyses of the solutions

The leaching tests were conducted in deionised water and pH buffered solutions. The glass was ground carefully and the sieved powder ($+60$ -45 mesh) was collected; the formula, $S = 250\ m/d$, was used to obtain the average surface area of the powder in terms of the density, d, and the mass, m, of the glass. Experiments were conducted with sufficient glass to have 5 cm^2 of surface area in 50 ml of solution (for a S/V ratio of 0·1 cm^{-1}). The experiments were performed at room temperature (27°C) in a polymethylpentene jar rotating at 50 rev/min. After a predetermined soak time, the solution was filtered with a polymethylpentene disposable filter. The cations were analysed by plasma emission spectroscopy and the fluoride anions by potentiometry with a F^- selective electrode. The amount of glass leached into the solution is defined by NC_i, the normalised mass loss of each element, i,

$$NC_i = \frac{C_i \cdot V \cdot 10^{-6}}{S \cdot \%W_i} \quad (\text{g cm}^{-2}) \qquad (1)$$

where C_i (ppm) is the concentration of element i in the leachant solutions, V (cm^3) is the volume of the solution, S (cm^2) is the calculated surface area of the glass powder, and $\%W_i$ is the mass fraction of component i in the glass.

Surface analysis

Bulk glass samples polished with a 1 μm diamond paste in an oxygen free organic lubricant were used. The experiments were conducted by soaking the samples in a stagnant solution at the same surface to volume ratio as the powders; the samples were then rinsed with methanol and toluene and dried in a vacuum oven at 100°C.

The corroded surface was observed under a scanning electron microscope coupled with an energy dispersive x-ray system for the identification of the cations. Some semiquantitative analyses of the surface were conducted by electron spectroscopy for chemical analysis and x-ray diffraction analysis was used to study the crystallinity of the surface.

Results

Behaviour in deionised water

pH measurements. The pH of the solution was found to fall from 5·8 (original deionised water) to about 4 in one day (Figure 1), the drift being much less severe in the case of uranium glasses than that observed for fluorozirconate compositions.[4] The steady state pH value for these uranium glasses was found to be ~3·5, while for fluorozirconate glasses the pH drifted to ~2·5 with time; this decrease is attributed to the hydrolysis of uranium species.

Compositions of leachant solutions. Figure 2 shows the normalised composition of the leachant solution for up to one day of corrosion for Fe, Mn, and Zn glasses. We noted that in all cases these transition metals
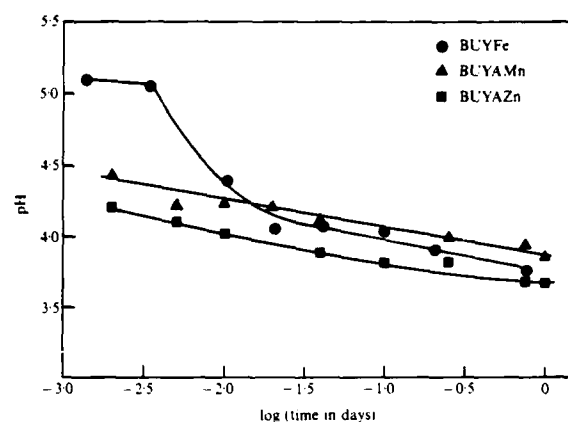
Figure 1. *Alterations in the pH of the deionised water after immersion of pieces of glass $10 \times 10 \times 2$ mm*
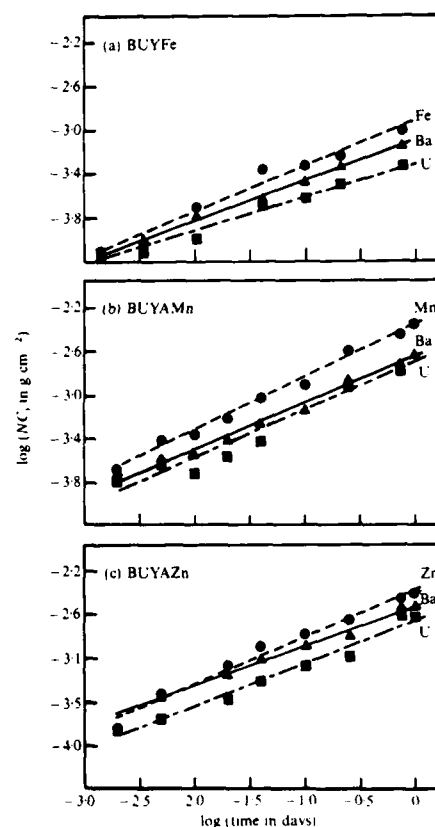
Figure 2. *Normalised concentration of the leachant solutions from the glasses*

leached into the solution at a higher rate than the other elements (1·5 times to twice as fast as F, Ba, and U); on the other hand, the yttrium concentration was low and constant, probably due to a rapid saturation of the solution by the corrosion product containing the Y. The same behaviour was also observed for zirconium and thorium based glasses where the leaching rate of lanthanum and thorium was found to be about one to two orders of magnitude lower than that of the other elements.[1,2,4,7,13]

Thus, the question of dissolution congruence cannot be addressed by this test, but rather the observed rates are dependent on the solubility of the hydrolysis products of the various elements. In this respect, it is clear that the transition metal fluorides are more soluble than the others. Scanning electron microscopy data indicate the formation of a layer rich in insoluble Ba, U, and Y species. However the concentration of elements increases continuously in the solution during one day so that, unlike in silicates, this layer plays no protective role in the leaching process.

NC_i increases linearly with log t, and can be expressed as: $NC_i = A_i t^x$. In each glass, all the fitted lines for the dissolution of the cations have about the same time exponent, $x = 0.40$ to 0.48 for the BUYAMn and BUYAZn glasses and 0.36 to 0.40 for the BUYFe glass. The calculations of x near 0.5 indicate that, in this dissolution process, diffusion may play a major role. The glass containing iron is more resistant to corrosion than those containing manganese or zinc; this lower rate of corrosion may be explained by its higher content of weakly soluble YF_3.

The stoichiometry between the cation and fluoride concentrations is maintained in the solution (Figure 3), indicating that the dissolution of the matrix is controlled by the dissolution of fluoride compounds, and that any $F^- OH^-$ ion exchange processes are negligible in deionised water.

Tests in pH buffered solutions

Investigations were conducted to determine the importance of the pH of the solution on the corrosion rate of the glasses over the pH range 2–10; the experiments were conducted with pH buffer solutions under the same conditions as the deionised water tests, lasting from 1 to 18 h.

Figure 4 represents the normalised concentration of cations leached out of the glasses after 18 h in the different solutions (because of its low solubility, Y is not mentioned) and it may be seen that the curves present a deep valley at pH values in the range 6–8. While the BUYFe glass indicates a near congruent dissolution, this is not the case for BUYA Mn or Zn glasses: in fact no Ba or U was detected at pH 6 for the ZnF_2 glass. In the acidic range (pH 2–4) the behaviour is similar for all glasses. The lack of congruency may correspond to the competition between dissolution by acidic hydrolysis and reprecipitation as was the case in the deionised water. Experiments at pH 10 showed a congruent dissolution for all glasses but, in view of the results of pH tests on fluorozirconates.[9] we find it surprising that the leaching rate of these glasses is as high at pH 10 as in the acidic range.

The data obtained after 18 h in deionised water are added to Figure 4 at the pH corresponding to the end of the corrosion time and show a slightly lower

Figure 3. Concentration in positive charges and F^- in the leachant solutions from the glasses
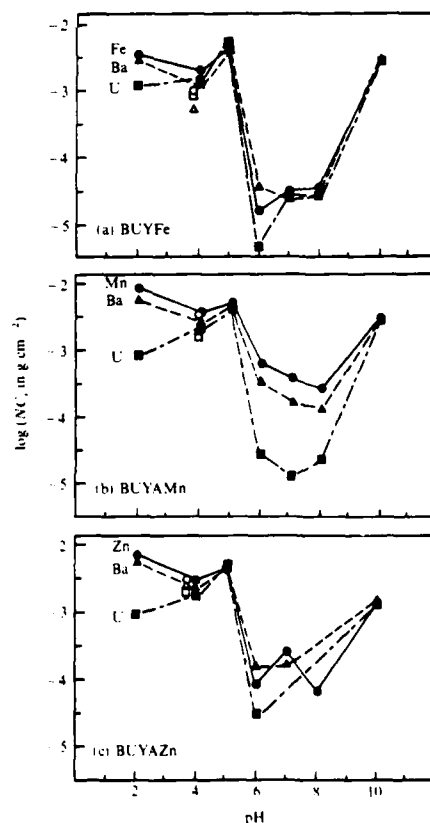
Figure 4. Normalised concentration of the leachant solutions in the range pH 2–10, after 18 h corrosion of the glasses

dissolution because the pH has changed continuously during the test.

We can compare the evolution of the corrosion with time by looking at the average leaching rate $(\Sigma NC_i/t)$ obtained from the two different times, 1 and 18 h shown in Figure 5; ΣNC_i is the total amount of leached cations (Ba, U, M) measured by plasma emission spectroscopy. After 1 h of reaction at low corrosion rates no Ba or U could be detected. In acidic and neutral solutions the leaching rate decreases with time.

At pH 10, the corrosion rate stays fairly constant. All the species are soluble, either as free ions or as complexes[14] such as $Zn(OH)_3^-$, $U(OH)_5^-$, or, more probably, UO_2^{2+}, because the solutions become yellow, the characteristic colour of the uranyl cation. This is a dissolution of the matrix, so the solution is continuously in contact with the surface of the glass and the corrosion keeps going at the same rate.

Figure 6(a) was obtained from the BUYFe glass after corrosion in deionised water; the plate like shape of the crystals may be seen better in Figure 6(b) which shows the surface after reaction in a buffer solution at pH 4. From the fact that crystals have nearly the same size after 18 h or 22 days in deionised water, it is believed that, in stagnant tests, crystal growth is promoted by a saturation of the corrosion products just above the surface and a steady state condition is established. The energy dispersive x-ray spectra of all these corroded surfaces are grouped in Figure 7 and are compared to the surface of the original glass. The iron peak is practically nonexistent in the spectra obtained after corrosion in solutions of pH 2, 4, and 5 and deionised water. The yttrium peak, on the contrary, increases slightly in all solutions. From pH 6 to 10 the composition of the surface does not significantly change from that of the original glass.

X-ray diffraction. Spectra were obtained directly from the surface of the bulk samples after 18 h of corrosion in stagnant tests. The diffraction peaks are broad and all the different glasses yield the same unidentified x-ray spectrum. The same experiments repeated on glasses in the ternary systems without any stabilising agent ($33BaF_2$, $33UF_4$, $33MF_n$) reveal a film of $BaUF_6$ (high temperature structure form), as shown in Figure 8, and these results are in good agreement with the known stabilising effect of YF_3 towards devitrification and corrosion.

Figure 5. *Average leaching rate as a function of pH after 1 and 18 h corrosion*
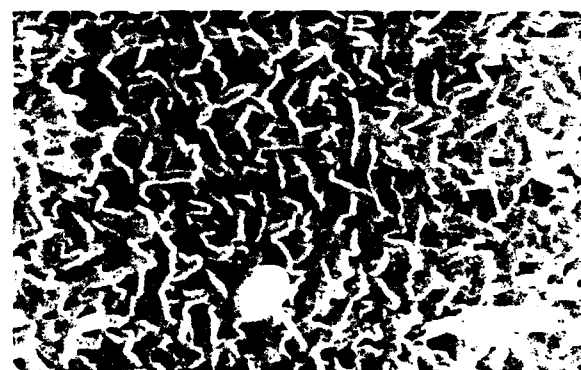
(a) 18 h in deionised water
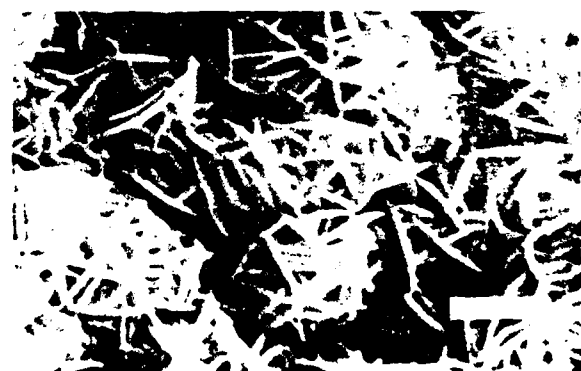
(b) 18 h in buffer solution of pH = 4

Figure 6. *Scanning electron micrograph of the surface of the glass BUYFe (bar = 1 μm*

Surface analysis

Scanning electron microscopy and energy dispersive x-ray analysis. The surfaces of bulk samples of BUYFe glass were examined under the scanning electron microscope after a stagnant corrosion test of 18 h. The neutral and basic solutions (pH 6–10) attack the surface only slightly, the least degraded surface being obtained from solutions at pH 7 where, after 18 h, it is still possible to see the polishing lines clearly.

Figure 7. *Energy dispersive x-ray spectra of the surface of BUYFe uncorroded (GL) and corroded for 18 h*
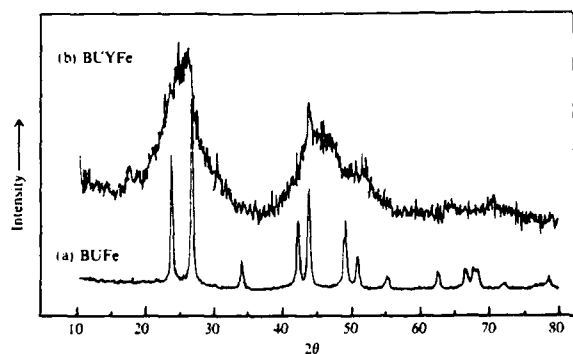
Figure 8. *X-ray spectra of glasses corroded in deionised water*

Figure 9. *Electron spectroscopy for the chemical analysis spectra of the surface of glass BUYFe*
(a) uncorroded polished surface
(b) surface corroded for 15 min in deionised water (rotation)
(c) surface corroded for 22 days in deionised water (stagnant)

Electron spectroscopy for chemical analysis. Figure 9 represents the spectra of the surface of samples corroded in deionised water: sample (a) is a polished piece of glass used as a reference, the surface of sample (b), prepared with the rotating test, does not have precipitated crystals, while on sample (c) crystals have grown due to the extended soaking time and the stagnant conditions. We observe on its spectrum the contamination by oxygen (O 1S) and carbon (C 1S and CF_2) from the atmosphere and the organic oil used to polish the samples.

The analysed composition of the surface of the sample shown in Figure 9(a) is in good agreement for Ba and U concentrations but the yttrium has a ratio

much higher than expected, whereas the fluorine concentration is lower and iron is not detected; the absence of iron may be due to its removal during polishing (or to a detection interference during the measurement). After corrosion, the samples gave similar spectra, as shown in Figure 9 (b) and (c), meaning that the composition of the corroded surface layer formed in the first few minutes is nearly the same as that of the crystal deposit formed at longer times. The decreasing oxygen content with time seems to indicate that corrosion does not give hydrated compounds as has been observed with ZBLA glasses.

Discussion

In deionised water, the corrosion of the glasses appears to be partly controlled by a diffusion process, the kinetics of which depend on the solubility of the basic fluoride compounds. The fluorides of the transition metals are the more soluble species and they leave behind an insoluble layer of $BaUF_6$. From previous studies on these types of glass,[12] it has been suggested that their network may be described as a

near close packing of F; $BaUF_6$ seems to be the major complex of the matrix and accepts the insertion of MF_n.[12] In aqueous environments, the transition metals leave their network and a porous structure is formed through which H_2O can diffuse easily allowing further dissolution of the transition metals because the water is always in contact with the original glass. This explains why $3d$ transition metal glasses are of low durability.[15] The same effect of layer porosity and thickness was discussed by Simmons & Simmons for fluorozirconate glasses.[4]

The glass containing the higher amount of YF_3 (BUYFe) has a lower corrosion rate and it appears that YF_3 slightly reduces the diffusion of water into the corroded surface by forming a less porous leached layer on the glass. The composition and structure of the corroded layer of these glasses is difficult to interpret and we have observed the growth of crystals on the surface without being able to identify them precisely.

Hench has described six types of surface on silica glasses.[16 18] In acidic and neutral solutions these fluoride glasses can be described as having a type IV surface on which a selective leaching film is formed, followed by a breakdown of the matrix and dissolution. The rate of reaction is slowed down as long as the pH remains in the neutral range but in basic solutions, with a pH of 10, the glasses possess a type V surface giving total and congruent dissolution.

Summary and conclusions

We have examined the corrosion of glasses whose common constituents are UF_4, BaF_2, and YF_3 with FeF_3, MnF_2, or ZnF_2 added; all the compositions gave very good, stable glasses. We believe that the reduction in leaching rate for the BUYFe glass results from the higher YF_3 content which appears to produce a less porous surface layer during corrosion. However, the replacement of MnF_2 by ZnF_2 has no appreciable effect on the leaching rate.

In contrast, when comparing the leaching in deionised water of this family of glasses containing UF_4 with that of other fluoride glasses not containing UF_4, the differences between the BUYFe glass and the BUYAMn and BUYAZn glasses become less accentuated and they appear to behave as a group with characteristics intermediate between the ZrF_4 family and the BaF_2-ThF_4 family.

Figure 10 shows a comparison of the durability in deionised water of the three families of glasses containing different tetravalent fluorides; this is a reproduction of Figure 6 from Reference 7, with the leaching rate of the UF_4 family added. Uranium based glasses exhibit the greatest time dependence and while their leaching rate is initially comparable to that of the fluorozirconate glasses it approaches that of thorium glasses after a few days; this is due to the relatively small drop in pH observed during the leaching of these glasses compared to the much larger drop observed with the ZrF_4 glasses.

Figure 11 shows the pH dependence of the leaching
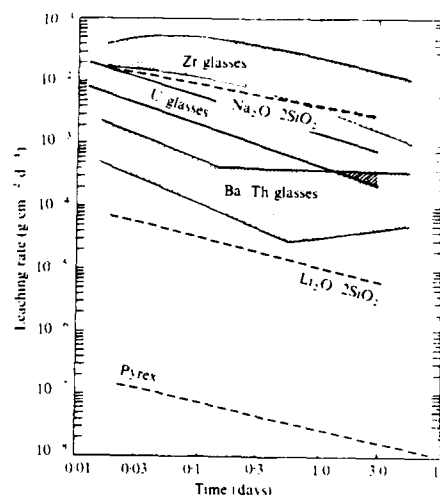
Figure 10. *Comparison of leaching rates in deionised water of fluoride glasses based on ZrF_4,[4] BaF_2-ThF_4,[7] and UF_4*
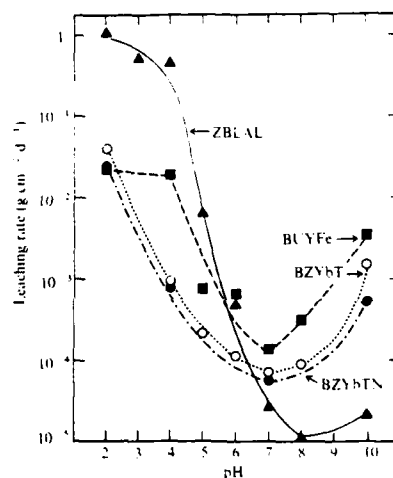
Figure 11. *Comparison of leaching rates as a function of solution pH for fluoride glasses based on ZrF_4,[7] BaF_2-ThF_4,[9] and UF_4*

rate of the BUYFe glass and compares it with that of ZBLAL, BZYbT, and BZYbTN glasses from Figure 6 of Reference 9. Aside from a difference in behaviour at pH 4, the uranium fluoride glass closely follows the broad minimum in the pH dependence observed in the thorium fluoride glasses, with a slightly higher leaching rate. It is interesting to note that the similarity between the two families of glasses extends to the minimum leaching rate which occurs at pH 7. By comparison, the zirconium fluoride glass has a markedly different pH dependence, varying over a greater range of leaching rates and having a minimum at pH 8.

References

1. Simmons, C. J., Sutter, H., Simmons, J. H. & Tran, D. C. (1982). *Mater. Res. Bull.* **17**, 1203.
2. Simmons, C. J. & Sutter, H. (1982). *First Int. Symp. on halide and other non-oxide glasses.* Cambridge, England.
3. Mitachi, T. A. (1983). *Physics Chem. Glasses* **24** (6), 146.
4. Simmons, C. J. & Simmons, J. H. (1986). *J. Am. Ceram. Soc.* **64** (9), 661.
5. Doremus, R. H., Murphy, D., Bansal, N. P., Lanford, W. A. & Burman, C. (1985). *J. Mater. Sci.* **20**, 4445.
6. Frischat, G. H. & Overbeck, I. (1984). *J. Am. Ceram. Soc.* **67** (11), C238.
7. Simmons, C. J. (1987). *J. Am. Ceram. Soc.* **70** (4), 295.
8. Robinson, M. & Drexhage, M. G. (1983). *Mater. Res. Bull.* **18**, 1101.
9. Simmons, C. (1987). *J. Am. Ceram. Soc.* **70** (9), 654.
10. Guery, J., Courbion, G., Jacoboni, C. & De Pape, R. (1983). *Second Int. Symp. on fluoride glasses,* Troy, N.Y.
11. Guery, J., Courbion, G., Jacoboni, J. & De Pape, R. (1982). *Mater. Chem.* **7**, 715.
12. Guery, J. (1984). *Thèse de 3ᵉ cycle,* Le Mans.
13. Simmons, C. J., Guery, J., Chen, D. G. & Jacoboni, C. (1986). *Mater. Sci. Forum* **5**, 329.
14. Baes, C. F. Jnr & Mesmer, R. E. (1986). *The hydrolysis of cations.* Krieger Publications, Malabar, Florida.
15. Auriault, N. (1986). *Thèse de 3ᵉ cycle,* Le Mans.
16. Hench, L. L. (1977). *Proc. 11th Int. Congr. Glass,* Prague. Survey papers, Vol. II, 343.
17. Hench, L. L. & Clark, D. E. (1978). *J. Non-Cryst. Solids* **28**, 83.
18. Hench, L. L. (1982). *J. Physique Colloq.* C9, **43**, 625.

Appendix I

Infrared Spectroscopic Studies of the Hydrolysis Reaction During Leaching of Heavy-Metal Fluoride Glasses

MICHEL LE TOULLEC, CATHERINE J. SIMMONS,* and JOSEPH H. SIMMONS*

Advanced Materials Research Center, University of Florida, Gainesville, Florida   32611

In this work, the interfacial reactions of heavy-metal fluoride glasses with water have been investigated by Fourier transform infrared spectroscopy. High dilution and stirring conditions were maintained to prevent any influence of pH drift and reprecipitation. From comparisons of the integrated absorption peak areas for the O–H stretching and H–O–H bending vibrations in the glass with those for molecular water, the contributions of metal hydroxyls formed in the corrosion layer can be separated from the total O–H band. The comparison between the infrared spectra for leached samples and hydroxides of the glass components show the presence of Zr–OH and La–OH groups in ZrF$_4$-based glasses after leaching and drying and of Th–OH groups in ThF$_4$ glass, indicating the existence of F$^-$/OH$^-$ ion exchange between the glass surface and water.

I. Introduction

HEAVY-METAL fluoride (HMF) glasses are strong candidate materials for optical waveguides because of their excellent transmission characteristics extending from the near-UV to the mid-IR, and their promise of lower attenuation at long wavelengths. However, these benefits are diminished by their relatively poor chemical durability, when compared to silicate glasses. It is essential to gain an understanding of the mechanisms involved in the corrosion process before control, or an improvement, of the chemical durability of these new materials can be affected. The chemical corrosion process in these glasses consists of many interacting reactions. We present here an analysis of hydrolysis at the glass–water interface.

The first results of aqueous leach tests on a fluorozirconate glass[1] suggested that (a) the corrosion occurs primarily by matrix dissolution, (b) the rapid penetration of water into the glass leads to the formation of a porous, poorly protective hydrated layer, called the transform layer, (c) under static leaching conditions, a crystalline outer layer develops due to a dissolution–reprecipitation process, and (d) a sharp decrease in solution pH arises from an F$^-$/OH$^-$ ion exchange. Subsequent studies reported by Frischat et al.[2] on the reaction of ZrF$_4$-based glasses with water lend support to these findings. More recently, several surface crystals contained in the precipitation layer were identified by scanning electron microscopy and X-ray diffraction to be ZrF$_4$·[1] and BaZrF$_6$.[4,5] This indicates that at least some of the glass components are being dissolved directly as fluorides (i.e., ZrF$_x^{4-x}$) without any prior hydrolysis step.

Recent studies by Simmons[3,6] developed a corrosion model involving the hydrolysis of dissolved fluorides (mainly ZrF$_4$) to account for the rapid decrease in solution pH and the drastic increase in leaching rate resulting from the increased solubility of the glass components in acidic media. The species formed in solution appear to be ZrF$_x$(OH)$_y^{4-x-y}$. Simmons described the pH drift as resulting from successive hydrolyses of zirconium fluoride and

determined that, on the average, two OH's are exchanged per Zr in solution. Since the presence of hydroxyfluorides has been determined for dissolved species, indicating an OH$^-$/F$^-$ ion exchange in solution, there are expectations of finding similar mixed species in the glass transform layer as a result of the exchange of OH$^-$ in solution for F$^-$ in the glass.

Investigations of the increase in surface hydration of leached samples as a function of the time and temperature of corrosion have been reported.[7,8] These studies, comparing the relative amplitudes of the OH and HOH absorption bands in leached fluorozirconate glasses (plotted as absorbance = log (T_0/T)), found that, despite an increase in absorbance with time, the ratios of peak heights for the stretching and bending vibrations yielded a constant (i.e., ~2.9). It has been suggested that the OH infrared absorption might be due exclusively to the presence of molecular water in the hydrated layer and not to the formation of metal–OH species. However, a recent study[9] of the application of a fluorozirconate glass as a fluoride-ion-selective electrode indicates the occurrence of anion exchange in the glass.

The aim of the present investigation is to study, by Fourier transform infrared (FTIR) spectroscopy, the reaction of ZrF$_4$- and ThF$_4$-based glasses, with water, and the possible formation of hydroxyl species in the glass surface during corrosion. It has been shown that these two families of fluoride glasses exhibit many similarities, and some differences, in their dissolution behavior.[10] The corrosion conditions, described below, were selected to prevent the formation of a precipitation layer in order to study the transform layer exclusively.

II. Experimental Technique

(1) Glass Preparation

The glass samples, whose compositions and commonly used mnemonics are given in Table I, were provided by the same laboratory and were all prepared from the fusion of oxide raw materials with added ammonium bifluoride.[11,12] The glasses were cast in a brass mold and annealed. Rectangular bars were polished on all sides to a 1-μm finish using diamond paste in water. The bars were cut into flat plates (15 by 10 by 4 mm) with polished faces. One ZBLA sample was repolished with diamond paste in oil (water and oxygen free) to remove the original water-polished surfaces. The IR spectra recorded before and after repolishing were compared and found to be identical. It was determined that the small OH (3430 cm^{-1}) absorption seen in the initial spectrum of this glass is due to water impurities in the bulk and not to surface reactions resulting from polishing in water.

(2) Procedure

The corrosion tests were conducted under highly dilute and

Table I.   Composition of Glass Samples

Mnemonic	Composition (mol%)						
	ZrF$_4$	ThF$_4$	BaF$_2$	LaF$_3$	AlF$_3$	YbF$_3$	ZnF$_2$
ZBL	62		33	5			
ZBLA	57		35	4	4		
BZYbT		27	19			27	27

Source   Laboratoire de Chimie Minérale D, Rennes, France.

Table II. Leaching Conditions

Mnemonic	Deionized water flow rate (L/h)	Temperature (°C)	pH	Figure
ZBL	9	27	5.3–5.4	3, 4, 5
ZBLA	9	27	5.3–5.4	1, 2, 3, 5, 7
BZYbT	2	100	5.6	6, 7

well-stirred conditions in order to minimize solution pH drop and its associated increase in glass leaching rate resulting from an increased solubility of the glass components. These conditions also eliminate the complication arising from the formation of crystalline surface deposits due to supersaturation at the glass–solution interface. Under high-dilution conditions, only a transform layer enriched with water forms at the glass surface.

Bulk samples were suspended in a 1000-mL polymethylpentene container. Fresh, constantly stirred deionized water was supplied at a rate of 9 L/h for the fluorozirconates and 2 L/h for the more durable BZYbT glass. Solution pH was monitored for each test. Since solution pH drift accompanies the buildup of corrosion products in solution, and both lead to complication of the leaching process,[3,6,10] the flow rates were selected to minimize solution pH drift, guaranteeing an adequate removal of dissolved species. Fluorozirconate samples were leached for different periods of time, resulting in total (or additive) immersion times of from ½ to 220 h; BZYbT leach tests extended to times of 30 d. The corrosion conditions are given in Table II. The corroded glass samples were removed from the solution at various intervals and rinsed briefly in methanol followed by toluene, in order to remove adhering liquid from the surface before recording spectra. As a final test, the corroded samples were heated in a hot stage under flowing N_2; transmission spectra were recorded in situ after a 5-min hold at each temperature to ensure equilibration.

(3) Measurements

FTIR is a very useful technique for investigating the reaction of water with glass and for studying the glass surface (e.g., for silicate systems, see Ref. 13). The IR spectroscopic study reported here was performed on a spectrometer* with a data analyzer. Scans of the order of 15 min corresponded to an accumulation of 500 spectra and led to an improvement in signal-to-noise ratio of a factor of 22 over a single scan. The optical measurements were recorded under flowing dry N_2.

In order to identify the different absorption phenomena, a spectrum of H_2O was recorded using a ZnSe liquid cell. KBr pellets containing 1% by weight of oxides and hydroxides of the glass components were prepared, and their spectra were recorded in the transmission cell used for the glass samples (see Table III). The spectrum of a pure KBr pellet was recorded and used for background subtraction.

III. Results

The series of glasses studied exhibit an order of leaching rate,

---

*Model 120-SXB, Nicolet Analytical Instruments, Madison, WI

with respect to the composition (ZBL · ZBLA ≫ BZYbT), which has been determined by previous soaking solution analyses.[5,10] The thorium-based glass is about 100 times more resistant to corrosion by liquid water than the zirconium-based series.[10,14,16] This is due, primarily, to its lower component solubility and the fact that the corrosion products tend to acidify the solution less than for fluorozirconates.

(1) ZrF₄-Based Glasses

Infrared transmission curves for the ZBLA glass are plotted as a function of cumulative immersion time in deionized water (Fig. 1). During the time of the measurements the pH value of the leaching solution remained constant at about 5.3, whereas the deionized input water pH was originally 5.7, indicating that glass dissolution was occurring at a constant rate. The broad absorption band, with a maximum intensity at 3430 cm^{-1}, corresponds to the fundamental stretching vibration of O–H bonds, and the peak at 1630 cm^{-1} corresponds to the bending vibration of molecular water in the transform layer. A weak, broad band at about 2100 cm^{-1} that appears at longer leaching times is also present in the IR spectrum of water. The appearance of these first two absorption bands is now well-known in the study of the corrosion of fluoride glasses. Their intensity and width, especially in the case of the OH band, grow with increasing time. The transmission base-line decrease with exposure time is due to scattering losses as a result of the increasing roughness of the corroded surface. A comparison of the relative areas of these bands, with the spectrum of water, enables us to separate the contribution of molecular water from that due to metal hydroxyls in the O–H stretching absorption band. Previously published measurements reported the increasing values of OH "absorption" with corrosion time;[17] however, since the sample surfaces appear to be well covered with crystal precipitates (see Figs. 3 and 5, Ref. 17), it is not possible to be certain that the measured OH absorbance is due exclusively to water contained in the transform layer. As mentioned previously, studies based on the Beer–Lambert law and peak height values[18,19] indicate the OH/HOH ratio as a constant. These results by Loehr et al. were confirmed when, by plotting log (T_0/T) versus time for ZBLA using peak amplitude, we obtained a constant OH/HOH ratio of 3 ± 0.1, in good agreement with their value of 2.9. However, since the stretching band exhibits a significant broadening with increasing intensity, the peak height alone is insufficient to yield a measure of the concentration of absorbing species.

Absorption peaks are generally recorded by spectroscopic instruments as transmittance or absorbance. From the Beer–Lambert law, the absorbance, A, is proportional to the molar concentration, c, of the absorbing species, whose extinction coefficient is ξ, as follows:

$$A = \log \frac{I_0}{I_t} = 0.4343\xi cl - 2 \log (1 - R) \tag{1}$$

where I_0 and I_t are the incident and transmitted intensities, respectively, l is the thickness of the absorbing layer, and R is the surface reflection coefficient of the sample (approximately 3% in the mid-IR for polished surfaces). Variations in the environment of the vibrating species will, however, cause shifts in the normal mode vibration frequencies and broaden the absorption spectrum. This could also result from the presence of different hydroxyl

---

Table III. Characteristic Frequencies for Hydroxides and Oxides

Compound	Characteristic absorption (cm^{-1})*
Al(OH)₃	3630–3200 stg, M; 1400–1250 wk; 1070–950 stg, <880 stg, M
Ba(OH)₂	3560 stg, sp; 3450–2600 stg, bd; 1700–1550 wk; 1500–1430 wk; <1100 m, M
La(OH)₃	**3610 stg, sp**; 3580–3150 m, bd; 1650–1100 m, M; <800 m, M
Th(OH)₄	3620–2800 stg, bd; **1650–1250 stg**, D; <900 stg, bd
Zn(OH)₂	3500–2700 stg, bd; 2250–2050 wk, M; 1100–1000 stg, D; <850 stg, M
Zr(OH)₄	3630–2800 stg, bd; 1630 m (H₂O), **1600–1300 m**, D; <800 stg, bd
ThO₂	1400±1000 wk, D; <600 stg, bd
ZrO₂	<900 stg, M

*stg = strong, m = medium, wk = weak, bd = broad, sp = sharp, D = doublet, M = multiple. Boldface data refer to absorption peaks matched to data in Figs. 3, 5, and 6.
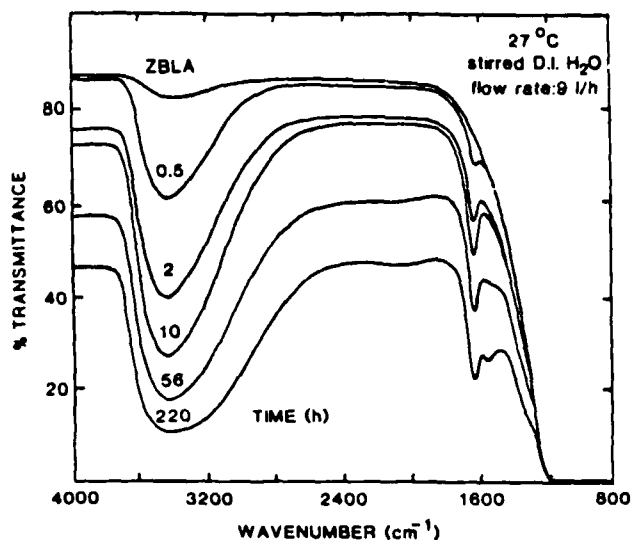
Fig. 1. FTIR spectra of ZBLA glass versus total immersion time in deionized water.

Fig. 2. Evolution with immersion time in water of the total OH integrated absorption peak area at 3430 cm^{-1}, metal OH and water OH peak areas at 3430 cm^{-1}, and HOH peak area at 1630 cm^{-1}.

species (such as metal hydroxides). In this case, the concentration of absorbing species must be calculated from the entire absorption band which coincides with the integrated amplitude of the absorbance peak. While the reflection coefficient for polished faces is negligible, our data show an increase in scattering with degree of corrosion. However, this effect is additive and can be separated from the integral by judicious choice of a base line.

In this work we calculated and compared the integrated areas of the absorbance bands. The HOH bending vibration peak partly superposes the multiphonon edge, but the additivity of the two absorption phenomena allows an accurate measure of the integrated intensity of this band. For molecular water the ratio of the integrated areas of the 3430- to the 1620-cm^{-1} bands is a constant independent of concentration. This was confirmed by measuring this ratio in a series of mixtures of water and acetone, respectively: 75/25, 50/50 (v/v). These exhibited the same ratio as pure water (9.4 ± 0.4), when measured as previously described. The relative contribution of water hydroxyls in the total OH absorbance (3430 cm^{-1}) was calculated from the HOH (1630 cm^{-1}) peak integrated area of the leach samples and the OH/HOH integrated area ratio of molecular water:

$$R_w = \sum{}^{3430} A[OH] \Big/ \sum{}^{1620} A[HOH] \qquad (2)$$

where $\sum{}^x$ is the integral over the peak whose maximum is at x wavenumber and A is the absorbance. (Note that the peak position is shifted slightly for HOH in glass compared to molecular water.)

The contribution of metal hydroxyls was deduced assuming the total OH integrated absorbance in the corroded glass to be the sum of the metal hydroxyl (MOH) and water hydroxyl peak integrated areas:

$$\sum{}^{3430} A[MOH] = \sum{}^{3430} A[\text{total OH}]$$

$$-R_w \sum{}^{1630} A[HOH] \sim \sum{}^{3430} A_d[\text{glass}] \qquad (3)$$

where A_d[glass] is the absorbance measured in the uncorroded glass. The concentration, c, of MOH species in the transform layers on both faces is thus proportional to the resulting difference in integrated absorbance as calculated in Eq. (3).

$$c_{MOH} \propto \sum{}^{3430} A[MOH] \qquad (4)$$
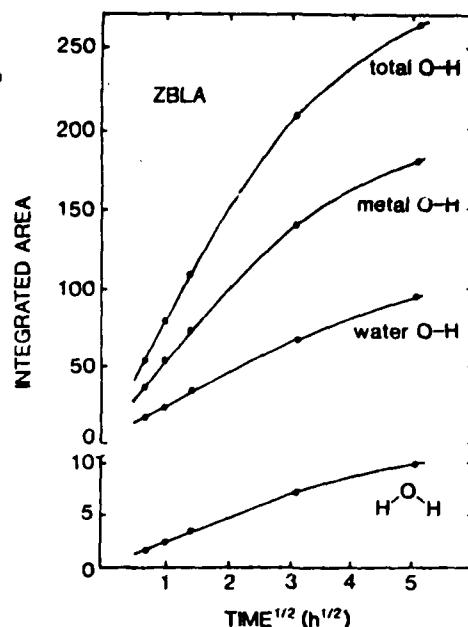
It should be noted that since the thickness of the transform layer grows with time, the proportionality constant in Eq. (4) will decrease with time. However, since we cannot accurately measure the depth to which each reaction occurs, our analysis is based on their relative contributions to the total absorbance, not on absolute concentrations, and the layer thickness can be neglected.

The values for integrated areas versus time$^{1/2}$ are plotted in Fig. 2. The percentage contribution of metal hydroxyls to the total OH band has been evaluated to be 73% initially, decreasing to 63% at longer times. The rate of penetration of molecular water into the transform layer follows a square-root dependence on time for the first 10 h before decreasing. This may imply a simple diffusion control during the early stages of layer formation, while at longer times some of the pathways may become blocked through precipitation of dissolved species. The fact that the linearity is not followed at 26 h may also be explained, in part, by the partial overlapping of the HOH peak at 1630 cm^{-1} with the band at 1550 cm^{-1}, which diminishes the accuracy in the calculation of the integrated area. The rate of formation of metal hydroxyls, although rapid initially, is seen to decrease after 2 h. This decrease is thought to result from changes occurring in the aqueous environment within the transform layer as hydrolysis leads to an increase in F concentration and a decrease in pH.

Figure 1 shows other absorption phenomena that appear at longer wavelengths: a peak at 1550 cm^{-1} and a shoulder on the multiphonon edge at about 1340 cm^{-1}. The latter has been reported[19] and attributed to a metal–oxygen bond. However, the clearly visible absorption band at 1550 cm^{-1} has not been identified previously. In order to determine the origin of these bands we recorded, systematically, the IR transmission spectra of KBr pellets containing the different glass components as oxides and hydroxides (Table III). A comparison of the transmission spectrum of the ZBLA glass leached for 220 h with that of Zr(OH)$_4$ at 1550 and 1340 cm^{-1} (Fig. 3) shows excellent agreement in peak positions. The transmission curve of the ZBL glass corroded for 44 h under the same conditions (Table II) confirms this result. Thus we can propose not only that the transform layer contains hydroxyls, but also that it contains, specifically, Zr–OH bonds.

Figure 4 shows the spectra of ZBL 44 (leached 44 h in deionized water) after in situ heat treatments at 60°, 80°, 100°, and 150°C
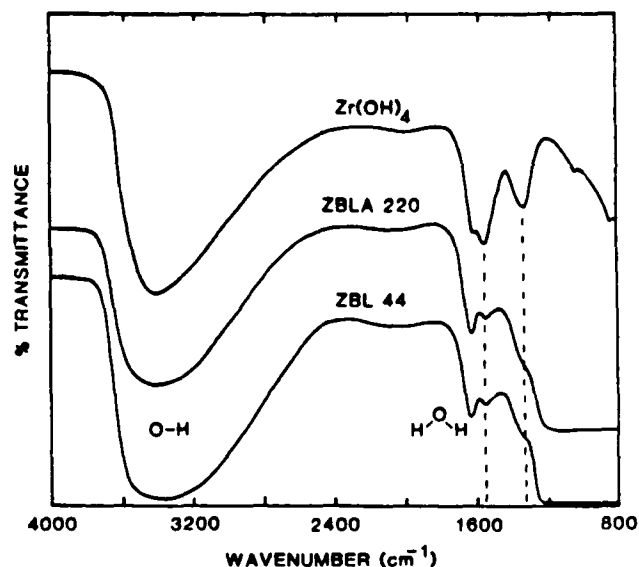
Fig. 3. FTIR spectra of ZBLA glass leached for 220 h, ZBL glass leached for 44 h, and Zr(OH)₄ in a KBr pellet.
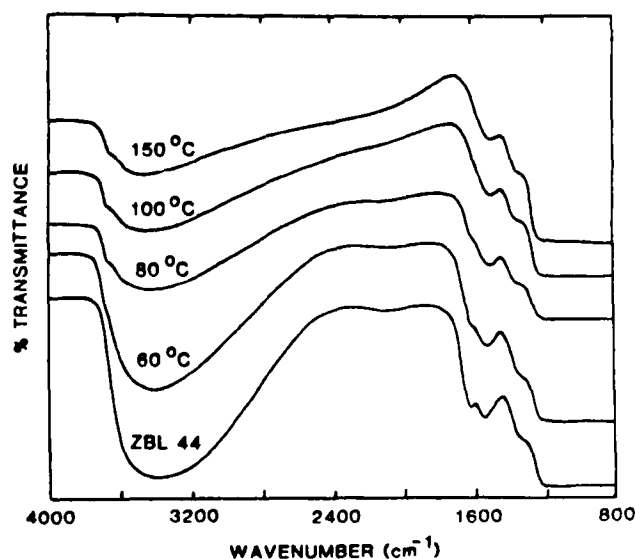
Fig. 4. FTIR spectra of ZBL 44 glass dried under nitrogen.

under N_2 atmosphere. It should be noted that the spectra have been shifted along the transmittance axis to improve clarity. The band at 1630 cm^{-1}, corresponding to molecular water, decreases rapidly in intensity during drying and is no longer apparent on the spectrum recorded at 150°C. The broad band at 3430 cm^{-1} also decreases and its maximum intensity is slightly shifted to higher wavenumbers, to 3470 cm^{-1}. The first value, 3430 cm^{-1}, corresponds to the peak position of the overlapping water OH groups. The rapid decrease of these absorption bands indicates that molecular water is very poorly hydrogen bonded in the transform layer. As the OH band decreases, in both amplitude and width, with increasing drying temperature, a shoulder at about 3620 to 3630 cm^{-1} is revealed. This result has also been observed for the same heat treatment carried out on the ZBLA 220 glass. Figure 5 shows the alignment of the shoulder in both ZBLA 220 and ZBL 44 glass with the peak at 3610 cm^{-1} present in the transmission spectrum of La(OH)₃ in KBr, indicating the presence of La–OH groups in the transform layer of the glass after drying.

(2) ThF₄-Based Glasses

The same measurements were performed on the BZYbT glass, whose composition is given in Table I. Because of the higher durability, the leaching tests were conducted under a stream of deionized water for which the flow rate and the temperature were controlled to maintain boiling water in the container, the pH value under these conditions remained about 5.6 (Table II). Figure 6 shows the variation of the IR transmittance with leaching time, on the same scale. The OH and HOH absorption bands appear at 3420 and 1630 cm^{-1}, respectively. The ratio OH/HOH, determined by Eq. (3), is higher than in the ZrF₄-based glasses, indicating that the contribution of OH due to surface hydration (i.e., molecular water) is smaller. The percentage of metal hydroxyls is about 90% of the total OH band. Two other weak bands appear at 1490 and 1370 cm^{-1}. Through a comparison with the oxides and hydroxides of the glass components, these can be traced to the presence of thorium hydroxyls. As in the case of ZrF₄-based glasses, these two bands are not specifically assigned to Th(OH)₄ in the glass but

Fig. 5. FTIR spectra of dried ZBLA 220 and ZBL 44. Comparison with La(OH)₃ in a KBr pellet.
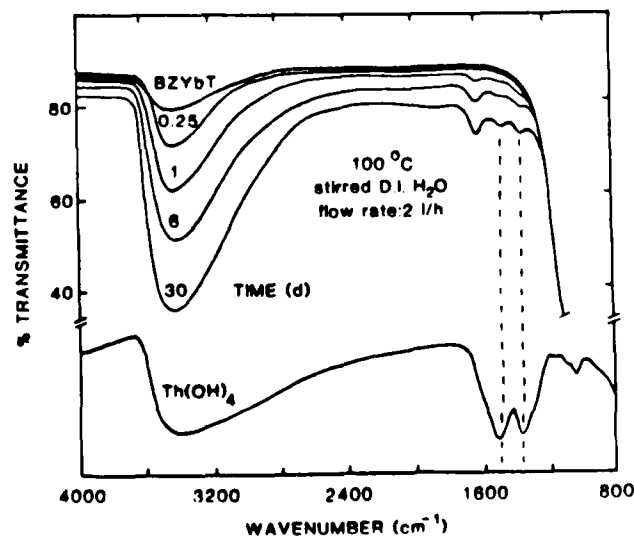
Fig. 6. FTIR spectra of BZYbT glass versus total immersion time in deionized water. Comparison with Th(OH)₄ in KBr pellet.

involve Th–OH species. A heat treatment was performed, as previously described, in the BZYbT glass leached for 30 d in boiling water. The transmission curves show a similar decrease in intensity for both OH and HOH bands, while the weak bands at 1490 and 1370 cm⁻¹ are not significantly affected.

IV. Discussion

The study of the corrosion of ZrF_4- and ThF_4-based glasses by FTIR spectroscopy shows mainly that, in both cases, formation of the hydroxide of the glass former metal occurs. Under the experimental conditions described above (flow of well-stirred deionized H_2O, pH ≈ constant), no local supersaturation, and therefore, no precipitation layer, can develop. Thus metal–OH groups are shown to exist in the transform layer and to account for a large portion of the OH band absorption. The leaching tests also show that the transform layer is enriched with water, whose contribution to the total OH absorption has been evaluated at 27% to 37% for fluorozirconate and 10% for BZYbT.

In the case of ZBLA and ZBL, the existence of the formation of $ZrF_x(OH)_y^{4-x-y}$ in solution was shown as a step in the corrosion process.[5] The presence of Zr–OH groups in the corroded layer now shows that the exchange of OH⁻ in solution with F⁻ from the glass also occurs. The presence of Zr–OH groups in the glass cannot be explained by the reprecipitation of hydroxyfluoride species in the soaking solution, because they are constantly removed from the surface and the solution by flow. The second main component of the glass is BaF_2, but the IR spectroscopic study did not show the presence of the corresponding hydroxide in the layer. Here an ion-exchange reaction may also occur; however, the high solubility of barium hydroxide in water could explain its absence from the transform layer. This is supported by the solution chemical analysis previously reported[5] showing that barium is rapidly depleted from the surface.

As far as La and Al are concerned, it is difficult to differentiate between their OH absorption bands by IR spectroscopy because of the overlapping of their sharp peaks at 3610 cm⁻¹. The spectra of ZBL and ZBLA glasses after heat treatment both show a shoulder at about that wavenumber. But the highly preferential normalized leach rate of Al compared to La[1,5] and its depletion from the surface show that the shoulder in Fig. 5 is more likely to be due to La–OH groups (rather than Al–OH) in the transform layer.

These results clearly contribute to confirmation of the role of the anion exchange between the F⁻ ions from the glass surface with OH from the water in the corrosion process, and are in good agreement with the study of Ravaine and Perera,[9] and recent work by Brow and Pantano,[20] who investigated, by XPS and semiquantitative analysis, the formation of zirconium (hydr)oxyfluoride species $(ZrF_x(OH)_{m-x})$ through hydrolysis reactions at the surface of a ZrF_4-based glass.

Figure 4 shows the decrease in the absorption in ZBL 44 as a function of the drying heat treatment. The OH band intensity decreases drastically as does the HOH band which is no longer apparent after drying at 150°C. The 1550-cm⁻¹ band decreases slightly and the 1340-cm⁻¹ band is not significantly modified at the temperatures reached by using the hot stage. The same treatment performed on a $Zr(OH)_4$-KBr pellet gave the identical result, confirming the correlation between both 1550- and 1340-cm⁻¹ bands with $Zr(OH)_4$. No further absorption phenomenon appears, and none increases in intensity. This is probably due to the fact that the maximum temperature reached by the hot stage (less than 200°C) was not sufficient to lead to the reaction

$$\overset{|}{\underset{/|\diagdown}{Zr}}-OH + HO-\overset{|}{\underset{/|\diagdown}{Zr}} \;\overset{\Delta}{\to}\; \overset{|}{\underset{/|\diagdown}{Zr}}-O-\overset{|}{\underset{/|\diagdown}{Zr}} + H_2O\uparrow \tag{5}$$
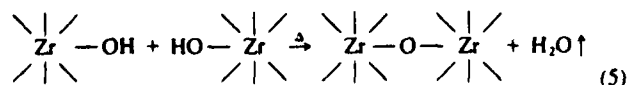
In the case of BZYbT, previous corrosion studies have shown that the leach rate order is Zn ≈ Ba > Yb ≈ F ≫ Th, the concentration of the last element being close to detection limits in the analysis of the soaking solution,[10] so that the surface is particularly rich in Th. This result is consistent with the fact that our study
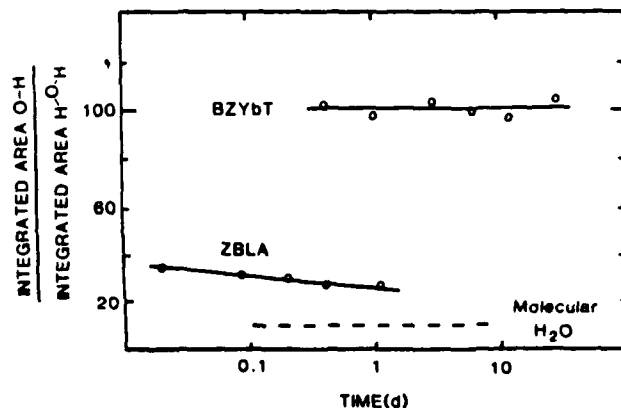
Fig. 7. Evolution of OH/HOH absorbance ratio for ZBLA and BZYbT. Comparison with the molecular water ratio.

shows a large concentration of thorium hydroxyls. The drying heat treatment, under the same conditions described above, showed an expected decrease in absorbance for both the OH and HOH bands. No further peak or shoulder appears, indicating clearly that the shoulder at about 3620 cm⁻¹ previously noted in ZBL and ZBLA glasses is not correlated to the presence of barium, which is the only common cation for both glass families. No other hydroxyls have been specifically determined; this may be explained by the fact that at a pH value of 5.6 (that remained roughly constant during the leaching tests) the hydrolysis of the glass involves ThF_4 solely,[21] while the other components present either do not undergo this reaction or dissolve into solution from soluble hydroxyl species.

The water content of the BZYbT corroded surface is much lower than in the case of ZrF_4-based glasses under these high-dilution conditions, as well as in static conditions[10] and under exposure to water vapor.[18]

Figure 7 shows the evolution of the OH/HOH integrated areas ratio versus time for ZBLA and BZYbT, and the dotted line represents the value of the ratio in molecular water. The ratio decreases slightly for ZBLA, but it remains roughly constant for BZYbT. For ZBLA, the water of hydration trapped in the transform layer has a more acidic pH than the stirred soaking solution. This acidity increases, with time and increasing layer thickness, and enhances the local dissolution of hydroxides formed. It may also explain the slight drop in the OH/HOH absorbance ratio. Furthermore, as the dissolved [F⁻] increases, Zr–F dissociation is inhibited. For the BZYbT glass, measurements show a lower percentage of molecular water in the transform layer and show that the leaching process leads to a less severe pH drift. Since the OH/HOH integrated absorbance ratio remains constant with increased leaching time, it can be concluded that the growth rate of the layer consists of equal rates of water penetration and metal hydroxyl formation.

The relative extent of the hydrolysis reaction for both ZBLA and BZYbT can be compared for the same degree of hydration, determined by the HOH peak integrated area. ZBLA leached 0.5 h and BZYbT 30 exhibit roughly the same $\Sigma A[HOH]$ value. We have estimated that the term $\Sigma A[MOH]$ is about 4 times greater in the case of BZYbT, indicating that it has fixed 4 times more hydroxyl groups per unit volume.

Figure 4 shows that in the case of the OH absorption band, because of the overlapping of the HOH band at 1630 cm⁻¹ with the 1550 cm⁻¹ band, the term $\Sigma A[HOH]$ (Eq. (3)) cannot be accurately estimated and therefore the respective contributions of metal and water hydroxyls during the first steps of the drying treatment cannot be calculated. However, the fact that the transmission curve recorded at 150°C no longer exhibits the HOH band indicates that the OH absorption is due entirely to metal hydroxyls at that point in the treatment. The decrease in the total integrated area of the OH stretching band is about 80% of that recorded for the room-temperature ZBL 44 leached sample. This indicates a

large reduction in the metal–OH concentration in the transform layer in addition to the loss of molecular water due to evaporation. In the case of ZBLA 220, the same analysis and calculations evaluated the total OH band in the dried sample at 28% of the total OH for ZBLA 220 before drying. Since our room-temperature measurements determined [MOH] to be 63% of the total area, it is apparent that the initial [MOH] has decreased by a factor of 2.25. The same calculations indicate a decrease of a factor of 4.5 for [MOH] in the case BZYbT 30. If we assume that the dehydration process involving reaction (5) does not occur in our experimental temperature range, the decrease of the metal hydroxyl concentration can be explained by (1) the dissolution of the hydroxyfluoride species or (2) the reversibility of the hydrolysis reaction. The first reaction may occur as a result of a decreasing pH with decreasing water concentration in the layer. The reaction can be followed by a reprecipitation due to saturation of the fluoride species formed:

$$MF_{4+x}^{-x}(gl) + H_2O \rightarrow MF_{4+x-y}(OH)_y^{-x}(gl)$$

$$+ [y(H^+,F^-) + (1-y)H_2O](sol) \qquad (6)$$

$$\xrightarrow[\;H_2O\uparrow\;]{\Delta}$$

$$MF_4(precip) + xF^- + yH_2O \leftarrow$$

$$[M^{4+} + (4+x)F^- + yH_2O](sol) \qquad (7)$$
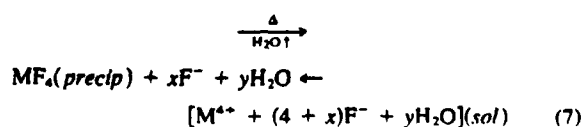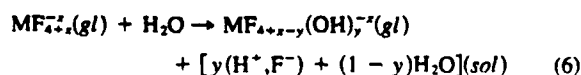
(Note that (gl) refers to the glass and (sol) to the solution in the transform layer.)

The second possibility is that, during evaporation, the concentration in F^- contained in the "water of hydration" increases and may lead to the reversibility of the reaction (according to the fact that, at equilibrium, the excess of one constituent in a reaction leads to its consumption and determines the direction of the reaction):

$$MF_{4+x}^{-x}(gl) + H_2O \rightarrow MF_{4+x-y}(OH)_y^{-x}(gl)$$

$$+ [y(H^+,F^-) + (1-y)H_2O](sol)$$

$$\xrightarrow[\;H_2O\uparrow\;]{\Delta}$$

$$MF_{4+x}^{-x}(gl) + yH_2O \leftarrow MF_{4+x-y}(OH)_y^{-x}(gl) + [y(H^+,F^-)](sol)$$

$$(8)$$
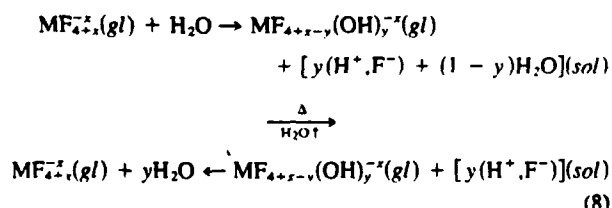
Figure 4 shows that the two absorption bands at 1550 and 1340 cm^{-1} (clearly present on the spectrum of Zr(OH)$_4$, Fig. 3) do not exhibit exactly the same behavior during the drying treatment. If we assume that the decrease in intensity of the first one is due to the reversibility of the reaction (Eq. (8)) concerning hydroxyfluoride species, the second band at 1340 cm^{-1}, which is less affected, may involve bridging oxygen species (very likely present in zirconium hydroxide).

V. Conclusion

The evolution of the hydrolysis reaction of ZrF$_4$- and ThF$_4$-based glasses has been investigated by FTIR spectroscopy, on glass samples leached in high-dilution and stirred conditions. Zirconium and lanthanum hydroxyls are present in the transform layer of ZBL and ZBLA glasses and thorium hydroxyls have been identified in BZYbT glass. By calculation of the integrated areas of the OH stretching and H$_2$O bending absorption peaks, the contribution of metal hydroxyls was determined at about 70% and 90% of the total OH band for ZBLA and BZYbT, respectively, indicating the importance of the ion exchange between F$^-$ ions on the glass surface and OH$^-$ ions in water, according to the reaction

$$F\ (gl) + OH^-(sol) \rightarrow OH\ (gl) + F^-(sol).$$

The drying heat treatment carried out in situ at temperatures below 200°C appears to lead to the reversibility of the reaction to a large extent. The reactions occurring in the transform layer during leaching followed by drying at these temperatures are

proposed to be
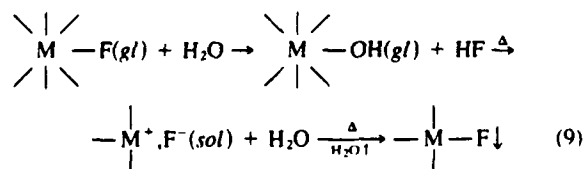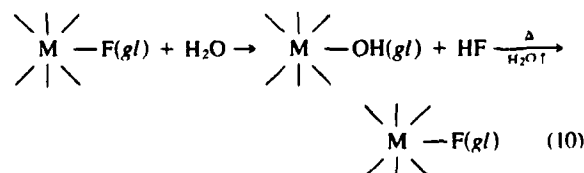
$$M-F(gl) + H_2O \rightarrow M-OH(gl) + HF \xrightarrow{\Delta}$$

$$-M^+,F^-(sol) + H_2O \xrightarrow[\;H_2O\uparrow\;]{\Delta} -M-F\downarrow \qquad (9)$$

or

$$M-F(gl) + H_2O \rightarrow M-OH(gl) + HF \xrightarrow[\;H_2O\uparrow\;]{\Delta}$$

$$M-F(gl) \qquad (10)$$

References

[1] C. J. Simmons, H. Sutter, J. H. Simmons, and D. C. Tran, "Aqueous Corrosion Studies of a Fluorozirconate Glass," *Mater. Res. Bull.,* **17,** 1203–10 (1982).
[2] G. H. Frischat and I. Overbeck, "Chemical Durability of Fluorozirconate Glasses," *J. Am. Ceram. Soc.,* **67** [11] C-238–C-239 (1984).
[3] R. H. Doremus, N. P. Bansal, T. Bradner, and D. Murphy, "Zirconium Fluoride Glasses Surface Crystals Formed by Reaction with Water," *J. Mater. Sci. Lett.,* **3** [6] 484–88 (1984).
[4] D. G. Chen, C. J. Simmons, and J. H. Simmons, "Corrosion Layer Formation of ZrF$_4$-Based Fluoride Glasses"; pp. 315–20 in Proceedings of the 4th International Symposium on Halide Glasses, Monterey, CA. Edited by M. G. Drexhage, C. T. Moynihan, and M. Robinson. TransTech Publications, Aedermannsdorf, Switzerland. 1987.
[5] C. J. Simmons and J. H. Simmons, "Chemical Durability of Fluoride Glasses I. Reaction of Fluorozirconate Glasses with Water," *J. Am. Ceram. Soc.,* **69** [9] 661–69 (1986).
[6] C. J. Simmons, "Chemical Durability of Fluoride Glasses: III. The Effect of Solution pH," *J. Am. Ceram. Soc.,* **70** [9] 654–61 (1987).
[7] S. R. Loehr, A. J. Bruce, R. Mossadegh, R. H. Doremus, and C. T. Moynihan, "IR Spectroscopic Studies of Attack of Liquid Water on ZrF$_4$-Based Glasses"; pp. 311–22 in Proceedings of the 3rd International Symposium on Halide Glasses, Rennes, France, 1985. Edited by J. Lucas and C. T. Moynihan. TransTech Publications. Aedermannsdorf, Switzerland, 1986.
[8] A. J. Bruce, S. R. Loehr, N. P. Bansal, D. M. Murphy, C. T. Moynihan, and R. H. Doremus, "IR Measurements of the Rate of Surface Layer Development on ZrF$_4$-BaF$_2$-LaF$_3$ Glass in Aqueous Solution"; Extended Abstracts, 2nd International Symposium on Halide Glasses, Troy, NY, 1983.
[9] D. Ravaine and G. Perera, "Corrosion Studies of Various Heavy-Metal Fluoride Glasses in Liquid Water: Application to Fluoride-Ion-Selective Electrode," *J. Am. Ceram. Soc.,* **69** [12] 852–57 (1986).
[10] C. J. Simmons, "Chemical Durability of Fluoride Glasses: II. Reaction of Barium-Thorium-Based Glasses with Water," *J. Am. Ceram. Soc.,* **70** [4] 295–300 (1987).
[11] M. Poulain and J. Lucas, "A New Family of Materials: ZrF$_4$-Based Fluoride Glasses," *Verres Refract.,* **32,** 505 (1978).
[12] G. Fonteneau, F. Lahaie, and J. Lucas, "A New Family of Infrared Transmitting Fluoride Glasses: Vitreous Fluorides in the System ThF$_4$-BaF$_2$-MF$_3$ (M = Mn, Zn)," *Mater. Res. Bull.,* **15,** 1143 (1980).
[13] G. Orcel, J. Phalipou, and L. L. Hench, "Structural Changes of Silica Xerogels During Low Temperature Dehydration," *J. Non-Cryst. Solids,* **88,** 114 (1986).
[14] C. J. Simmons, S. Azali, and J. H. Simmons, "Chemical Durability Studies of HMF Glasses"; Paper No. 47 in Extended Abstracts, 2nd International Symposium on Halide Glasses, Troy, NY, 1983.
[15] C. J. Simmons, J. Guery, and D. G. Chen, "Leaching Behavior of Heavy Metal Fluoride Glasses", pp. 329–34 in Proceedings of the 3rd International Symposium on Halide Glasses, Rennes, France, 1985. Edited by J. Lucas and C. T. Moynihan. TransTech Publications, Aedermannsdorf, Switzerland, 1986.
[16] D. Tregoat, G. Fonteneau, and J. Lucas, "Aqueous Corrosion of a HMFG," pp. 335–38 in Proceedings of the 3rd International Symposium on Halide Glasses, Rennes, France, 1985. Edited by J. Lucas and C. T. Moynihan. TransTech Publications, Aedermannsdorf, Switzerland, 1986.
[17] G. H. Frischat and I. Overbeck, "Chemical Durability of Fluorozirconate Glasses Against Aqueous Solutions"; pp. 299–303 in Proceedings of the 3rd International Symposium on Halide Glasses, Rennes, France, 1985. Edited by J. Lucas and C. T. Moynihan. TransTech Publications, Aedermannsdorf, Switzerland, 1986.
[18] P. S. Christensen, G. Fonteneau, and J. Lucas, "OH and H$_2$O in Fluoride Glasses: Determination of Molar Extinction Coefficients", pp. 303–15 in Proceedings of the 4th International Symposium on Halide Glasses, Monterey, CA. Edited by M. G. Drexhage, C. T. Moynihan, and M. Robinson. TransTech Publications, Aedermannsdorf, Switzerland, 1987.
[19] M. G. Drexhage, C. T. Moynihan, B. Bendow, E. Gbogi, K. H. Chung, and M. Boulos, *Mater. Res. Bull.,* **16,** 943 (1981).
[20] R. K. Brow and C. G. Pantano, "Surface Analyses of Corroded Fluorozirconate Glass" presented at the 89th Annual Meeting of the American Ceramic Society, Pittsburgh, PA, April 29, 1987 (Glass Division, Paper No. 117-G-87).
[21] C. F. Baes, Jr., R. E. Mesmer, The Hydrolysis of Cations. Krieger, Malabar, FL, 1986.

Appendix J

GLASS/WATER INTERFACE REACTIONS DURING THE
CORROSION OF FLUOROZIRCONATE GLASSES

BY

DIN-GUO CHEN

A THESIS PRESENTED TO THE GRADUATE SCHOOL
OF THE UNIVERSITY OF FLORIDA IN
PARTIAL FULFILLMENT OF THE REQUIREMENTS
FOR THE DEGREE OF MASTER OF SCIENCE

UNIVERSITY OF FLORIDA

1987

ACKNOWLEDGMENTS

TABLE OF CONTENTS

LIST OF TABLES

LIST OF FIGURES

Abstract of a Thesis Presented to the Graduate School
of the University of Florida in Partial Fulfillment of the
Requirements for the Degree of Master of Science

GLASS/WATER INTERFACE REACTIONS DURING THE CORROSION
OF FLUOROZIRCONATE GLASSES

By

Din-Guo Chen

August 1987

Chairman: Dr. Joseph H. Simmons
Major Department: Materials Science and Engineering

A study of the mechanisms of the fluorozirconate
glass/water interface reactions and the effects of
experimental variables, such as S/V ratio, static or flow,
stirring speed and temperature, on glass leaching behavior
has been conducted. In this study, fluorozirconate glasses
were exposed to various corrosion conditions for several
periods of time. Then the leachate and glass surface were
analyzed by various solution and surface analytical
techniques, such as ICP-AE, FTIR and SEM-EDS, to understand
the leaching mechanisms.

Solubility of the glass components, especially that of
ZrF_4, is the dominant factor controlling the chemical
durability of fluorozirconate glasses in aqueous
environments. It was found that, in the leaching process,
the glass begins to dissolve as soon as it comes into

contact with the solution. The degree of the dissolution depends upon the solution pH. A sharp pH excursion toward the acidic range will occur, especially in static conditions, due to the ion-exchange process of F^- and OH^- and the hydrolysis of the dissolved species in the solution, particularly ZrF_4. Both a thick precipitation layer and a transform layer can form with increasing corrosion time. The porous precipitation layer plays a minor role as a diffusion barrier for the dissolved species, while a thick transform layer can interfere with the leaching process and cause reprecipitation inside the layer.

In dynamic flow conditions, no thick precipitation layer was observed to form. Some precipitate crystals could be found if the stirring speed was not high enough to disperse the accumulation of the corrosion products in the solution film adjacent to glass surface. A gel-like layer enriched in Zr, La and their metal-hydroxyl groups was found on the glass surface due to the ion-exchange processes and high extraction rates of the soluble species. Colloidal precipitates, with a composition of higher Ba/Zr ratio than the bulk glass, can form within the transform layer. High temperature flow tests were also performed.

Based on the solubility gradient thought to exist in the solution within the transform layer, and in the bulk solution, and electrokinetic effects, a corrosion model is proposed.

CHAPTER I

INTRODUCTION

Infrared-transmitting glasses are of interest as
materials for a broad range of components, such as laser
windows, IR domes, laser hosts, lenses, filters and mid-IR
optical fibers. In particular, there are many promising
applications in both the industrial and military sectors for
mid-IR fiber optics, including ultralong repeaterless
underwater links, nuclear radiation resistant links, high-
capacity wavelength multiplexed fiber optics system, remote
IR focal plane arrays, IR laser devices, IR power delivery,
long-length fiber optics sensor systems, and nonlinear
optical elements. The attainment of these goals places
stringent requirements on the optical properties of
candidate materials: i.e. intrinsic absorption coefficients
of the order of α= 0.01 dB/Km are needed for some applica-
tions. Heavy metal fluoride glasses(HMFG) appear to be
among the promising candidate materials and have drawn a lot
of attention due to their excellent transparency. The
minimum intrinsic loss in high quality fibers is determined
by the intersection of two curves, see Fig.1.1,[1]
corresponding to the residual vibrational (or multiphonon)
absorption from the low frequency side and to the Rayleigh

1
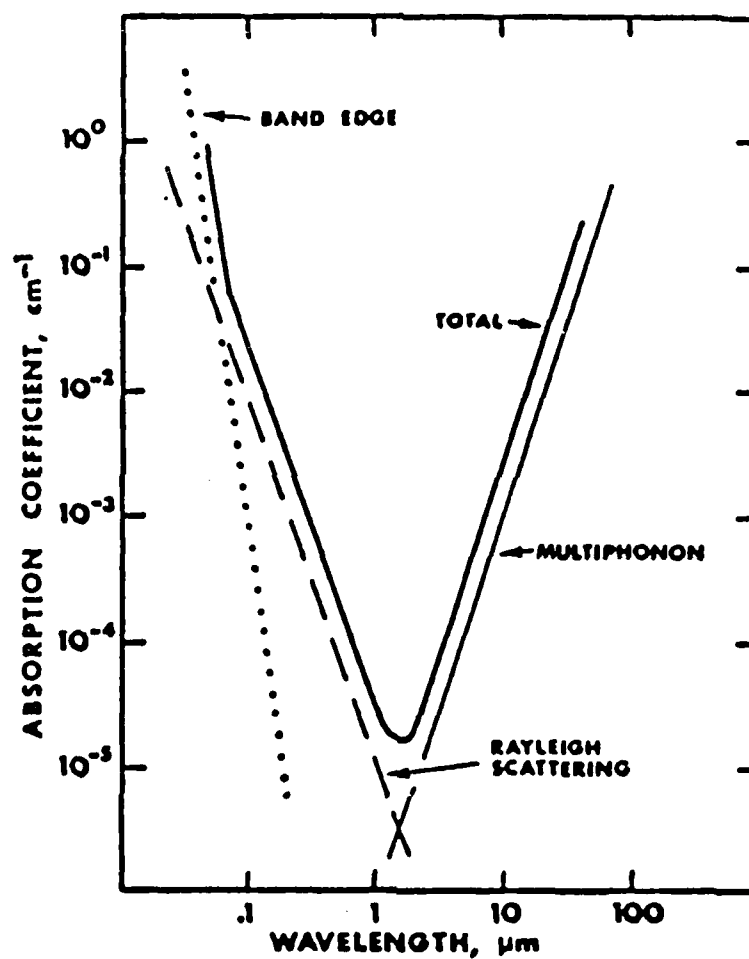
Figure 1.1. Schematic plot of intrinsic optical absorption
coefficient vs. wavelength in an insulator. (Drexhage et
al.[1])

scattering loss from the high frequency side.

The ZrF_4-based family of fluoride glass compositions, at present, promises the best opportunity for applications both in optical fibers and bulk optical elements. The typical glass transition temperatures of ZrF_4-based glasses are between 300°-340°C, much lower than those of oxide glasses, and consequently the frozen-in density fluctuations in fluoride glasses are lower than those in oxide glasses.[2] Therefore, the intrinsic Rayleigh scattering for fluoride glasses will be lower than silicates, despite a larger absolute scattering cross-section which is shown in the following equations:

$$I_{Rayleigh} = (c/n^4) \{[kT_f(\beta_T-\beta_S)+kT_f\beta_S^r]+[kT\beta_{\infty S}]\}$$
$$\beta_T-\beta_S = \alpha_f^2 T_f/\sigma_o c_{pf}$$

where n=wavelength; c=scattering cross-section; β_T=isothermal compressibility; β_S=adiabatic compressibility; $\beta_{\infty S}$=high frequency adiabatic compressibility; T_f=fictive temperature; β_S^r=relaxational adiabatic compressibility; α_f=expansion coefficient at T_f; c_{pf}=specific heat at T_f; σ_o=density.

For silicate glass fibers a loss minimum of about 0.2 dB/Km has been achieved. Since the Rayleigh scattering losses, which result from local imhomogeneities whose size is comparable to the wavelength of light, show a n^{-4} wavelength dependence, lower losses than obtained for

silicate glasses are possible when using materials which transmit light further into the infrared region, i.e. longer wavelengths of light. Fluoride compounds have been known to have better infrared transparency than oxides owing to the replacement of the light oxygen by the heavier fluorine atom. The glasses of interest contain heavy metal cations and thus show a greater IR transmission window. For instance, the fluorozirconates and fluorohafnates exhibit high transparancy from the ultraviolet to the mid-infrared (transmission between approximately 0.2 and 7 micrometer(μm) is achievable with certain compositions), while fused silica stops slightly above 3μm, see Fig.1.2.[3] HMFG glasses, therefore, offer the opportunity of a lower Rayleigh scattering loss by transmission at longer wavelengths, and consequently, the opportunity for much longer optical links.

Fluoride glasses, however, have two major intrinsic problems: The first problem is their high susceptibility to chemical attack. Because of the hygroscopic nature of fluoride components, they have much poorer chemical durability than silicate glasses in aqeous environments. This appears to be a severe limiting factor to their practical applications. The second problem is glass phase stability. Although fluoride glasses have the advantage of much lower liquidus temperatures, which rarely reach above 900°-1100°C, their relatively low viscosity at the liquidus makes them very susceptible to crystallization. The low
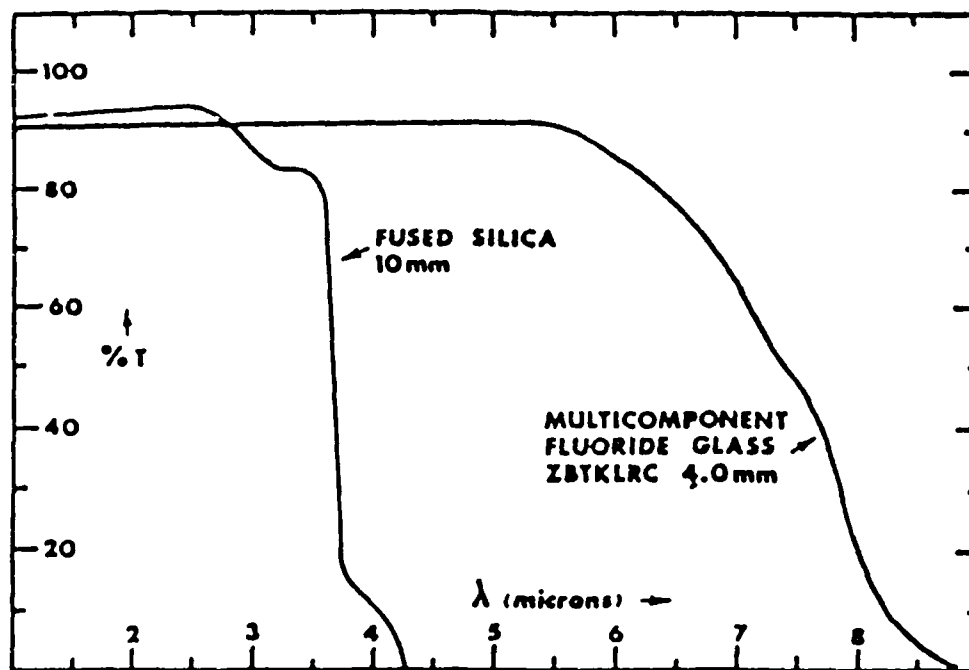
Figure 1.2. Infrared transmission spectra of fused silica (Suprasil W. Heraeus-Amersil Inc.) and a typical multicomponent fluoride glass.(Drexhage et al.[3])

temperature crystallization limit(Tx) of fluoride glasses is between 390°-450°C, yielding a broad range of temperatures (including the fiber-drawing temperature range) where crystallization is favored. A very steep viscosity increase in cooling below T_x yields a rapid approach to the glass transition temperature,Tg. The relative proximity of Tg and Tx in these glasses and the strong variation of viscosity with temperature result in devitrification during slow cooling from the melt, and thus limit the size of castings.

There are additional extrinsic loss problems: The first consists of impurities from melt contamination or from batch raw materials, which can cause extrinsic losses at shorter IR wavelengths(2-10μm) either due to bulk or surface absorption, see Fig.1.3.[4] Among them OH absorption is possibly the most important, since the absorption coefficients are very high and the peak wavelength is at 2.87μm close to the minimum intrinsic loss region. 3d transition metal impurities are another source of extrinsic absorption. In particular, Fe^{+2} , Co^{+2} , Ni^{+2} and Cu^{+2} introduce losses at 2.55μm. Fe is probably of most concern among them, since it is normally present at higher concentrations. Fortunately , by melting the glasses under oxidizing conditions, the Fe impurities are shifted toward the Fe^{+3} state which does not absorb at 2.55μm. Rare earth metal impurities can also cause absorption, in particular Pr, Nd, Sm, Eu, Tb and Dy absorb near 2.55μm. Of these Nd is the worst offender,
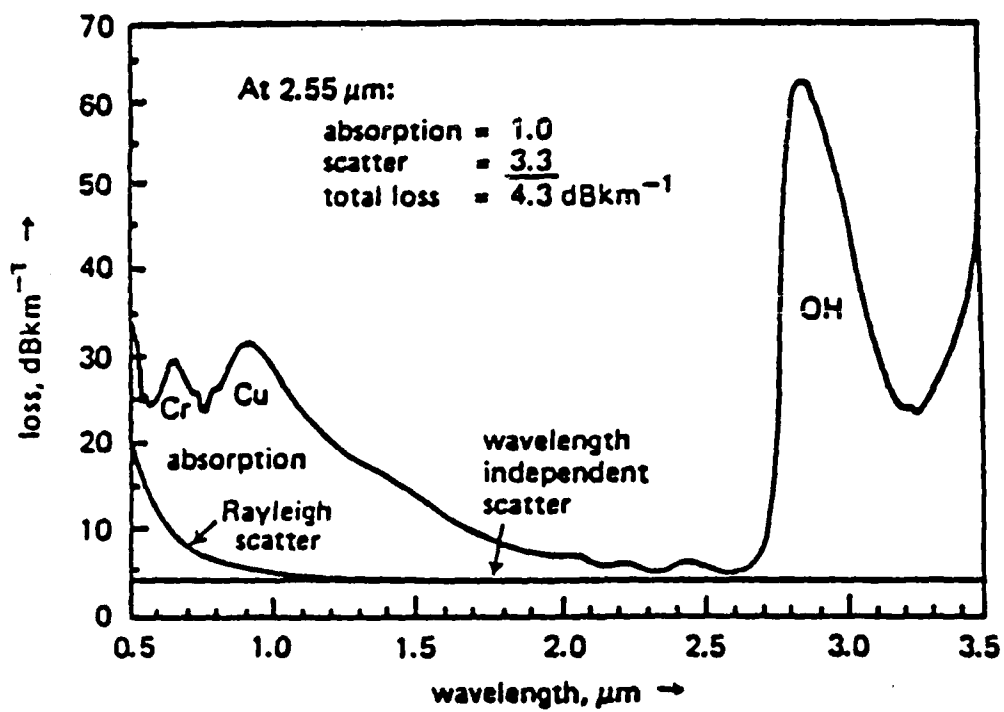
Figure 1.3. Break down of total loss in fluoride fibre.
(France et al.[4])

since it has an absorption at 2.51μm and is often found as a contaminant of LaF_3 which is a component of the glass. All rare earth ions apart from Eu exist only in the tripositive form and so redox control cannot be used to shift their absorptions to different wavelengths.

The principal source of the residual bulk absorption in the IR transmitting materials is believed to be largely associated with substitutional molecular impurities. Other sources such as macroscopic inclusions can also exist. In addition, oxide ions and the oxygen in -OH will be bonded to the cations in the glass and these metal oxyfluoride species can contribute to excess absorption at ≈7μm.

In addition, imperfections, such as inclusions, microcrystals and bubbles in the glass can also cause extrinsic scattering loss. Mie scattering is caused by imperfections whose size is of the order of the wavelength of the exciting light and is generally in the forward direction. Wavelength independent scattering is caused by large defects and is in both forward and backward directions at low angles.

Finally, there are severe problems associated with fiber drawing. This results from the the relative proximity of Tg and Tx in these glasses and the steep viscosity drop above Tg. For drawing optical fibers above Tg, rapid quench rates are needed to prevent phase separation or crystallization problems. Only preforms are used, because if melt drawing

were attempted, the likelihood of crystals forming in the crucible is very high. Detailed viscosity measurements are required before the parameters involved in the draw process can be determined.

In this thesis, we will study the intrinsic problem of chemical durability of fluoride glasses, with an attempt to understand the corrosion mechanisms in aqueous environments. The corrosion problem is central to both fiber waveguides and bulk optical components. The ZrF_4-based fluoride glasses were chosen for the study because of their current technological value due to their better stability, lesser toxicity and lower cost to fabricate. The goal of this thesis is, therefore, to elucidate the major mechanisms which control the reaction between water and ZrF_4-based glasses by studying the glass-water interface under a variety of exposure conditions. Together with solution analysis studies of the corrosion of these glasses, this investigation will attempt to model the leaching process. Only after the mechanisms are fully understood, will it be possible to assess the behavior of these glasses under use conditions.

Owing to the highly ionic bonding in fluoride glasses, their structure cannot be explained by the Zachariassen theory which gives criteria for the formation of vitreous structures with highly directed three dimensional bond arrays,i.e. covalently-bonded network glasses. For ionic

glasses, the bonding forces are primarily Coulombic; and the mobility of highly charged cations in the structure is low. The cation can possess several different coordination numbers. In fluorozirconate glasses, the Zr^{+4} ion exhibits a medium field strength (i.e. charge/ionic radius ratio), but it can appear in various sites with coordination numbers of 7, 8 and 9, and acts as a glass former. Thus these glasses are made up of units of ZrF_7, ZrF_8 and ZrF_9 linked by corner, edge and even face sharing bridges.[5] BaF_2 stabilizes the glass structure by contributing its fluoride ions to Zr^{+4} ions while the large Ba^{+2} ions are randomly distributed in the glass to maintain the electrical neutrality. Ba^{+2} acts as a network modifier.

Trivalent cation fluorides are added to the basic fluoride glass system as network stablizers. They can incorporate into the vitreous network and enhance the stability of local sites.[6] Rare earth elements act similarly to Zr and can have various coordination numbers and a large variety of values for the angles and distances of their fluorine bridges.[7] Consequently, LaF_3 is usually added to glass to create additional sites in the network and lower the strain energy of the network thus stablizing the glass.

Although AlF_3 has usually an octahedral coordination in glass, it is often added as another stablizer by Zr^{+4} /Al^{+3} substitutions. This can be achieved by localization of 4

Al^{+3} ions in free sites of the anionic packing structure to compensate for removing 3 Zr^{+4} ions. This results in an increased average cationic concentration (which is measured by the number of moles per unit volume), while the anionic concentration also undergoes a small but significant increase, which suggests that greater compactness and therefore greater thermodynamic stability can be obtained through this substitution. Because of this high ionic bonding characteristic of the HMFG structures, their chemical reactivity and leaching behavior is different from that of silicates which have SiO_4 tetrahedra bonded by strong directional O^{-2} bridges.

CHAPTER II

BACKGROUND

In this thesis, the term "leaching" is defined as the release of glass component fluorides or elements through glass-aqueous solution reactions without regard to mechanisms of release. Likewise, the term "corrosion" is also associated with the deterioration of glass surfaces due to the reactions that occur when water interacts with glass. Therefore, both of these terms are used synonymously.

The terms such as selective leaching and congruent dissolution are used in discussing the glass leaching mechanisms. Selective leaching pertains to the partial removal of glass species.[8] It may includes ion exchange of the mobile species in the glass and selective dissolution of the glass matrix, structural or network species, with or without precipitation. Ion exchange involves a process in which exchange between mobile species such as fluoride ions(F^-) from the glass and hydroxyl ions (OH^-) from the solution occurs. During this process the remaining constituents of the glass are not altered.

Congruent dissolution occurs when the species comprising the glass are dissolving into solution in the same ratios as

12

the stoichiometry of the glass and the composition in the glass surface is not changed. However, large dimensional changes often accompany such kinds of corrosion processes. These processes may or may not be followed by precipitation of dissolved species, depending on the composition of glass and solution. If there were no precipitation occuring, when solution saturation of species "i" is reached, the driving force for that species to leave the glass surface would no longer exist; consequently, species "i" will accumulate at the glass solution interface as the matrix dissolves, leaving species "i" behind in the glass. The extent of apparent noncongruent dissolution of the glass is thereby increased. The sequence of events that occurs is predictable, based on the solubility limits of each species at the given solution PH value.[9]

2.1. General Leaching Processes of Silicate Glasses

To understand the aqueous leaching mechanisms of fluoride glasses, it is best to review the well established framework of processes for the analysis of silicate glass corrosion.[10-12] Briefly described, silicate glasses leach by the competing mechanisms of alkali ion exchange processes and silica matrix dissolution, see Fig.2.1.[13] In general, positively charged ions in water(protons or hydronium ions) diffuse into the glass and ion exchange with alkali ions which causes the formation of a dealkalized layer at the

14

DEALKALIZED
SURFACE
LAYER

EXTERNAL
BATH

BULK GLASS

Na

H

Ln,Fe,Th

Si

CONCENTRATION PROFILES

Si

H

Na

Ln Fe Th
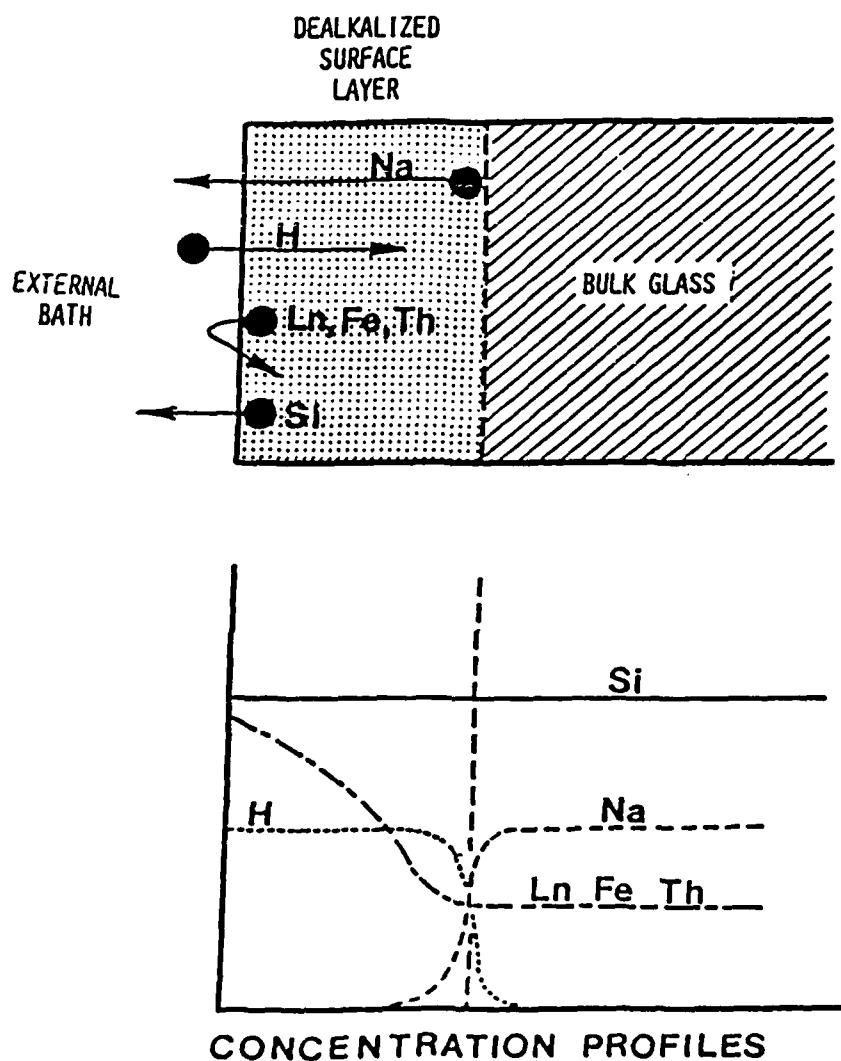
Figure 2.1. Mechanism of layer formation in silicate
glasses.(Simmons and Simmons[13])

glass surface. Usually, as the thickness of the dealkalized layer grows the interdiffusion and ion exchange processes slow down sufficiently that the corrosion process becomes dependent upon the rate of matrix dissolution at the outer edge of the dealkalized layer. The behavior of the dealkalized layer and its effectiveness in protecting the glass matrix from further dealkalization and from matrix dissolution are dependent upon alkali diffusion through the layer, layer porosity, layer thickness, precipitation or species adsorption and the pH of the solution before and during corrosion. Under stagnant conditions, corrosion products can accumulate near the solution/glass interface and the rapid dealkalization process raises the solution pH to basic values, whose limit is determined either by the other glass component reactions, such as dissociation of boric, phosphoric and silicic acids, or by buffers in the soaking solution. Since the solubility of silica is greatly increased in basic solutions, the increase in solution pH accelerates the matrix dissolution rate. In stirred or flowing conditions, less solution PH drift occurs and the concentration of silica from durable silicate glasses generally increases, first with a $(time)^{\frac{1}{2}}$ law due to the rate controlling interdiffusion of alkali metal ions and H^+ or H_3O^+ ions, and then as $(time)^1$ due to matrix dissolution through a steady state dealkalized layer. If the concentration of major glass components in solution

approaches saturation, the leach rate will be drastically lowered, however, complexes are usually formed by these corrosion products which precipitate in the form of crystals or colloids. At this point, the dissolution rate is reduced to the rate of precipitation of these components from the saturated solution. Multivalent ions are strongly adsorbed on the glass surface. They can either adsorb in the dealkalized layer or form precipitates in it which can both slow down the interdiffusion necessary for dealkalization to occur, and reduce the rate of attack of the silica network.

2.2. Solution pH Effect

The major difference between the behavior of fluorozirconate and silicate glasses lies in the measurement of solution pH during the leaching process. Silicate glasses containing alkali oxides exhibit a solution pH drift to basic values generally above 10. This results from a dominating ion-exchange process between alkali ions in the glass with protons or hydronium ions in solution. Fluorozirconate glasses by contrast exhibit a solution pH excursion to acidic values, which was first pointed out by Simmons et al.[14] and confirmed by many subsequent studies.[15-17] Solution pH drift behavior was measured by Simmons and Simmons[18], for several compositions of fluoride glasses. All showed a marked decreased in pH within the first few hours. By soaking an excess of fine ZBLAL glass powder in

deionized (D.I.) water at a pH of 5.6, a final solution pH= 2.46 was measured.

This pH drop could be accounted for either by an ion exchange of OH$^-$ in the solution for F$^-$ in the glass[14] or by the hydrolysis process of corrosion products which occured by OH$^-$/F$^-$ exchange of dissolved species in solution[18]. Ravaine et al.[19] have studied the ion exchange process between fluoride glasses and buffered basic solutions by measuring the OH$^-$ interference effect on the potential response of a fluoride glass membrane, used as a fluoride ion selective electrode. The authors suggested that the ion exchange reaction could be an important factor in the corrosion of fluoride glasses.

A study of the pH drift effect for the crystalline fluoride component of the investigated glasses was conducted by Simmons et al..[18] It showed that the hydrolysis reaction occurs in solution and that ZrF_4 was almost exclusively responsible for the large pH drop in the solution. The solution species formed was suggested to be $[ZrF_x(OH)_y]^{+4-x-y}[H_2O]_n$. It was also proposed that the stable $[ZrF_x]^{+4-x}$ species which exist in solution depend upon the fluoride ion concentration in the soluton.(i.e. for $[F^-] \geq 0.01$ ppm the dominant species are $[ZrF_2]^{+2}$, $[ZrF_3]^+$ and $[ZrF_4]$. In the range $1 \leq [F^-] \leq 10$ ppm, only $[ZrF_4]$ and $[ZrF_3]^+$ dominate.)

The effect of pH on the leaching process of fluoride

glasses was studied systematically by Simmons et al..[20,21].
For three fluoride glass families, i.e.ZrF_4-based, ThF_4-BaF_2-based and UF_4-based glasses. They were studied by
soaking solution analysis, and all exhibited similar
behavior with a minimum leach rate near neutral pH. The pH
dependence of the leaching rate of different glass
components was thought to be related to the difference in
solubility of the fluoride components over the range of
different solution pH values studied.

Houser et al.[22,23] reported a composition depth profile
study conducted by SIMS spectroscopy which showed the
hydration layer formed on ZBLA glass surfaces, corroded at
different solution pH for 10 min.. The study concluded that
at high pH,i.e. pH10, almost no corrosion occured, while at
low pH, i.e. pH2, surface films several micron thick formed
due to much higher corrosion rates in acidic environments.

2.3. Glass Composition Effect

Most of the detailed investigations on this aspect was
done by Simmons et al..[13,14,20,21,24]. Through soaking
solution analysis, they measured the leached elements and
fluoride ion concentrations in solution as a function of
both time and solution pH values on ZrF_4-based, ThF_4-BaF_2-based and UF_4-based glass families.

For fluorozirconate glasses, despite the difference in
solubility of the components and their different roles in

the glass structure, the measurements of normalized leach rate versus time showed that within a factor of 10 most of the ions leach out at a nearly congruent rate especially during the earlier stage of corrosion. La is an exception most likely due to the extremely low solubility of LaF_3, see Fig.2.2.[18]. The measurements of normalized leach rates versus solution pH showed, for all glass families, a minimum near neutral. In the acidic range, leach rates are several order of magnitude higher than at neutral pH and there is a small increase in basic media (i.e. pH10), see Fig.2.3.[21] Moreover, between pH4~pH7. the differences in leach rate between the components are more prominent than those in more acidic and more basic cases where all solubilities are higher and the glasses leach more congruently,[21] Within each family of glasses, the average leach rates measured were very close[24] regardless of variations in composition. This is very different from silicate glasses whose leach rate is changed drastically by adding only very small amount of modifier oxides or by using different modifier oxides. For fluorozirconates glasses, the order of leach rate with respect to composition is ZBLALPb>ZBLAN>ZBLAL>ZBL>ZBLA,[18] where the compositions (in mol %) of these glasses are: ZBL-62.0 ZrF_4, 33.0 BaF_2, 5.0 LaF_3; ZBLAL-57.5 ZrF_4, 34.5 BaF_2, 4.0 LaF_3, 4.0 AlF_3; ZBLAL-51.8 ZrF_4, 20.0 BaF_2, 5.3 LaF_3, 3.3 AlF_3, 19.6 LiF; ZBLAN-54.0 ZrF_4, 15.0 BaF_2, 6.0 LaF_3, 4.0 AlF_3, 21.0 NaF; ZBLALPb-50.4 ZrF_4, 15.5 BaF_2, 4.9 LaF_3,
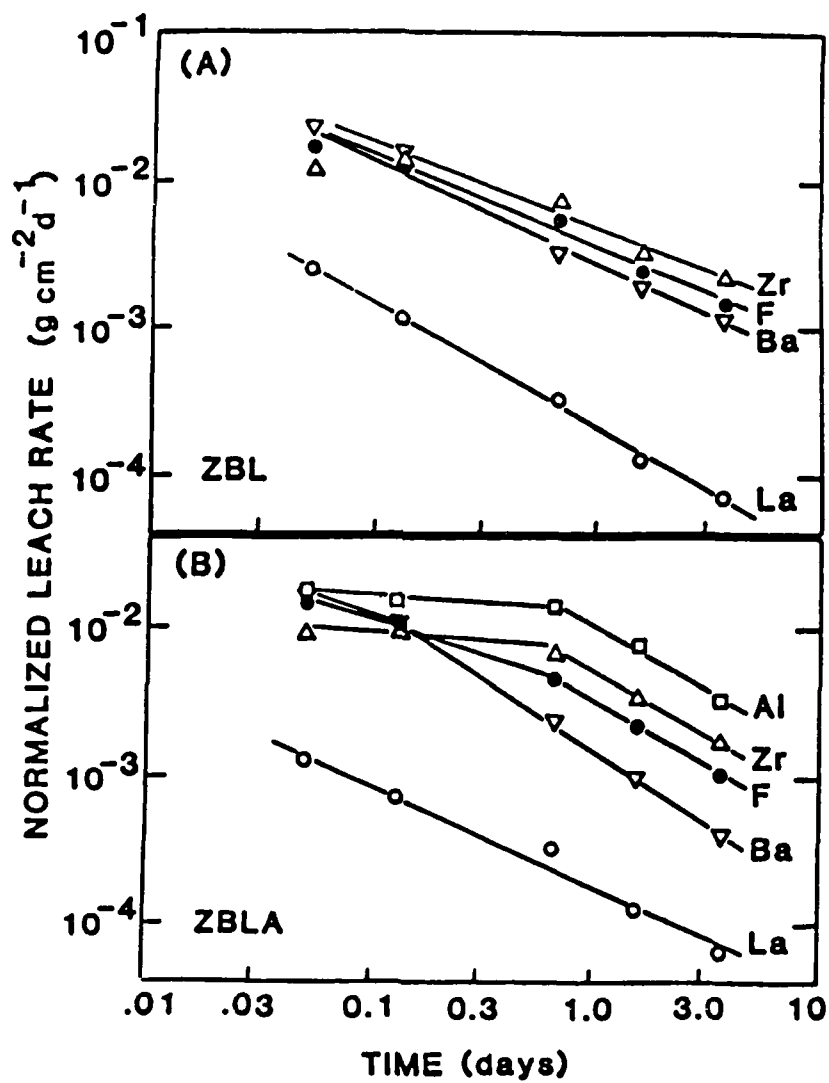
Figure 2.2. Normalized leach rates vs. time from leachate analysis fcr individual elements of glasses: (a) ZBL; (b) ZBLA. (Simmons and Simmons[18])
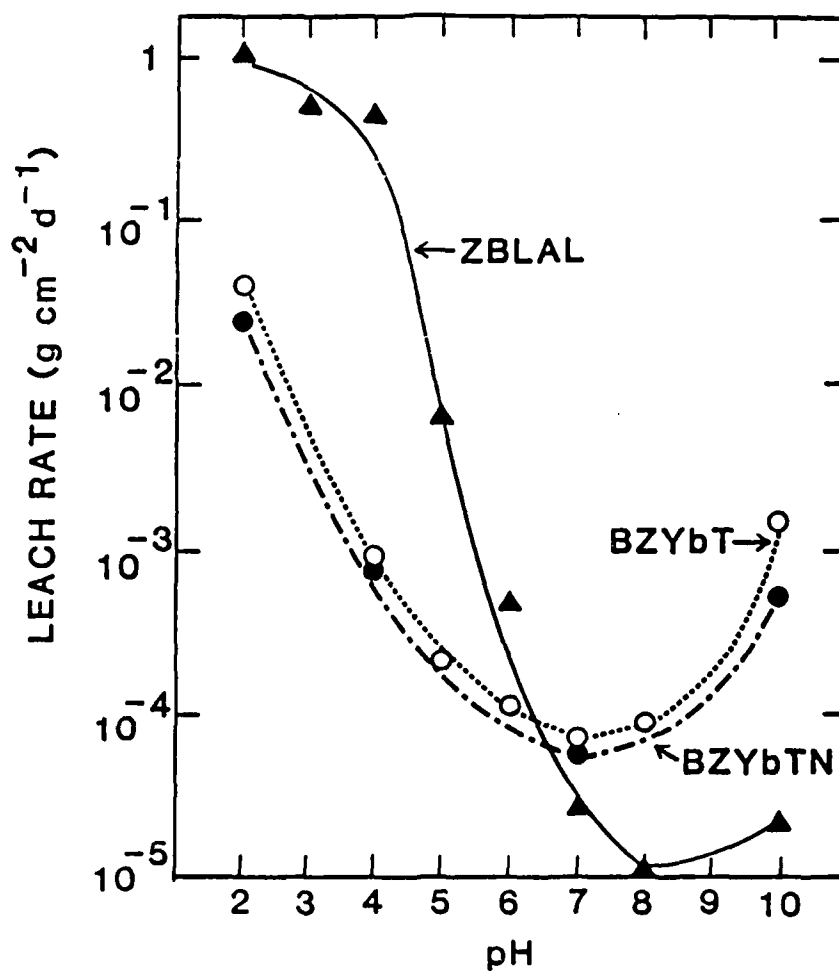
Figure 2.3. Overall leach rates vs. solution pH for all three compositions: ▲: ZBLAL; O: BZYbT; ◉: BZYbTN. (Simmons[21])

3.1 AlF$_3$, 20.2 LiF, 4.9 PbF$_2$. This has also been confirmed by Loehr et al..[17] Generally, the glass containing alkali elements, e.g. LiF, NaF, or highly soluble fluorides, e.g. PbF$_2$, is less durable and will exhibit a higher leach rate.

However, there is a marked difference in leach rate between different glass families.[13,25] For instance, ThF$_4$-BaF$_2$-based glasses have leach rates nearly two orders of magnitude lower than fluorozirconate glasses in D.I. water. This is partially due to the lower solubility of ThF$_4$ than ZrF$_4$. Moreover, the pH drift of these ThF$_4$-BaF$_2$ glasses in unbuffered deionized water was less severe than those observed in the ZrF$_4$ glass family, reaching an equilibrium value of pH 4.8 instead of pH 2.46. This difference in the solution pH drift behavior is due to the extensive hydrolysis of ZrF$_4$ species in solution for Zr-containing glasses, while no such pronounced effect was seen in ThF$_4$-BaF$_2$ glasses where the hydrolysis of thorium fluoride species was observed to be very limited. This particularly interesting solution pH dependence for leaching behavior of fluoride glasses suggests that, if there is no buffering agent in the glass and/or in solution to balance this self-induced pH drift effect, the acidic pH environment produced by the glass dissolution process and by the associated hydrolysis process will cause a severe increase in the corrosion rate.

2.4. Glass Surface Area to Solution Volume Ratio (S/V)

The fraction of various constituents released by a glass under corrosion conditions is proportional to the surface area exposed to the solution. The ratio of the exposed surface area of glass to the volume of aqueous corrosion solution is an experimental parameter that affects the corrosion kinetics drastically and can change the leaching mechanisms entirely. Systematic studies in silicate glasses by Ethridge et al.[26] demonstrated this effect, and subsequent corrosion studies have considered the S/V ratio as a primary parameter in determining leaching conditions. The S/V parameter is especially important for closed systems under either static or stirring conditions. The S/V ratio determines the extraction rates of glass components into the solution environment, which in turn control the time it takes to reach saturation of glass component in solution and the extent of solution pH drift. All these effects will change the dissolution rates of glass components and will influence the reprecipitation processes occurring in the system. In the case of silicate glass leaching, as we described earlier, an initial stage of ion exchange between H^+ or H_3O^+ in solution with alkali ions in the glass causes the solution pH to drift into the basic range. If the solution pH reaches above 9 or 10, the controlling leaching process becomes the dissolution of the major glass matrix compoment, (i.e. SiO_2), and the corrosion

kinetics switch from the process of diffusion controlled selective leaching to the network dissolution rate controlled process. Since alkali salts are highly soluble in water, the leach rate of alkali ions does not vary appreciably with the ratio of the surface area of the glass to volume of the solution. Under high S/V ratio conditions, the rapid accumulation of corrosion products results in a rapid transition from an initial selective leaching process to a matrix dissolution process. On the other hand, for corrosion conducted in a larger volume of solution compared to the exposed surface, the transition from ion exchange to matrix dissolution will occur much later.

2.5. Static, Stirred or dynamic condition

From the work done on the leaching behavior of silicate glasses in an aqueous solution enviroment, we know that according to thermodynamic considerations, the glass components will leave the glass phase to go into solution to try to reach the thermodynamic equilibrium of each element. It has been shown[27] for oxide glasses that the long term chemical resistance of a glass is mainly determined by the thermodynamic activity and stability of its component oxides in aqueous solutions, whereas for tests carried out at low temperatures, or for shorter duration times, the kinetic stability should be predominant. In static, closed systems,

if the leach rate of glass components is comparatively
higher than their diffusion rate in aqueous solution, a
highly concentrated solution film forms adjacent to the
glass/solution interface. Depending on the glass system,
this could cause a more severe solution pH drift and create
a different pH environment at the interface with a resulting
change in leach rate. Further the saturation of the near
interface solution can cause reprecipitation to occur. On
the other hand, in stirred closed systems, mechanical mixing
of the solution is rapid enough to allow the corrosion
products from the glass to redistribute evenly in the bulk
solution and thus, end up uniformly distributed throughout
the bulk solution. However, since the reaction products are
still in solution, saturation/reprecipitation processes can
still occur if the reaction time is long enough or S/V ratio
high enough to allow an accumulation of reaction products to
reach saturation. In addition, solution pH drift can occur
in this case and influence the leaching process. In the
case of an open dynamic system, which can be achieved by
flowing fresh solution through the reaction vessel and
continuously removing the attacking medium, with its
corrosion products, no saturation of leach species can
occur. In this case, it is very difficult to accumulate the
corrosion products in solution and thus the solution pH
stays nearly constant, while the saturation/ reprecipitation
process becomes difficult to achieve.

2.6. Surface Layer Formation

Some corrosion studies[14,16,18] have been conducted on
fluorozirconate glasses by observing the corroded glass
surface topography, which was formed under either static,
stirred or frequently replenished solution conditions. The
results showed that crystals can form on the staticly
corroded glass surface. Houser et al.[22,23] reported
secondary ion mass spectroscopy (SIMS) data on the hydration
layer thickness of fluorozirconate glasses, claiming that
for agitated (rotated) samples there is an increase in the
layer thickness when compared to the staticly corroded
sample; however, these samples were corroded for relatively
short times (1 hour).

C. J. Simmons et al.[14] examined the corroded sample
surface of fluorozirconate glasses by scanning electron
microscope (SEM) and found precipitated crystal deposits of
2 kinds over the entire glass surface. Below the crystals,
the glass was heavily hydrated and cracked, for a depth of
several microns. These authors suggested these layers did
not appear to protect the interior of the glass as commonly
seen in durable silicate glasses.

Doremus et al.[28] reported that one of the crystals
observed to have a blade shape by Simmons et al.[14] exhibited
the same X-ray diffraction spectra as crystalline ZrF_4. They
also studied the crystals formed on glass corroded at high
temperature in dilute H_2SO_4. The X-ray diffraction spectra

before and after dehydration heat treatments were found to be the same, indicating that these crystals are not hydrated. The same authors suggested that since these crystalline deposits appear to be embedded on glass surface, they could be formed right at the glass surface by diffusion through the solid or as a result of surface segregation after the original glass surface leached of other ions. They saw no need for hydration or dehydration of the Zr or fluoride ions that are incorporated into the crystal.

The same crystals were also identified by C. J. Simmons et al.[13] as ZrF_4. The other commonly seen surface crystal consisted of a semi-spherical segregates composed of thin platelets which they identified as a Ba and Zr containing crystal. They suggested that these crystalline deposits result from a saturation of the aqueous solution at the glass-solution interface which is caused by the stagnant conditions of the tests. Furthermore, this saturation and precipitation processes can occur rapidly, before the corrosion products have an opportunity to diffuse into the bulk solution. This model contradicted Doremus' analysis but its conclusions were supported by the observation that a hydration layer is present below the crystal layer and clearly forms as a result of water-glass reactions. This layer which can be very thick for long corrosion times[18] serves as a substrate for the crystal precipitates.

2.7. Time Dependence of Corrosion Process

Houser et al.[22] studied the composition depth profile of corroded glasses with SIMS analysis for a ZBLA glass corroded in S/V=10⁻³ deionized water at room temperature for 5 to 60 minutes. The Zr, Ba, F, and Al profiles showed a slight surface build-up followed by a depleted region. For longer exposures, the depth profiles, particularly that of carbon showed additional structure, which they interpreted as resulting from the formation of several corrosion layers.

Bruce et al.[17,29] measured the IR transmission spectra, by monitoring the OH stretching (2.9 μm) and HOH bond bending(6.1 μm) peak height changes, to see how these two peaks develop with corrosion time. The time dependence of the growth of the water and hydroxyl peaks appeared to follow a t^1 power law for the first 10 minutes and then a $t^{\frac{1}{2}}$ law for longer times. Moreover, from the constant ratio between peak heights of these two bands they concluded that only molecular water is present in the hydrated layer of glass. By measuring the peak heights, these authors could not separate, in the hydroxyl vibration, the contribution due to molecular water from that due to metal hydroxides. However, these two absorbing peaks broaden as well as increasing their heights as they develop, as has been pointed out by Simmons and Simmons[18], therefore the integrated intensity of whole absorption band should be considered instead of the peak height, and this could lead

to very different conclusions.

C. J. Simmons also reported solution analysis results
from five different fluorozirconate glasses, showing that
most of the glass components leach at a slower rates as the
corrosion time increases, particularly Ba and La. This was
observed for all the glasses tested. For ZBLA glass, Zr and
Al leach at a relatively constant rate at the beginning and
this rate decreases as time exceeds more than one day. Ba,
La and F leach at a more rapidly decreasing rate with time.

2.8. Temperature Effect

The importance of temperature in silicate glass
corrosion is well established. The reaction temperature not
only alters the kinetics of the reaction but also dictates
the rate controlling mechanism of corrosion[30]. At
temperatures below 27°C selective leaching is rate
controlling, while above 80°C the corrosion rate is
controlled by the total dissolution process. However, for
fluoride glasses no systematic study has been conducted.
Houser and Pantano[22] studied the ZBLA glass surface
hydration layer development for short times, i.e. 20 minutes
at room temperature in D.I. water, by using SIMS O, H and C
depth profiling. They found that the layer thickness
increases as the temperature increases for three different
temperatures used. Infrared transmission spectra of these
samples by these authors show the same results.

Mitachi[31] investigated the BaF_2-GdF_3-ZrF_4 glass system and measured the solution pH value as a function of temperature. This data showed a steep pH drop between 20° to 40°C and then a decrease at a much slower rate from 40°to 100°C.

Pantano[32] studied the water and oxygen adsorption on a fractured ZBLA glass surface under ultra high vacuum conditions and monitored their concentration with a low energy ion scattering spectrometer (ISS). He concluded that neither oxygen nor water is adsorbed on the clean fluoride glass surface even at atmospheric pressure. A similar study done by Strecker[33] showed no adsorption of water on single crystals of calcium fluoride until the temperature was reduced to less than 0°C, at which point the water vapor was physically adsorbed. Thus it seems clear that chemisorption of water does not occur at the surface of ZBLA or CaF_2 under ambient conditions. This explains why the ZBLA glass shows essentially no attack if exposed under high humidity enviroment even for a long time, when there is no liquid water condensation.[14,34-37].

However, if the glass is exposed under high temperature, i.e. 220°-320°C, to wet gaseous environments which are enriched in ^{18}O, ISS spectra showed that two independent diffusion processes occur: one is due to hydration or hydroxylation and the other is from oxydation. Moreover, the rate of oxidation is much less than that of the hydration

reaction. Tregoat et al.[35] reported that a ThF_4-BaF_2-based glass reacted with atmospheric water at high temperature $(212°-347°_C)$. The main corrosion process was written as follows:

$$F^-_{(glass)} + H_2O_{(gas)} \rightarrow HF_{(gas)} + OH^-_{(glass)}$$
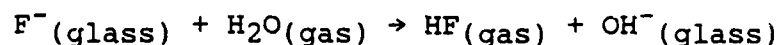
They concluded that since hydroxylation reaction can occur rapidly and hydroxyl ions can diffuse into the glass at high temperatures, the presence of water vapor can cause severe problems in glass processing operations such as fiber drawing.

2.9. Corrosion Mechanism Proposed for Fluoride Glasses

Although fluorozirconate glasses show almost no reaction with atmopheric water at room temperature even when exposed for a long time, they leach rapidly in liquid water and the solution pH drifts to acidic values quickly. Thick hydrated layers can form with crystal precipitates on the hydrated glass surface. Data has been collected by a combination of solution composition analysis[18], IR work on the extent of hydration,[17,22] surface topography observation by SEM, composition and morphology study of surface crystals by X-ray diffraction and electron microprobe studies 18,28,39-41. A corrosion mechanism for static leaching of fluorozirconate glasses was proposed by Simmons and

Simmons[18] which can be described as follows;

(1). Owing to the highly ionic structure of fluoride glasses, the ZrF_4-based fluoride glasses corroded primarily by matrix dissolution. Unlike silicates which go into solution as hydroxides, the components of these glasses can go into solution as fluorides without a prior hydroxylation step.

(2). Preliminary IR absorption work by calculating the integrated peak area of OH and HOH peaks of corroded glass indicates the OH stretching peak grow slightly faster than the HOH bending peak, suggesting that hydroxides can form on the glass surface and the fluorozirconate glasses undergo a small amount of ion exchange but that the corrosion occurs primarily by selective extraction of some fluoride components, i.e. Na, Al, followed by matrix dissolution.

(3). LiF, NaF, AlF_3 and in some cases BaF_2 dissolve at faster rates than either ZrF_4 or LaF_3. This difference in extraction rates, coupled with the rapid penetration of water into the glass leads to the formation of a porous, hydrated corrosion layer at the glass surface.

(4). With time the leach rates of LiF, NaF and AlF_3 remain high, while that of BaF_2 decreases significantly as a possible result of (i) an increase in [F] ion concentration which can interfere with BaF_2 solubility and (ii) the depletion of BaF_2 from the glass surface. LaF_3 is highly insoluble in water and therefore remains in the

surface layer.

(5). ZrF_4 dissolves into solution as ZrF_4. This is supported by the fact that ZrF_4 appears in this form as a precipitated crystals on the glass surface. Moreover, the increase of $[F^-]$ in solution also favors the existence of $[ZrF_4]$ in solution as a stable species.

(6). A decrease in solution pH with corrosion time results from succesive hydrolysis of the zirconium fluoride species in solution. By measuring the equivalent hydroxyl concentration exchanged with a titration method, these authors concluded that two hydroxyl groups are exchanged per Zr in solution as shown below;

$$2[OH]^- + [ZrF_4] \rightarrow [ZrF_2(OH)_2] + 2F^-$$
$$2[OH]^- + [ZrF3]^+ \rightarrow [ZrF(OH)_2]^+ + 2F^-$$
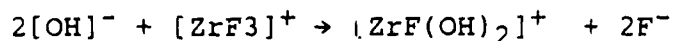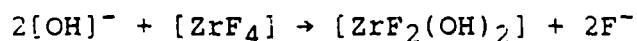
(7). Two distinct crystal types are formed on the hydrated layer surface, i.e. blade or needle like ZrF_4 crystals and spherical assemblages of thin platelike $ZrBaF_6$ crystals. These crystals are formed by precipitation due to a saturation at the glass-solution interface. The two crystal types appear to form simultaneously. Under dilute and well stirred conditions, the corrosion layer appears to be similar in character; however, no crystals are formed, even after leaching for 10 days.[41]

(8). The thick porous layer plays a minor role in

protecting the unreacted bulk glass and acts as a diffusion barrier to reduce the leach rates. The porosity of the layer reflects the molar volume of highly soluble species, i.e. NaF, LiF, PbF_2, AlF_3 etc., in the glass compositions and can be related to the comparative leach rates of different glasses. For example, the less durable glasses form a thick and highly porous layer.

(9). The pH drift of the solution into an acidic range during leaching raises the solubility of ZrF_4, which accelerates the glass dissolution by several order of magnitude. The addition of any buffer to the solution can have a profound effect on the leach rate, if it retards or eliminates the pH drift.

CHAPTER III

OBJECTIVES

In this thesis, we are interested in investigating the corrosion processes of ZrF_4-based glasses in aqueous environments, and in trying to determine the primary reactions occuring at the glass/water interface under a variety of exposure conditions, from stagnant to rapidly flowing dynamic conditions.

Stagnant conditions allow us to study the effect of corrosion products on the leaching proceses. In the extreme of this case, it can simulate the result of water penetrating through the coating of optical fibers, resulting in the exposure of the glass to a very small amount of water. In flow conditions, the glass is exposed to large amounts of water, flowing or stirred, which simulates the exposure condition found by immersion in a river, an ocean, or lake etc., where most of the corrosion products can be carried away from the glass environment by the continuous flow, thus the effect of corrosion products can be eliminated.

To achieve the objectives, a series of experiments have been conducted:

1. Raw materials study

2. Short time leaching and solution pH effect

3. Solution precipitation study

4. Stagnant tests

5. Zeta potential measurements

6. Flow tests

7. Hydration/ dehydration tests

A combination of analytical techniques were used for evaluating the leaching behavior of fluorozirconate glasses and the surface layer formation. Figure 3.1 shows the sampling depth for various techniques used in this study.[30]

For solution analysis, inductively coupled plasma(ICP) emission spectrometer was used to measure the element concentration in the solution, with a detection level of sub-ppm concentrations. The solubility of the various fluoride compounds in D.I. water and in different pH buffer solutions at room temperature was determined by ICP measurement. pH electrodes were used to monitor the solution pH drift both in bulk solution and at the glass surface during the corrosion. Fluoride ion concentration was measured from potentiometry by using fluoride ion selective electrodes.

SEM is one of the most widely used tools for morphology and microstructure characterization of glasses. The use of energy dispersive X-ray spectroscopy (EDX) with the SEM makes possible the compositional analysis of the observed structural features. The combination of high resolution,

FTIR-TS   SEM/EDX

XRD   Solution analysis
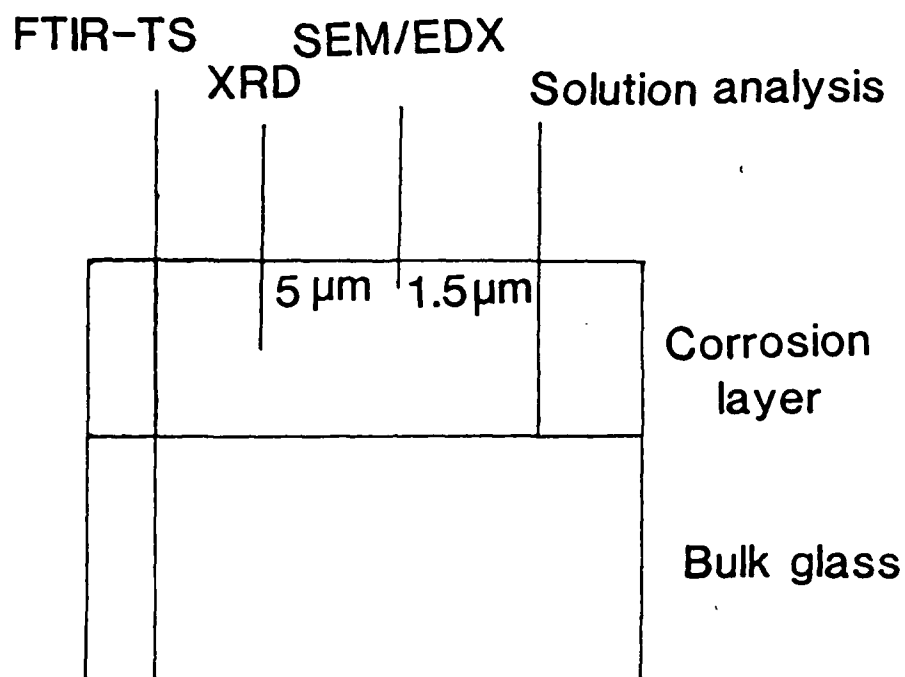
5 μm 1.5μm

Corrosion
layer

Bulk glass

Figure 3.1.   Sampling depths of various techniques used in
this study.

near three dimensional image and compositional analysis of the microstructural features observed makes the SEM perhaps the most powerful general characterization tool currently available. However, its depth of analysis is relatively large, i.e. ~1 μm, and it is not capable of detecting low atomic mass, Z (Z$\leq$9), elements. The thick corrosion layers formed on fluoride glasses during leaching are well suited to this technique, while the study of corroded silicate glasses must resort to more surface sensitive techniques, such as AES, XPS and SIMS. However, it is important to recognize that the accuracy of electron microprobe measurement is dependent upon the surface roughness and severe surface roughening may occur with extensive aqueous corrosion, thus, there are analytical uncertainties resulting from the surface roughness and porosity. Nonetheless, composition profiles can be obtained by analysis done on a polished fractured sample surface; composition dot mapping may also be conducted.

X-ray diffraction spectroscopy in the reflection mode is the most convenient technique for identifying the crystalline precipitates on the glass surface. Samples are either collected by gently scratching off the corrosion layer or they are measured directly.

Thermal Gravitometry Analysis (TGA) was used to analyze the total weight loss of the corrosion layers during dehydration. This was coupled to a Differential Thermal

Analysis (DTA) at the same time to monitor the enthalpy change of the system.

Particle electrophoresis was used for measuring the surface charge of glass powders. Suspensions made up of solution and microscopically visible fluorozirconate glass powders were prepared for the measurement. The movement of a charged surface plus attatched material, i.e. dissolved or suspended material, relative to the stationary liquid, under an applied electric field was measured. The mobility measured can be related to the surface charge (or Zeta potential) of the measured particles.[42]

Another commonly used technique in this study for examining glass structure and compositin is Fourier-transformed Infrared Transmission Spectroscopy (FTIR-TS). By measuring the integrated area of the O-H stretching vibration band at $2.9 \mu m$ and H-O-H bending vibration band at $6.1 \mu m$, we can monitor the change of hydroxyl groups as well as molecular water existing in the corroded fluoride glass.

CHAPTER IV

EXPERIMENTAL STUDY

4.1. Sample Composition

Tests of chemical durability were conducted on solid samples of fluorozirconate glasses obtained from various sources with the compositions shown in Table 4.1

Table 4.1   Compositions of fluorozirconate glasses (mol%)

mnemonic	ZrF_4	BaF_2	LaF_3	AlF_3	LiF	source
ZBLA	57	36	3	4	--	RADC[*]
ZBLA-F	51.16	38.62	5.66	4.56	--	Le Verre Fluore[#]
ZBLAL	51.8	20.0	5.3	3.3	19.6	NRL["]

[*] Rome Air Development Center, Hanscom AFB, MA (Dr. El Bayoumi)

[#] Le Verre Fluore' Co., LeMans, France

["] Naval Research Laboratory, Washington, DC (Dr. D. C. Tran)

These glasses were melted under a variety of conditions varying from the use of oxide raw materials with added ammonium bifluoride[43] to the direct use of anhydrous fluoride raw materials, melted under an Ar or CCl_4 atmosphere.[44,45]

4.2. Sample Preparation

4.2.1. Raw Material Study

High purity anhydrous fluoride compounds were used for the raw material study. Each compound was weighed precisely and put into 100 ml D.I. water in polymethylpantene (PMP) container to prepare a solution of 100ppm cation concentration if the compound dissolves completely. The solution was shaken periodically and kept for sufficient amount of time to reach its dissolution limit (i.e. solubility), it was then filtered with a PMP disposable filter immediately before the measurement with an ICP. The solution pH modification due to the hydrolysis of each raw material was measured by potentiometry with a pH electrode.

Excess amount of each fluoride compound was also put in different pH buffer solution after a similar preparation as described above. The ICP was used to measure the solubility of different fluoride compounds in the solution. The standards were prepared by using different buffer solutions as matrix solution.

The zeta potential of each fluoride raw material was measured in D.I. water at different pH values adjusted with 0.01N HCl and 0.01N NaOH solutions by using a Laser Zee (model 501) instrument. The specific conductivity (SC) of the solution was also measured at the same time.

4.2.2. Glass Powder Samples

The ZBLA glass powder was ground carefully with mortar and pestal for 15 minutes and its surface area was measured by BET nitrogen gas adsorption/desorption method as $8175cm^2/g$. Different amounts of glass powder were weighed precisely and each was put into the same amount (i.e. 30ml) of D.I. water to study the effect of corrosion conducted under different glass surface to solution volume ratios (S/V). The solution pH modification was measured with a pH electrode.

The same glass powder was also used for short time leaching studies to measure the cation and fluoride ion concentrations for an initial short period of corrosion time. Solution analysis was conducted by ICP and a fluoride ion selective electrode. The solution pH drift was also measured. The solution samples were prepared by filtering through a polystyrene (PS) disposable filter after being shaken for predetermined periods of time.

A glass powder/D.I.water suspension was prepared for zeta potential measurement as a function of corrosion time using the Laser Zee instrument. The specific conductivity which is related to ionic strength was also measured at the same time. A separate suspension was prepared with the same procedure for solution pH drift measurements with a pH electrode.

Excess amounts of ZBLAL glass powder were added to D.I.

water to prepare a solution saturated with corrosion

products for a solution precipitation study. After putting

fused silica slides on one side of the container carefully

without disturbing the glass powder settled at the bottom on

the other side of the container, the solution was then air-

dried and the precipitated crystals on the SiO_2 slide were

observed under SEM.

4.2.3. Bulk Samples

Bulk fluoride glasses were polished down to 1 μm

diamond paste with halocarbon oil, which is oxygen and water

free, as lubricant, in order to remove the aged or corroded

surface layer and obtain a reproducible surface finish

without aqueous contact. After polishing, the samples were

rinsed in methanol and then toluene for a very short time to

remove the oil. Polished samples were used for corrosion

tests conducted under various conditions which will be

described in the following section.

4.3. Exposure Conditions and Measurements for Bulk Samples

4.3.1. Solution Precipitation Study

Besides using powdered glasses to produce saturated

solutions for a reprecipitation study, bulk glass samples

were also used. A polished glass plate was placed

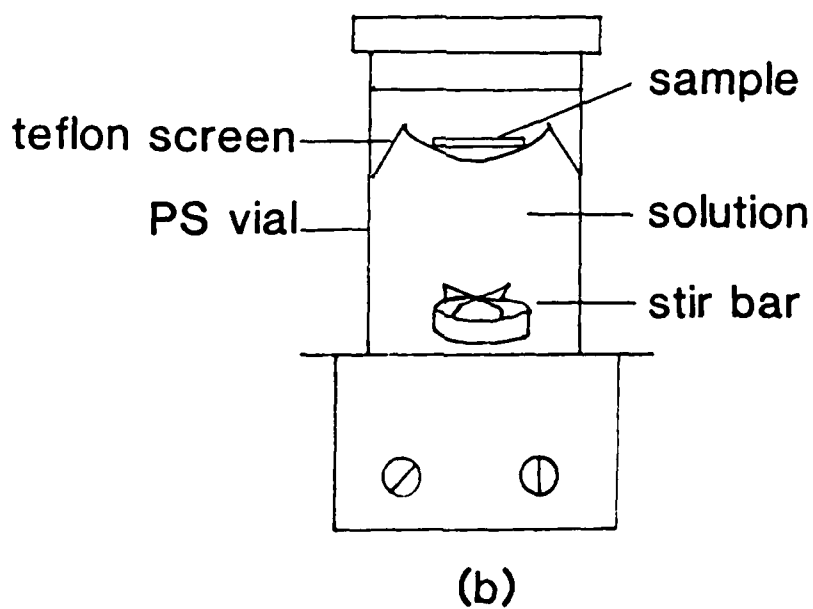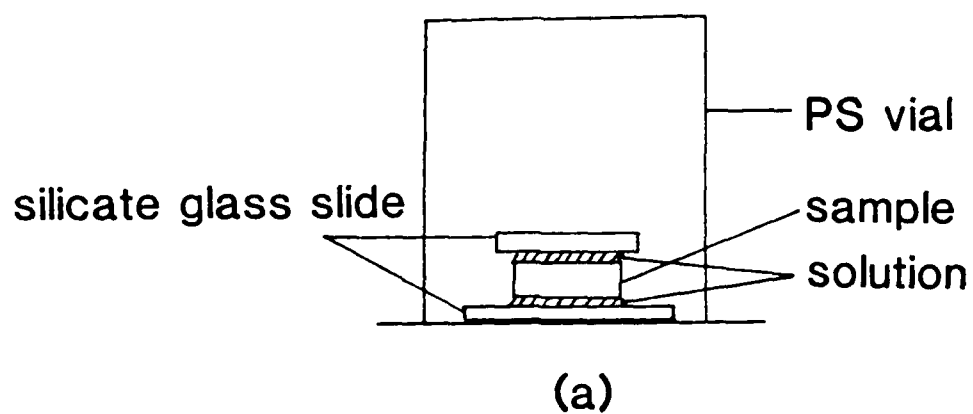between two silicate microscope cover slides, with a very

(a)

(b)

Figure 4.1. (a) Corrosion configuration for both high S/V
ratio and solution precipitation study; (b) experimental
set-up for glass corroded in stirred pH buffer solutions.

small amount of D.I. water in between to produce a high S/V ratio, i.e. S/V=15, corrosion environment, see Fig.4.1(a). After 4 hours, the sample was removed and the solution on the bottom slide was left to air-dry, causing precipitation to occur. The precipitated crystals on the bottom glass slide were examined under SEM/EDX and were collected for X-ray diffraction studies also.

Another crystalline precipitate sample was collected from the solution of a ZBLA glass corroded for five days at S/V=1.5. After the sample was taken out, the solution was left to evaporate for a long period of time to have the dissolved crystals precipitate out and suspend in the solution. These suspended crystal were collected for examination.

4.3.2. Corrosion in Stirred pH Buffer Solutions

Small ZBLA glass plates were put on a pre-cleaned teflon screen placed in buffer solutions of different pH values in clean polystyrene vials. The S/V ratio is 0.01 and the solution was stirred at a preset speed, see Fig.4.1 (b). Since the leach rate at different pH values varies, in order to obtain samples with a comparable extent of leaching, samples were corroded for different times depending on the pH buffer solution used. At pH2 and pH4, the samples were corroded for 2 hours, while at pH6, 8 and 10, the samples were corroded for 201 hours. After

corrosion, the samples were rinsed in methanol and then toluene to remove the residual liquid solution on the sample surface. These samples were observed under SEM for surface topography and were fractured perpendicular to the exposed surface to see the resulting corrosion layer in cross-section.

4.3.3. Stagnant Tests

(a). Surface pH measurements: A Ross, flat-surface, combination pH electrode was used to measure the pH drift on the glass surface by locating it above and directly on the polished glass surface with a small drop of D.I. water in between. In this test, a S/V ratio ranging between 10-20 was used depending upon the amount of water present. The pH drift was directly measured on a chart recorder. The measurement was conducted for short times to avoid affecting the results with the evaporation of the water.

In order to determine the effect of small amount of KCl to the leach processes, a KCl of concentration of 3M was added to solutions saturated with individual glass components and with combinations of glass components. Neither precipitation nor significant solution pH drift were observed in the tested solutions. Thus a small amount of KCl which had diffused from the electrode during the measurement should not affect the leaching process.

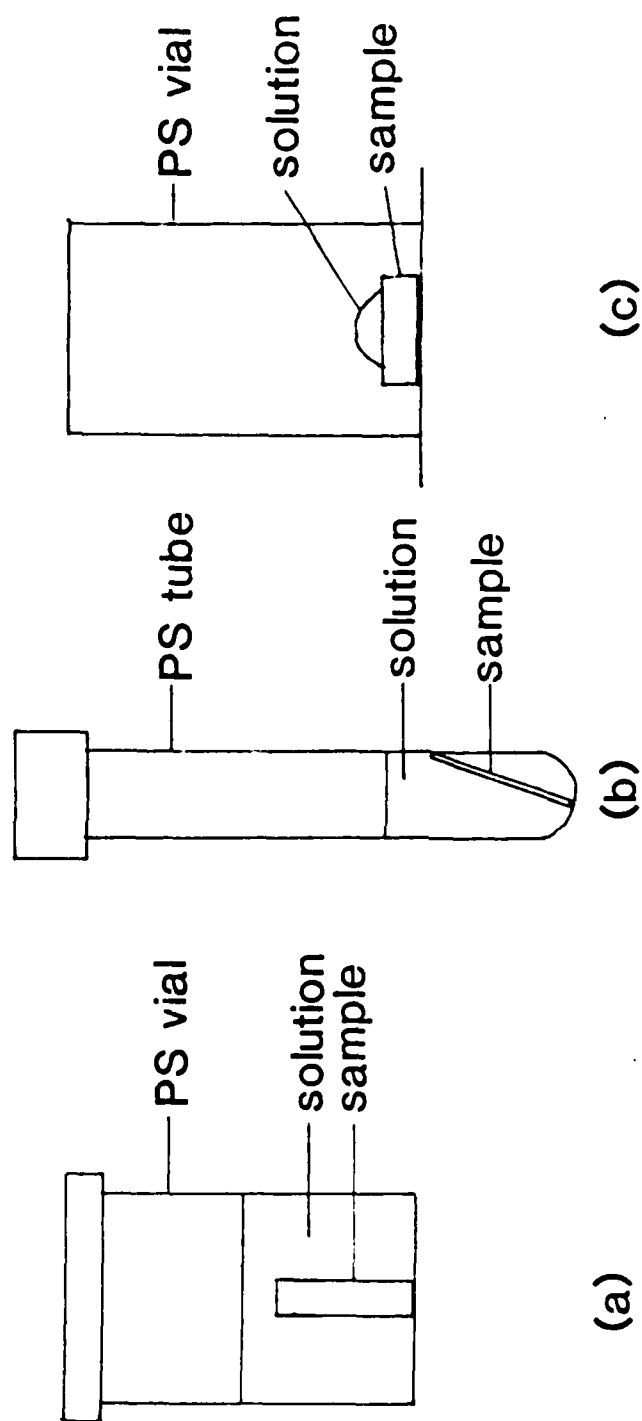(b). Intermediate S/V stagnant tests (S/V=1-5): The

Figure 4.2.   Three types of corrosion configurations for static condition.
(a) for thick glass plate in S/V=1; (b) for thin glass plate; (c) for glass
plates in S/V=5.

dimension and thus the surface areas of polished bulk samples were determined by micrometer. For S/V=1 test, see Fig.4.2, a PS 20ml vial was used as the corrosion vessel with a thick fluoride glass plate standing upright which was completely immersed in the D.I. water, see (a); for the case of a thin glass plate, the sample was laid against the wall of a narrow polystyrene tube, see (b), for different periods of times. Corroded thin glass plates can be fractured easily and the corrosion layer developed with time may be observed directly with SEM. EDX compositional analysis for different spots and X-ray line scan analysis for composition profiles along the fractured cross sectional surface were conducted. The corrosion layer was scratched off carefully for X-ray diffraction analysis to identify the crystals formed on the corroded surface. A TGA/DTA analysis was also conducted on these scratched layers. FTIR transmission spectra were acquired for short time corroded samples to compare with those of samples corroded by solution flow.

A sample corroded at S/V=5, see Fig.4.2 (c), which will be denoted as drop test, was prepared by putting a drop of D.I. water, usually around 0.1 ml, onto a polished glass plate. The glass was covered with a small vial to retard evaporation. After corrosion, the sample was rinsed in methanol and then toluene to remove residual water. This experimental set-up was only used for short time corrosion tests. The corroded samples were observed under SEM to study

the glass surface corroded for different short time periods.

(c). High S/V ratio (i.e. 10-40) static test: Samples corroded under this condition were exposed by using two thin D.I. water films to corrode a polished glass plate for short periods of time; one thin silicate glass slide was used on each side of the fluoride glass to produce the water film. After rinsing the corroded samples, they were examined with SEM/EDX. Corrosion layers were scratched off carefully for X-ray diffraction analysis.

4.3.4. Zeta Potential Measurement

To achieve a better understanding of the corrosion process and corrosion layer formation, a series of zeta potential measurements were conducted on ZBLA glass powders. Scratched corrosion layers and individual fluoride compounds were also measured using a Laser Zee (model 501) instrument. Microparticle electrophoresis was used for the measurements, and very dilute suspensions were used. This measurement was combined with SEM examination of both the fractured cross-section and surface topography of corroded glasses.

The glass powder used in this measurement was prepared by grinding in mortar with pestal for 10 minutes. The surface area was measured by BET, N_2 gas adsorption / desorption, method to be 8175 cm^2/g. To measure the zeta potential of the glass powder as a function of time, a small amount of glass powder was used for corrosion. For low S/V,

0.0125g powder was added to 40 ml D.I. water. Measurements were made after shaking the solution for 3 minutes to prepare a homogeneous suspension. The sample was syringed into the rectangular liquid cell which has two built-in electrodes. The cell was then mounted onto the optical microscope. Under the preset d.c. voltage the glass particles with a certain surface charge can move under the applied electric field. By measuring the charged particle mobility at stationary level, the zeta potential of the glass particles can be obtained; solution specific conductivity which is related to its ionic strength was also measured at the same time. The same suspension was used throughout the zeta potential measurement; while another suspension, which was prepared the same way, was used to monitor the solution pH drift.

To correlate the zeta potential measurement with the corrosion layer formation, which can be observed by SEM, four thin small ZBLA glass plates with a comparatively negligible total surface area of 1.5 cm^2 were added with 0.03g glass powder into 40ml D.I. water, and the suspension was slowly rotated, i.e. 15 rpm, to promote a more uniform leaching environment. Zeta potential and solution specific conductivity were measured. The thin glass plates were taken out of the PMP corrosion vessel successively at proper intervals, and then these samples were fractured and observed under SEM.

The zeta potential of the glass powder, corrosion layers and various fluoride compounds were measured in solutions of different pH values in order to find the isoelectric point (IEP) of each species measured. The solution pH was adjusted by 0.01N hydrochloric acid (HCl) and 0.01N sodium hydroxide (NaOH) solution. After the solution was prepared, the powder sample was added and the solution pH was taken after the suspension was shaken vigorously for a few minutes. The suspension was not put into the cell for measurement until the solution pH had remained constant for several minutes. After the measurement, the solution pH was checked to insure that the value had not drifted significantly.

4.3.5. Flow Tests: High Dilution Condition

The experimental set-up for dynamic flow tests is shown in Fig.4.3. Ultrapure (i.e. 18M Ohm) D.I. water from a Milli-Q water system was passed through two valves, used to control the flow rate, along 100 feet of tygon tubing with one end connected to the water system outlet while the other end led to the cleaned polypropylene (PP) corrosion vessel. The tygon tubing was coiled in a thermostatically controlled bath to heat the D.I. water. Within the vessel, either a teflon thread or teflon screen basket, which had been pre-cleaned, was used to hold the glass sample. Solution pH and temperature were monitored with a pH electrode and a
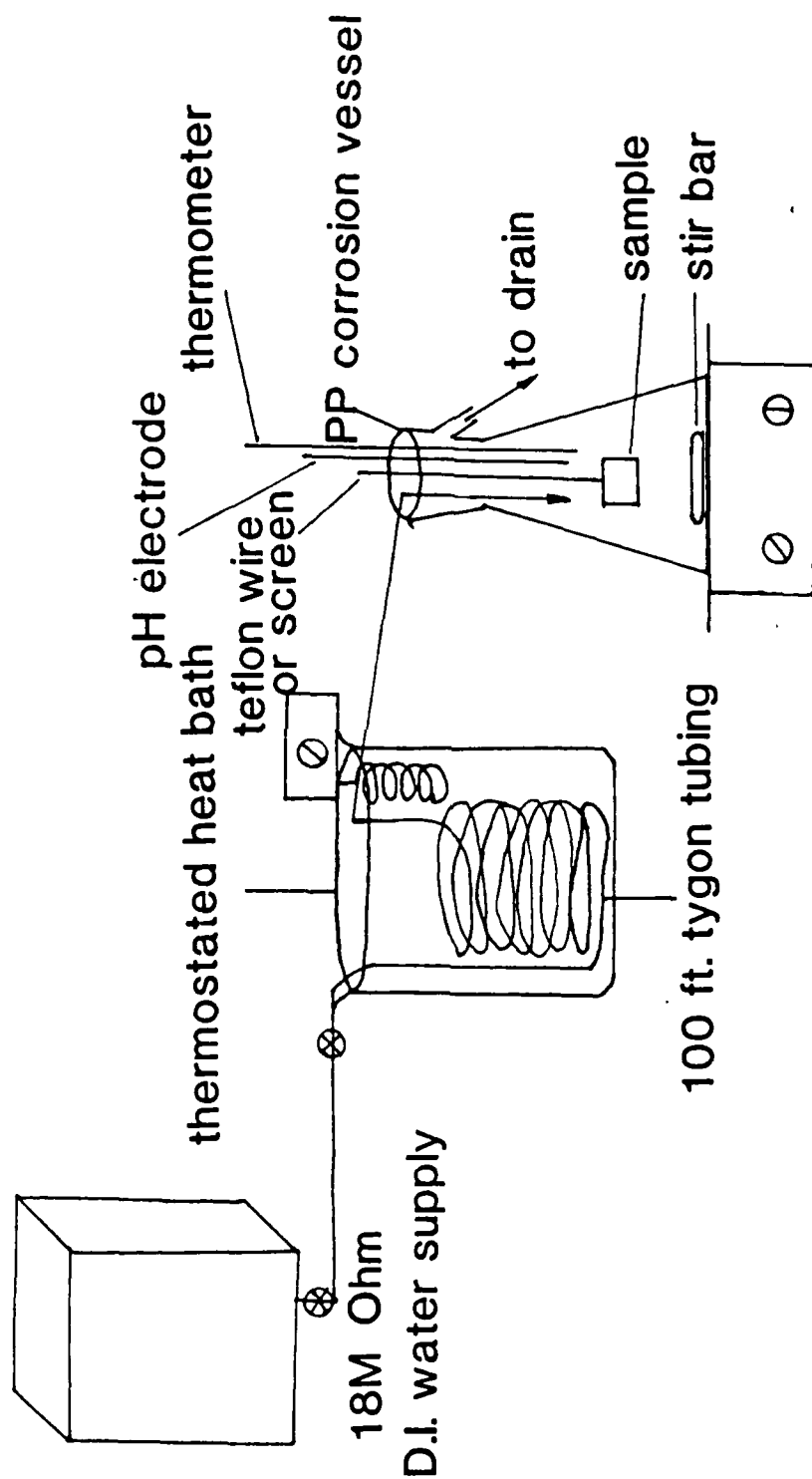
Figure 4.3. Corrosion configuration for dynamic flow condition.

Table 4.2. The flowing conditions for flow tests

Test #	Sample	Flow rate (ml/min.·cm²)	Stirring	Temp.(°C)	Time
(a)-1	ZBLA	139.9	N	25°	6 hr.
(a)-2	ZBLA	228	slow	25°	6 hr.
(a)-3	ZBLA	333.3	strong	25°	9 hr.
(a)-4	ZBLA-F	312.5	N	25°	1 hr.
(b)-1	ZBLA	608.4	medium	25°	0.5-0.3 days
(c)-1	ZBLA	638.2	medium	10°-85°	6 hr.
(c)-2	ZBLA	123.6	N	37°	6 hr.
(c)-3	ZBLA	64.2	strong	63°	6 hr.
(c)-4	ZBLA	65.9	strong	35°	6 hr.

thermometer during the experiment. A stir bar was placed in the vessel to stir the solution, if necessary, and the stirring speed was controlled by setting the dial on the hot plate. The flow rates used ranged from 120 to 1150 ml/min.. The variables of flow rate, temperature and stirring speed are shown in Table4.2.

(a). The effect of stirring speed: Polished ZBLA glass samples were corroded in the vessel for 6 hours. One sample used a flow rate,which has also been normalized to the sample surface area as the value given in the parenthesis, of 0.75 l/min. (139.9 ml/min.$\cdot$cm^2) without stirring, i.e. Test(a)-1. The other sample was corroded at a higher flow rate of 1.15 liter/min. (228 ml/min.$\cdot$cm^2), using slow stirring speed, i.e. Test(a)-2. Corroded samples, after a rinse in methanol and toluene, were observed under SEM both for surface topography and fractured cross section to examine the corrosion layer formed. EDX analysis, X-ray compositional line scan analysis were conducted, X-ray diffraction spectra were also acquired. In order to further test the effect of stirring speed, a ZBLA sample was held in a teflon holder and corroded in water flowing at a rate of 0.5 liter/min (333.3 ml/min.$\cdot$cm^2) with a very high stirring speed for 9 hours, i.e. Test(a)-3. After rinsing and drying in a vaccum oven for a short time, both surface and fractured cross section were examined with SEM, and X-ray diffraction. Another ZBLA-F glass was

clamped in the sample holder which is made of two thin teflon plates with a 1 cm diameter aperture on each, i.e. Test(a)-4. After exposing the sample in the holder to the D.I. water, at a flow rate of 1 liter/min. (312.5 ml/min.·cm^2) for 1 hour, the sample was removed from the holder, rinsed, then observed under SEM.

(b). Corrosion layer formation: To find out how the corrosion layer forms with time, a series of ZBLA samples was corroded under a flow rate of 166 ml/min (608.4 ml/min.cm^2). with stirring at medium speed, for different periods of times, i.e. Test(b)-1. After rinsing, the corroded samples were fractured and the corrosion layer formed was observed and measured by SEM. An average thickness was determined for the transform layer.

(c). High temperature flow corrosion condition: The effect of temperature on leaching of fluoride glasses was studied by corroding several thin ZBLA glass plates with stirred D.I. water flowing at a rate of 120ml/min (638.2 ml/min.·cm^2) at temperatures from 10°C to 85°C for 6 hours, i.e. Test(c)-1. The solution temperature was controlled with a heat bath, and for the temperatures lower than room temperature, ice cubes were used to fill the bath tank. The corrosion layer formation was examined by SEM on a fractured surface.

High temperature flow tests were also conducted at rates of 272 ml/min (123.6 ml/min.·cm^2) flow at 67°C without

stirring, i.e. Test(c)-2. Surface crystal precipitates were observed by SEM. Both Test(c)-3 and 4 were conducted in a D.I. water flow, having a rate of 250ml/min. (65 ml/min.·cm^2), for 6 hours with a high stirring speed at different temperatures. The corrosion solutions used for both the high temperature, i.e.63°C, and room temperature flow tests were sampled at different times during the experiment for I.C.P. solution analysis. Also, an X-ray diffraction spectrum was taken of the high temperature flow corroded sample.

4.3.6. Hydration/Dehydration Tests

Infrared spectroscopy has been commonly used to study the corrosion process in fluoride glasses, mainly by monitoring the change in size of the water (H-O-H at 6.2 μm) and hydroxyl (O-H at 2.9μm) bands. In this work, a Fourier-Transformed Infrared Spectrometer (Nicolet 20SXB FTIR Spectrometer) was used to study the hydration and dehydration processes of ZBLA-F fluoride glass samples corroded in flow conditions at both room temperature and higher temperatures.

A sample corroded for a short time in a static solution was also studied to compare with the same glass exposed to flowing water for the same duration of time. Two samples were obtained by corroding the ZBLA-F glass in a flowing solution at the rate of 250ml/min.. The solution was

stirred for 3 hours. For comparison, the same glass was corroded under static condition, S/V=2, for 3 hours. After rinsing the samples, transmission spectra were taken and SEM was used to measure the depth of attack.

Samples were also corroded at different temperatures but the same flow conditions to study the difference in spectra. The hydration test is the test which measures the growth of OH and H-O-H band with increasing corrosion time. Two series of tests were conducted at 56°C and 20°C. The solution was stirred and the flow rate was 250 ml/min.. The sample was placed into a corrosion vessel for a predetermined period of time and then was removed, rinsed in methanol and toluene to remove adhering water, for spectral measurements. The sample was put back into the corrosion vessel for an additional period of time and the same steps were repeated again. To eliminate the possible error caused by cracking which could occur during rinsing and air-drying, the same sample was used either for no more than two measurements or for a short cumulative leaching time. The integrated areas of the OH band and HOH band were measured. By using a liquid cell, the transmission spectrum of pure D.I. water was taken as a standard to analyze the spectra of the corroded glasses. The ZBLA-F glass was also corroded at 166 ml/min. water flow for 9.5 days to obtain a thick corrosion layer. FTIR spectra and X-ray diffraction spectra were acquired.

A dehydration test was conducted on a sample corroded at 68°C under flowing conditions. The rinsed corroded sample was put into a hot stage which has two cartridge heaters installed and the temperatures used to dehydrate the corroded sample were maintained by a controller. The hot stage was mounted in the FTIR sample compartment without changing the position throughout the experiment. N_2 gas was used to purge the compartment continuously. The FTIR transmission spectra were taken at different stages of the dehydration process.

CHAPTER V

RESULTS AND DISCUSSIONS

5.1. Raw Material Studies

The raw material components of the glasses tested were dissolved in aqueous solutions to measure their saturated concentrations and their equilibrium pH in solution in order to separate the behavior of each individual glass component in the aqueous environments from the observations made on the composite glasses.

5.1.1. pH Drift of Fluoride Compounds

Predetermined amounts of high purity anhydrous fluoride compounds, ZrF_4, BaF_2, LaF_3 and AlF_3, were dissolved in water. After waiting for a sufficient period of time to assure the achievement of equilibrium, the supernatant solution was filtered and used for measuring the pH values and ion concentrations.

The results of pH measurement are shown in Table 5.1. The only fluoride compound that caused a distinct pH drop is ZrF_4 while the others only showed minor pH changes. BaF_2 showed little pH change in spite of its high solubility in the aqueous environment. This will be discussed in the next section. The pH drop resulting from the dissolution of

Table 5.1.   Solution pH drift measurement of   fluoride
compounds

Compound	pH drift	Observation
ZrF_4	5.70→3.29	clear
BaF_2	5.70→5.51	clear
LaF_3	5.70→5.26	clear
AlF_3	5.70→5.01	clear
LiF	5.70→6.21	clear
ZB	5.70→3.29	ppt. formed
BLA	5.70→5.57	clear
ZBLA	5.70→3.29	ppt formed

Table 5.2. Solution Analysis of Fluoride Compounds,
[ ] (10^{-5} mol)

	[Zr]	[Ba]	[La]	[Al]	[Li]	[F]
ZrF_4	40.6	---	---	---	---	129.0
BaF_2	---	35.9	---	---	---	29.5
LaF_3	---	---	0.06	---	---	0.18
AlF_3	---	---	---	1.1	---	2.3
LiF	---	---	---	---	677.0	684.0
ZB	34.0	21.1	---	---	---	112.9
BLA	---	32.5	0	0	---	23.2
ZBLA	28.5	19.1	0	0.8	---	104.2

fluoride compounds, particularly ZrF_4, is due to the hydrolysis of the dissolved species. For example, the hydrolysis reaction of ZrF_4 is responsible for a large part of pH drop during the corrosion of fluorozirconate glasses. This conclusion is strongly supported by the difference of pH drop observed by mixing together powders of ZrF_4, BaF_2, LaF_3 and AlF_3 in different combinations including a mixture of the same composition as the ZBLA glass. The BLA combination caused a pH drop similar to that obtained from BaF_2 alone, while the ZBLA combination had the same pH drop as ZrF_4 alone. For ZrF_4, the effect of ion exchange reaction on the solid plays little role here because the powder used was nearly completely dissolved. Another thing worth noticing is that a layer of precipitate coats the bottom of the container whenever ZrF_4 is mixed with BaF_2 for a certain period of time. The small pH rise resulting from the LiF dissolution was attributed to its high solubility because a sufficient amount of hydrogen ion (H^+) will associate with fluoride ions (F^-) in the solution to form HF. The solution cation concentration was measured by I.C.P. and the fluoride ion concentration was measured by potentiometry with a fluoride ion selective electrode. Powders were mixed to reach a concentration in solution of 50ppm for complete dissolution. The results are listed in table 5.2. The LiF and BaF_2 experienced nearly complete dissolution, and the concentration of ZrF_4 was also high,

whereas LaF_3 and AlF_3 dissolved very little. The measurements also showed a stoichiometrically defficient fluoride ion concentration in solution when compared to the cation concentration measured. This result confirms Simmons' titration study of ZBLAL glass powder.[18] These authors suggested that, on the average, each Zr and Ba ion retain one fluoride ion despite the addition of a strong complexing agent (TISAB), and therefore, that in the pH range covered by the tests, the metal does not release all its fluoride ions. In addition, the results presented here show that Al will also retain one fluoride ion. Simmons further showed that the more highly dissociated species can only be expected in appreciable relative concentrations in solution in the very early stage of corrosion where the fluoride concentration is relatively low. They found that the $[ZrF_4]$ species can be dominant in solutions where the fluoride ion concentration is higher than 1ppm.

When dissolving the combined powders, the [Zr] and [Ba] concentrations measured were lower than their individual solubility. This explains the observation of precipitation products at the bottom of the container, mentioned earlier.

5.1.2. Solubility of Fluoride Compounds

Solubility of the substance has been considered as the most important factor that affects the mineral dissolution process and the rate controlling mechanisms.[46] Moreover,

for the case of nuclear waste glass leaching, if the flow rate of ground water is slow, aqueous solubilities rather than kinetics of the dissolution process have been used to impose a limit on the maximum concentration of many elements that dissolve from the nuclear waste forms.[47,48.] Therefore, in order to gain a basic understanding of the leaching behavior of glass itself, it is necessary to study the solubilities of the glass components.

The solubility of fluoride compounds in solutions of different pH are measured by adding a sufficient amount of each fluoride compound to the solutions, that undissolved material remains in the container. The saturated solution is then analyzed by ICP. Figure 5.1 shows the strong pH dependence of the solubility of fluoride compounds, all of which exhibit a dramatical increase of solubility in acidic environments. LaF_3 has the lowest solubility at nearly all pH values with a minimum around pH=5.26; AlF_3 shows a range of low solubility between pH5-6 and a sharp increase below pH5; BaF_2 has the highest solubility among these four compounds. In the solution pH used, ZrF_4 is relatively difficult to measure because the precipitation of hydroxide can occur in solution pH 4 and pH 6, therefore the minimum solubility shown at pH3.29 was taken from a measurement using D.I. water instead of a buffer solution. The dotted line for ZrF_4 between pH 3.29 and 10 indicates an uncertainty of the minimum solubility point which should
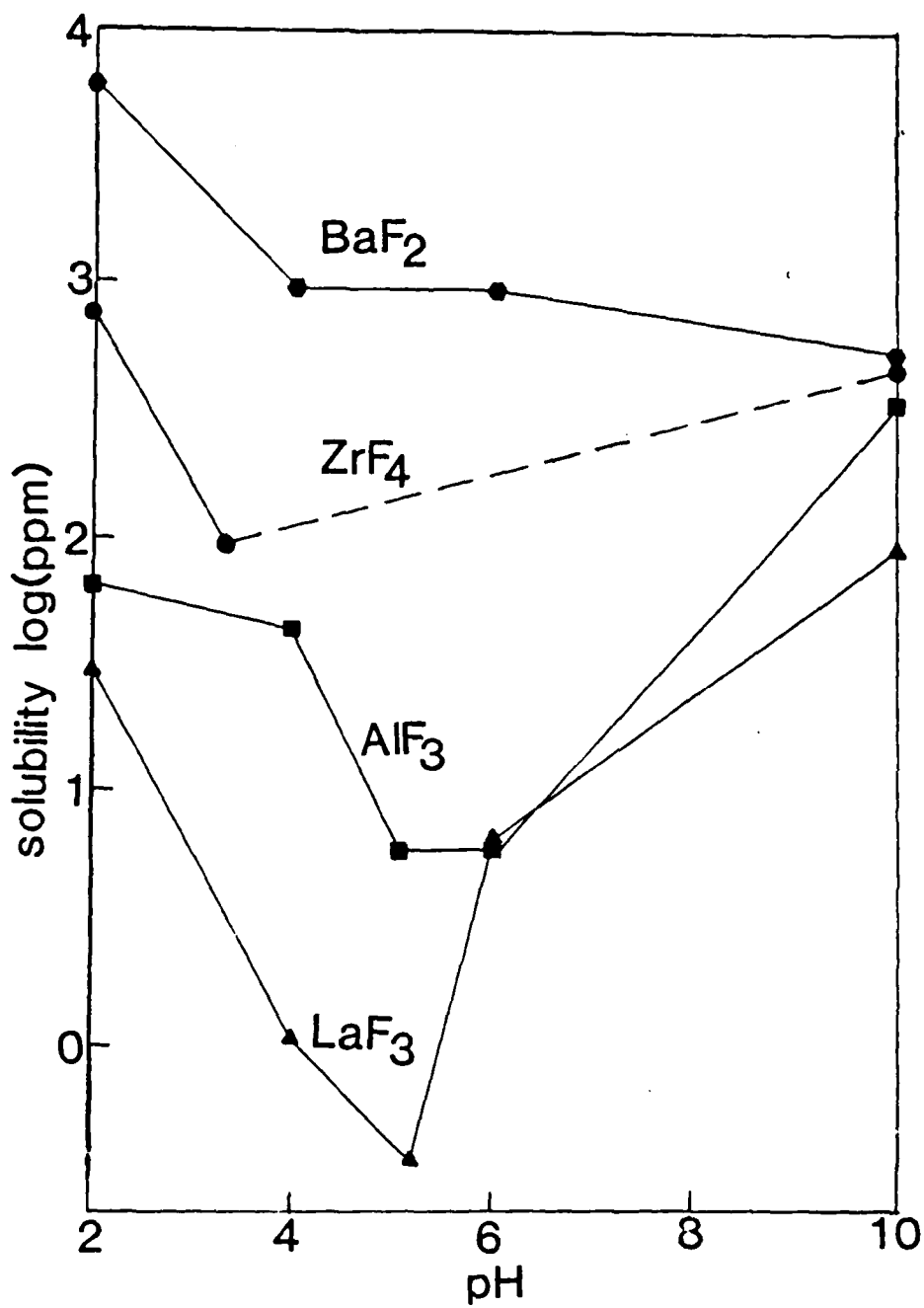
Figure 5.1. Solubilities of fluoride compounds, ZrF_4, BaF_2, LaF_3 and AlF_3, in aqueous solutions of different pH.

fall within this range. The high solubility of all the glass components at both ends of the pH scale is responsible for the high leach rate of the glass in acidic solutions.[21] The decrease near neutral pH is consistent with a minimum leach rate at pH 8. A small increase in more basic solutions, i.e. pH 10 can be explained by the increase of solubility of LaF_3, AlF_3 and ZrF_4 and still relatively high solubility of BaF_2. More solution pH effect on the corrosion of fluorozirconate glasses will be discussed in the next section.

5.2. Short Time Corrosion and pH Effect

A short time leaching study was conducted on glass powders to determine how glass components leach from the very beginning after contact with D.I. water.

5.2.1. pH Drift

Different amounts of ZBLA glass powder were used with the same amount of D.I. water to vary S/V ratio. After being shaken for predetermined period of time, the solution was filtered and the solution pH vs. time were measured as shown in Figure 5.2.. Solution pH experienced a sharp drop, at all three tested S/V ratios, for soaking times as short as 10 seconds and then the decrease leveled off and continued to drop slowly. In all cases the higher the S/V ratio the more pH drift with time.
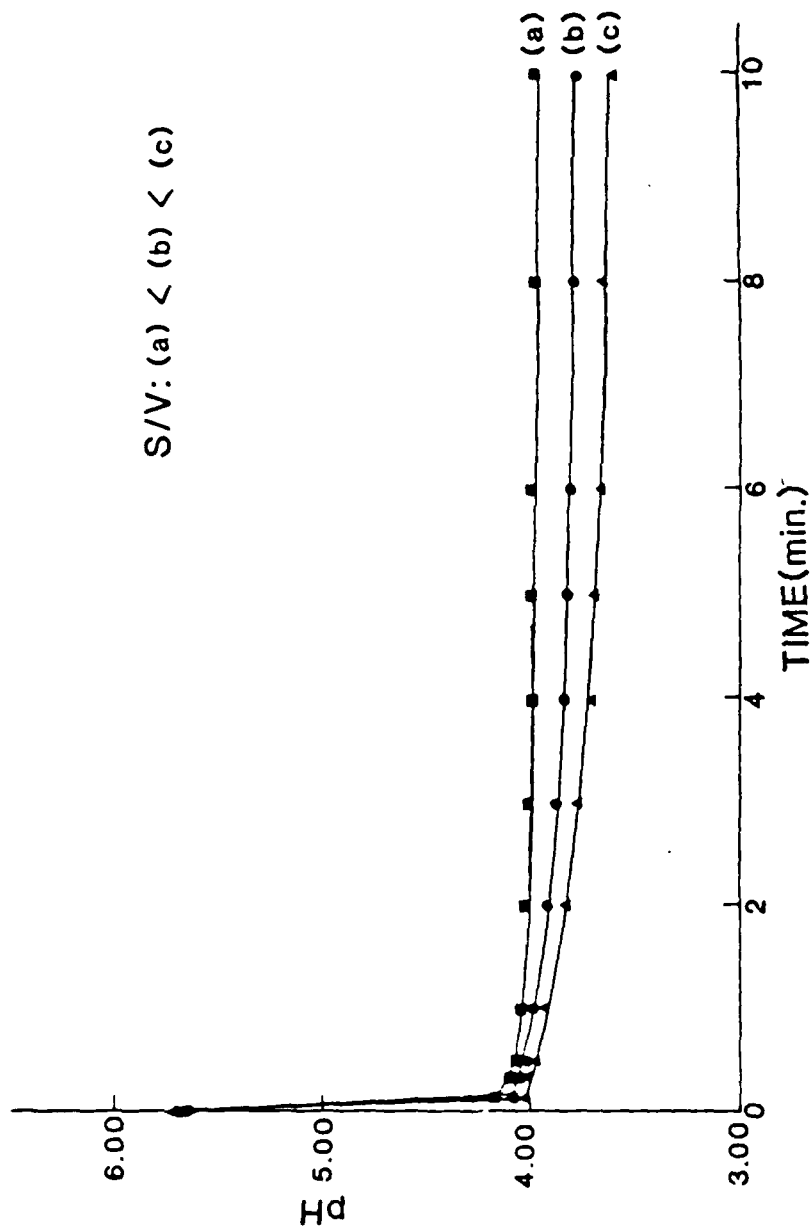
Figure 5.2. PH drift during short time leaching of ZBLAL glass powder at different S/V ratios.

5.2.2. Short Time Leaching

Using ZBLA glass powders, the test samples were prepared in a similar way as in the pH drift measurements. Cation concentrations were measured by I.C.P. spectroscopy and fluoride ion concentration was monitored by means of a fluoride ion selective electrode. The result was plotted as normalized leach rate versus time, see Fig.5.3. The normalized leach rate (NLR) was calculated from the following equation:

$$NLR = [x]\ V/\ (S\ t\ w) = \mu g/cm^2\ day$$

where x= ppm in solution measured, V= solution volume (ml), S= surface area (cm^2), t= soak time (days) and w= weight fraction of element in the original glass. In this study since the soaking time is so short the measurement of cation concentration with I.C.P. is critical. A sufficient amount of glass powder was needed and the most sensitive wavelengths were chosen for increased detection sensitivity. The detection limits of the various components are Zr=0.007ppm, Ba=0.001ppm, Al=0.01ppm and La=0.028ppm. All the elements are present in solution at concentrations much higher than the detection limits except La which is slightly lower. The leach rate of Al, Ba and F are higher at the very beginning, however, this could be due to the small fines, or surface irregularities on the glass powder used.
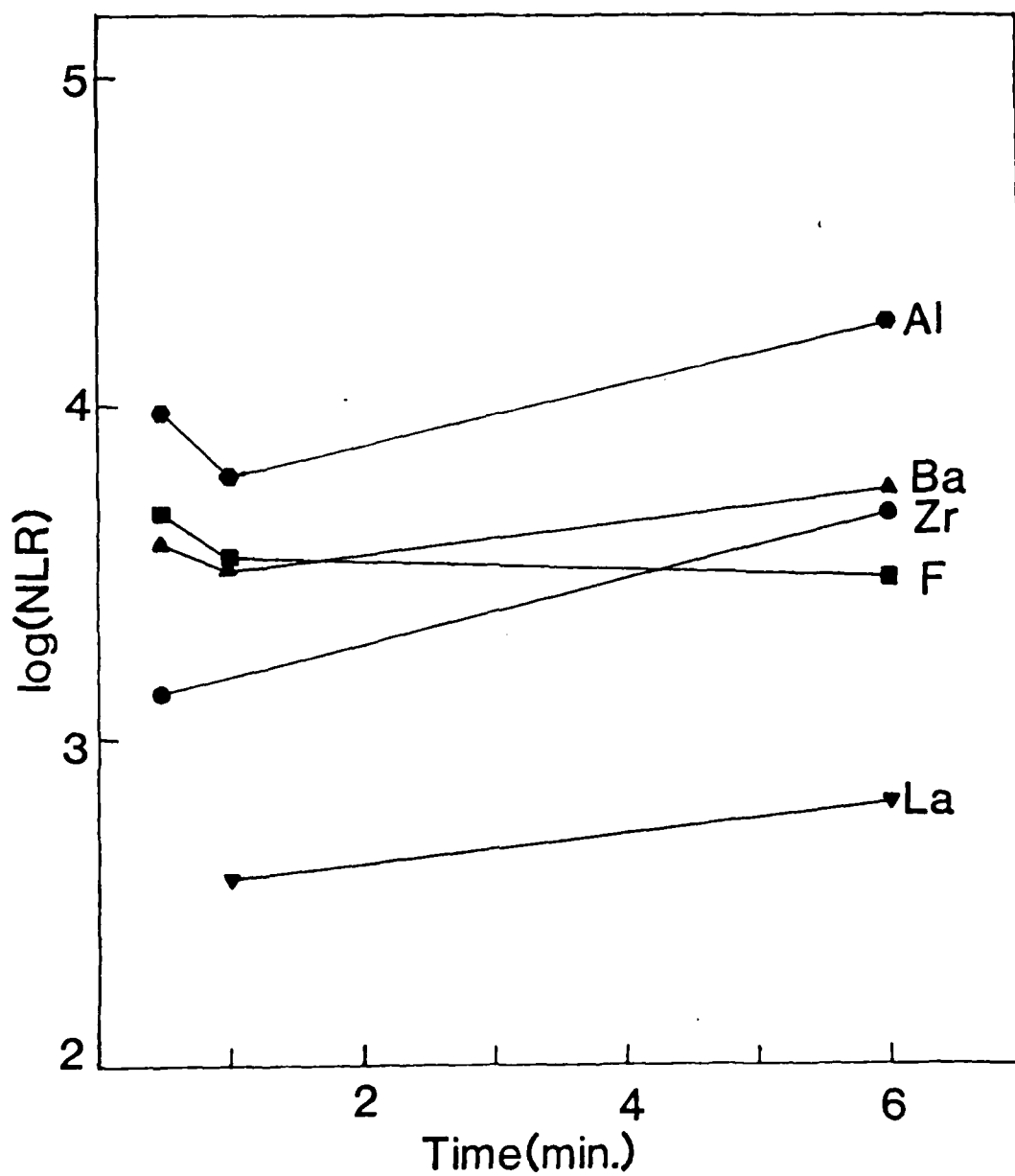
Figure 5.3.   Normalized leach rates vs. time for individual elements of ZBLA glass from solution analysis.

The increase in leach rate at longer time can be attributed to the effect of solution pH drop to a more acidic range.

This result proved that the dissolution of glass occurs as long as it remains in contact with D.I. water, including the glass network former ZrF_4. This leaching process is a combination of network break-down plus selective leaching. The glass network breaks down at a certain rate which is represented by the leach rate of Zr from the very beginning. This can be confirmed by the short time pH drift measurement discussed in last section, i.e. 5.1.2., where a sharp solution pH drop occurs as soon as the glass comes into contact with water. Moreover, The leach rate reported here is comparable to that of longer time leaching studies done by Simmons.[18]

5.2.3. Corrosion of Bulk Glass in Different pH Buffer Solutions

Polished ZBLA glass plates were corroded in an $S/V=10^{-2}$ environment of different buffer solutions; the solutions were stirred. After Corroding at pH values of 2,4,6,8 and 10 for 2 hrs., 2 hrs., 201 hrs., 201 hrs., and 201 hrs., respectively, both the sample surface topography and the fractured cross-sectional surface were examined with SEM. see Fig.5.4. For pH2, the most acidic case, very severe network dissolution occured, forming extensive broad pits over the glass surface with some precitates covering the top
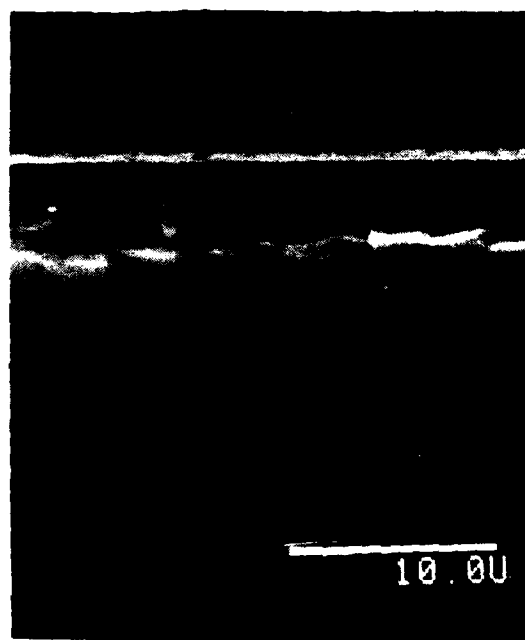
Figure 5.4. ZBLA glasses(top view and cross-section) corroded in different pH buffer solution under stirred condition, $S/V=10^{-2}$, (a)(b) pH2; (c)(d) pH4; (e)(f) pH6; (g)(h) pH8; (i)(j) pH10.

(e)
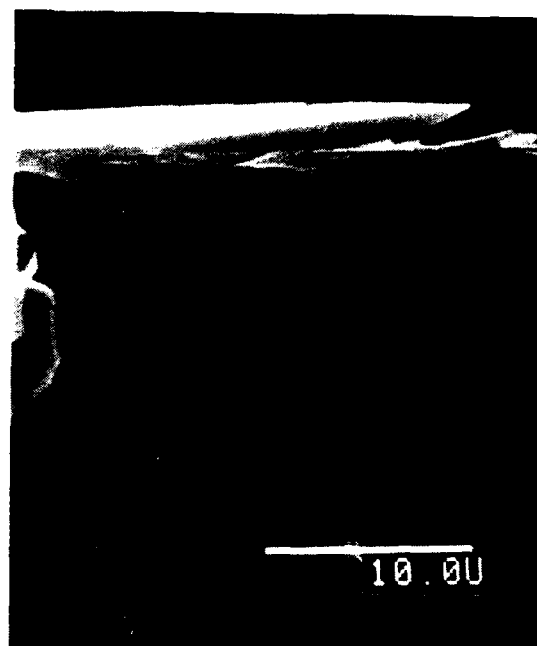
(f)

(g)
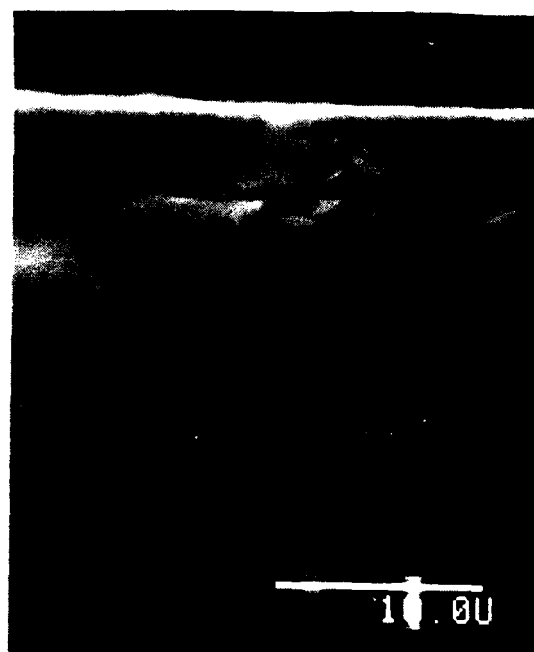
(h)

Figure 5.4 (continued)
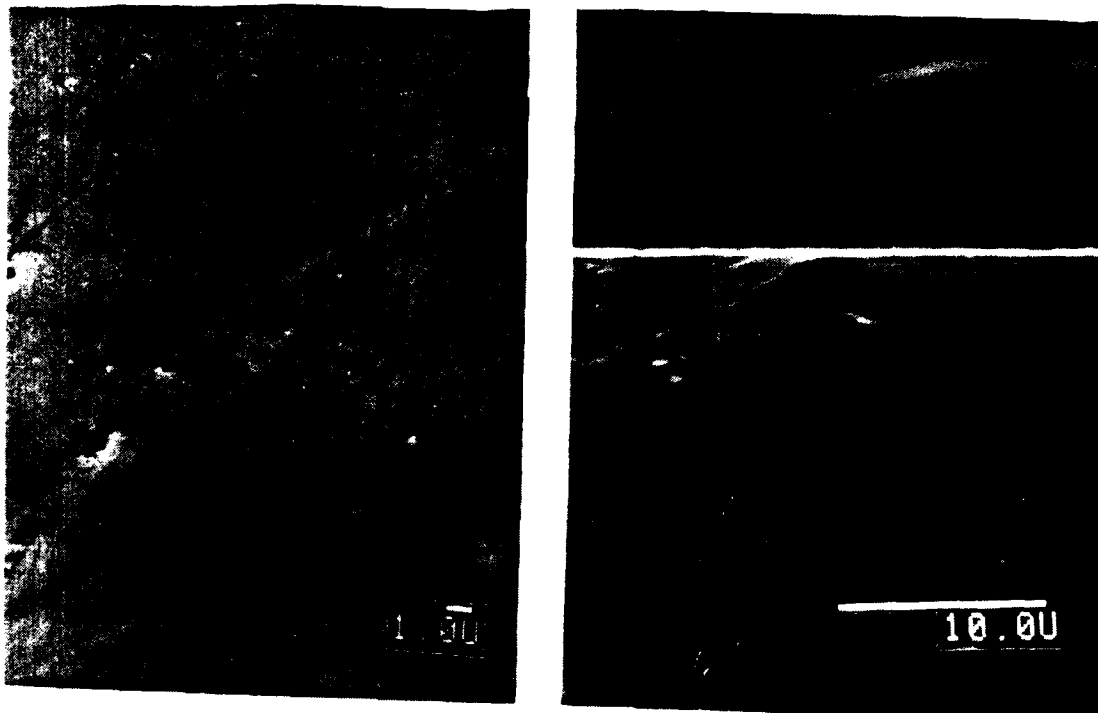
Figure 5.4 (continued)

of the surface, see (a). In some regions, instead of broad
extensive pits, severe disssolution left irregular pits and
remnants on the glass, see (b). At pH4, where the
solubility of ZrF_4 is much lower than at pH2, a thick
transform layer forms in two hours, see (d), although the
surface topogrophy exhibits little change, see (c). This
can be explained by the difference of solubilities of two
main components in glass, i.e. ZrF_4 and BaF_2,. The
phenomenon of an altered layer remaining behind as the
aqueous solution leaches soluble and moderately soluble
species from the glass matrix has been observed in the
corrosion of nuclear waste glasses.[49] A similar argument
could also apply to the layer formation of pH6, see (e) and
(f), and pH8, see (g) and (h). In a pH 10 solution, where
BaF_2 has its lowest solubility and which is very close to
that of ZrF_4, (see Fig.5.1), there is no distinct
transformed layer, see (j), only numerous pits on the
surface due to a matrix dissolution processes, see (i).
Although the solubilities of AlF_3 and LaF_3 are high at pH10,
they only make up small proportions of the glass, thus the
effect will be small. Moreover, the solubility of ZrF_4 here
is about half that measured at pH2, but the degree of
corrosion is much smaller. More work still needs to be done
to obtain a better understanding of the corrosion process in
basic environments. However, the selective leaching of more
soluble species, i.e. BaF_2, can drastically enhance the

(a)

(b)

(c)

(d)

Figure 5.5. ZBLA glass corroded in PH2 buffer solution under S/V=40 for 6 hours.

(a) $\overline{100\ \mu m}$

(b) $\overline{1\ \mu m}$

(c) $\overline{1\ \mu m}$

Figure 5.6.   ZBLA glasses corroded in pH10 buffer solution under S/V=40 for 6 hours.

glass leaching processes. Because of the microporosity produced after leaching of BaF_2 it is possible for the solution to penetrate into the bulk glass and the effective glass surface area accessible to reactions with the solution will be greatly increased. Another conclusion which can be drawn from this test is that for corrosion in acidic aqueous environments, the leaching process is drastically accelerated and the solution saturation/reprecipitation process can occur faster.

The 6 hours stagnant tests with S/V=40 were conducted on ZBLA glass in pH2 and pH10 buffer solutions to observe the corrosion layer formation. At pH2, see Figure 5.5, the surface was covered by spherical crystalline precipitates, see (a), which were composed of many small colloids, see cross-section (b). In some regions, below these spherical crystals another smaller spherical type of precipitate can be found in the broad etch pits, see (c), with microstructure as shown in (d). For the case of pH10, only a few pits were formed, mostly along polishing lines, see Fig.5.6 (a), with some small colloidal precipitate formed, along the polishing lines, see (b), and in the pits, see (c).

5.3. Solution Precipitation Study

Precipitate crystals have been found formed on the corroded glass surface. However, the formation mechanisms

are still subject to debate. Doremus et al.[28] proposed that the ZrF_4 crystal deposits on the glass surface grow from the glass surface and that surface diffusion and surface depletion of other ions may be involved. These authors also suggested the dissolution processes of glass should not be controlled by the diffusion in solution. Frischat et al.[38] made a similar suggestion that the crystals which form on the surface can be due to a part of the leached/dissolved glass components segregating at the glass surface. On the other hand, Simmons et al.[14,18] proposed that crystals are formed through a supersaturation/reprecipitation process from the solution. This study was conducted to resolve this conflict. The solution precipitates were collected through three methods:

(1). Through the corrosion solution of ZBLA glass corrosion, S/V=1.5, 5 days. After the sample was removed, the solution was left sitting for enough time to have precipitates form and suspend in the solution. This could then be collected for analysis, see Fig.5.7. Two types of crystals were found in this case. There were spherical crystals (a) which have also been found on the samples corroded in a stagnant solution. Their composition is shown in EDX spectra, see (b)-(1), to be mainly a Ba/Zr containing crystals; with a small La peak. The other type of crystal is extensive, exhibiting network texture and covers the spherical crystal, see (a), its composition is
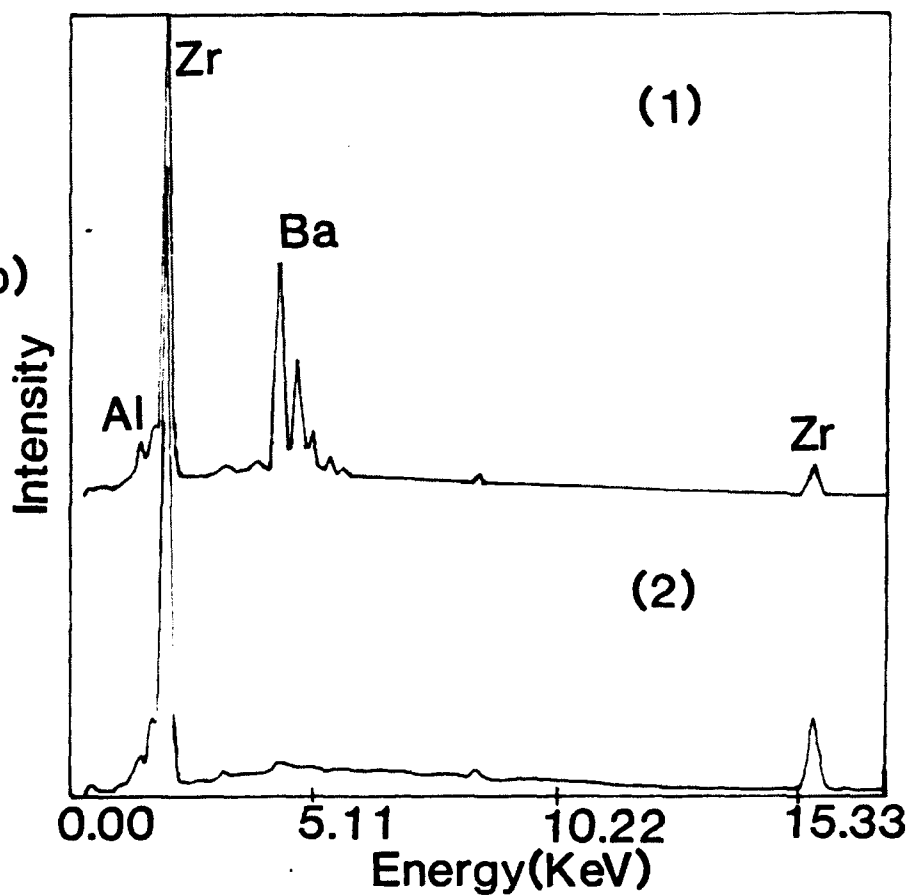
(a)

(b)

Intensity

Energy (KeV)
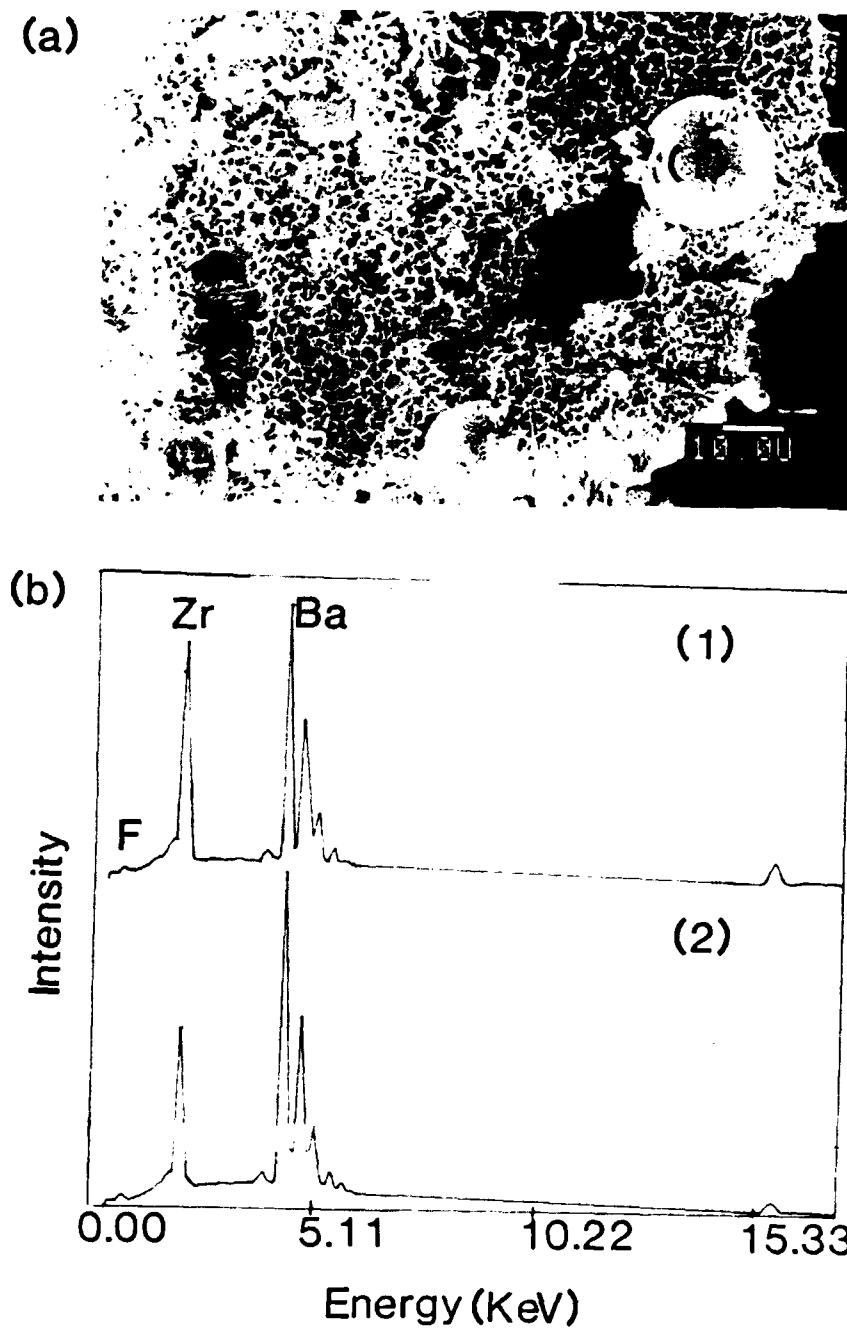
Figure 5.7.   (a)   The crystal precipitated from solution by method, (1), (b)-(1) The EDX spectrum of spherical crystal, (b)-(2) EDX spectrum of network-like crystal.
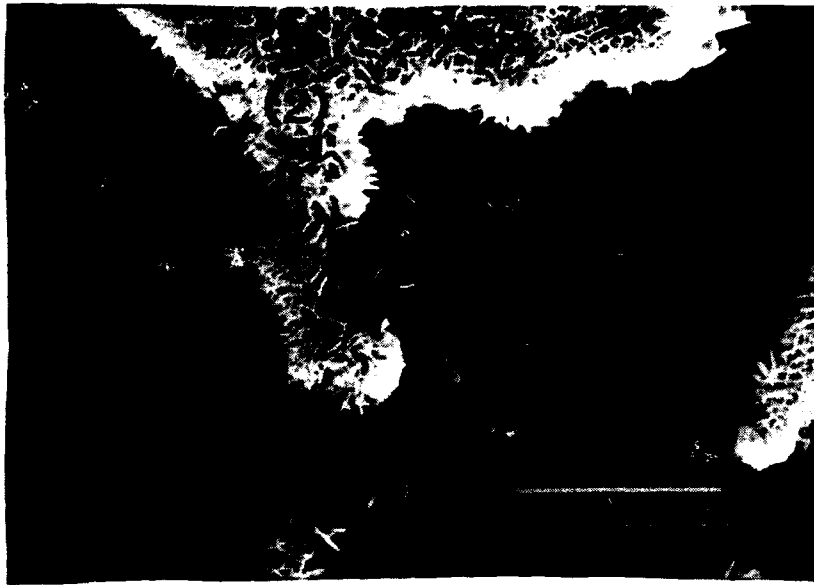
indicated in (b)-(2) as a Ba/Zr containing crystal with a higher Ba/Zr ratio than the spherical crystal.

(2). Precipitates prepared from the solution of ZBLA glass, corroded under S/V=15 condition for 4 hours. After the sample was removed, the solution was air-dried to cause supersaturation/ reprecipitation processes to occur and the precipitated crystals were examined under SEM. see Fig.5.8. Two main types of crystals were found, see (b). These two crystals are similar to the cystals formed on the glass surface which was corroded under a dilute and nearly static condition, see Fig.5.8 (a). These crystals have a composition as shown in Fig.5.9 (b)-(2), and are basically ZrF_4 crystals composed of laminae shaped into thick rods. The spherically shaped crystals consist of thin platelets and are composed mainly of Zr,Ba, see Fig.5.9 (b)-(1). However, Al also appears in the spectrum. X-ray diffraction spectra of these precipitates are shown in Fig.5.10 (a), in which α-$BaZrF_6$ and ZrF_4 crystals can be identified, similar to the spectra of the glass corrosion layer, see (b); yet there were many other peaks which could not be identified. The existence of Al in the EDX spectrum for the $BaZrF_6$ crystals could come from, the bottom glass slide used or from Al containing precipitates created by supersaturation of Al in the reduced solution volume.

(3) precipitated crystal were also collected from a solution saturated by the leaching products from the ZBLAL

(a) 1 $\overline{\mu m}$

(b) 1 $\overline{\mu m}$

Figure 5.8. Comparision between the crystal precipitate on corroded glass (a), and that from the saturated solution,(b).

Figure 5.5.   The crystals precipitated from solution by
method (2); (b)-(1) The EDX spectrum of spherical crystal;
(b)-(2) of ZrF$_4$ crystal.
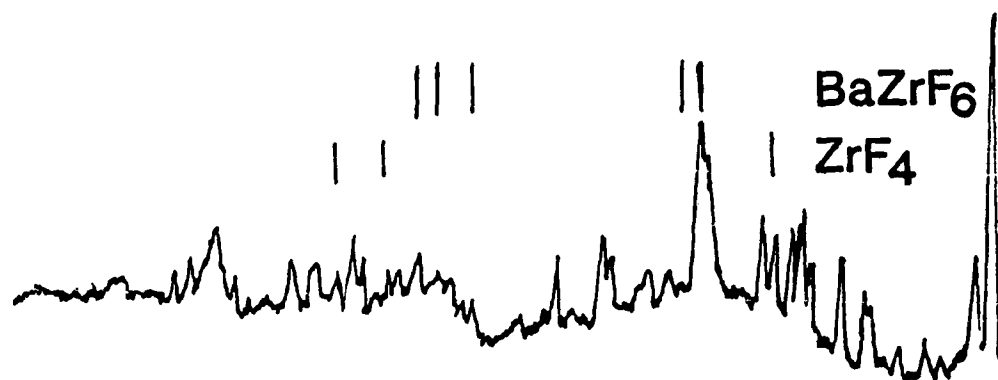
(a) Precipitated crystals from solution
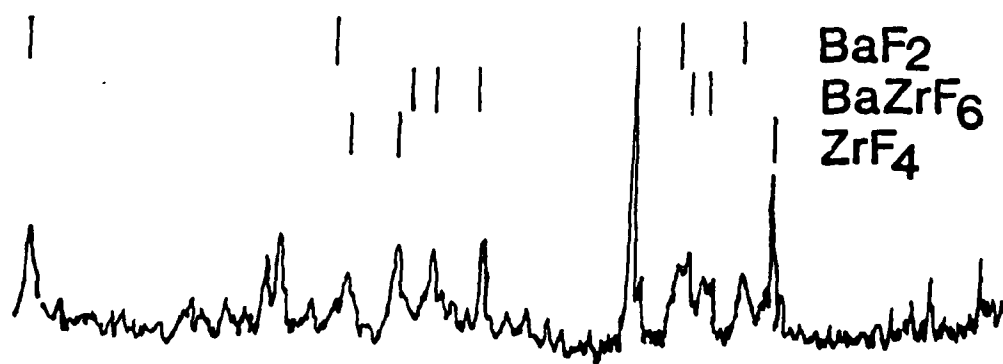
(b) Precipitated crystals on corroded glass

Figure 5.10.   (a) X-ray diffraction spectrum of crystal
precipitated by method (2), compared to that of corrosion
layer formed at S/V=1 for 7 days, see (b).
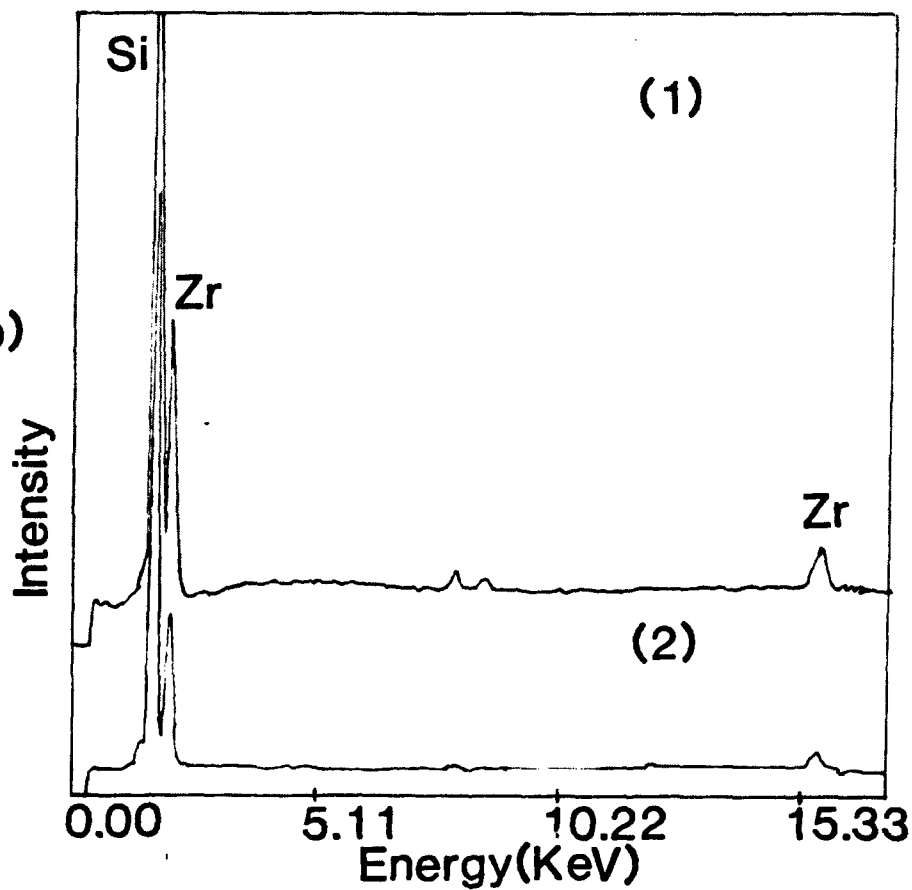
Figure 5.11.   The crystals precipitated by method (3); (b)-
(1) The EDX spectrum of plate crystal; (b)-(2) of cluster
crystal.

glass powder from which the precipitated crystals were deposited on fused silica slides. Figure 5.11 (a) shows badly formed large plate crystals with extensive crystalline cluster deposits on them. The EDX spectra of the plate precipitates only contain Zr see Fig.5.11 (b)-(1), whereas (b)-(2) shows that the cluster crystals have Zr, Al in them.

The results of a comparison of precipitated crystal that formed through saturation /reprecipitation processes from the solution, with those formed on the corroded glass surface,indicate that the precipitates formed on the corroded glass surface are due to the saturation of the solution near glass/solution interface and the repricipirtation of crystals onto the glass surface.

5.4. Stagnant Tests

Various stagnant tests have been conducted, which allow the study of the effect of reconcentration of the corrosion products on the leaching processes. In the extreme of this condition, it can simulate the result of the exposure of optical glass fibers by very small amount of water penetrating through the coating. In this section the following subjects will be included:

(1) Introduction

(2) Surface pH measurement

(3) Intermediate S/V ratio (i.e. S/V=1-5.)

    (a) Short time static test at S/V=5.

(b) Long time static test at S/V=1.

(c) Corrosion layer formation vs. time

(4) High S/V ratio static test

5.4.1. Introduction

From the earlier discussion it is clear that the glass begins leaching as soon as it contacts the D.I. water and the leach rate of each glass component is strongly dependent on solution pH, thus the concentration of corrosion products in the solution will also be pH dependent. Reprecipitation will occur when the solution reaches saturation, and the types of crystal formed on the surface depend upon various corrosion conditions. This statement can be illustrated by comparing glasses corroded at different S/V ratios as shown in Figure 5.12.   (a) shows a glass corroded at S/V=2 exhibiting mainly ZrF_4 crystals on the surface, while the same glass corroded at higher S/V ratio for 9 hours has mostly spherical precipitate crystal on its surface, see (b), which contains Ba, Zr. Two different glass compositions corroded under the same corrosion condition exhibit different surface precipitates indicating different degrees of species saturation, see Fig. 5.13. (a), (b). In order to obtain a better understanding of the corrosion under stagnant conditions, it is necessary to first consider the solution pH value at the glass/water interface.

(a)
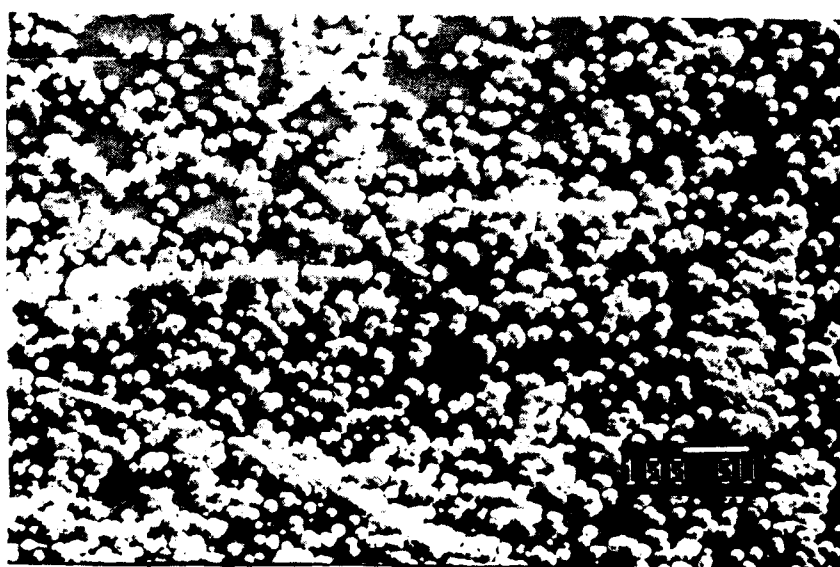
(b)

Figure 5.12.   ZBLA-F glass corroded under different static corrosion conditions. (a) S/V=2, 3 hours, (b) high S/V, 9 hours.
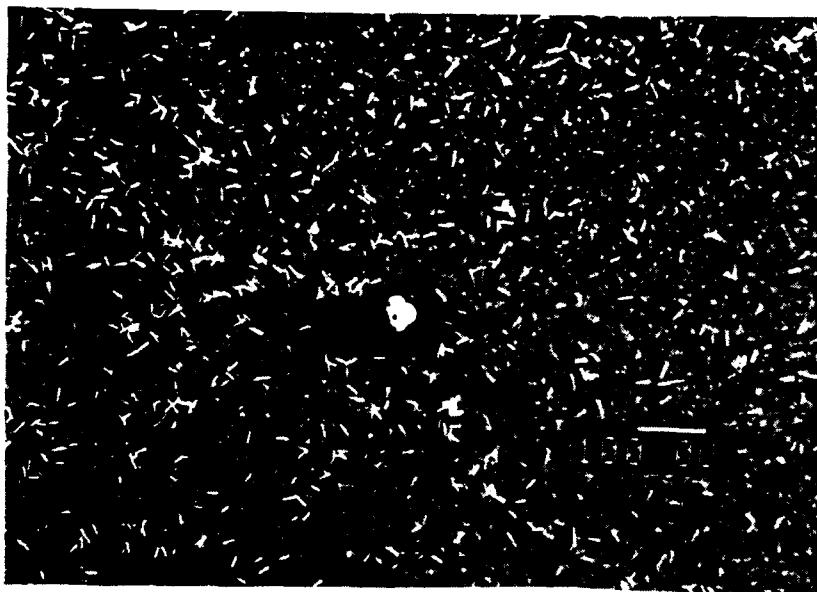
(a) $\overline{100\ \mu m}$

(b) $\overline{1\ \mu m}$

Figure 5.13. Static corrosion at S/V=15 for 4 hours.
(a)ZBLA-F glass, (b) ZBLA glass.

5.4.2. Surface pH Measurement

Surface pH values of fluorozirconate glasses were measured as a function of time with a Ross flat-surface, epoxy-body combination electrode. Different glasses were used for the first measurements where the S/V ratios were adjusted between 9-13. Figure 5.14 shows the measurement results. A sharp pH drop at the surface was experienced for all the sample measured which then levels off at a pH value between 4-3.45. After that the pH continues to drift downward gradually and a second levelling off occurs at a pH value between 2-1.6. The corroded samples were also examined by SEM, see Fig. 5.15. In all cases, a thick layer was formed with spherical Ba, Zr containing crystal. ZrF_4 was only found on the glass surface of the ZBLA-F sample. By controlling the amount of water used in the measurement to achieve the conditions of different S/V ratios the pH drift of ZBLA-F glass is reported in Fig. 5.16. After the measurement, samples were observed under SEM to find that for higher S/V only spherical crystals were found on the surface, see Fig. 5.17 (a). Similarly to the bulk solution pH measurement, the higher the S/V ratio the more rapid was the drop in solution pH value. Moreover, the pH drop on the surface is proceeding in steps instead of a continuous drift indicating that some buffering effect of the solution hydrolysis species must occur. The importance of buffers was demonstrated in corrosion studies of silicates for
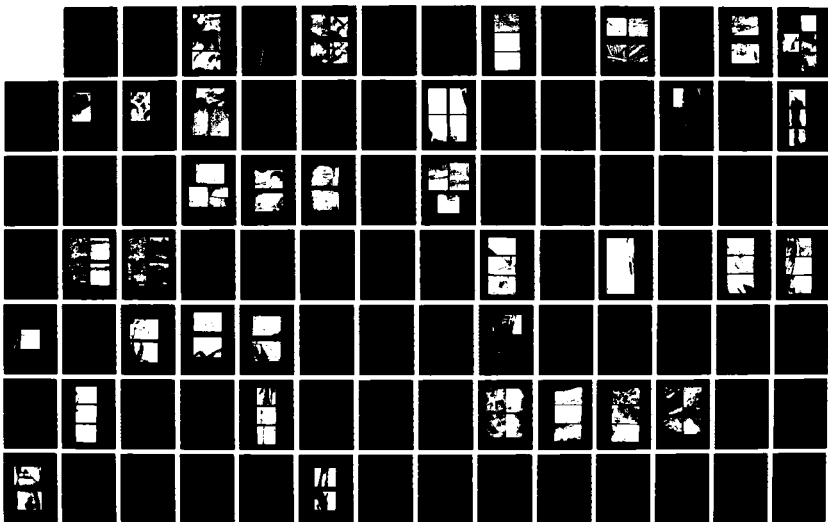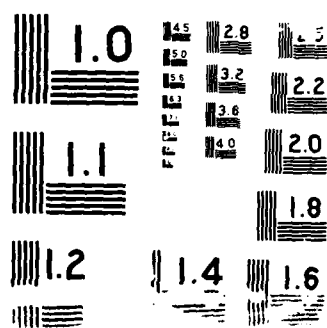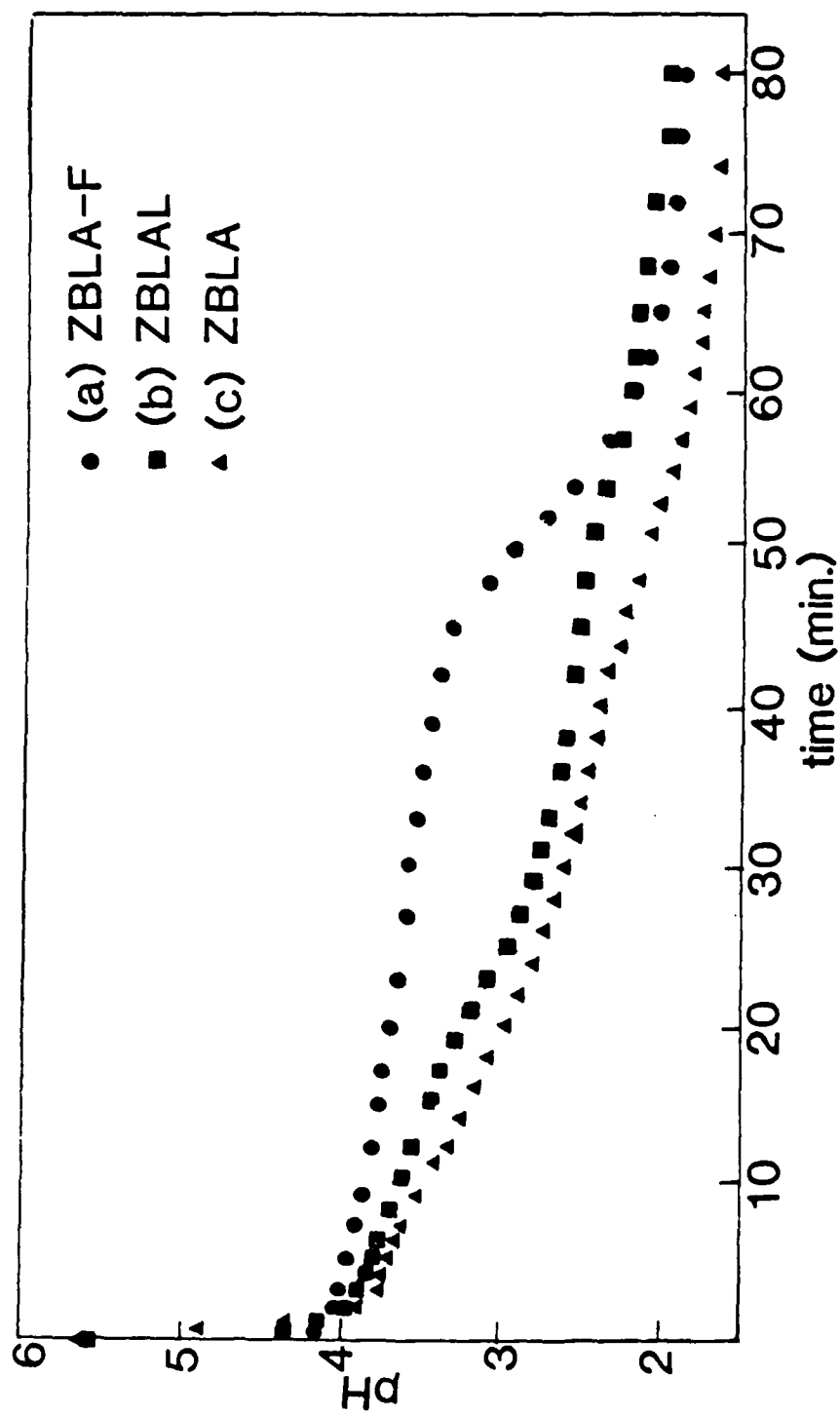
Figure 5.14. Solution pH drift near glass surface vs. corrosion time. (a) ZBLA-F; (b) ZBLAL; (c) ZBLA.
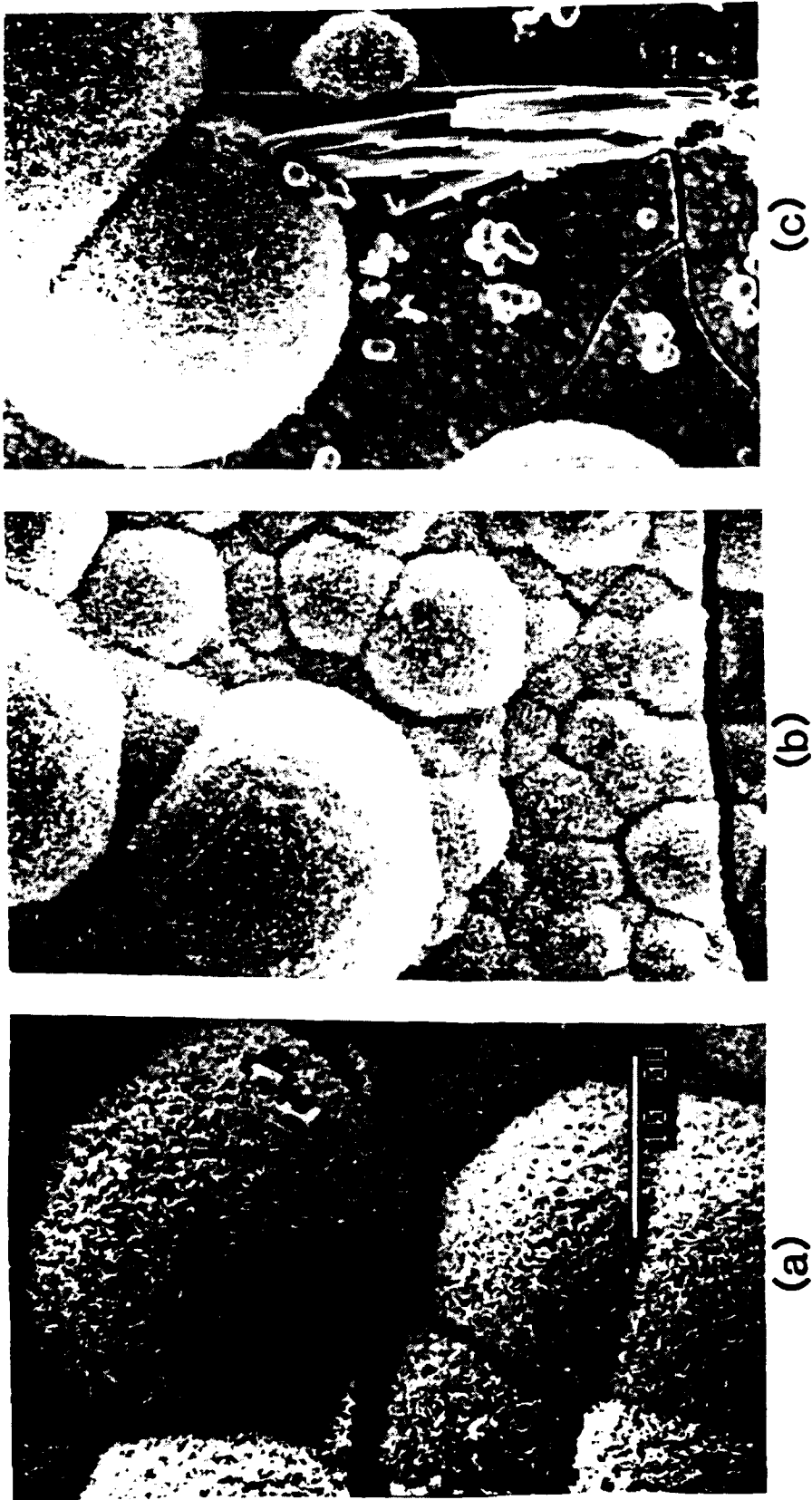
Figure 5.15. SEM micrograghs of different glasses staticly corroded at S/V=10 for 80 minutes. (a) ZBLAL, (b) ZBLA, (c)ZBLA-F.
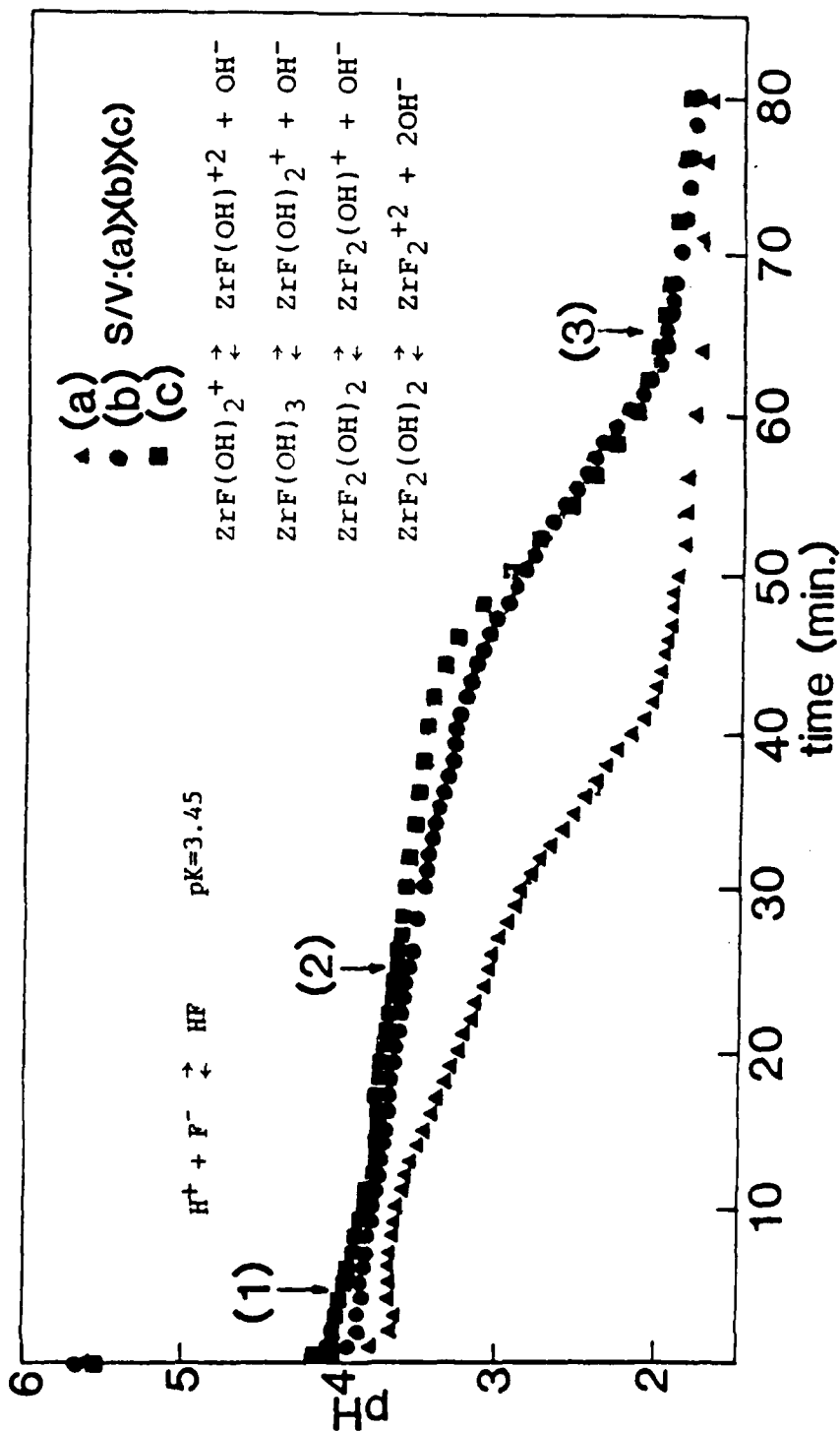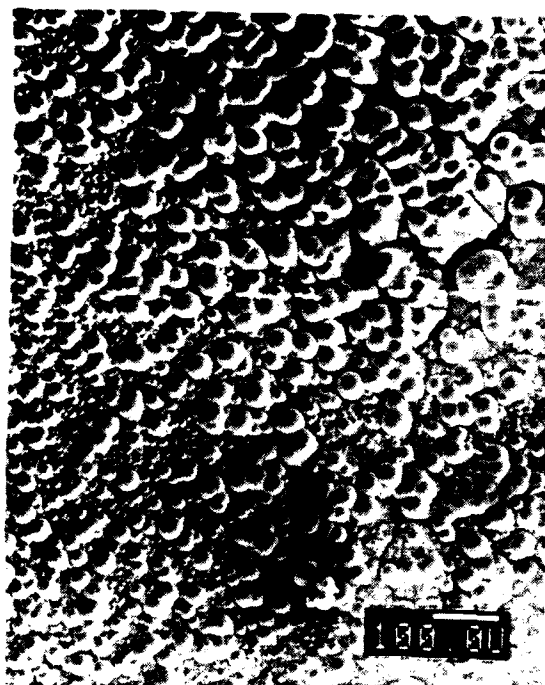
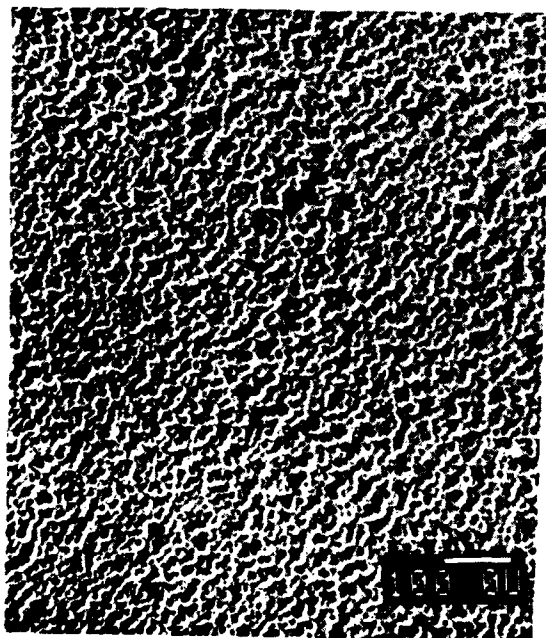Figure 5.16. Solution PH drift near ZBLA-F glass surface at different S/V ratios, for 80 mins. S/V:(a)>(b)>(c).

100 µm   (b)   10 µm
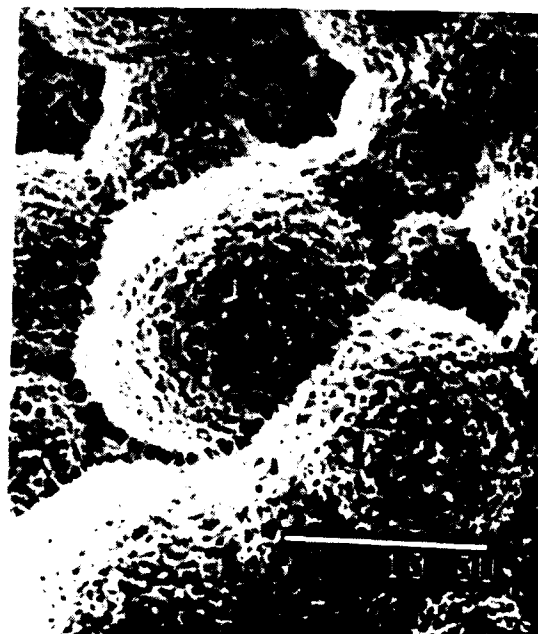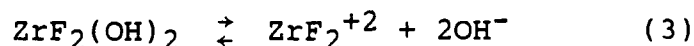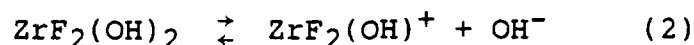

(a)

Figure 5.17.   ZBLA-F glass surface topography after corroded
at different S/V for 80 minutes, S/V: (a)>(b).

nuclear waste disposal. There, important buffers were CO_2 from the atmosphere, silicates and $CaCO_3$ from ground water, and silicic and boric acid and phosphoric acid generated by the dissolution of the glass.[50] Unlike nuclear waste glasses, fluorozirconate glass leaching causes the solution pH to drift toward the acidic range. The first plateau in the pH drop is attributed to the buffering effect of hydrofluric acic, which can form during the leaching process, as shown below:[51-1]

$$H^+ + F^- \rightleftarrows HF \qquad pK=3.45$$

As the leaching process proceeds and the fluoride ion concentration increases, fluorine ions react with hydrogen ions in the solution to form HF and temporarily buffer the solution pH until the fluoride ion concentration in solution is insufficient to buffer sufficiently the increasing amount of H^+ ions released in solution. Then the solution pH will start to drop more rapidly again. Aqueous solutions saturated with ZrO_2 react to form stable hydrolysis products, $Zr_x(OH)_y^{+(4x-y)}$, where x and y are a function of solution pH and vary from (1,4) at pH=5.7-5.0, and to gradually more dissociated species as the solution pH decreases.[52] Simmons and Simmons[18] have calculated the relative $[ZrF_x]^{+4-x}$ species concentrations and showed that they are strongly dependent on the fluoride ion

concentration in solution. $[ZrF_4]$ and $[ZrF_3]^+$ will be the dominant species for fluoride concentrations greater than 10ppm. They also determined that if hydroxyls are available, the most probable zirconium species in solution are the hydrolyzed forms: $ZrF(OH)_2^+$ and $ZrF_2(OH)_2$ with the neutral species favored at higher fluoride concentrations, i.e. $[F^-] >$ 10ppm. The buffering effect shown after the second drop in the pH measured near the glass surface occurs around 1.7-2.0. It seems likely that this is due to the dissociation of hydroxyl groups from the hydrolyzed species proposed by Simmons et al. through the following reaction:

$$ZrF(OH)_2^+ \rightleftharpoons ZrF(OH)^{+2} + OH^- \qquad (1)$$

$$ZrF_2(OH)_2 \rightleftharpoons ZrF_2(OH)^+ + OH^- \qquad (2)$$

$$ZrF_2(OH)_2 \rightleftharpoons ZrF_2^{+2} + 2OH^- \qquad (3)$$
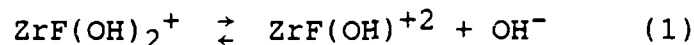
Moreover, the samples on which the surface pH measurements were conducted for different times, have been collected to observe the precipitation crystals formed on their glass surface at different stages of the measurement, as indicated on curve (c) in Fig. 5.16. Figure 5.18. shows the samples corroded for (1) 4.5 min., (2) 25 min. and (3) 65 min. respectively. In (1) we can see only very few irregular precipitates on the surface. After 25 min, (2) shows some ZrF_4 crystals on the surface and in this case the solution pH still appears to be buffered at 3.45 by the

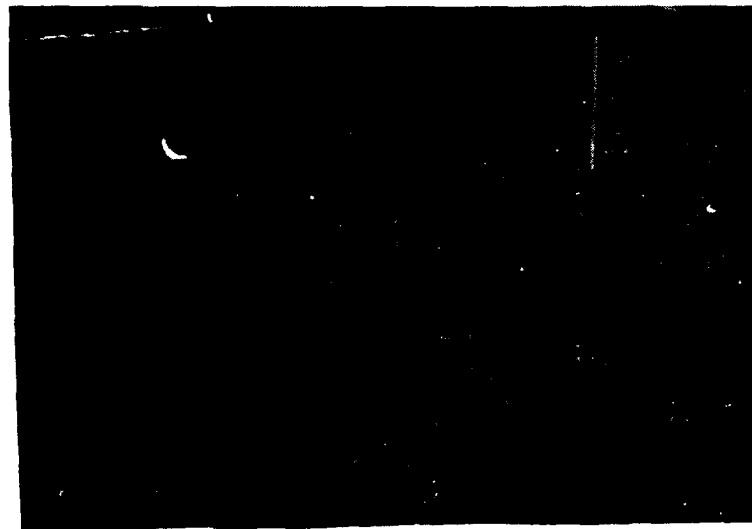(1) $\overline{100 \quad \mu m}$

(2)

(3)
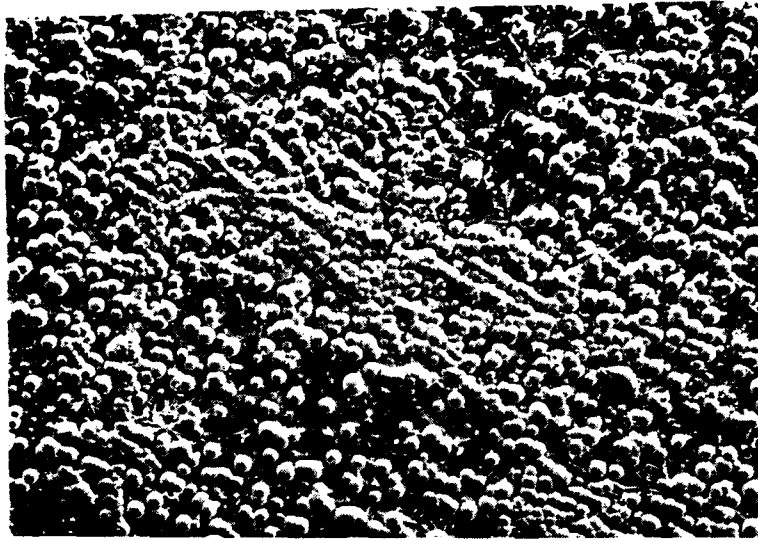
Figure 5.18. Surface topography of ZBLA-F glass corroded for different times corresponding to the curve (c) in Figure 5.16. (1) 4.5 min, (2) 25 min, (3) 65 min.

formation of HF in solution. Since only a small amount of solution was used in the measurement, the fluoride ion concentration in the solution builds up very rapidly, thus the $[ZrF_4]$ and $[ZrF_3]^+$ species are the dominant species at this time. In 65 min, however, the corrosion solution has experienced another rapid pH drop, and we can find numerous spherical Ba/Zr crystal on the glass surface. Higher S/V ratios lead to a faster solution pH drop, see curve (a) in Fig. 5.16, and a thicker spherical Ba/Zr crystal layer formed in place of the ZrF_4 crystal as shown in the previous figure.

5.4.3. Intermediate S/V Ratio

(a). Short time static test at S/V=5. In order to understand how static corrosion proceeds with time during the early stage of corrosion, a series of short time tests were conducted by putting a drop of D.I. water on top of a polished ZBLA-F glass plate, for given periods of time. Figure 5.19. shows that under this corrosion condition, within a time as short as 5 minutes a large number of pits, which formed due to the matrix dissolution of the glass, will be produced preferentially along the polishing lines, see (b). This occurs because in concave regions, such as polishing lines, corrosion products have a greater difficulty in diffusing out thus the accumulation of these corrosion products more easily occurs, which in turn cause a
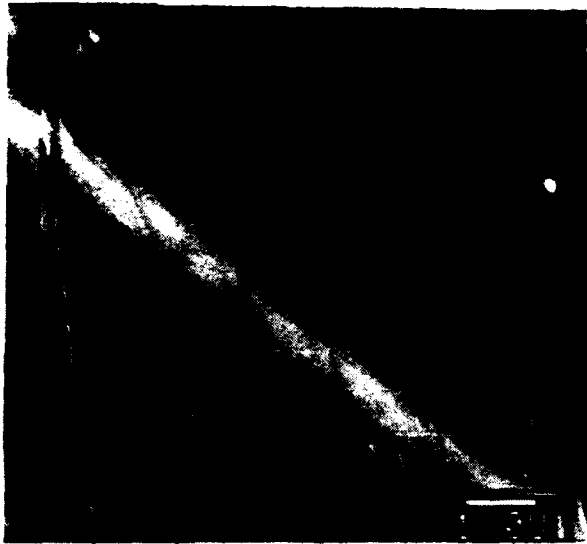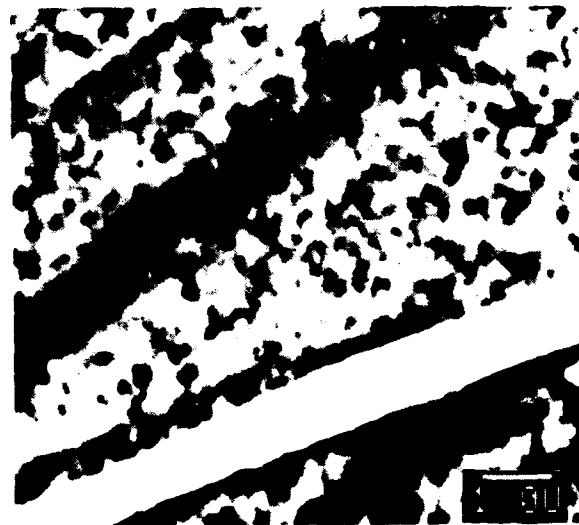
(a) 0 min. ($\overline{1 \ \mu m}$)

(b) 5 min.
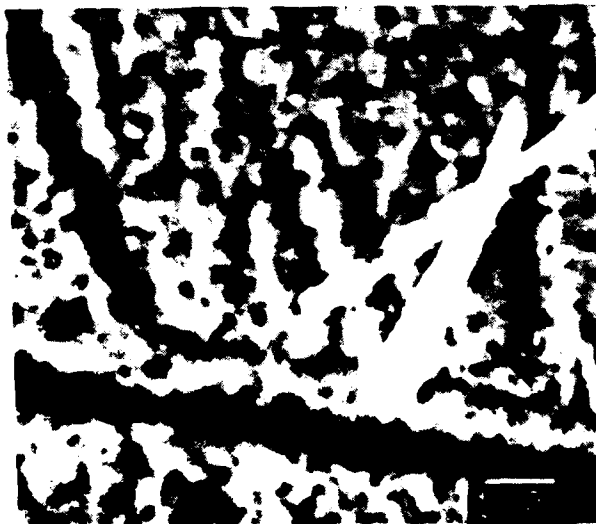
(c) 15 min.

(d) 30 min.

Figure 5.19. Short time static corrosion of ZBLA-F glass at S/V=5.

more severe pH drift and so more rapid dissolution. As time
proceeds, the precipitation of ZrF_4 crystals occurs and the
glass surface becomes rougher due to extensive pitting on
the glass surface, see (c), (d). Figure 5.20.(a) shows
clearly the difference of surface topography between the
areas inside of and outside of the corroded region. Within
the corroded region, corrosion does not proceed uniformly;
some regions, such as compositional inhomogeneities,
experience more severe corrosion. The boundary between the
corroded and uncorroded region exhibited severe corrosion
due to the evaporation of water and corresponding reduction
in solution pH during the experiment. Fig.5.20(b) shows
that in some areas, the glass network breaks down and water
starts to penetrate into bulk glass.

(b). Long term static test at S/V=1. These tests were
conducted to examine the corrosion layer formation of
fluorozirconate glass under static condition. A sample of
ZBLA glass was immersed in D.I. water at S/V=1 for 7 days.
Figure 5.21 shows the typical statically corroded glass
surface with two distinct layers formed, see (a), due to the
leaching processes. The outer layer is composed of three
main types of precipitated crystals, see (b), thus this
layer will be refered to as the precipitation layer in the
rest of the text. Below the precipitation layer is a layer
which was originally glass and has reacted with water. On
the top of this layer polishing marks still can be seen, see
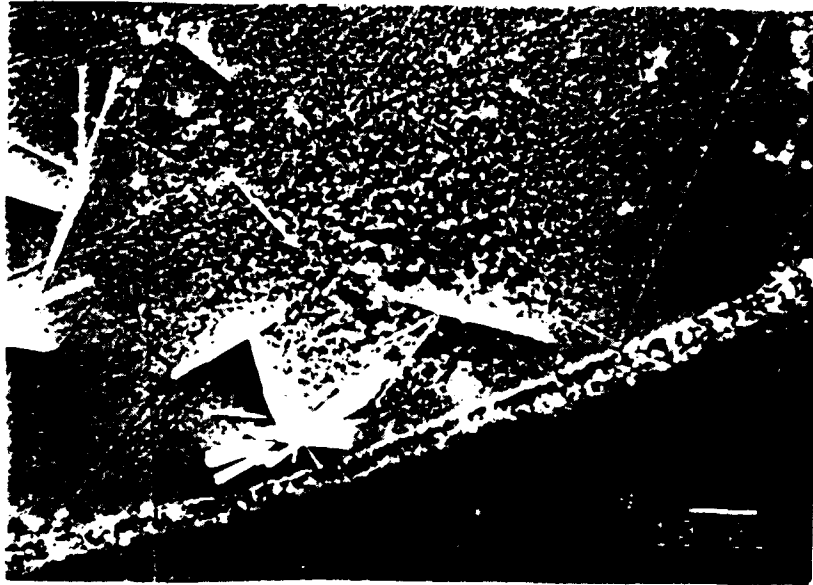
Inside and outside of corroded region

Water penetration

Figure 5.20.   Surface   topography of   ZBLA-F glass staticly
corroded at S/V=5 for 4 hours.
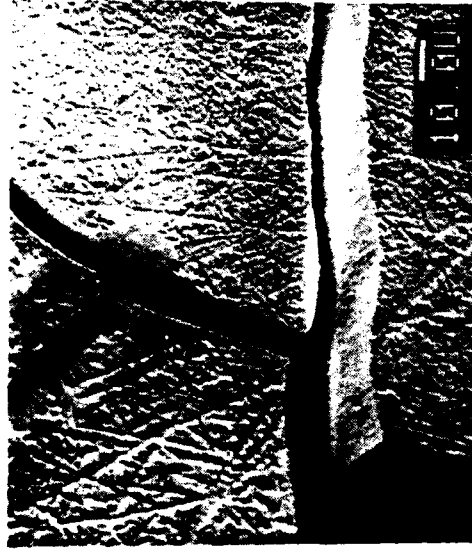
Precipitation layer(10 $\overline{\mu m}$)   Transform layer(10 $\overline{\mu m}$)   Bulk glass($\overline{10\ \mu m}$)

Figure 5.21. Corrosion layers formed on ZBLA glass, which was staticly corroded at S/V=1 for 7 days.

(c), this layer will be called the transform layer. Below the tranform layer is the bulk glass on which pits can be found, see (d), due to the reaction of the penetrating water with the glass.

(1). Precipitation layer. In addition to the ZrF_4 crystals in this layer are two other main crystals whose EDX spectra are shown in Fig.5.22 and Fig. 5.23 respectively. Both of these crystals contain Ba and Zr and the spherical crystals in Fig.5.23 contains a much higher Ba/Zr ratio than the other crystals. If we look at the cross-section of the precipitation layer, see Fig. 5.24, the bottom part of this layer consists mainly of spherical crystals composed of spikes and having a very porous texture, see (b), while the outer part of this layer, composed of the crystal shown in Fig.5.22, has a random texture and appears to be less porous than the bottom crystals, see (c). The upper crystal is identified as α-$BaZrF_6$ from an X-ray diffraction study, see Fig. 5.25. The existence of this kind of crystal was confirmed by the observation of an endothermic peak near 570°C in DTA measurements of the corrosion layers, corresponding to the transition temperature of $BaZrF_6$ crystal from α phase to β phase.[53] Furthermore, from this X-ray diffraction study BaF_2 appears to be one of t' $_{5}$ crystalline phases in the corrosion layer, thus the crystal shown in Fig. 5.23. (i.e. the lower crystal), may be BaF_2 since there is only a weak Zr signal detected in the EDX
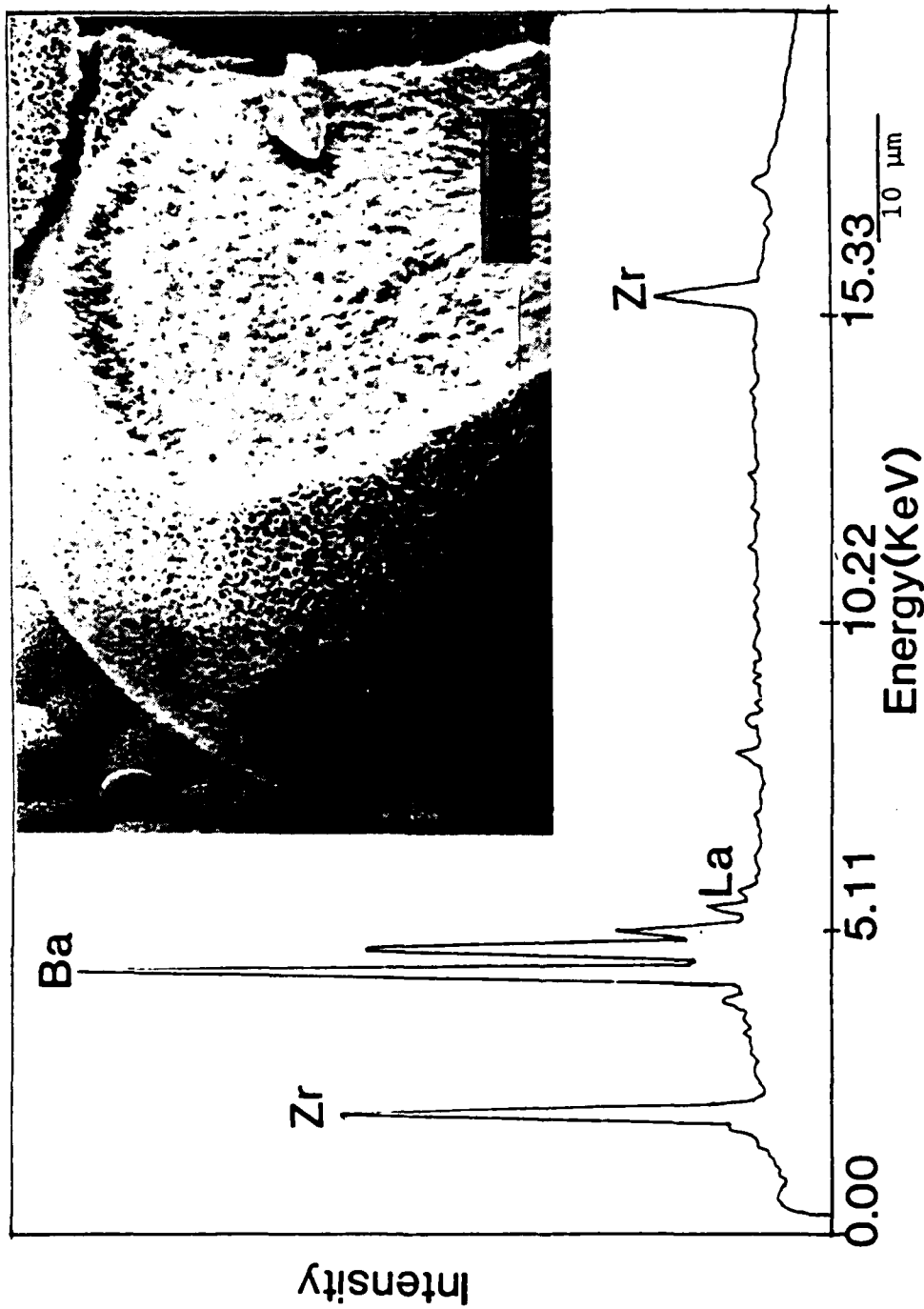
Figure 5.22. Spherical crystal at the outer portion of precipitation layer, which formed on ZBLA glass corroded at S/V=1 for 7 days and its EDX spectrum.
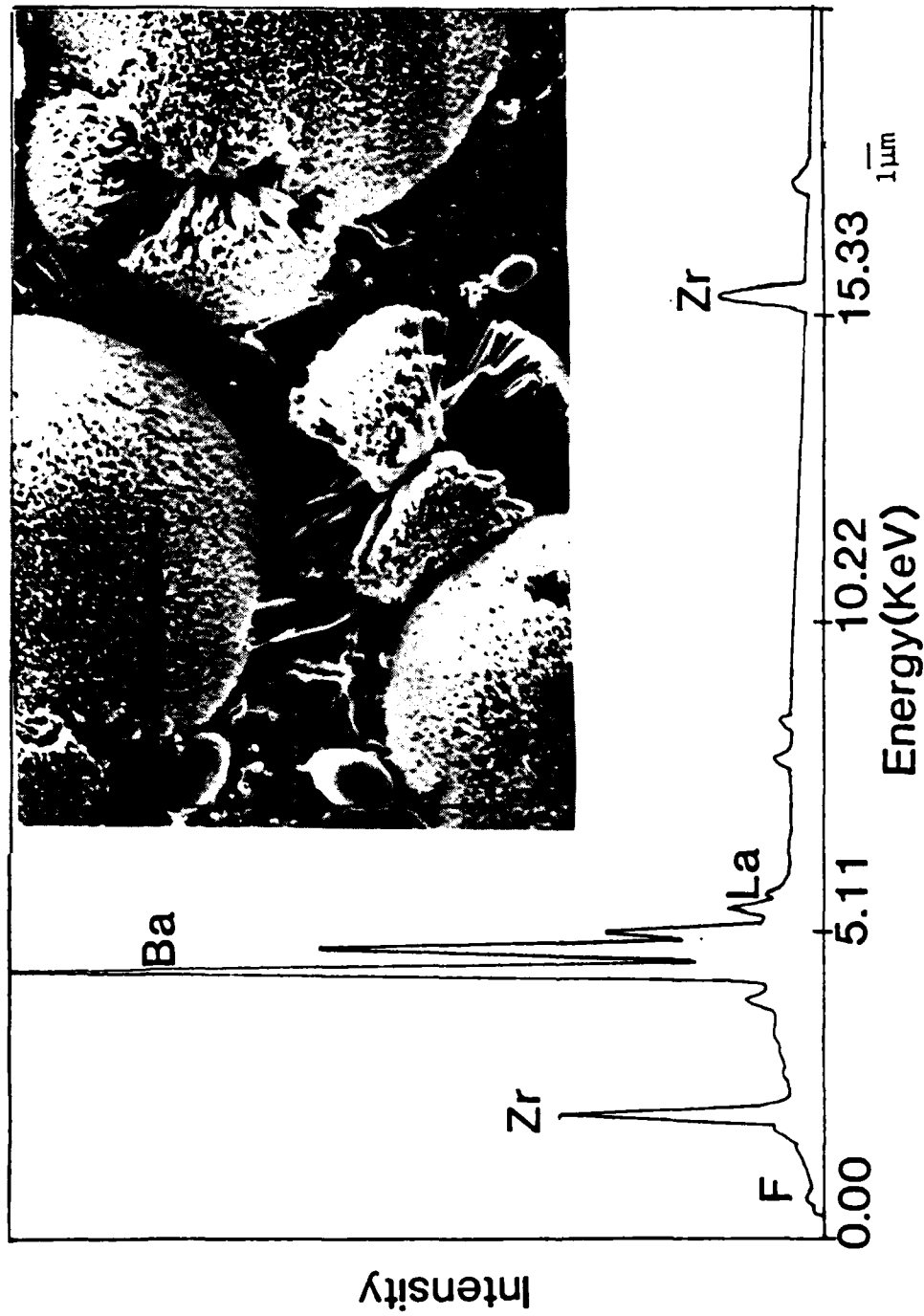
Figure 5.23. Spherical crystal consisting of spikes in the inner portion of precipitation layer, which formed on ZBLA glass corroded at S/V=1 for 7 days, and its EDX spectrum.
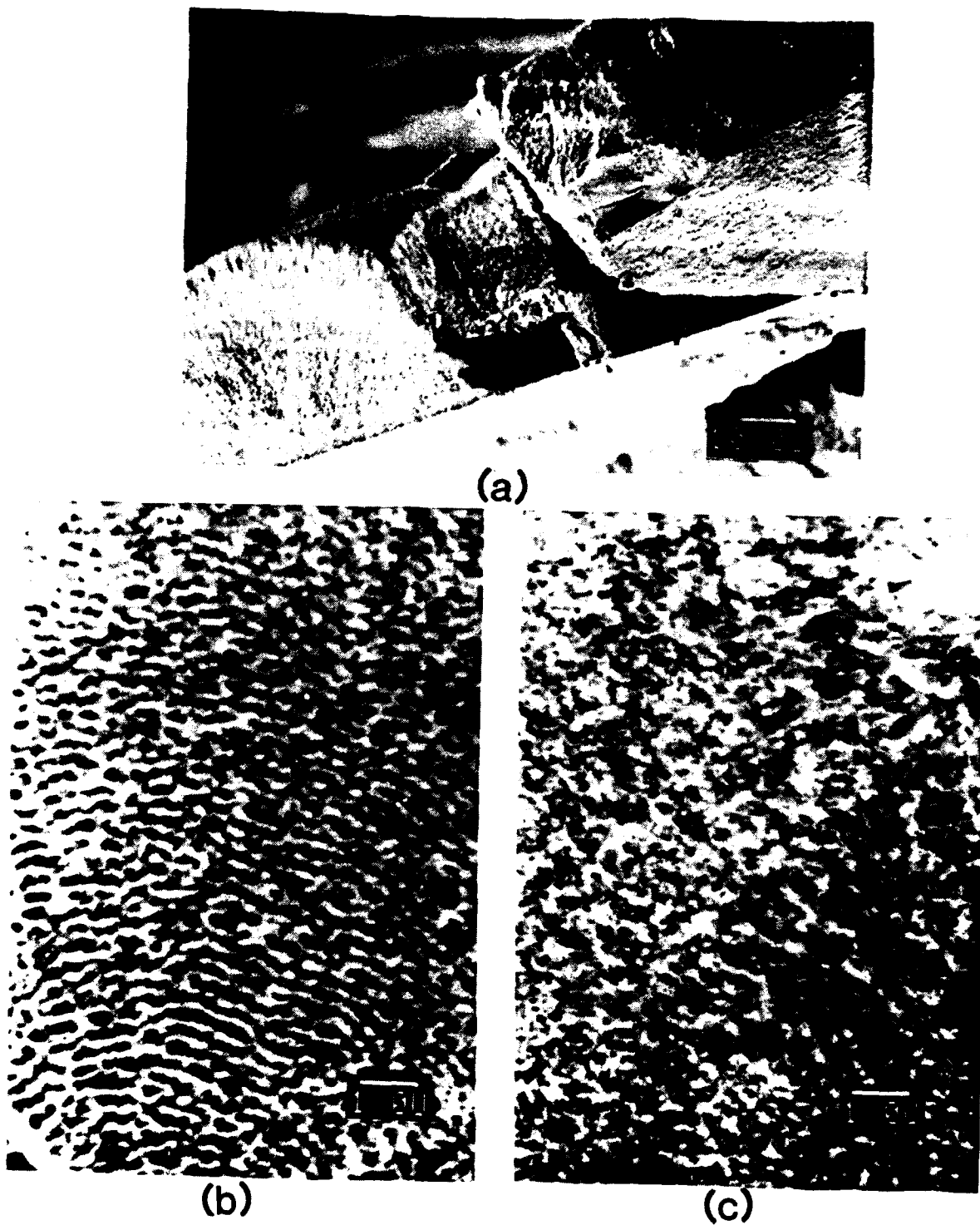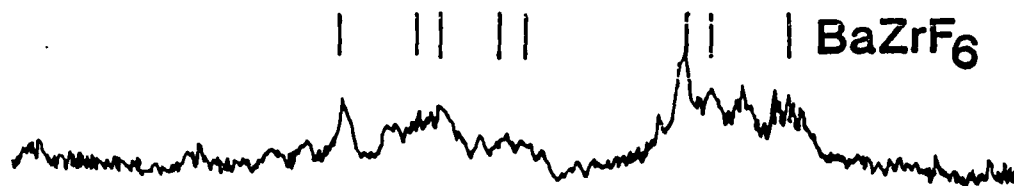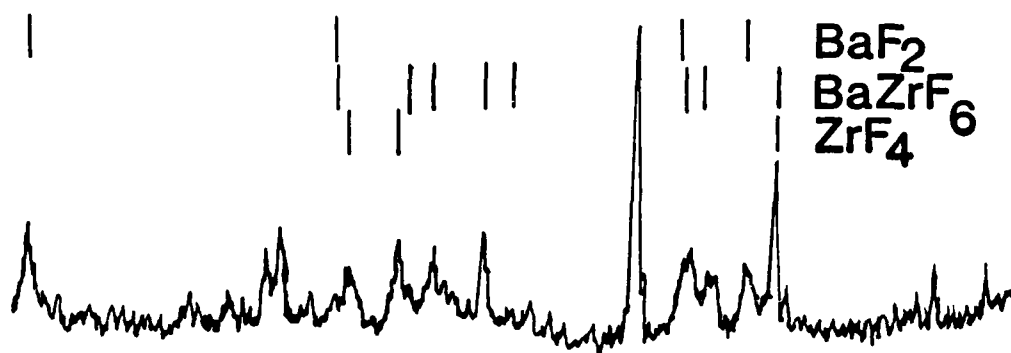
Figure 5.24. Cross-sectional view of precipitation layer formed on ZBLA glass after being corrodd at S/V=1 for 7 days, (b) inner portion of the layer, (c) outer portion of the layer.

(a) Unccraped corroded glass

(b) Scraped corrosion layer

Figure 5.25. X-ray diffraction spectra of corrosion layer of ZBLA glass in S/V=1 for 7 days. (a) unscraped corroded glass; (b) scraped corrosion layer.

spectrum. Because of the highly porous texture of this crystal, the signal coming from material below this crystal such as either ZrF_4 crystals or the transform layer, may have contributed to the spectrum recorded.

The formation of several precipitation layers can be shown by comparing the X-ray diffraction spectra from the corroded glass itself where the X-ray only samples the top few microns of the precipitation layer, see Fig. 5.25. The spectrum (a) show that the top of the crystalline layer is made up of α-$BaZrF_6$ crystals, while the diffraction spectrum of material removed from this layer by scraping shows the peaks of ZrF_4 and BaF_2 crystal in addition to α-$BaZrF_6$. During the noncongruent dissolution of the glass, several processes control the nature of the precipitates. These are the degree of supersaturation, the solution pH, the species in solution and the rate of material diffusion away from the corrosion regions. As various portions of the precipitated layer form, it is conceivable that the material removal process and the pH can be sufficiently altered on a local basis to lead to the rapid dissolution, saturation and precipitation of crystals of different composition or different Zr/Ba content. More discussion of the formation of the precipitation layer will be seen in section 5.5.

(2) Transform layer. The original glass surface which was altered by reacting with water is shown in Fig.5.26.(a)-(d). (a) shows the surface topography of this layer which

is severely corroded, (b) indicates, in cross-section, that this layer is very thick and porous and was formed through selective dissolution of more soluble species from the glass on a local scale, e.g. at inhomogeneities or high strain areas. Moreover, water can penetrate through this layer further into bulk glass, and as in (d), can react with the bulk glass below the transform layer.

When we removed these corrosion layers carefully and conducted TGA weight loss analysis on them, the results of Fig.5.27 were found. (a) shows a 17.5 wt% loss due to the removal of water in the layers during heating. The differtial curve (b) indicates most of the water was removed by raising the temperature up to 120°C. Assuming the average density of the solid portion of these corrosion layers to be 4.0 then these layer would contain about 70 vol% of water, which suggests these layers are very porous.

EDX analyses on different regions of the corroded glass are shown in Fig.5.28.. Compared to the uncorroded glass, see(a), the transform layer has less F and Al which agrees with the leaching rate measurement where both of these elements exhibit a higher dissolution rate. Moreover, the transform layer contains a higher Ba/Zr ratio than the glass. Lanthanum(La) seems not to change concentration noticeably. The precipitation layer, see (c), contains essentially no Al, little La and has a higher Ba/Zr ratio than the bulk glass.
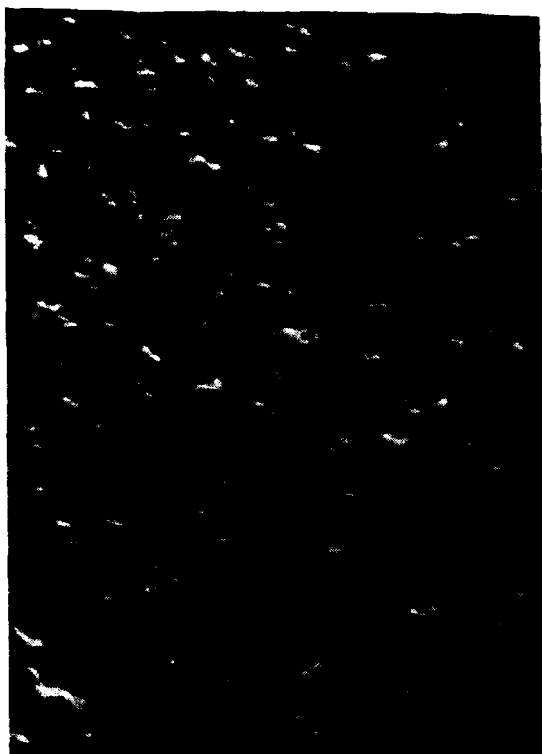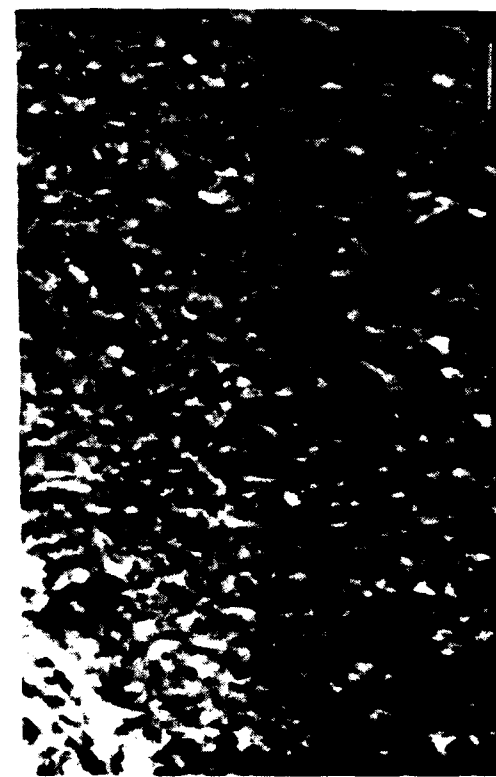
Figure 5.26. (a) Cross-sectional view of transform layer formed on ZBLA glass after being corroded at S/V=1 for 7 days; (b) top view of the layer; (c) enlarged cross-sectional view of the layer; (d) water penetration marks at the reaction front between transform layer and bulk glass.
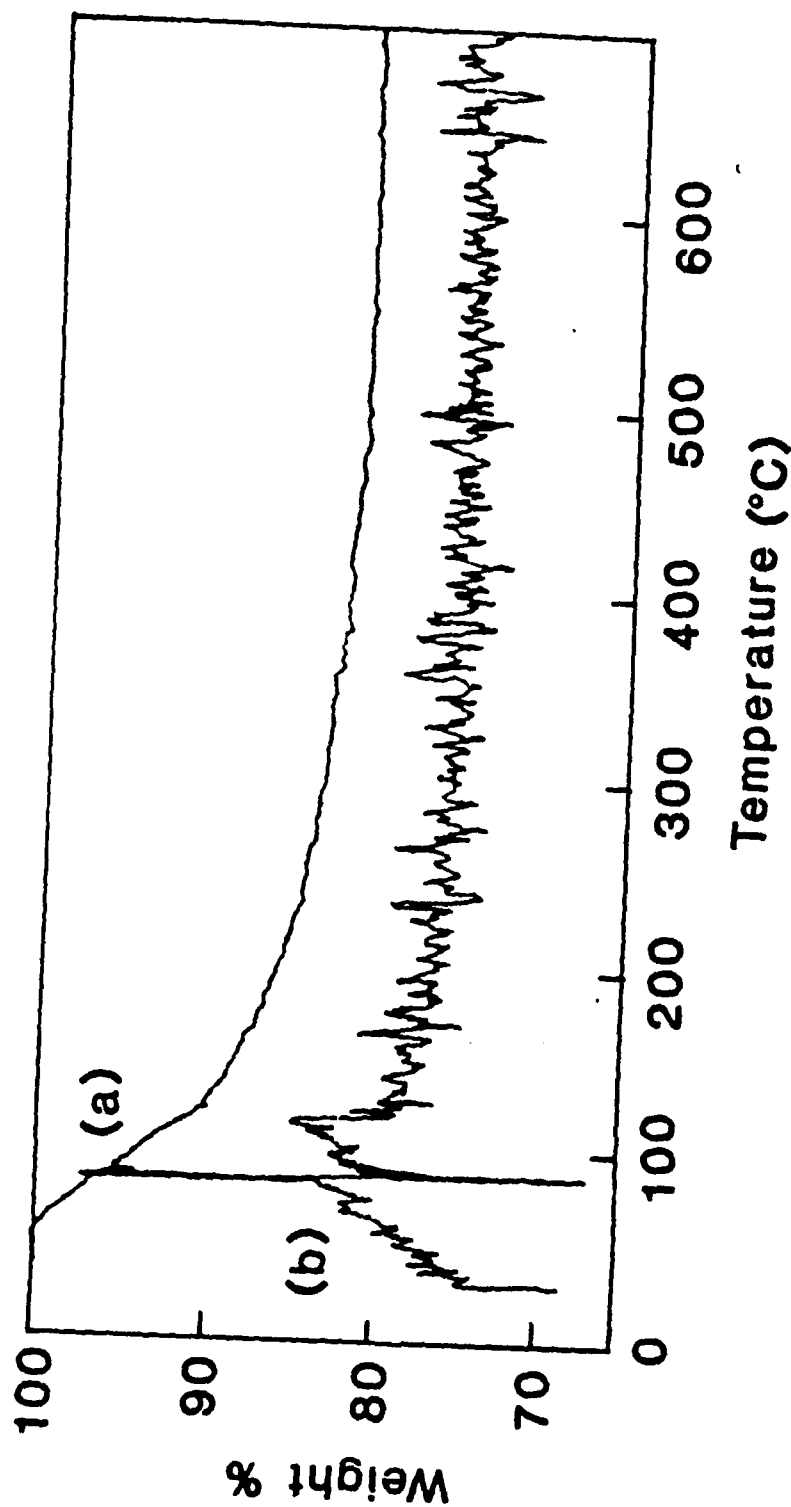
Figure 5.27. (a) TGA weight loss measurement of corrosion layers of the 7 days ZBLA stagnant test sample, corroded in D.I.water, S/V=1, (b) differential curve of (a).
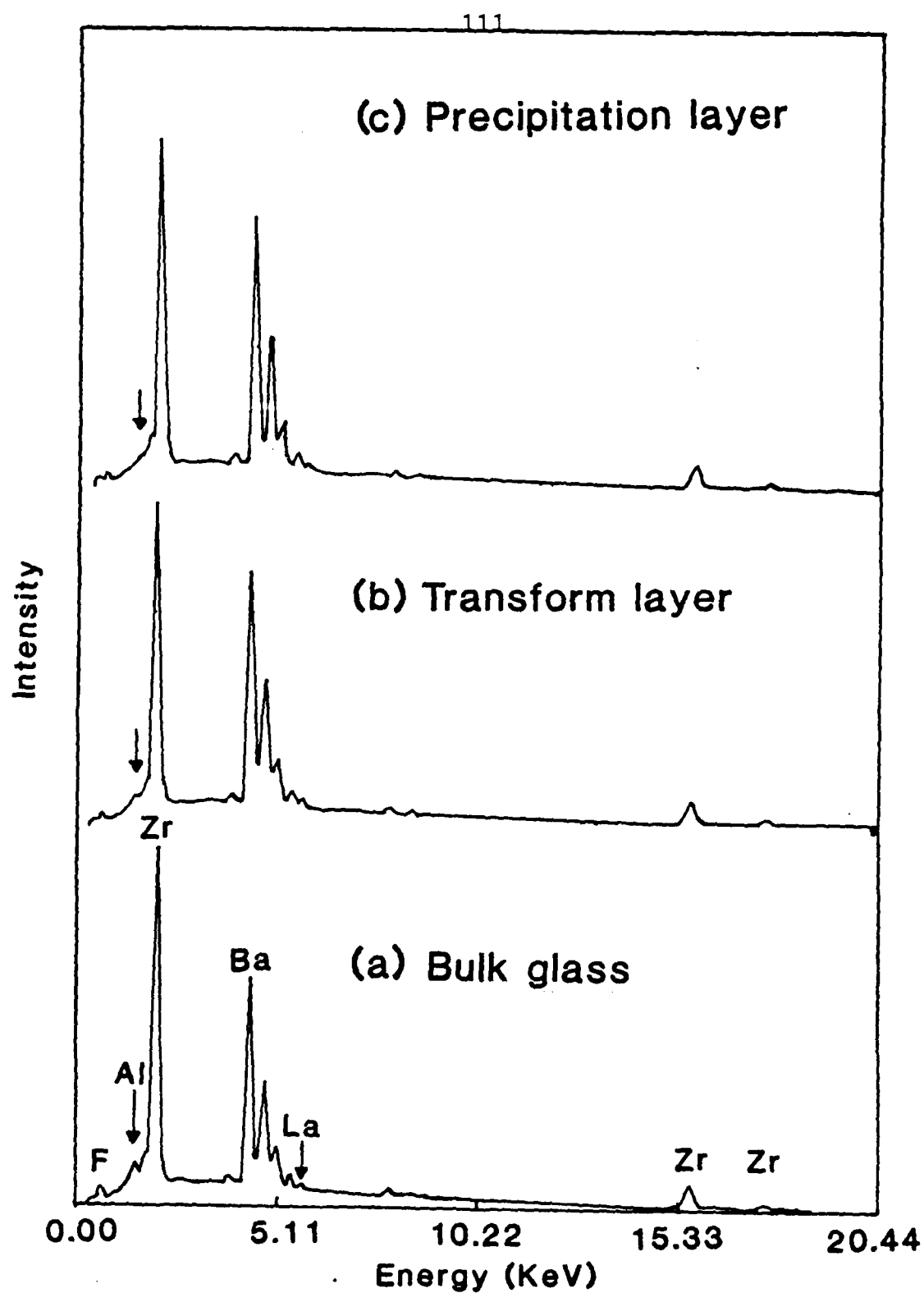
Figure 5.28.   EDX spectra of corrosion layers of ZBLA glass, staticly corroded at S/V=1 for 7 days. (a) bulk glass, (b) transform layer; (c) precipitation layer.

An X-ray compositional line scan was conducted on the polished fractured surface of a corroded sample to study the composition profile of the glass corroded under static conditions. The region scanned is shown in Fig.5,29. and the results of elemental analyses for Zr,Ba and F are plotted. By comparing the results to the bulk glass, the tranform layer has less Zr due to selective dissolution, especially at the reaction front. Moving further out toward the original glass surface, the Zr concentration increases a little, going to a region that has relatively higher Zr concentrations than the other regions of the tranform layer. Beyond this higher concentration region, the Zr concentration decreases again until it approaches the original glass surface. For Ba there is also a low concentration region near the reaction front and there is a region having a higher concentration when getting closer to the original glass surface. A small region having lower Ba concenrtation near the onginal glass surface also exists. For fluoride (F) concentration, which is relatively more difficult to analyze reliably with this technique, one sees no distinct decrease near the reaction front and a relatively lower concentration of F at the outer region of this layer. Those regions having higher Zr and Ba concentrations than at the reaction front are attributed to the precipitation which occurs because corrosion products could not be transported out effectively, thus accumulating
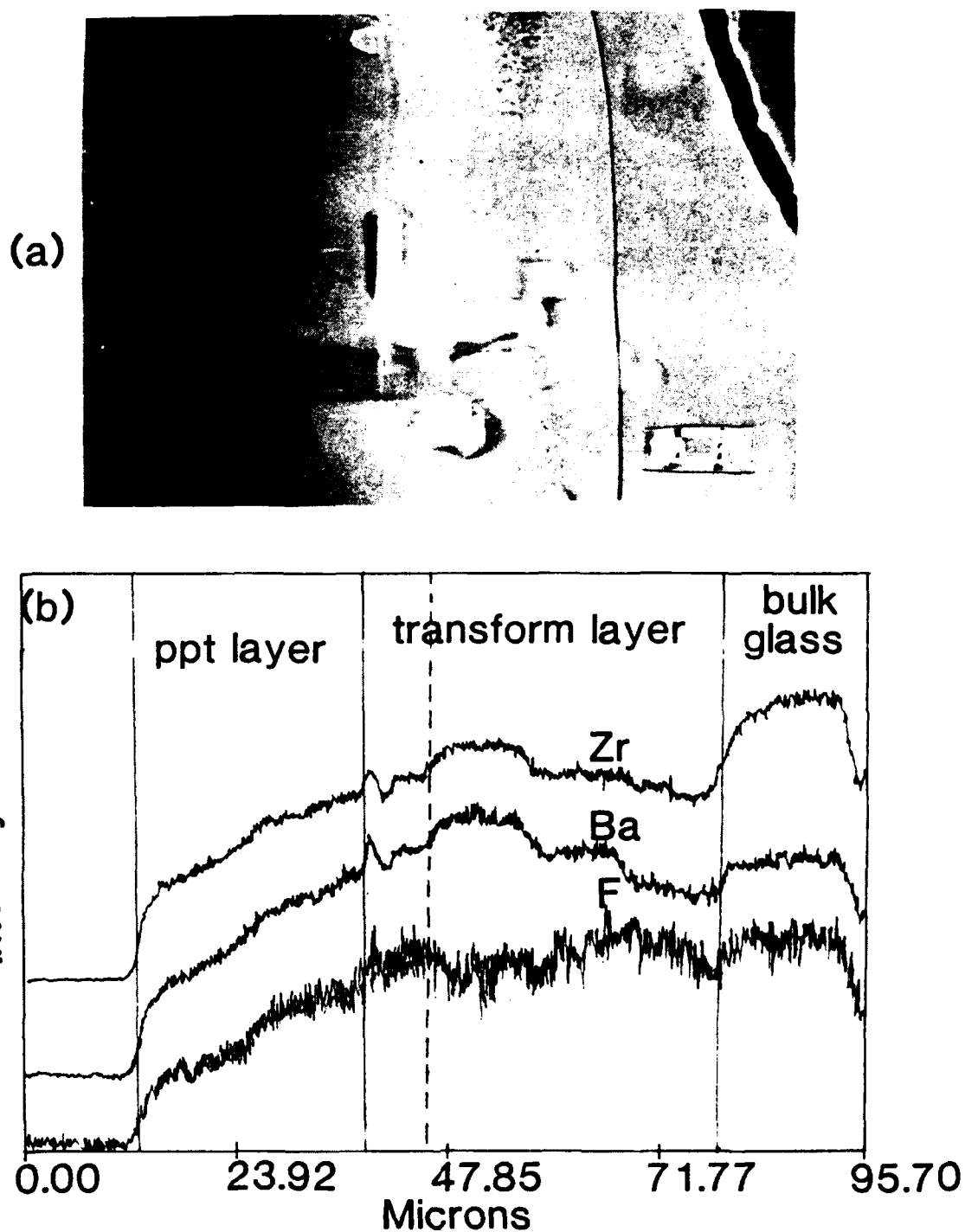
Figure 5.29.   (a) Polished fractured surface of ZBLA glass, corroded at S/V=1.5 for 115 hrs.;   (b) X-ray compositional line scan analysis along the cross-sectional surface to reveal its composition profile.

in the solution in this layer. This agrees with the fact that the region close to the original glass surface isrelatively depleted, because the transport path is shorter. Considering the precipitation layer, these conclusions are comfirmed by the result of EDX selective spot analysis which show higher Ba/Zr than the bulk glass. The lower signal in this layer is due to its porous structure.

(c) Corrosion layer fomation vs. time. The growth of the corrosion layer was studied by measuring the average thickness of the tranform layer with time using fractured corroded glass. Figure 5.30 shows for 0.5 day, (a), the primary precipitate consists of ZrF_4 crystals, and the transform layer is relatively thin. As time passes, the spherical crystals begin to precipitate and cover the ZrF_4 crystals, see (b). Both a precipitation layer and a transform layer are formed, with an increasing thickness with corrosion time, see (c). The reaction front is not uniform; however, measurments of the average thickness of the transform layer, Fig.5.31. show that the leached transform layer thickens more rapidly during the early stages of corrosion than during the later stages. No steady state was reached within the experimental time. The precipitation layer while becoming thicker could possibly act as a rate limiting barrier because the formation of the precipitate creates new precipitation sites further and
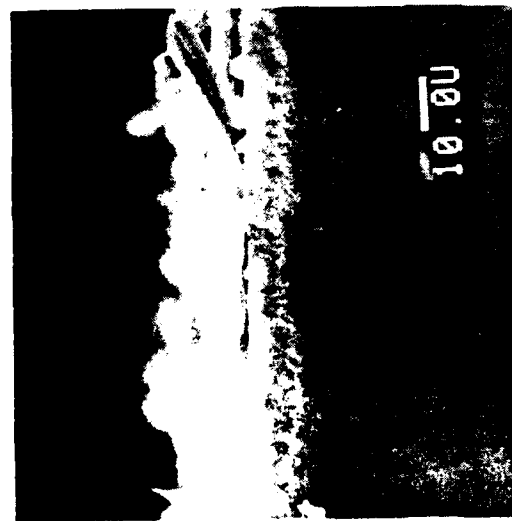
(a) 0.5 Day (b) 2 Days (c) 8 Days

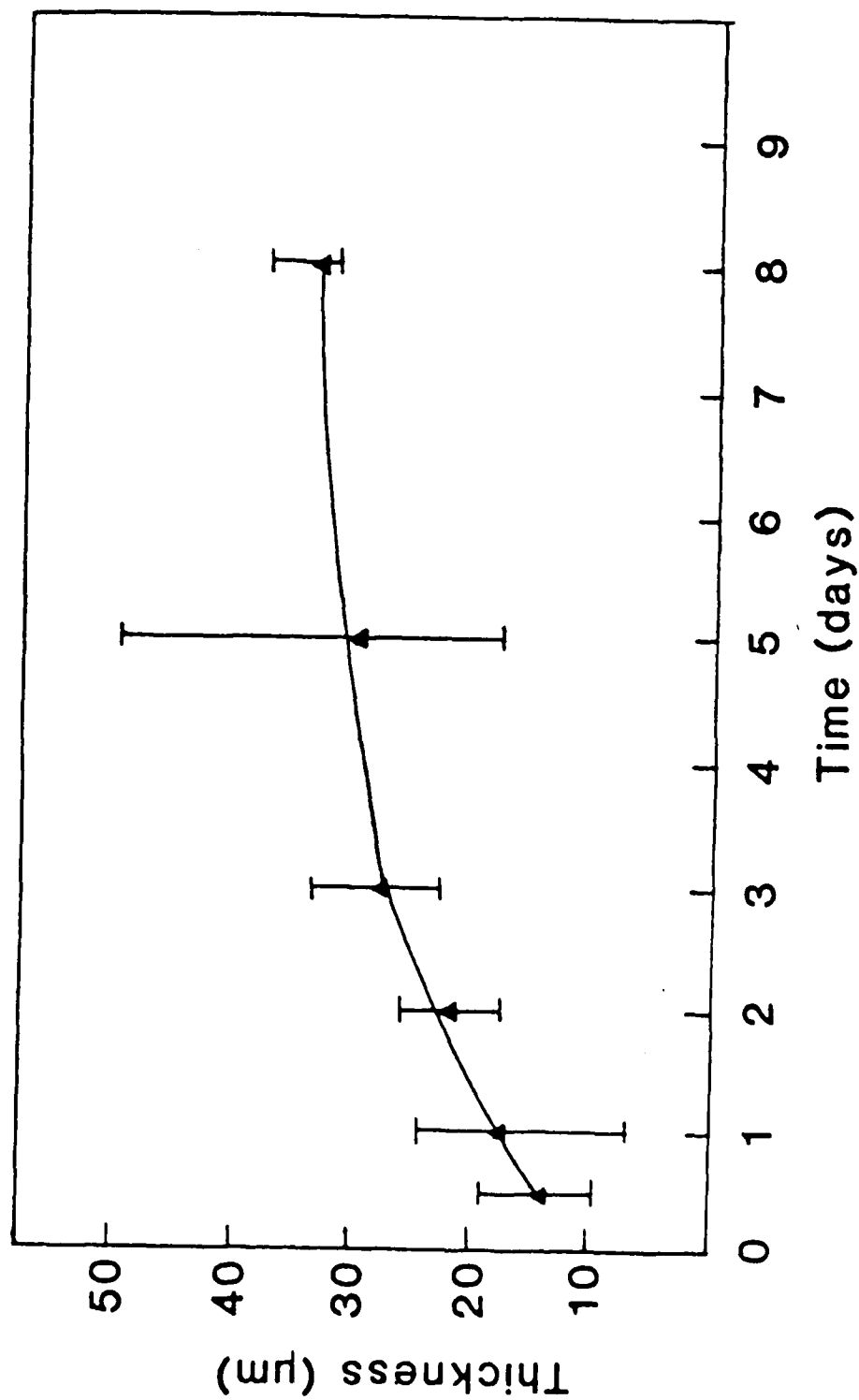Figure 5.30. Corrosion layers developed after different periods of corrosion time, under S/V=1 static conditon.

Figure 5.31. Average thickness of transform layer vs. corrosion time; ZBLA glass staticly corroded in D.I. water, S/V=1.

further away from the surface of the dissolving solid if the
precipitation layer is very compact.[46] However, this
interference of a thick precipitation layer with the
diffusion of water and the dissolved species to and from the
interface between the dissolving solid and the solution
should play an insignificant role as a diffusion barrier due
to its porous texture. Moreover, for a porous precipitation
layer, the corrosion species do not necessarily have to
diffuse through the whole precipitation layer to find a
precipitation site. Instead, crystals can precipitate out
from solution while still inside the pore channels. This
non-protective role can be supported by the relatively
depleted region in the transform layer adjacent to the
original glass/solution interface, see Fig.5.29. The cause
of the decrease in the leach rate is more likely to be
associated with the formation of a thick transform layer
which is less porous than the precipitation layer according
to the SEM micrognaphs shown previously. From X-ray line
scan results, see Fig.5.29., a region of higher Zr and Ba,
especially Ba, was observed. Selective dissolution of glass
produces a porous transform layer resulting in a dramatic
increase in surface area is and thus the S/V ratio in this
layer can be very high and cause a greater pH excursion
toward more acidic values. Due to the enhanced leach rates
in acid solutions, accelerated dissolution can saturate the
solution in the pores rapidly. As the transform layer

becomes thicker, the diffusion path for the dissolved species becomes longer and thus supersaturation can be reached inside the transform layer and precipitation can occur inside the layer. The large ionic radius of Ba could be responsible for slowing down the diffusion process of its dissolved species and hence could enhance the precipitation process even further. The observation that precipitation could occur in the thick transform layer is supported by the results reported by Simmons and Simmons[18], that the leach rate of the glass components, especially Ba, experience a decrease at longer times; although this decrease in leach rate can also be related to the common ion effect caused by the increase of fluoride ions in solution.

5.4.4. High S/V Ratio Static Test

In this section are considered the results of corrosion of fluorozirconate glasses conducted at high S/V ratios in D.I. water. In order to simulate the effect of a very small amount of water penetrating through the coating of optical fibers, the ZBLA glass was exposed to stagnant water in a low dilution test with S/V=40 was conducted on a ZBLA glass. Figure 5.32 shows that two precipitates can form on the surface, consisting mainly of large spherical crystals and small spherical precipitate below them, see (a) (b). In some regions, selective dissolution still occurs to form a thick transform layer under the compact large spherical
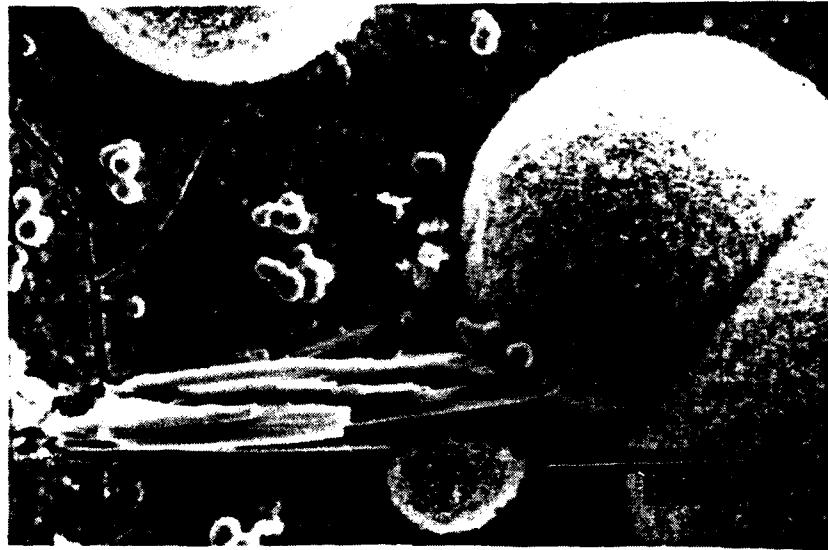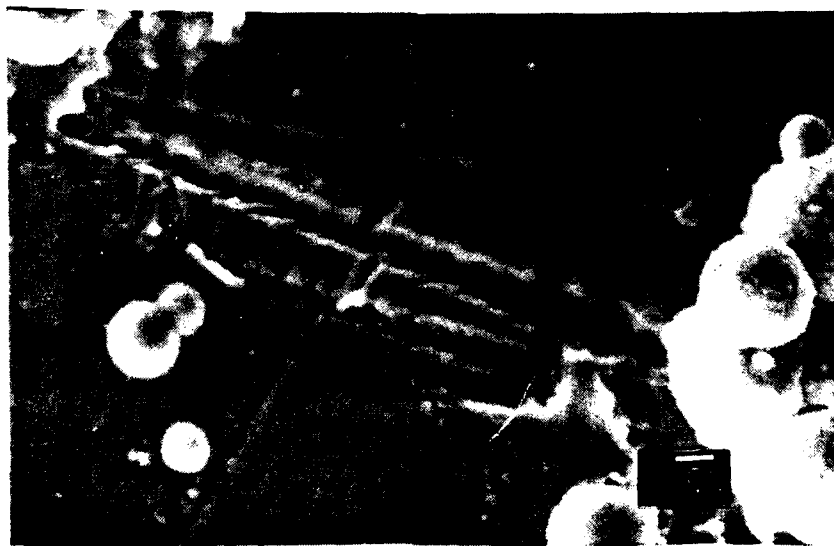
(a)
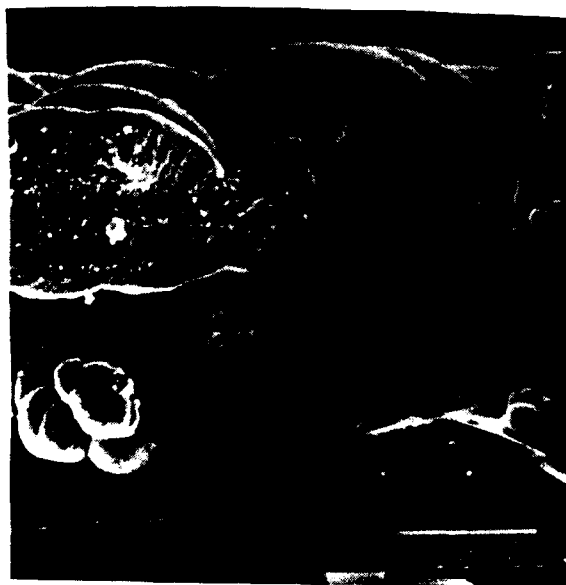
(b)   (c)

Figure 5.32. (a) Surface topography of ZBLA glass corroded in D.I. water, S/V=40 for 6 hrs.; (b) cross-sectional view of the region where two layers of precipitates formed on extensive broad pits; (c) cross-sectional view of the region where the glass suffered severe selective dissolution instead of complete matrix dissolution as in (b).

120

(a)

(b)

Figure 5.33. (a) Surface topography of ZBLA-F glass corroded in D.I. water, S/V=10 for 80 min.; (b) the edge of the corroded region.

(a) $\overline{1 \ \mu m}$

(b) $\overline{1 \ \mu m}$

Figure 5.34. The corrosion layer formed on (a) ZBLA glass, staticly corroded in pH2 buffer solution S/V=40 for 6 hours; (b) ZBLA glass staticly corroded in D.I. water, S/V=40 for 6 hours.

crystals. These spherical crystals were identified as α-BaZrF$_6$ from X-ray diffraction spectra to be shown later. Figure 5.33 (b) shows extensive, broadly etched grooves similar to those in Figure 5.4(a), suggesting that for high S/V ratio conditions, matrix dissolution processes dominate as occurs in highly acidic environments. The precipitated spherical crystals from the glass corroded at high S/V ratio in D.I. water has the same appearance as those from glass corroded in a pH2 buffer solution with the same S/V ratio, see Fig. 5.34. This suggests that the corrosion in D.I. water of high S/V ratio is similar to the corrosion in a highly acidic environment.

5.4.5. Summary

The corrosion layer formation is very much dependent upon corrosion conditions. One of most important phenomena that control the leaching behavior of fluorozirconates is the solution pH drift due to the hydrolysis of dissolved species, especially ZrF$_4$, and any ion exchange process between hydroxyls (OH$^-$) in solution and fluoride (F$^-$) ions in the solid, to be discussed in Section 5.7.. The rate of pH drift can be affected by S/V ratio, therefore it will change with the composition of the solution and the relative degree of supersaturation. Figure.5.35 illustrates the corrosion layer formation for ZBLA glasses corroded for the same time under different S/V ratios. In high dilution

123

(a)High dilution(S/V:10^{-5})   (b)Low dilution(S/V:40)
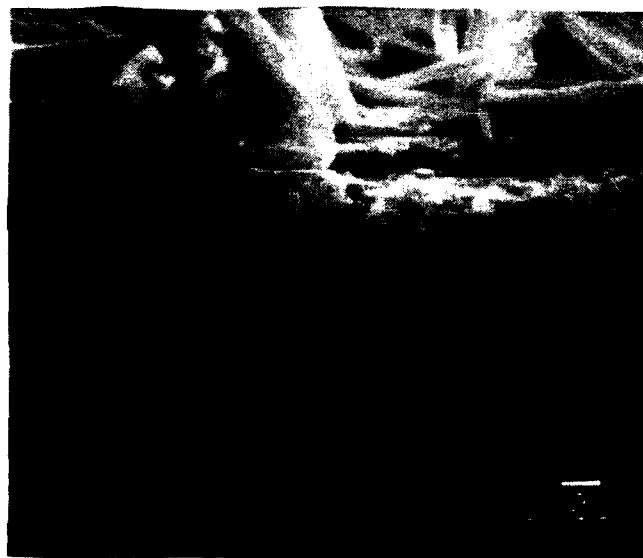
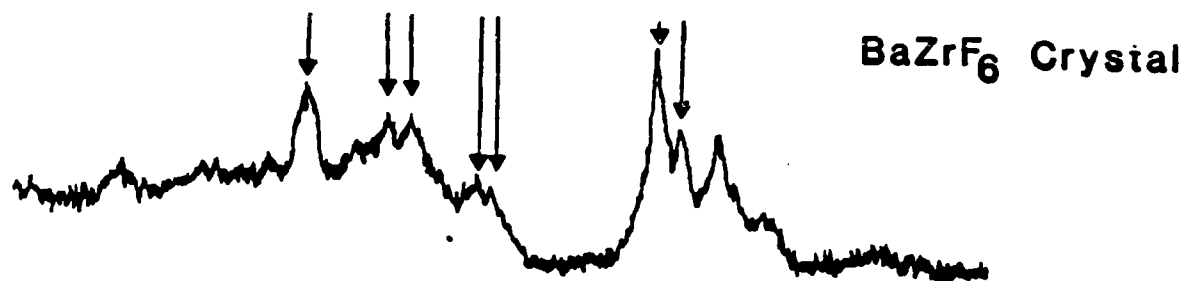(c)Intermediate dilution(S/V:1)

Figure 5.35.   Corrosion   layer   formation   of   ZBLA glass
corroded   under   different   S/V   ratios   for 6 hrs. (a) high
dilution; (b) low dilution; (c) intermediate dilution.

conditions, which correspond to flow conditions that will be discussed in section 5.6., most of the corrosion products can be carried away by the solution flow. Since little accumulation of corrosion products occurs at the solution/ glass interface, the solution pH does not experience as large a drop as measured in static solutions. No precipitation layer forms in this case except for a few small ZrF_4 crystals. Many colloidal particles precipitate within the transform layer and some deep pits extend into the bulk glass indicating a significant water penetration. At the other extreme, at very low dilution conditions which simulate fibers attacked by a small amount of water penetrating through the coating, enchanced leaching and accelerated precipitation can produce both thick precipitation and transform layers. In the intermediate case, the transform layer is not as thick as in (b), and the precipitated crystals are mostly ZrF_4, see (c). The results of X-ray diffraction studies of the corrosion layers of ZBLA glasses corroded under different conditions are shown in Fig. 5.36. In the low dilution case, α-$BaZrF_6$ crystals make up the primary precipitate and appear as large spherical crystals composed of small particles as shown in Fig.5.34., while for intermediate conditions many crystals can precipitate out, including α-BaZrF6, ZrF_4 and BaF_2.
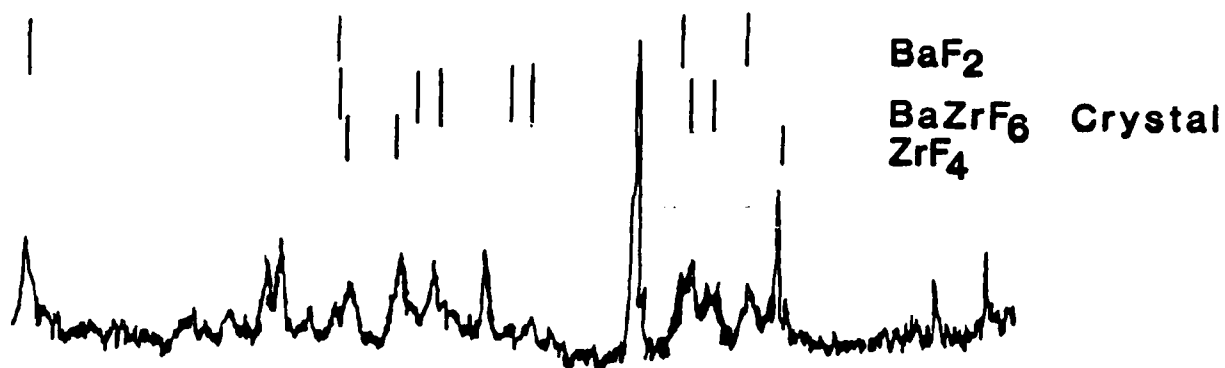
Under static corrosion conditions, it is expected that if no precipitation occurs in the leaching solution, the

(a) Uncorroded glass

(b) Low dilution condition (S/V=40,) 6 hours

(c) Intermediate dilution condition (S/V=1,) 7 days

Figure 5.36. X-ray diffraction spectra of the static corrosion layers of ZBLA glass formed under different S/V ratios.

leach rate of individual elements will decrease and even
cease as the leaching progresses and the accumulation of
elements in solution reaches saturation levels. However,
precipitation of saturated species can effectively remove
elements from solution and thus reduce the saturation
effects that normally occur in static leaching. Therefore,
static corrosion rates are very much dependent upon the
precipitation kinetics.[54] Moreover, the thick precipitation
layer itself could act as an effective diffuson barrier and
interfere with leaching processes, if the structure is
compact enough. Unfortunately, this is not the case for
fluorozironate glasses, at least for the case of
intermediate S/V ratio conditions, where the precipitation
layer has a porous structure. This layer thus plays only a
small role in limiting the rate of further leaching.
However, the thick transform layer of staticly corroded
fluorozirconate glasses can act as a diffusion barrier to
slow down the leaching process, and additional precipitation
can occur within this thick layer.

5.5   Zeta Potential Studies

5.5.1   Introduction

When glass sample is immersed in an aqueous solution,
electrical charges can develop on its surface[55] resulting
from the adsorption/desorption of ions between the glass
surface and solution[56]. These surface charges will change

the distribution of neighboring ions in solution by attracting oppositely charged ions (i.e. counter-ions) toward the surface and repulsing co-ions from the surface. This, together with the mixing tendency due to Brownian motion, leads to the formation of an electrical double layer made up of the charged surface and a neutralizing excess of counter ions in a diffuse layer in the aqueous solution. Electrokinetic behavior depends upon the electrical potential at the plane of shear, which is just outside the layer of adsorbed ions that constitute the charge of the surface. This potential is called the zeta potential.

The Zeta potential has been shown to play an important role in the leaching of silicate glasses. The diffusion of the charged species through the glass/solution interface is affected by this potential[57]. Moreover, the stability of colloidal precipitates in the leachate is closely related to the glass zeta potential, as colloids may be attracted to the glass surface by Van der Waals force and become part of the surface film or be repelled from the glass surface by either a hydration barrier layer or an electrostatic repulsion force between the similarly charged glass and colloids.[58]

5.5.2. Zeta Potential vs. Corrosion Layer Formation

In order to obtain more insight into the formation of the precipitation layer at the fluorozirconate glass

surface, electrophoresis was used to measure the zeta
potential of ZBLA glass powder in D.I. water as a function
of leaching time. The specific conductance, which is
related to the ionic strength of the solution, and solution
pH were also measured. The result is shown in Fig.5.37.;
the zeta potential first increases slowly, experiences a
maximum and starts to decrease. Negative values were
reached after longer times. To correlate this with the
corrosion layer formation on glass, four small thin glass
plates were put into the solution with the glass powder, and
they were taken out one by one at different times as
indicated in Fig.5.38. Because of their relatively small
surface area compared to that of glass powder, the
experimental results were not noticeably affected by their
presence. The plates were rinsed and used for SEM
examination. Sample (1), in Fig.5 39, was partially covered
by small ZrF_4 crystals. Sample (2) shows a second
spherical crystal precipitated on ZrF_4 and the whole glass
surface is almost covered by precipitates. Sample (3) was
found to have a third crystal type, which contains Ba and Zr
as found in the solution precipitation study, covering the
other two types of crystals, so that the whole glass surface
was covered by precipitate crystals. In sample (4) thick
platelets cover the precipitation layer and form a very
thick layer. Two main conclusions are suggested by these
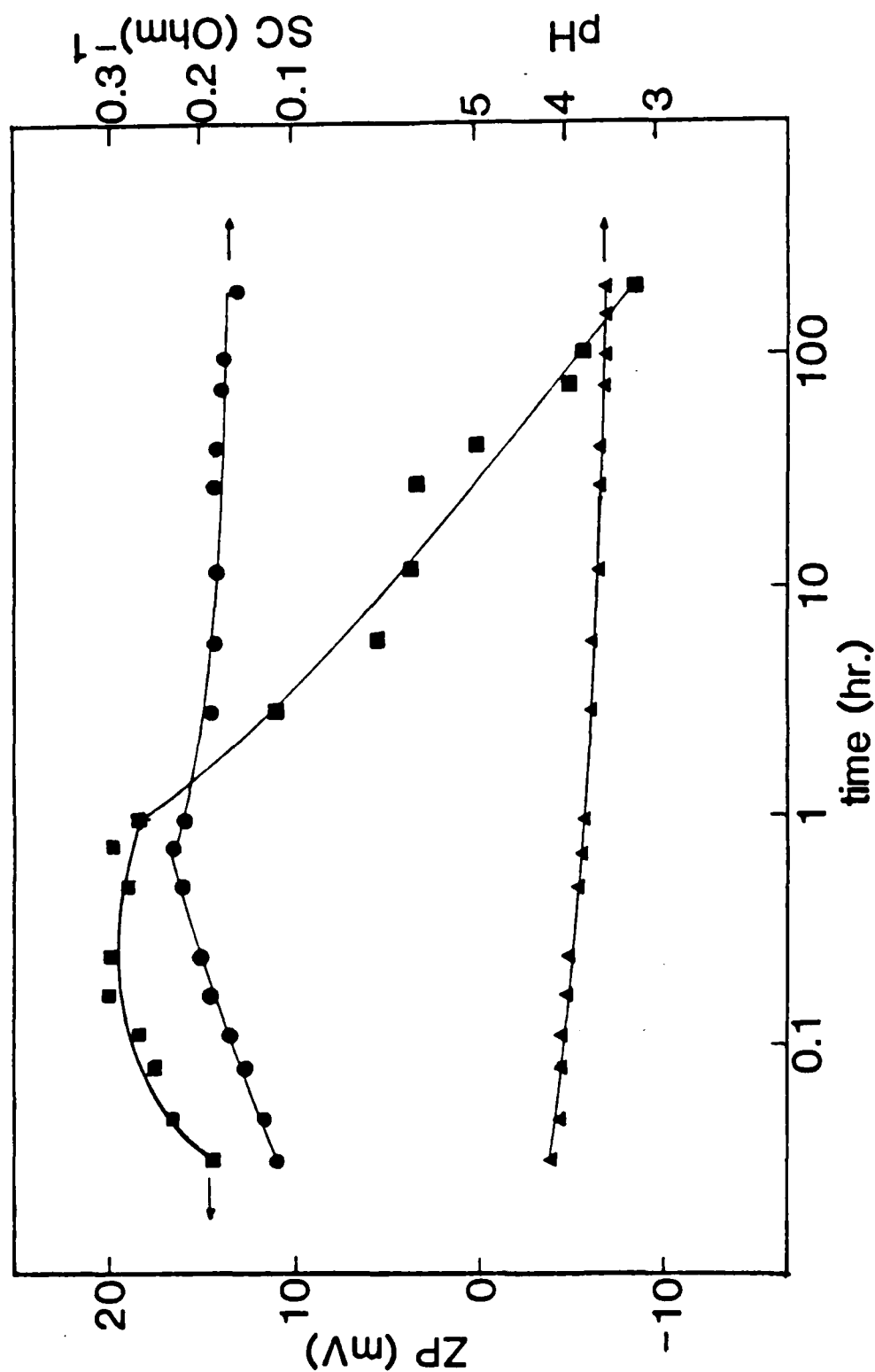results: (a) As time proceeds, the potential measured was

Figure 5.37. The time dependence of zeta potential, specific conductance and solution pH of ZBLA glass powder in D.I. water.
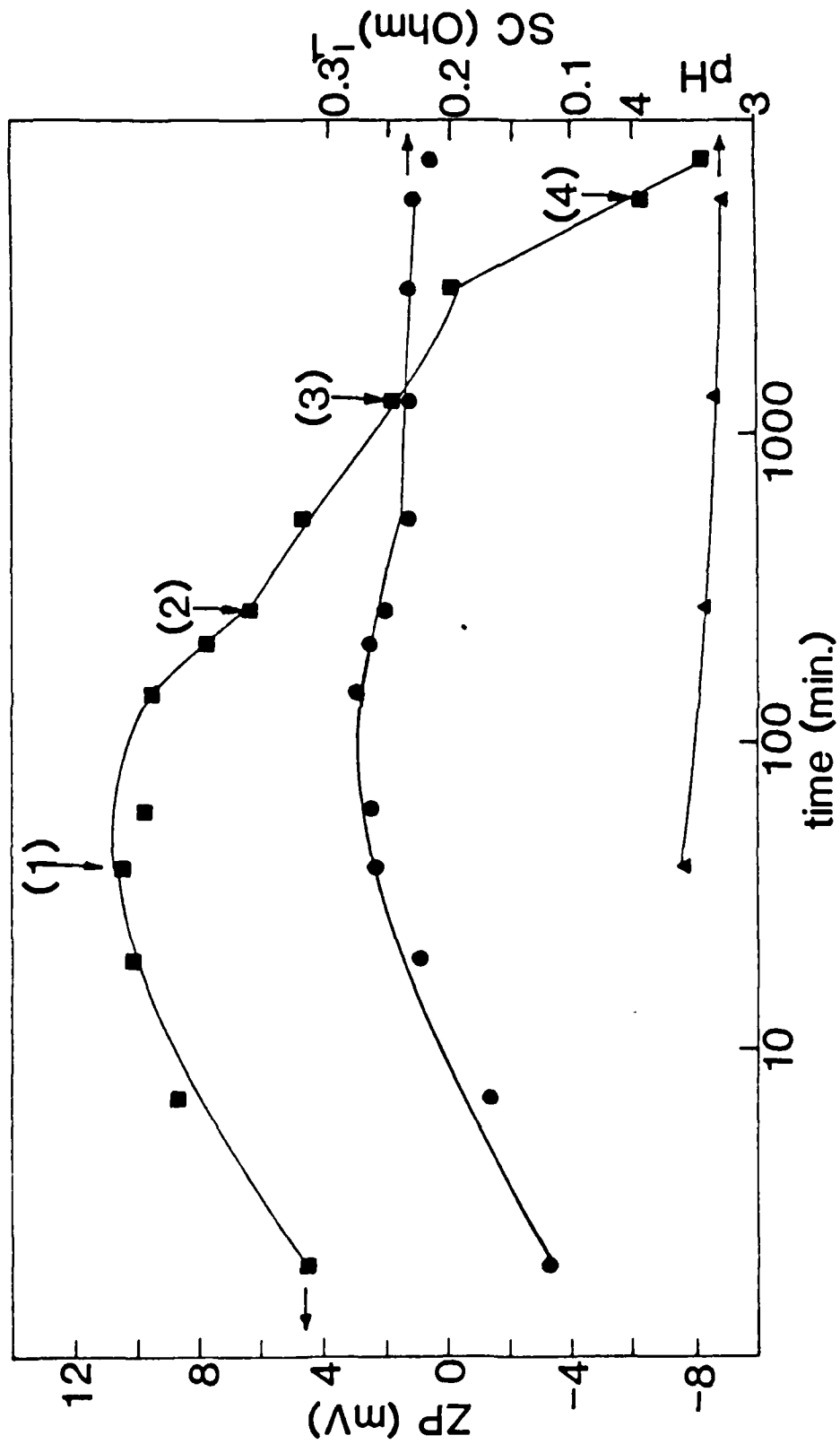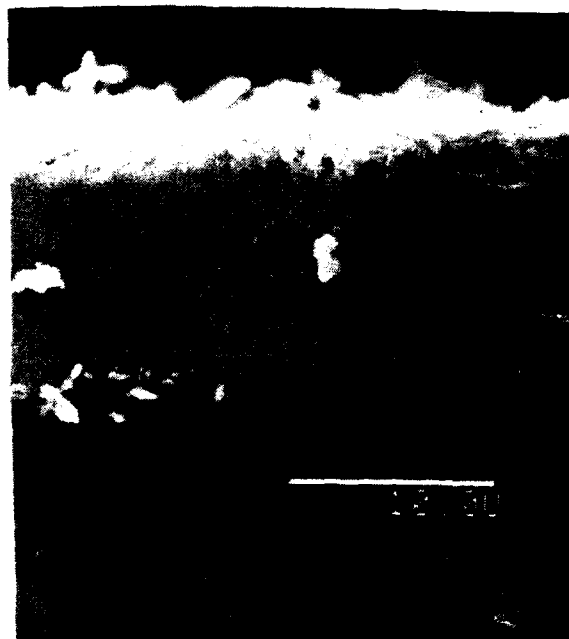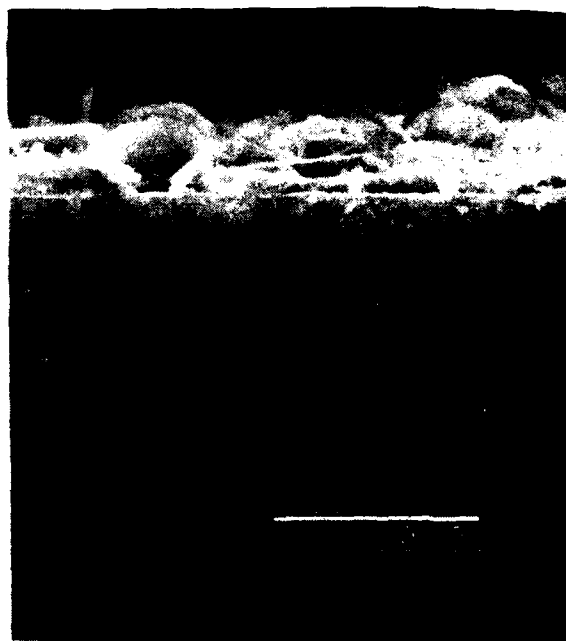
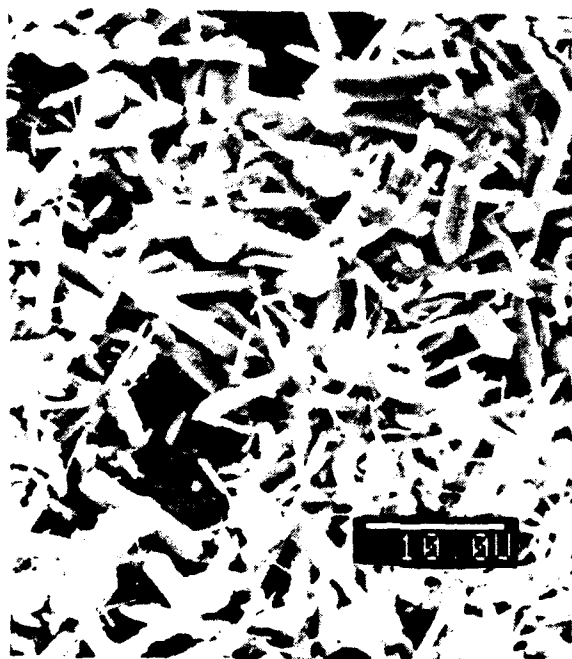Figure 5.38. The time dependence of zeta potential, specific conductance and solution pH related to corrosion layer formation.
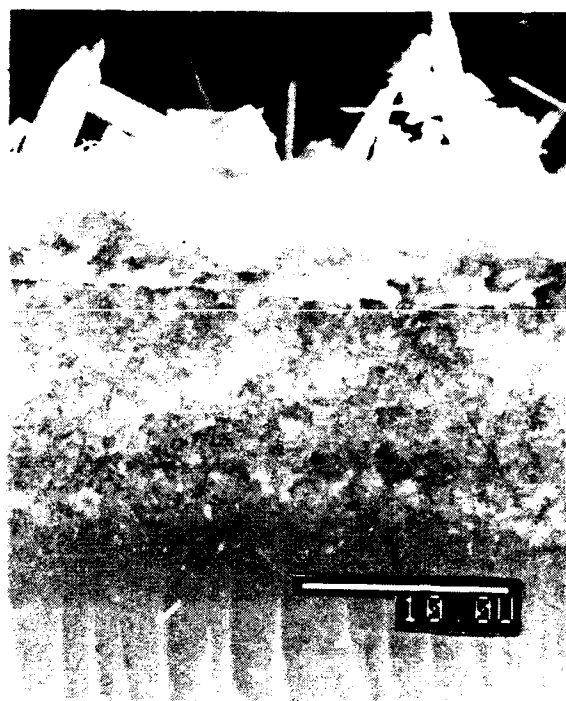
(1)

(2)

Figure 5.39. Top view and cross-section of the corrosion layers formed, corresponding to different stages of zeta potential developed at ZBLA glass surface (1) 40 min.; (2) 4.5 hrs.; (3) 21.75 hrs.; (4) 93.66 hrs..

(3)

(4)

Figure 5.39 (continued)

more and more influenced by the precipitation layer instead of the original glass surface, which becomes covered gradually, as the precipitates form; (b) The precipitation layer was formed by precipitation of different crystals which formed at different times.

5.5.3. Zeta Potential vs. Solution pH

In order to understand how this multicrystal precipitation layer was fomed, tests were conducted on ZBLA glass powder, ZrF_4 and BaF_2 fluoride compounds and sections of the corrosion layer formed under S/V=40, in solutions of different pH. Solution pH was adjusted by mixing 0.01N HCl and 0.01N NaOH solutions. Results are shown in Fig.5.40., the isoelectric point(IEP) of ZBLA glass powder is at pH=4.38, see (c), while that for ZrF_4 crystal is at pH=3.2, see (b). The negative surface potential generated when silicate glass is immersed in water produces an electrostatic potential gradient in the surface region of the glass which greatly modifies the kinetics of alkali ion migration and hence the dissolution rate.[57] Similarly, at solution pH higher than 4.38, which occurs during the very early stage of static corrosion of the fluorozirconates, the glass surface has a negative surface charge. This could not only affect the diffusion of positively charged dissolved species in the near glass surface region but also help to prevent these species from diffusing away into the bulk
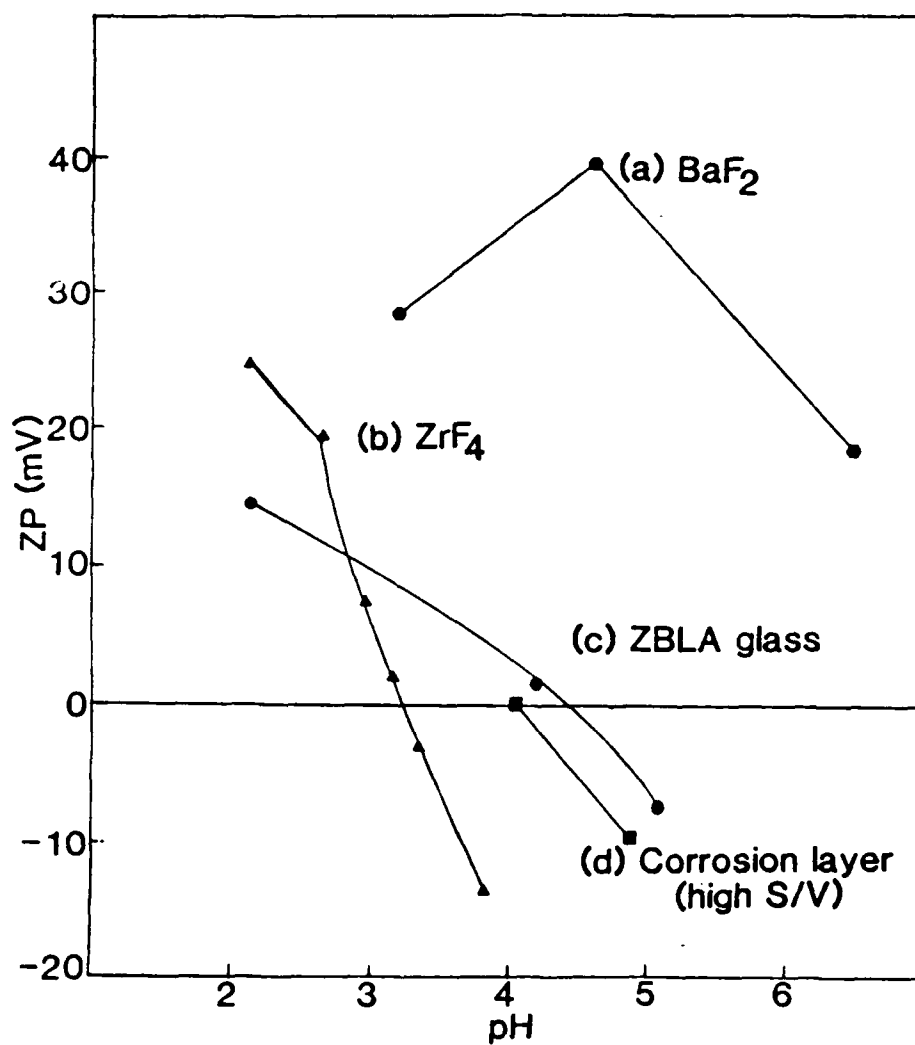
Figure 5.40. The solution pH dependence of zeta potential of (a) BaF_2 crystal powder; (b) ZrF_4 crystal powder; (c) ZBLA glass powder; (d) powdered corrosion layer of ZBLA glass corroded at S/V=40 for 8 1/6 hrs..

solution. This will enhance the formation of a near surface solution layer concentrated with corrosion products, which in turn accelerates the pH drift and hence dissolution and reprecipitation processes. Moreover, a supersaturation condition can develop in the solution near the glass surface due to the large pH gradient which results from the lower solution pH in the transform layer and higher solution pH in the exterior solution. The solubility gradient caused by this abrupt change in solution pH can enhance supersaturation in the water film near the glass surface. This will be discussed in more detail in section 5.6.1.. ZrF_4 might precipitate from the saturated solution near the surface by either nucleating directly on the glass surface or nucleating in the solution and being attracted to the glass surface.

The surface potential of the glass changes from negative to positive as the solution pH drifts below 4.38 with increased leaching time. The solution pH decreased from 5.6 to 3.59 by the time sample (1) was removed from the glass powder/water suspension. The zeta potential measurements show that the crystals made up initially of ZrF_4 have an IEP at solution pH of 3.25, thus exhibiting a negative charge for pH higher than 3.20 and positively charged for pH lower than 3.20, possibly due to the ionization of the Zr ion.

The correspondence between the charges on both the

leached glass surface and the ZrF_4 crystals during the initial phase of leaching thus explains why no precipitates are found in the solution during the static corrosion experiments. Because in these conditions, solution pH adjacent to the glass surface can decrease rapidly below 4.38, and for solution pH values between 4.38-3.20 the ZrF_4 precipitates will form on the glass surface due to the electrostatic forces between the glass surface and the crystal. Throughout these zeta potential measurements the solution pH values are above 3.27.

The increasing precipitation of ZrF_4 crystals on the surface can cause a decrease of average zeta potential. Furthermore, these surface ZrF_4 precipitates can act as sites to attract other types of crystal precipitates. In these sequences, the formation of multiple layers of precipitates process is possible. The IEP of the corrosion layer corroded at high S/V ratios under static conditions, see (d), is around pH=4.05. Thus it is possible to form α-$BaZrF_4$, which is the main crystal precipitate in low dilution corrosions. BaF_2, which was found present in the precipitation layer of the intermediate S/V case, is also likely to precipitate on either the ZrF_4 crystals or the glass surface due to its high positively charged surface. Unfortunately, the difficulty with this experiment is the measurement of the zeta potential of the last precipitated crystal, which formed on the very top of precipitation

layer, i.e. the platelet cluster shown in Fig.5.27.(4),
which is believed to cause the charge reversal of the longer
time zeta potential measurements.

5.6.   Flow Test

Under flow conditions, the glass was exposed to a large
amount of water while mixing was enhanced by stirring at
various speeds. In this dynamic environment, the corrosion
products can be transported not only through diffusion
processes but also by solution flow. Thus transport
processes are greatly enhanced and most of the dissolved
species can be carried away. However, the accumulation of
corrosion products depends on the stirring speed, i.e. how
rapidly these species can be transported away from the glass
surface. If the solution is stirred sufficiently, the
effect of solution pH drift can be eliminated.

A sample of ZBLA glass was corroded for 6 hours in the
corrosion vessel with D.I. water flow at a rate of 0.75
l/min (139.9 ml/min.·cm^2). but no stirring. The surface
topography was examined with SEM. Figure 5.41. shows that
the corroded glass surface was covered by a transform layer,
which severely cracked during drying, with a few ZrF$_4$
crystal precipitates on top. This cracked layer tended to
curl up see (a), suggesting the existence of stress
gradients in the layer. Some fibers, see Fig.5.41, appear
to join adjacent pieces of the top surface of the cracked
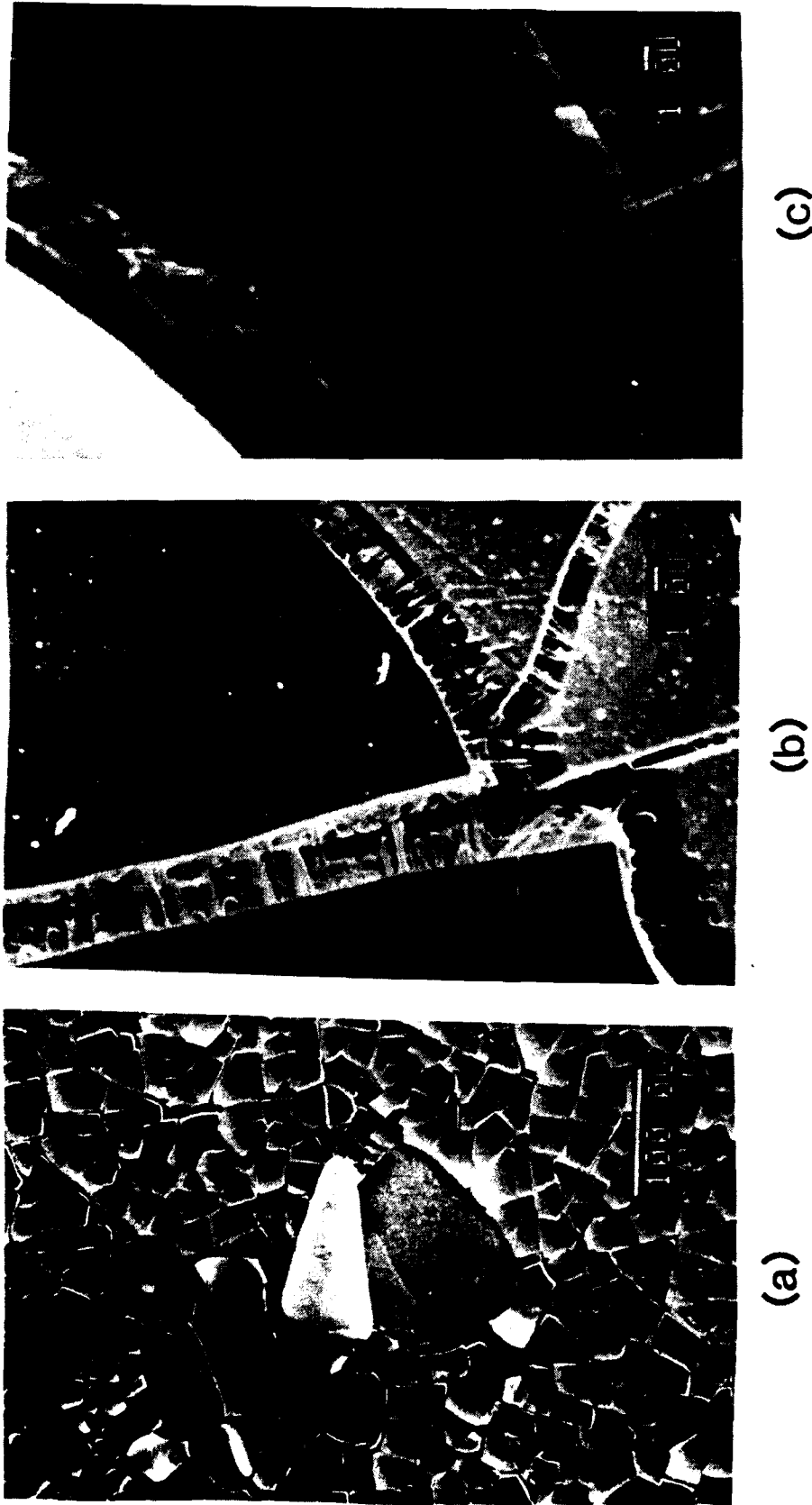
(c)

(b)

(a)

Figure 5.41. (a) Typical surface topography of solid corroded by water flow for 6 hours; (b) close-up of cracked transform layer, (c) pits beneath the layer.

hydrated layer, which is shown later to be an amorphous colloid layer. On the top of the surface, polishing marks still can be seen, therefore, it may be justified to assume that the surface of the trasform layer is nearly the same as the original glass surface without having experienced the degree of matrix dissolution seen in static corrosion, especially at high S/V cases. Colloidal particles were found in this layer. Below the transform layer etch pits were also observed. see (c). The existence of small ZrF_4 crystals on the surface suggested that the solution immediately next to the glass surface had experienced saturation and reprecipitation processes.

5.6.1. The Effect of Stirring Speed

To illustrate the effect of stirring, a clean teflon holder was used to clamp a sample of ZBLA-F glass causing a static condition at the corners, while the center area was exposed to fresh water flowing at a rate of 1 l/min. (312.5 ml/min.·cm^2) . The SEM micrographs of different areas are shown in Figure 5.42. The exposed area has a similar transform layer, shown previously, while the covered region has numerous pits covered with ZrF_4 crystals precipitates resembling a surface corroded in a stagnant solution.

A systematic analysis of the stirring effect was then conducted. A series of flow tests were conducted with different flow conditions. Figure 5.43 shows the surface
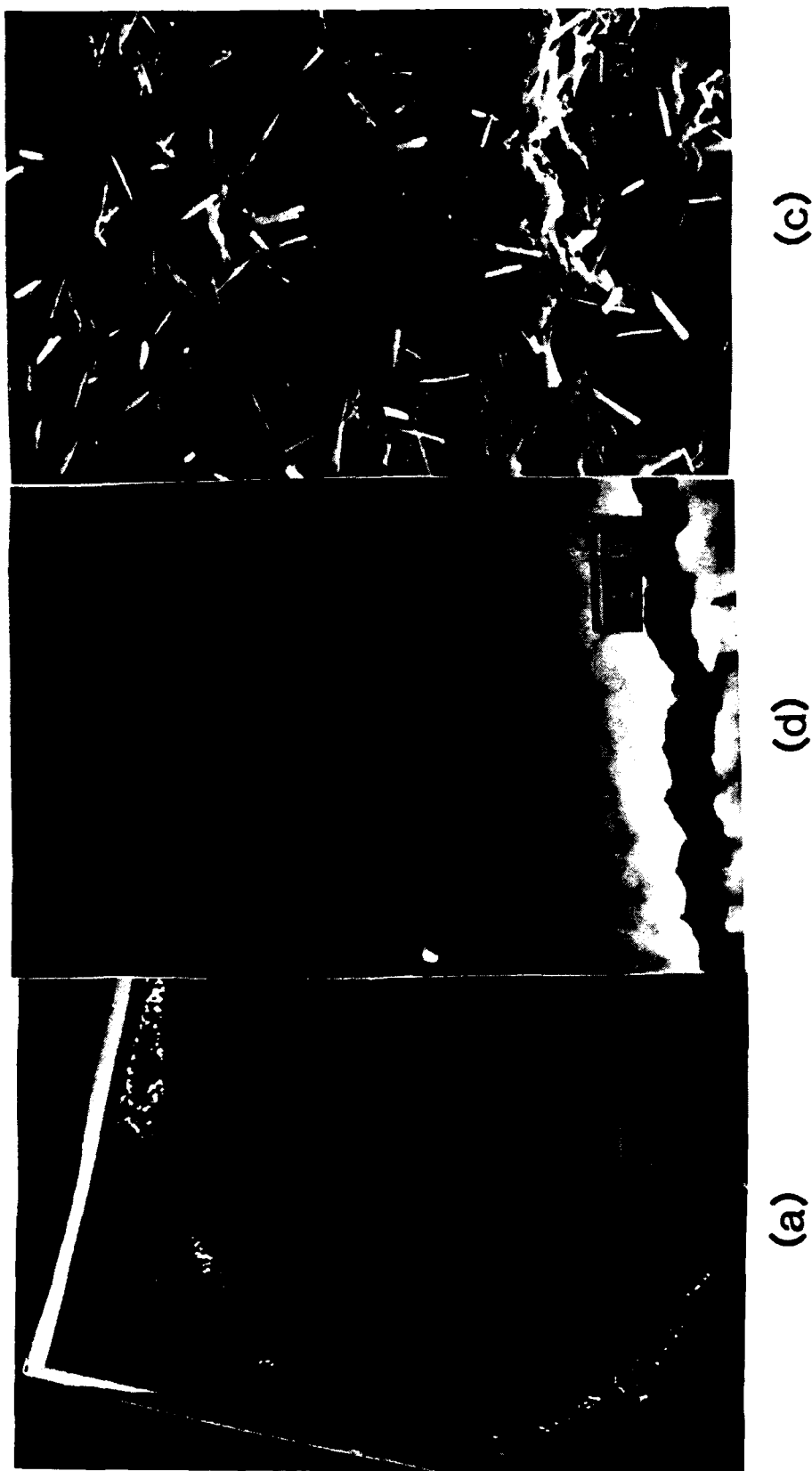
(c)

(d)

(a)

Figure 5.42. (a) Corroded ZBLA-F glass, held in teflon sample holder, for 1 hour; (b) the region exposed to flowing water; (c) the region where the water flow was blocked by sample holder.

topography of glasses corroded at flow rates of 0.12 - 1.15
1/min (124-228 ml/min.·cm^2). with different stirring speeds.
(a) is with slow stirring speed, at a flow rate of 228
ml/min.·cm^2. No surface precipitate was found exept for
colloids in the transform layer. (b) is without stirring
but flowing, at a rate of 0.75 1/min. (139.9 ml/min.·cm^2),
of water through the corrosion vessel. Few small ZrF_4
crystal can precipitate out. In (c), smaller samples were
used and a proportionately smaller amount of flow was used
without stirring, (i.e. at a flow rate of 124 ml/min.·cm^2).
Because there was less disturbance of water in this case,
large crystals were seen to precipitate from solution,
including ZrF_4 and α-BaZrF6 crystals. An investigaion of
samples fractured in cross-section was conducted to see the
corrosion layer formed under the different flow conditions
shown in Figure 5.44. (a) shows a sample corroded by flow
at a rate of 0.5 1/min (333.3 ml/min.·cm^2). with strong
stirring speed for 9 hours, which leads to a relatively
thin, dense transform layer with few colloids in it. The
pits are relatively few and shallow with some small colloids
in them. (b) shows a sample corroded at a low stirring
speed for 6 hours, at a flow rate of 228 ml/min.·cm^2. A
transform layer was formed with a relatively smooth top
layer composed mainly of an amorphous deposit and smaller
colloidal procipitates while the bottom portion of the
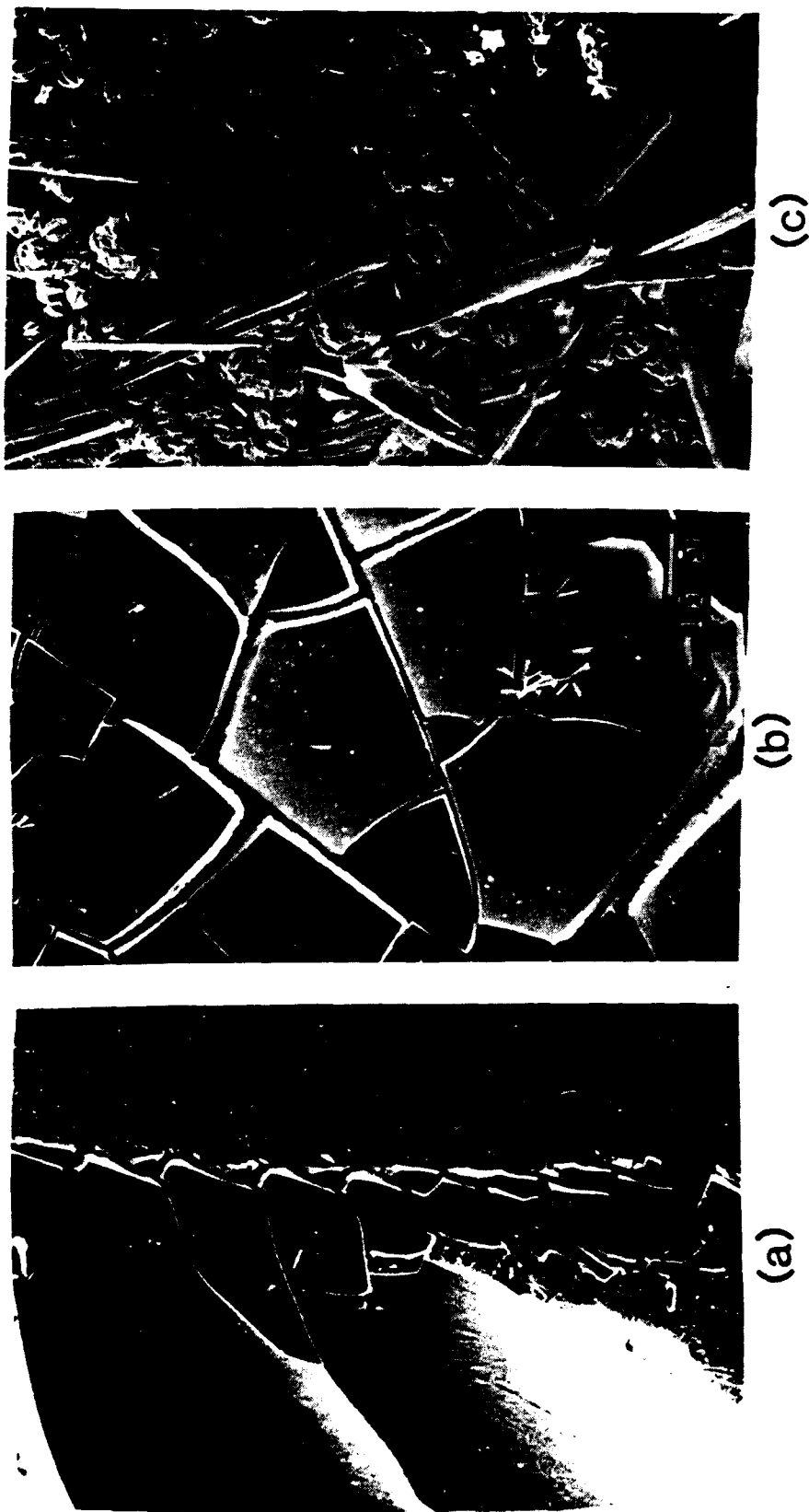transform layer had larger colloids. The pits are deep with

Figure 5.43. (a) The surface topography of ZBLA glass corroded in stirred, rapidly flowing water; (b) same glass corroded only in flowing water without stirring; (c) ZBLA glass corroded in slow flow rate without stirring.
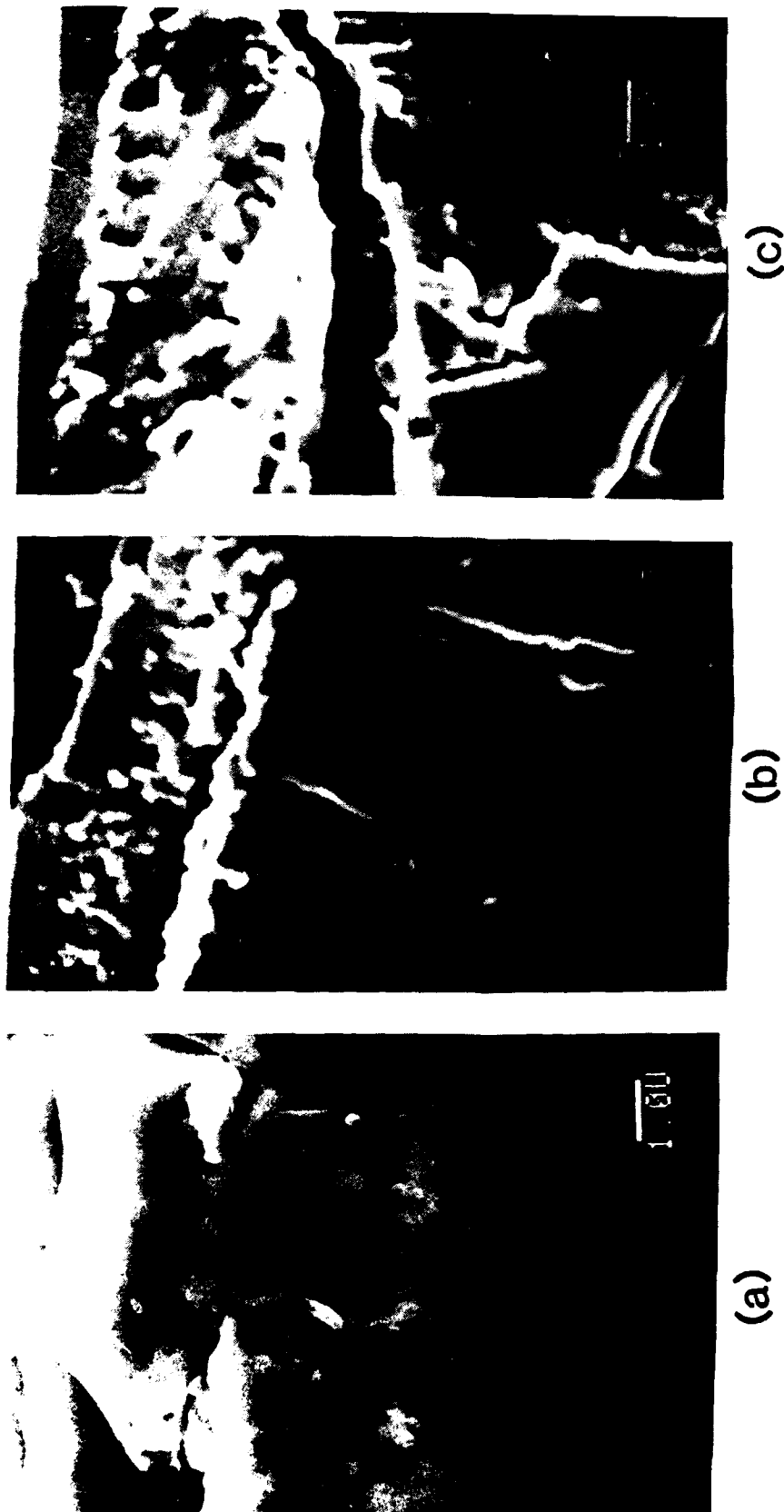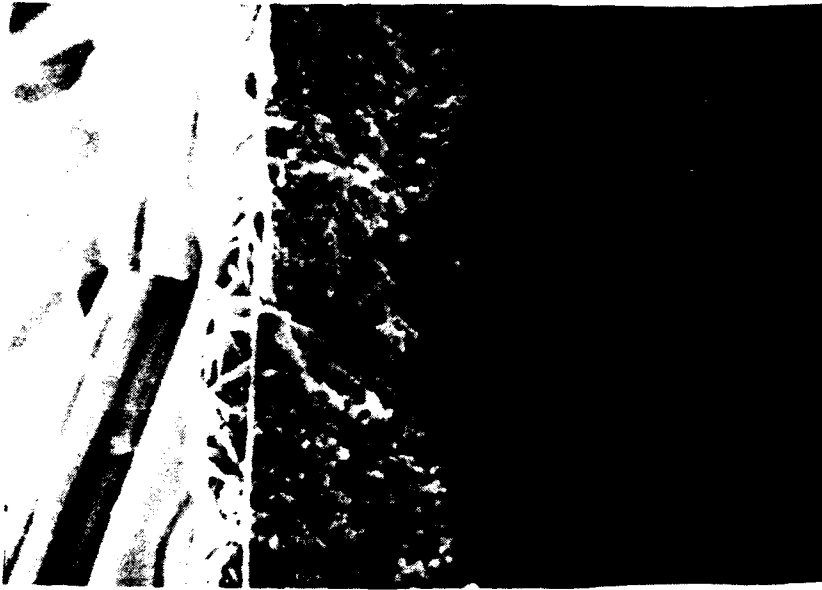
Figure 5.44. Cross-sectional view of corrosion layer formed under different flow conditions; (a) rapid flow with very strong stirring for 9 hours; (b) rapid flow with low stirring speed for 6 hours; (c) rapid flow without stirring, for 6 hours; (d) slow flow rate without stirring for 6 hours.

(d)

Figure 5.44. (continued)

smaller colloids precipitated in them, see Figure 5.45(b).
The sample, corroded only by flow at a rate of 139.9
ml/min.·cm^2 without stirring, as shown in Figure 5.44(c),
has a relatively thicker transform layer, which was
identified as amorphous, see Figure 5.53(c), with a smoother
top layer and larger colloid precipitates in the bottom
portion of the layer. Deep pits were also found. Figure
5.44(d) shows the sample corroded under lower flow, (i.e.
124 ml/min.·cm^2) without stirring. In addition to some
large crystal precipitates on top of the glass surface a
thick transform layer was found, which looks more like
samples corroded under static conditions. The difference in
colloidal sizes between sample (b) and (c) in Figure 5.44,
was examined in Figure 5.46. In general, unstirred samples
have larger colloidal precipitates than slowly stirred
samples and the variation in colloid size within the
transform layer can cause stress gradients when dried.

The EDX spectra of different regions of the samples
corroded under flowing water are shown in Figure 5.47.
Compared with the bulk glass, the colloids in the transform
layer contain less F, and Al and have higher Ba/Zr ratios,
while La stays nearly the same, see (b). In (c), very
little F and Al were found in the top gel layer. This
region is enriched in Zr and La while the Ba concentration
is relatively low when compared to the remainder of the
transform layer.

(a)
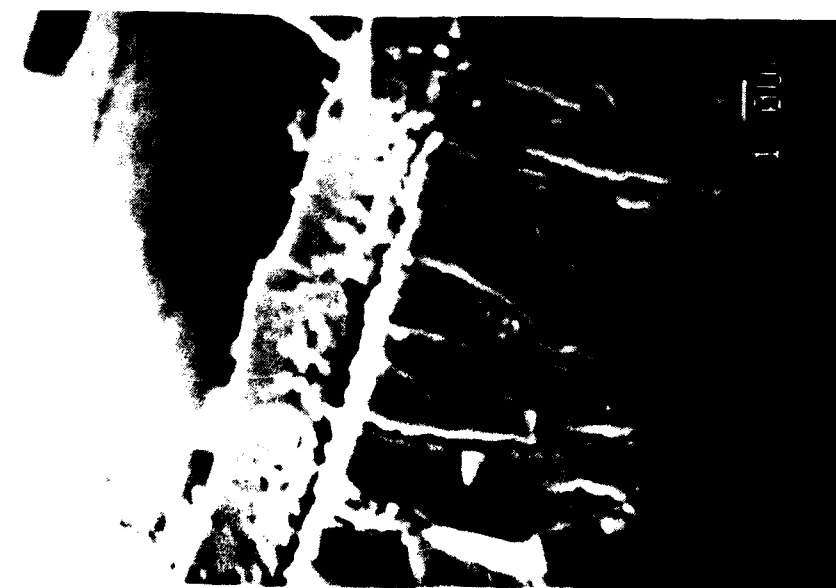
(b)

Figure 5.45. (a) Corrosion layer formed on ZBLA glass corroded by flow and slow stirring speed; (b) pits formed below the transform layer.
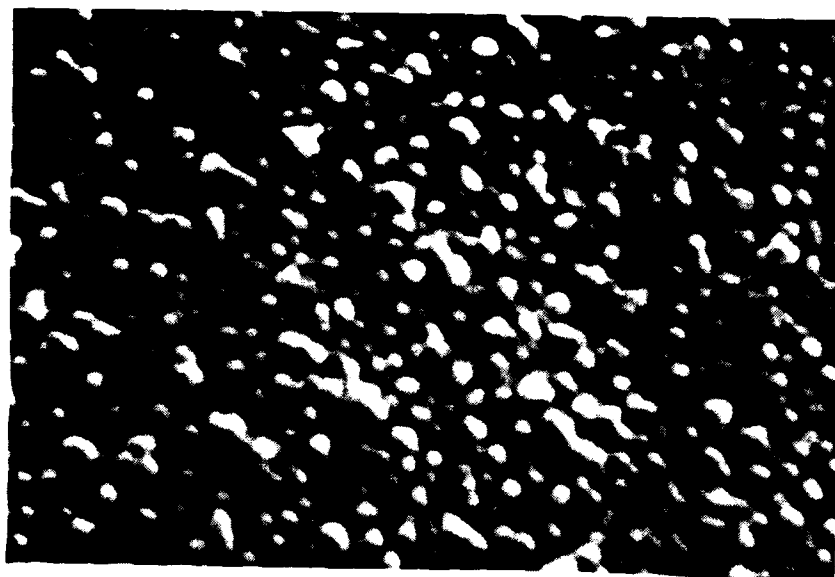
(a)

(b)

Figure 5.46. Different colloidal sizes in transform layer
of flow samples (a) the region close to glass surface of
unstirred sample; (b) the region close to the bulk glass of
unstirred sample; (c) the region close to the glass surface
of slowly stirred sample; (d) the region close to the bulk
glass of slowly stirred sample.
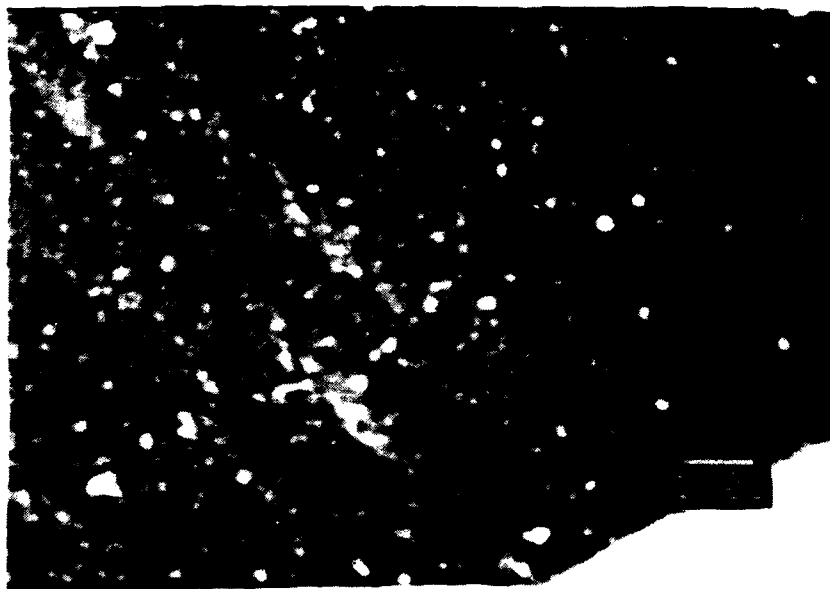
(c)
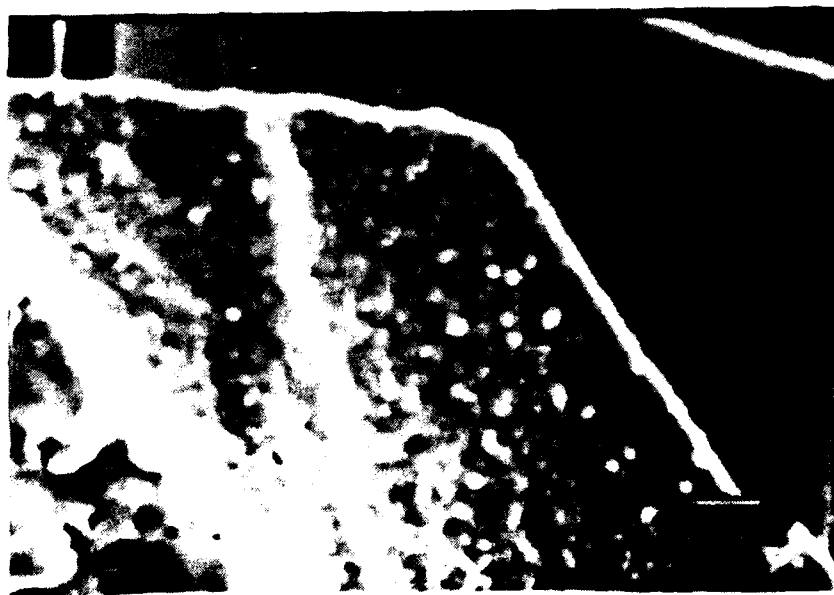
(d)

Figure 5.46 (continued)

Figure 5.47.   EDX spectra of the transform layer of stirred flow sample of ZBLA glass corroded for 6 hrs..

Despite the high dilution conditions used, the high solubility of Ba makes it possible to be measured by the ICP solution analysis for the early stage of leaching. Figure 5.48 shows that both high temperature and room temperature conditions experience a rapid increase in Ba concentration in solution in a short time, which may be due to t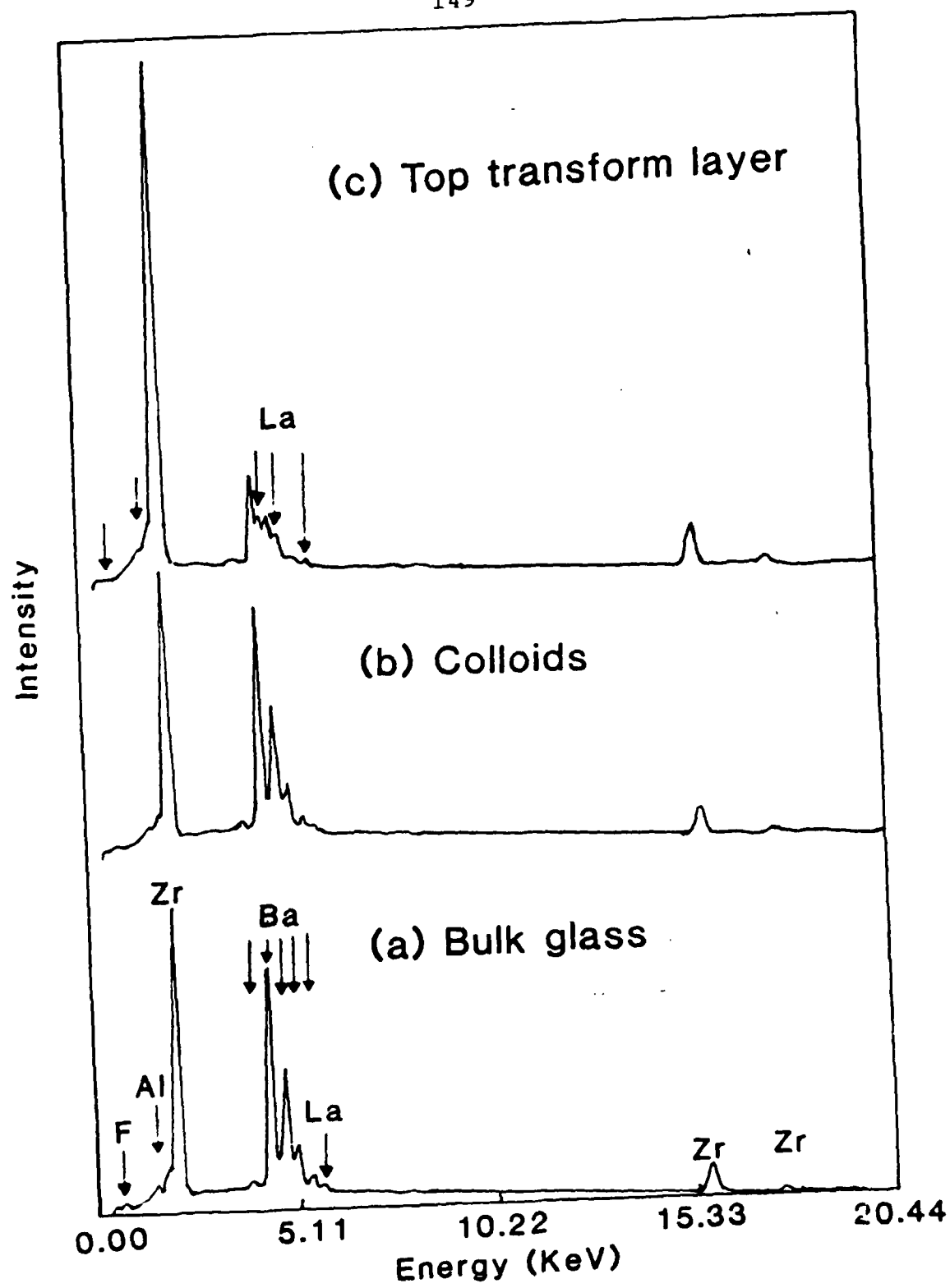he rapid dissolution of fines, surface irregularities and the initial glass surface, which was reported composed of primary F and Ba atoms.[32] After a maximum in the leach rate Ba decreases rapidly and drops to below the detection limit of the instrument, i.e. 0.001ppm, after 30 minutes for room temperature tests.

A fractured corroded ZBLA sample was polished for X-ray line scan analysis to determine the composition profile at the surface. Figure 5.49 shows the Zr, Ba, and F profiles. The top of the transform layer, or the gel layer (IV), is enriched in Zr and contains very little Ba and F, while the bottom of the transform layer (III) which has numerous large colloids exhibits a higher Ba/Zr ratio which confirms the result of EDX spectra. The composition of the pitted area (II) is basically the same as the unaltered base glass (I).

Based upon the observations that crystal precipitates still occur on a glass surface if the stirring speed is not high enough, that a gel layer forms with colloids of various sizes within the transform layer causing stress gradients,
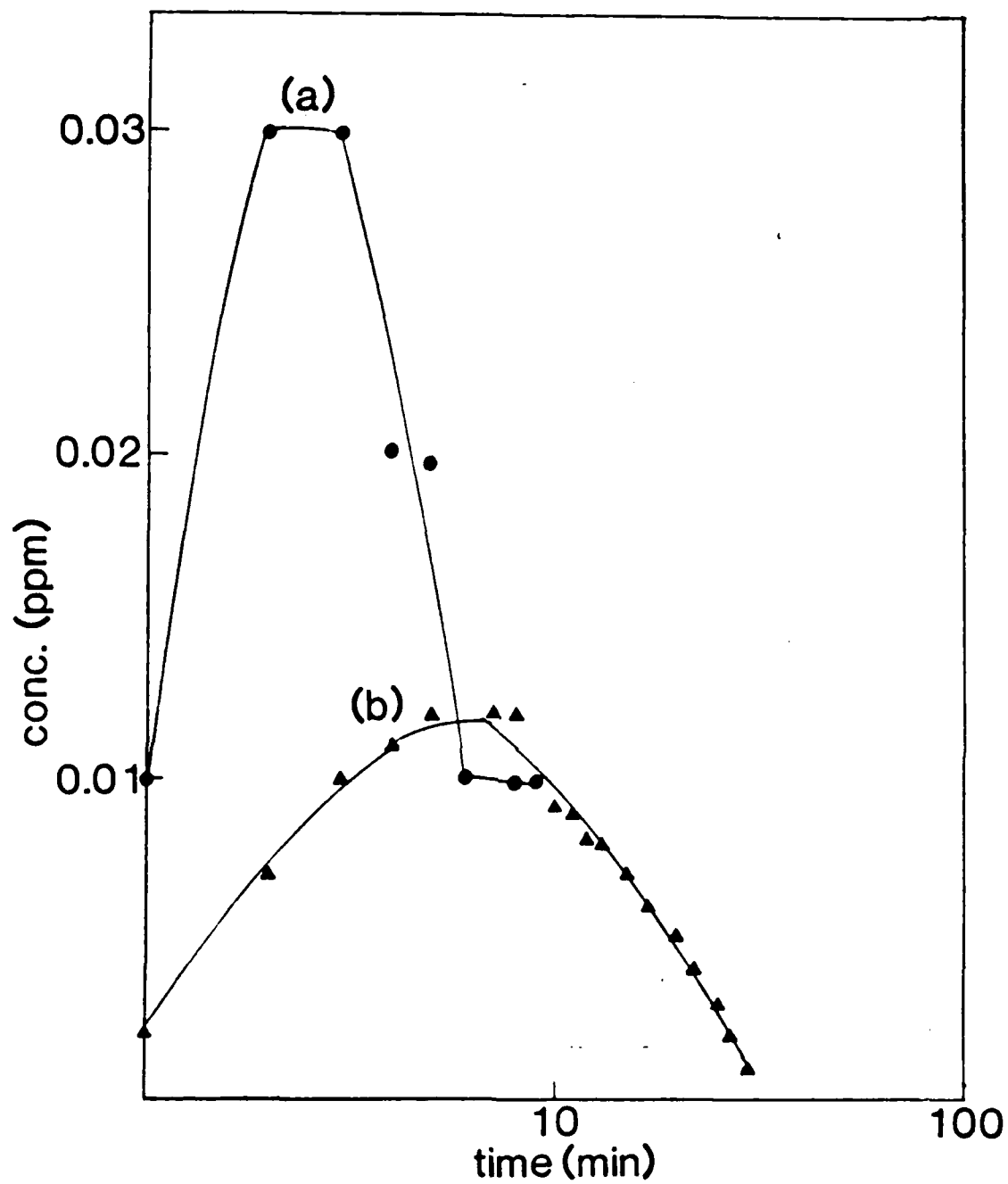
Figure 5.48. The Ba concentration in flowing solution at the initial stage of leaching of ZBLA glass (a) 62.5°C; (b) 25°C.
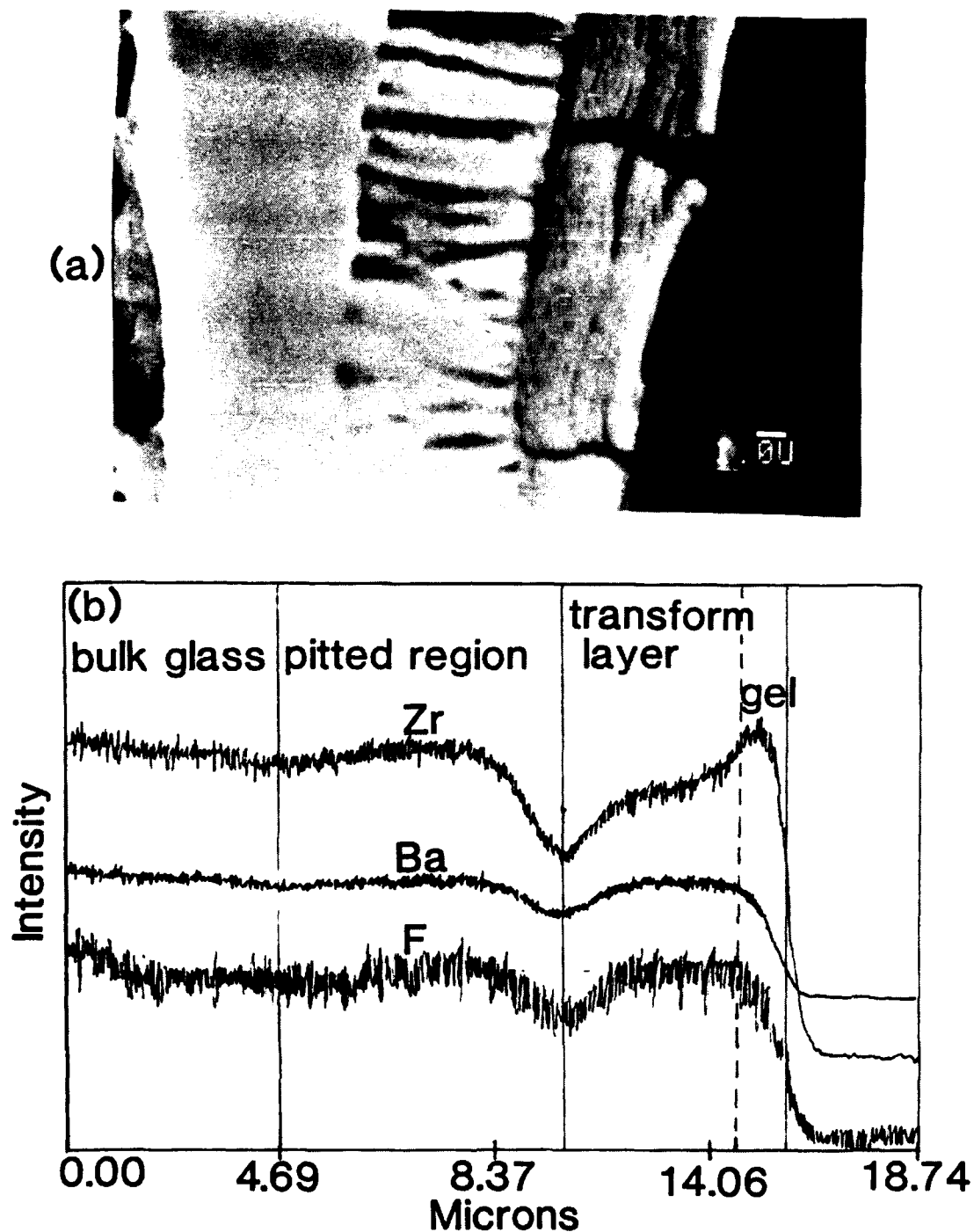
152

Figure 5.49. (a) The polished fractured surface of ZBLA glass corroded in slowly stirred flow for 6 hrs.; (b) X-ray line scan analysis on ZBLA glass to show its composition prifile.

and that a variation of colloidal size is due to different stirring speeds, a corrosion mechanism may be suggested.

For room temperature flow conditions, the bulk solution pH value is usually maintained above 5.0. The glass components have low solubility at this pH, with Ba higher than the others. Since the solubility of ZrF_4 is low, the leach rate of Zr, and the matrix dissolution rate, should be low. This agrees with the fact that polishing marks still can be seen on the surface of the transform layer.

The selective leaching of more soluble species, e.g. Ba, plus very slow matrix dissolution processes are responsible for the corrosion processes of fluorozirconate glasses under this flow condition. The selective leaching of soluble species causes numerous micropores which not only allow water to penetrate into the glass but also create a high S/V ratio condition within the transform layer which could enhance the dissolution processes. Moreover, the localized lower pH plus the stress concentration which could occur in the porous transform layer produced by a non-uniform attack of selective leaching, together with an uneven size distribution of colloids within the transform layer can cause the extension of etched pits far into the bulk glass, similar to the case of stress corrosion in silicate glasses.[59,60] The mechanism of spontaneous cracking for silicate glasses is believed to be due to the high tensile stresses generated in the surface layer by the

contraction of the layer when alkali ions are replaced by protons, i.e. ion exchange processes. The extent of the contraction depends upon the rate of ion exchange and the initial alkali metal content in the glass. In fluoride glasses the pits can form because of a localized accumulation of corrosion products which decrease the nearby solution pH and accelerate dissolution process thus driving the pits into the bulk glass. In our system, this accelerated dissolution process may be coupled with stress existing in the transform layer to form the pits. A porous layer formation leads to severe cracking due to the large shrinkage of the transform layer after drying, see Figure 5.55(a) in section 5.6.3.

The fact that ZrF_4 crystal precipitates form on the surface of samples exposed to flowing water suggests that the diffusion of corrosion products in solution is still an influencing factor to be considered in the leaching processes, even under flow conditions. However, the most important clue to the precipitation process lies in the solution pH gradient existing between the flowing solution and the solution inside the micropores in the transform layer.

In dynamic flow conditions, the transport process of dissolved species is greatly enhanced by water flow. Moreover, the flow speed and the stirring speed determine how rapidly and to what extent the solution in the

micropores is replenished, and how fast the corrosion
products are transported out of the glass. These two
parameters determine the distribution of corrosion products
and thus the solution pH gradient. The solubility gradient
which results from a solution pH gradient can induce a
competing process which causes precipitation both inside the
transform layer, i.e. colloids, and outside the transform
layer, i.e. crystalline precipitates. The high effective
S/V ratio inside the transform layer and the accumulation of
corrosion products cause a lower solution pH in the
micopores which leads to higher leach rates resulting in a
large concentration of corrosion products in the solution in
the pores. While these dissolved species experience a
solubility gradient during outward diffusion from deep
inside the pores to the more freshly replenished solution
near the glass surface, they encounter a reduction in
solubility as they approach the glass surface. This will
cause a supersaturation condition in the lower solubility
regions. If the rate of solution replenishment can be fast
enough to lower the concentration of corrosion products by
transporting them into the bulk solution, then no
precipitation processes are expected to occur. Otherwise,
the amorphous colloidal particles will precipitate out
inside the transform layer. The region closer to the glass
surface experiences a reduced supersaturation because the
corrosion products experience a smaller pH gradient and have

a shorter diffusion path to the bulk solution, thus the size of colloids is smaller. Similarly, the crystal precipitation on the glass surface is also affected by the interplay of a reduced solubility at higher pH values at the surface with increased transport rates in the dynamic flow environments. Moreover, the electrokinetic influence resulting from a zeta potential at glass surface can help sustain the corrosion products near the surface and enhance supersaturation conditions as has been discussed in section 5.5, as long as the solution pH next to the glass surface is in the appropriate range, i.e. lower than pH=4.38.

The formation of the amorphous colloidal precipitates in dynamic flow conditions is not unexpected if one considers the relative supersaturation at which precipitation takes place. Owing to the large pH gradient in the solution adjacent to the glass surface, the relative supersaturation remains high and yields one of the well accepted conditions for forming amorphous precipitates.[46]

The Zr, La enriched gel layer formed on the top portion of the transform layer could contain large amounts of metal-hydroxyl groups which may be expressed as $ZrF_x(OH)_y$ and $LaF_x(OH)_y$, and even some metal hydroxides can possibly form because the higher solution pH near glass surface than the static conditions. Three experimental results can support this hypothesis. First, the hydration/dehydration studies, which will be discussed in section 5.7, show that a

large amount of metal-hydroxyl groups will form in corroded samples, especially under flow conditions. Second, EDX composition analyses shows that the gel layer is enriched in Zr, La and has little Ba and F. This follows the relative solubilities of barium hydroxide [$(Ba(OH)_2 \cdot 8H_2O$] which is very soluble in water,[51-2] and $Zr(OH)_4$[51-3] and $La(OH)_3$[51-4] which are not. Furthermore, colloidal precipitates in lower transform layer contain Ba, Zr, La, and F. Third, the strong tendency of ZrF_4 to hydrolized at solution pH values between 4-8 and forming hydroxide precipitate, which was found during solubility measurements and zeta potential measurement, suggests that the gel layer should contain Zr-OH groups mainly with a small amount of La-OH groups because of the low La content in glass. Some $Zr(OH)_4$ and $La(OH)_3$ could possibly form, if the hydroxyl group concentration is sufficient in the solution.

5.6.2. Corrosion Layer Formation vs. Time

To investigate the development of the transform layer with corrosion time, thin ZBLA glass plates were used for stirred flow experiment. Samples were exposed to flow for different time periods then rinsed and fractured for SEM observation.

Figure 5.50 shows that the thickness of the layer grows with time. Since the flow rate was ample, (i.e. 608.4 ml/min.$\cdot$cm^2) and an intermediate stirring speed was used, no

distinguishable colloids were formed in this layer. The average thickness of these layers was measured and is shown in Figure 5.51. The average transform layer thickness grows nearly linearly with time. This can be explained by the effect of a relatively strong water flow which can replenish the pore solution fast enough to eliminate the precipitation processes which otherwise occur at a slower stirring speeds or slower flow rates. Moreover, owing to the rapid replenishment of the pore solution the solution pH within the transform layer does not experience any large excursion. Thus, the leach rates of the glass components remain relatively unchanged, which in turn produces a constant layer formation rate resulting from the near constant difference of leach rates between glass components.

The layer formation rate measured by taking the slope of the curve is much smaller when compared to that of the early stages of static corrosion, which was conducted at S/V = 1, see Figure 5.30. This is due to the different corrosion mechanisms for these two conditions, which is mainly caused by the severe solution pH excursion resulting from the accumulation of corrosion products in static conditions. However, the transform layer of the flow sample has similar formation rate as that of the later stages of static corrosion, where the precipitation inside the transform layer of the staticly corroded sample can partially block the diffusion paths in the transform layer
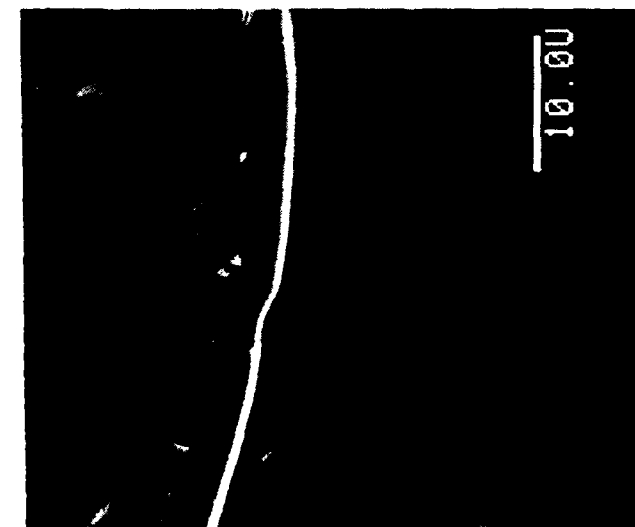
Figure 5.50. Corrosion layer formed on ZBLA glass corroded in stirred flow for different periods of time.
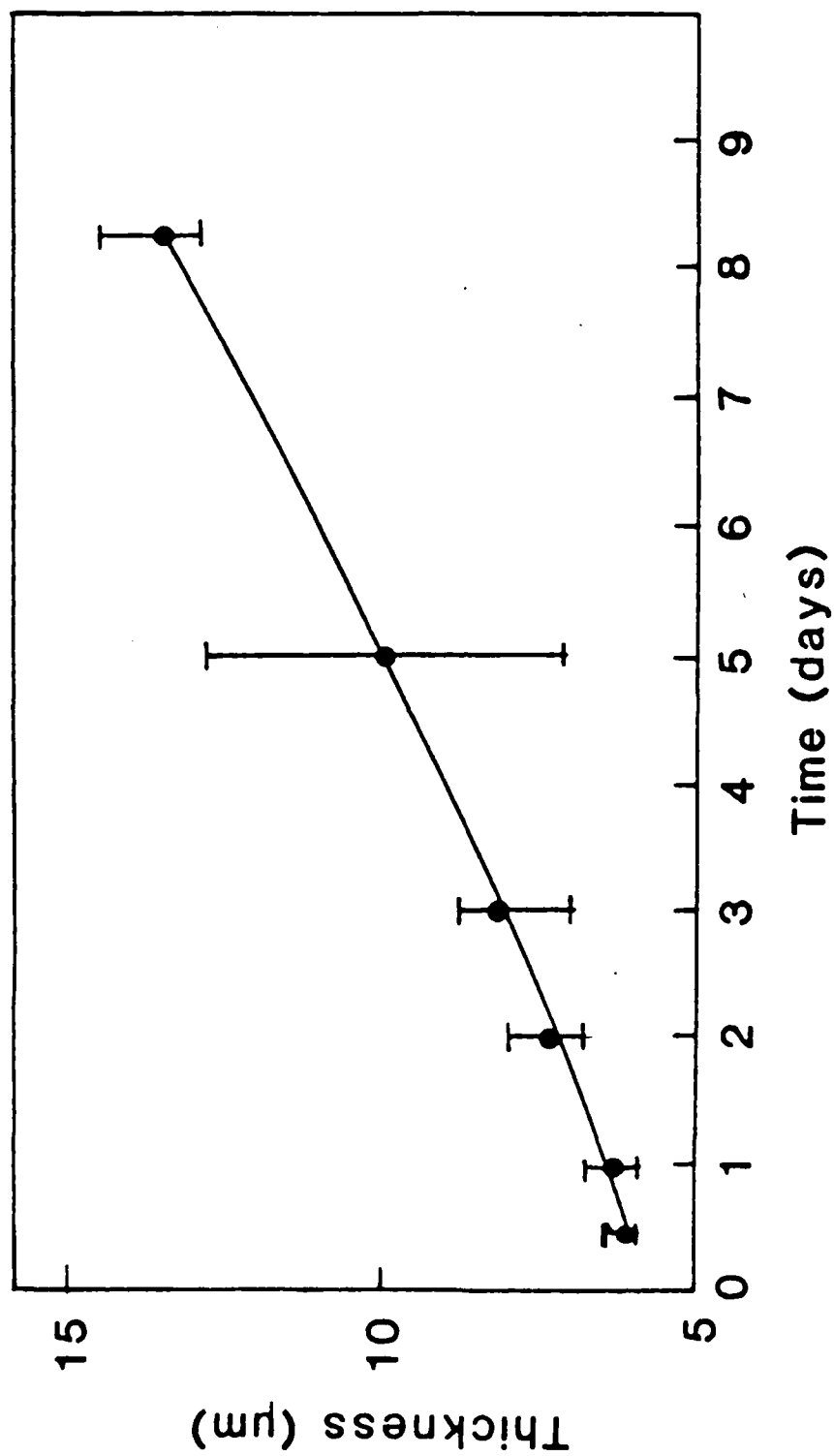
Figure 5.51. Time-dependence of the average thickness of the transform layer formed in stirred flow conditions.

and begin to interfere with the leaching processes.

5.6.3 Temperature Effect

A series of flow tests, with a flow rate of 638.2 ml/min.$\cdot$cm^2, were also conducted at different temperatures, which were controlled by a thermostated heat bath. The development of a transform layer at different flowing solution temperatures was monitored by SEM. The results are shown in Figure 5.52. As the temperature is raised the layer thickness increases, especially for temperatures higher than 45°C where the layer thickens drastically and the microstructure also appears different. The average thickness measurements are shown in Figure 5.53 as a function of corrosion temperature. Two distinct regions suggest different corrosion mechanisms for the higher and lower temperature ranges, and a much higher corrosion rate at temperatures above 45°C. X-ray diffraction analysis was conducted on the transform layer formed at both high temperature and room temperature, Figure 5.54 shows that $ZrF_4 \cdot H_2O$ crystals can precipitate within the transform layer for the high temperature corrosion tests, while only an amorphous layer is formed at room temperatures even after a long corrosion time.

The comparison of the suface topography between dried ZBLA-F glass corroded at different temperatures is shown in Figure 5.55. Besides different layer thicknesses, the
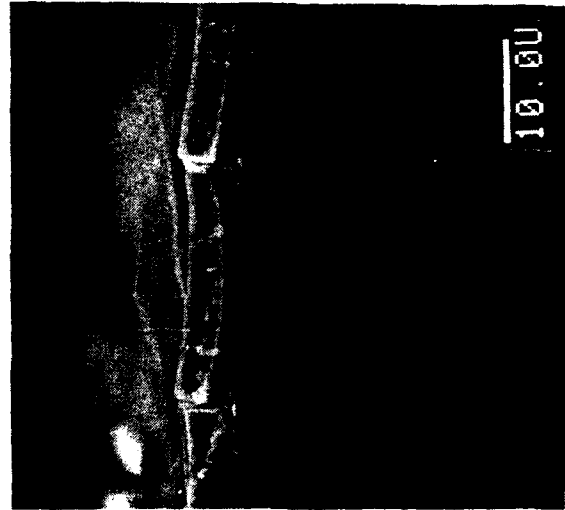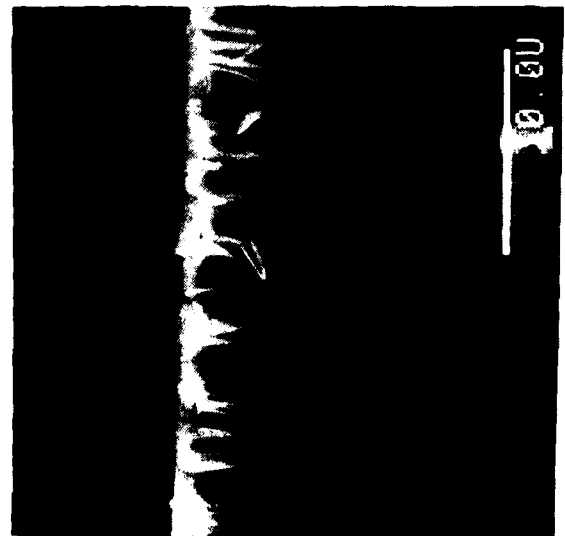
Figure 5.52. Transform layer formation of ZBLA glass corroded in stirred flow condition for 6 hours at different temperatures.

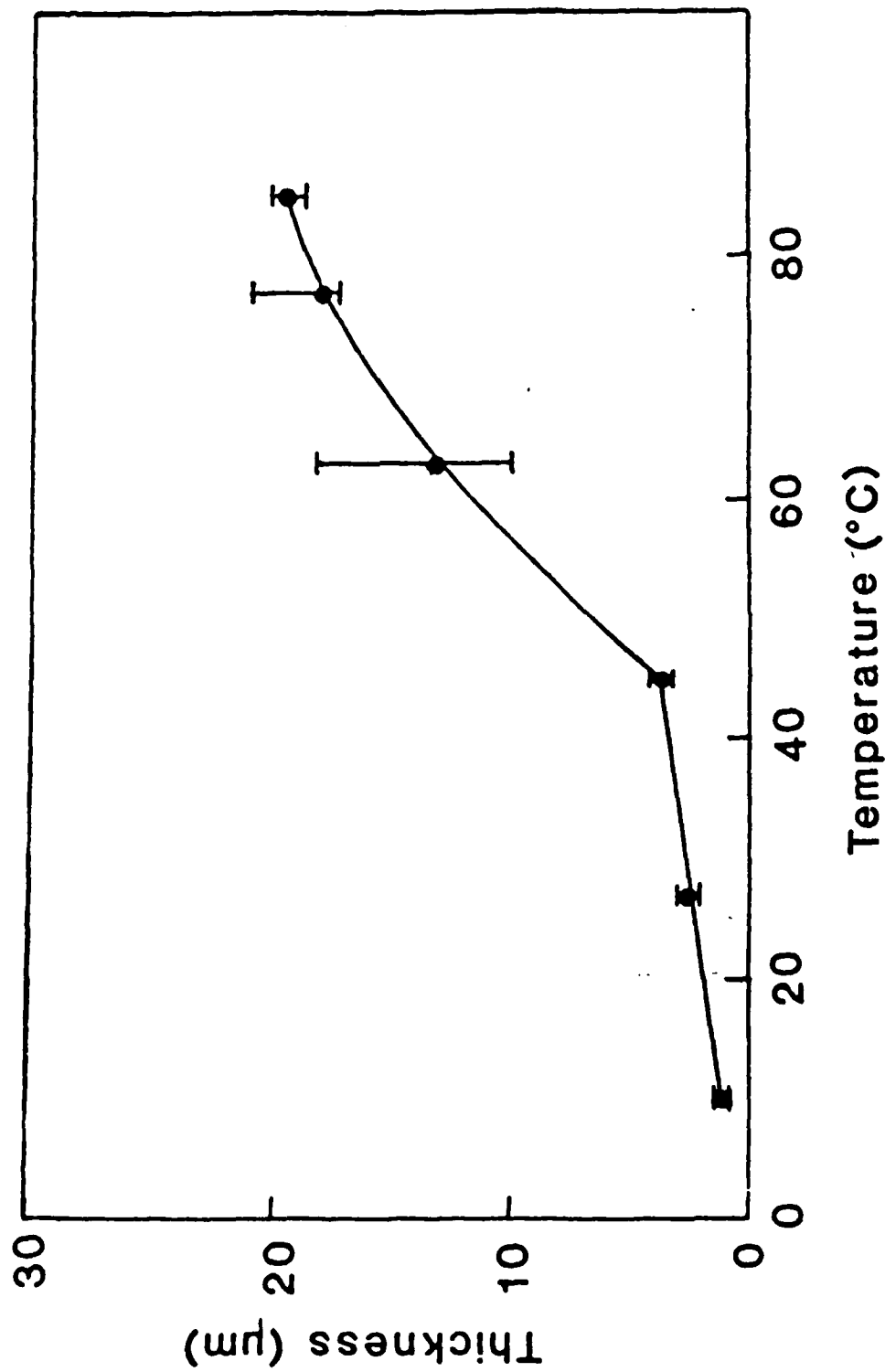Figure 5.53. Temperature dependence of the average thickness of the transform layer formed on ZBLA glass after being corroded in stirred flow for 6 hrs..

(a) Uncorroded glass

ZrF$_4$·H$_2$O crystal

(b) Stirred flow test at 78°C, 7 hours

Amorphous layer
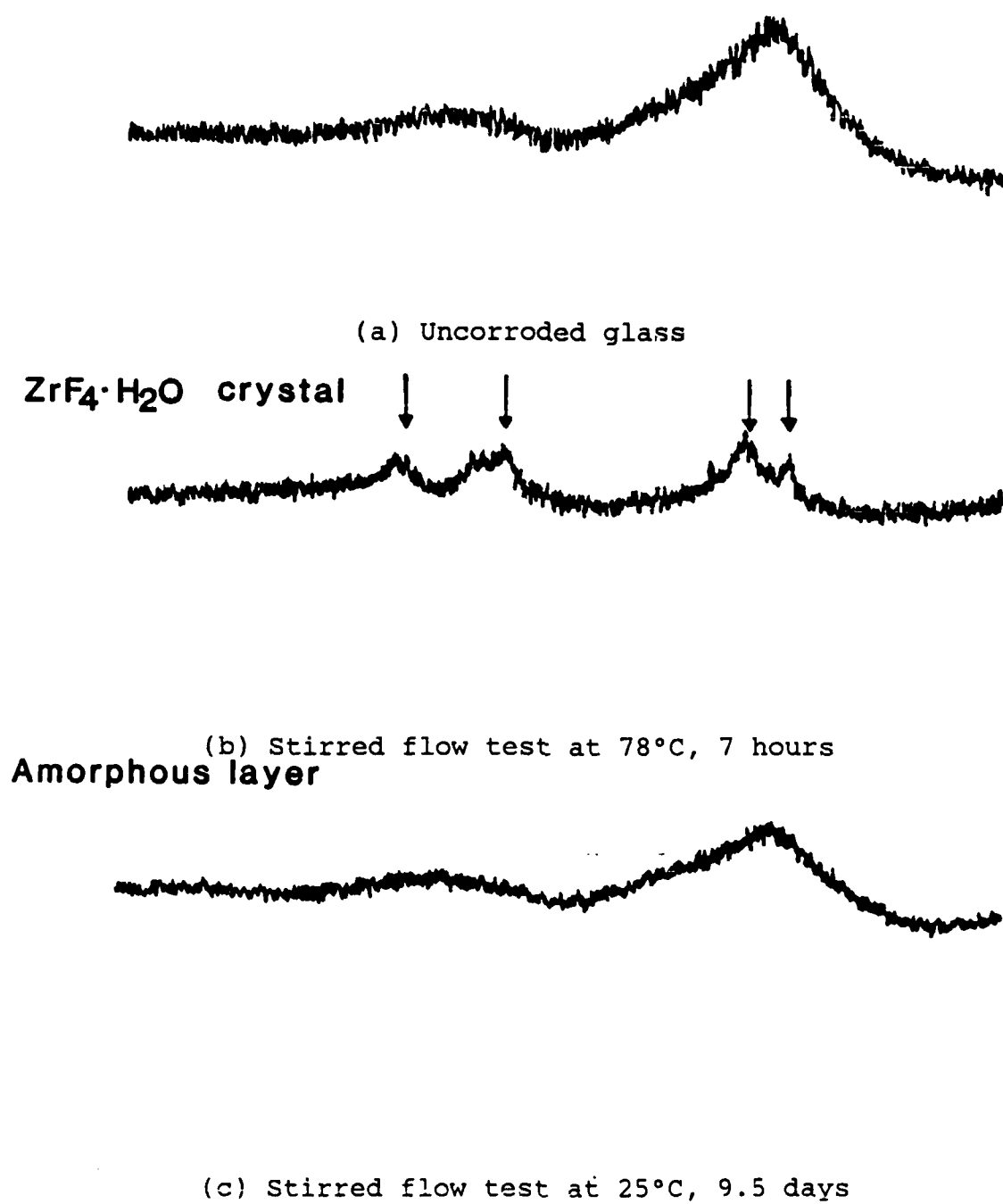
(c) Stirred flow test at 25°C, 9.5 days

Figure 5.54. X-ray diffraction spectra of the stirred flow corrosion layer formed at different temperatures.

surface of the sample corroded at high temperatures is covered by more small colloids than the room temperature case. In both cases, the hydrated layer cracks severely when dried due to the stress gradients existing in these layers. Moreover, it also suggests that the porous transform layer was formed by a leaching process. A closeup of the hydrated layer formed at 65°C in stirred solution is shown in Figure 5.56. In addition to the pits at the bottom, see (a), and the fine colloids on the top of the layer, see (b), we find that this hydrated layer is composed of fine colloidal particles around 0.1μm sizes, see (c). Figure 5.57 shows the same glass corroded at 66°C for two hours in a flowing solution without stirring. In this case, two types of crystals have formed on the glass surface, see (b), needle-shaped ZrF_4 crystal and rosette type Ba-Zr crystal whose EDX spectra will be shown later. Small colloids were also formed on the surface, see (c). The cross-sectional view of the corrosion layer is shown in Figure 5.58. (a) shows that the transform layer is also formed of fine particles and, (b) that the colloidal size is larger further away from the glass surface. There is relatively more porosity at the bottom of the layer which has a sponge-like texture, see (c), and which is formed by severe selective dissolution and reprecipitation. Below the sponge-like reaction front, pits can also be found, see (d). The results of EDX composition analyses of the polished ZBLA
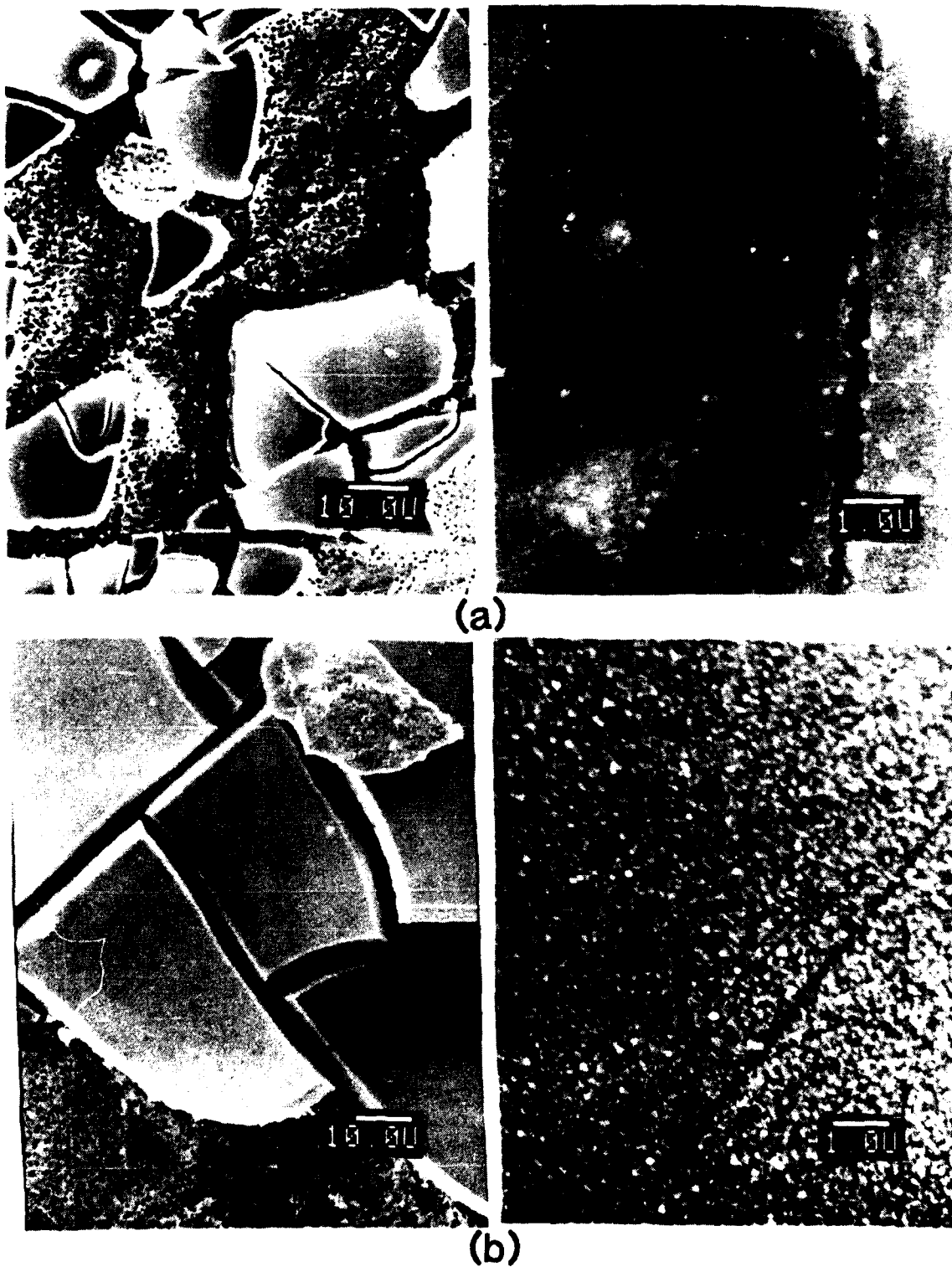
Figure 5.55. Surface topography of dried ZBLA-F glass corroded in flow at different temperatures with intermediate stirring speed for 3 hrs. (a) 21°C; (b) 65°C.
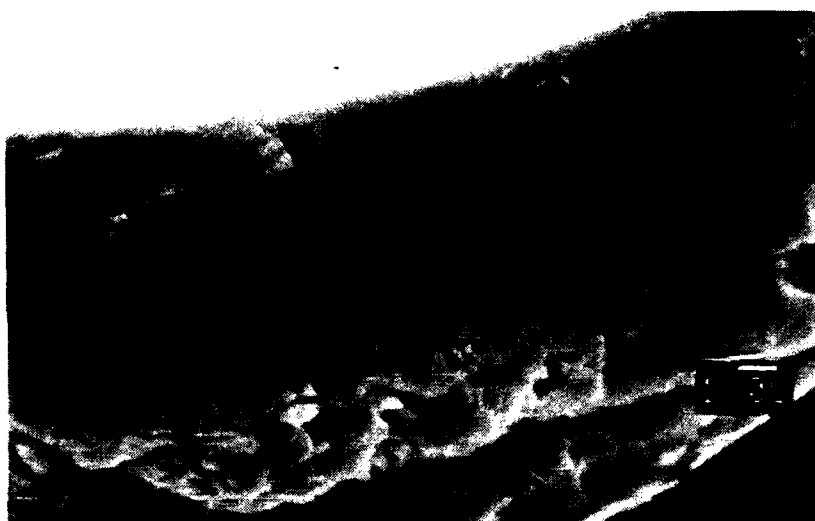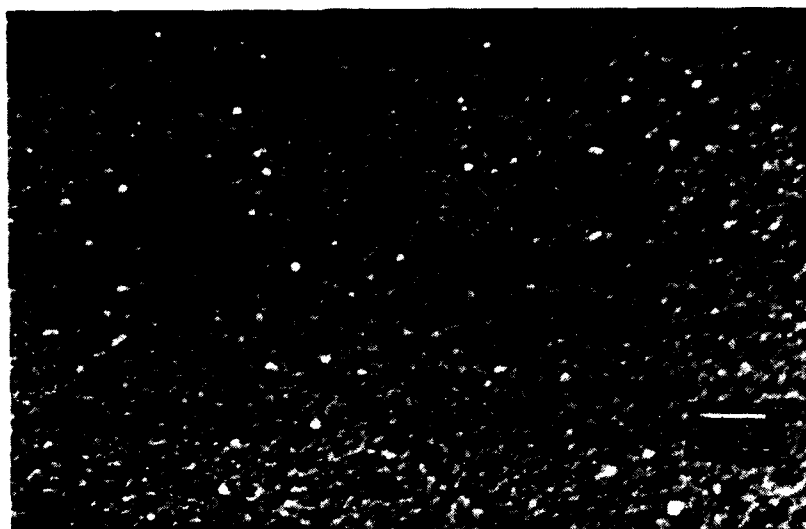
Figure 5.56.   The corrosion layer formed in stirred D.I.
water flow at 65°C for 3 hrs..   (a) cross-sectional view;
(b) top view; (c) enlarged cross-sectional view.
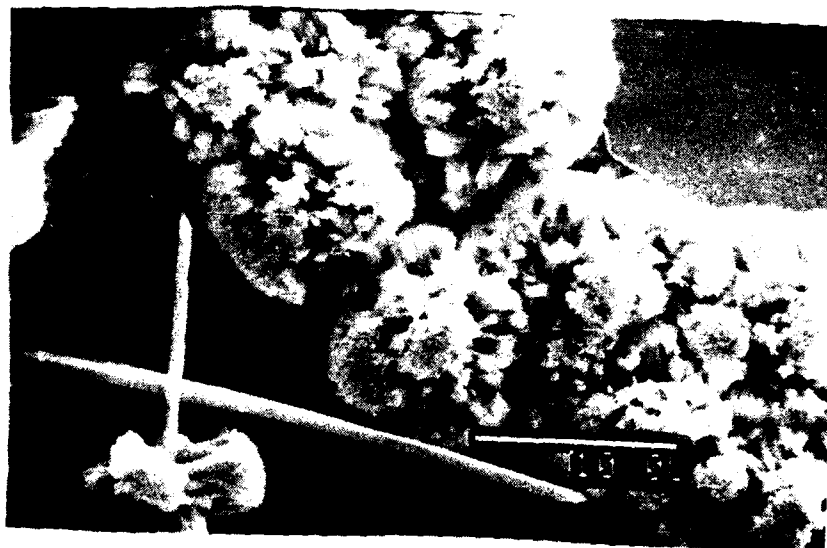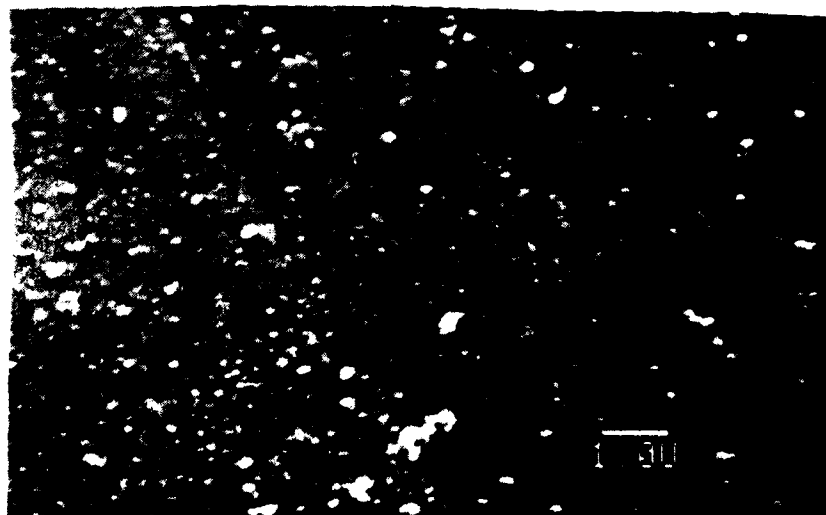
Figure 5.57. (a) Surface topography of ZBLA-F glass corroded in D.I. water flow at 65°C for 2 hrs. without stirring; (b) surface crystals; (c) top view of transform layer.
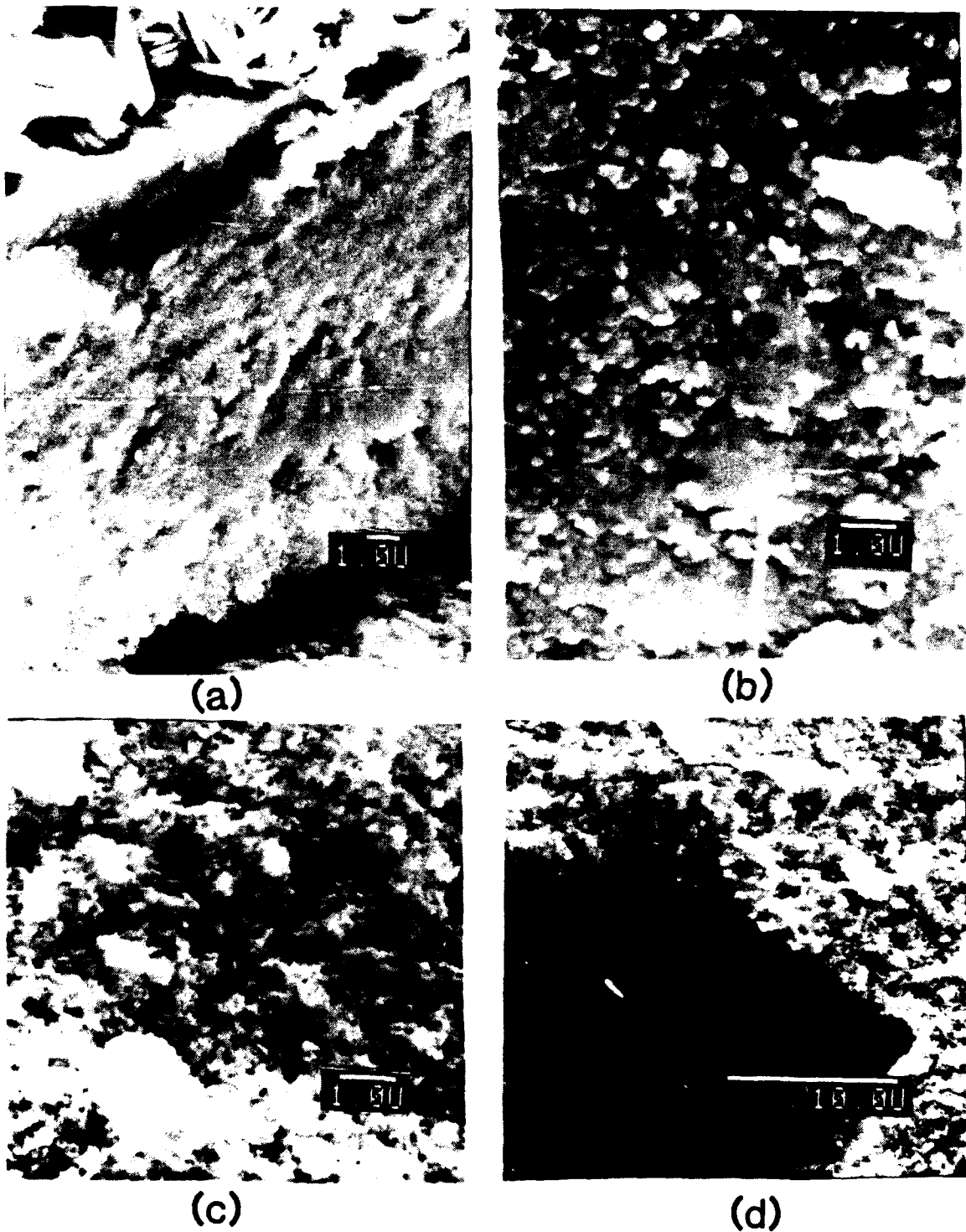
Figure 5.58. (a) Transform layer of ZBLA-F glass corroded in D.I. water flow at 65°C for 2 hrs. without stirring; (b) colloids formed within the layer; (c) sponge-like reaction front; (d) pits formed due to water/glass reaction.

sample which was leached for 6 hours at 67°C in flow without stirring are shown in Figure 5.59. Compared to the bulk glass, transform region 1, which is closer to the bulk glass, has a higher Ba/Zr ratio while Al decreases significantly. Transform region 2, which is close to the original glass surface has little Al and a much lower Ba/Zr ratio. The rosette precipitate crystal has a high Ba/Zr ratio without containing Al, which agrees with the EDX studies of the similar crystal deposits reported by Frischat et al.[38] X-ray line scan analysis was conducted to show the compositional make-up of the whole layer. Figure 5.60 (c) indicates that throughout the transform layer, Ba/Zr is higher than that of the bulk glass except in region 2, which is close to the original glass surface, and has a relatively depleted Ba and enriched Zr content. According to X-ray diffraction data, this region should be where most of $ZrF_4 \cdot H_2O$ crystals form, since the penetration depths of the X-ray beam in the reflection configuration should be only a few microns. Fluoride (F) is relatively depleted throughout the transform layer, especially in region 2. Two different crystal precipitates on the glass surface were also shown in spectra having two different Ba/Zr ratios, that is low Ba/Zr for ZaF4 crystals and high Ba/Zr for Ba-Zr containing rosette crystals.

The solubility of ZrF_4 is increased at higher temperatures[51-3] and the increase of BaF_2 solubility can also
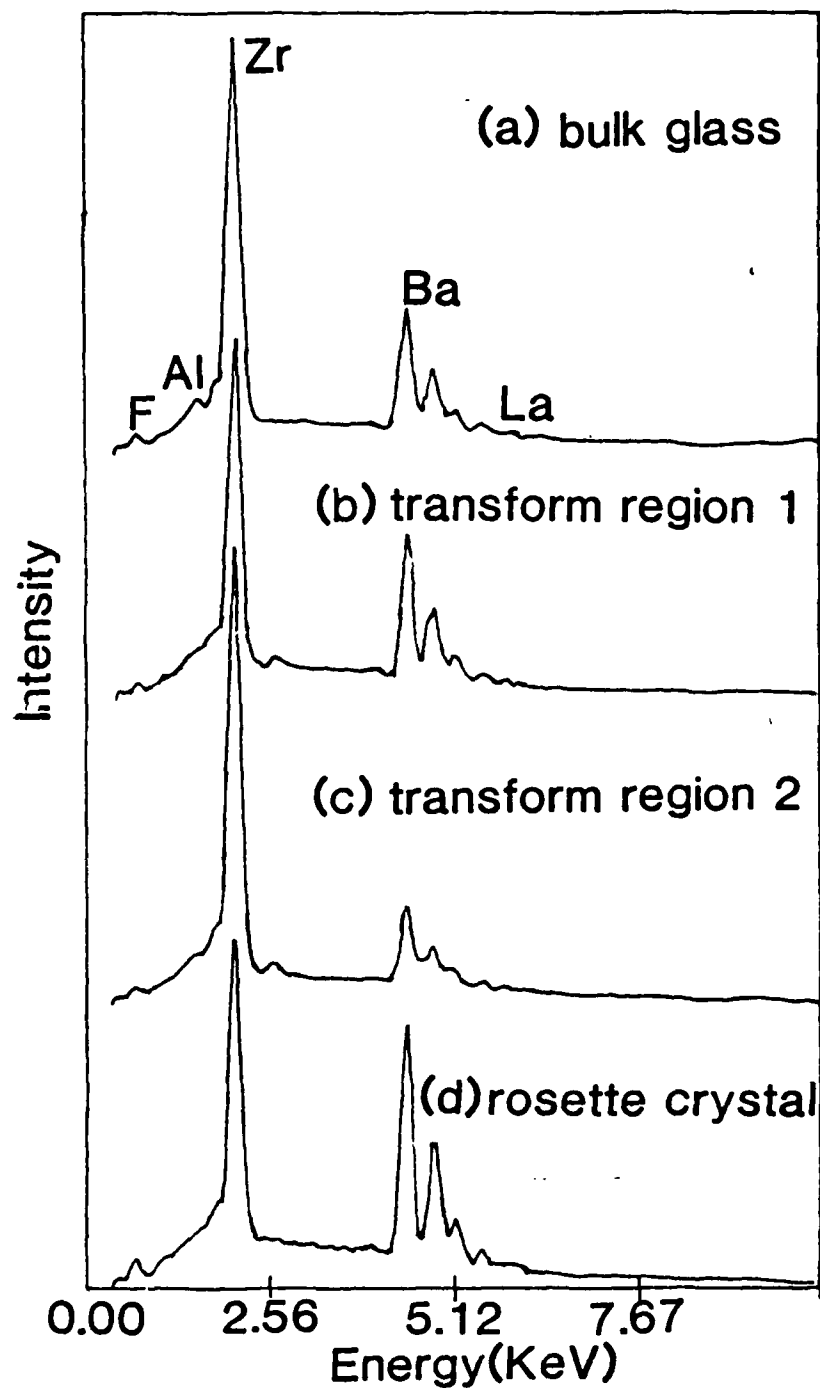
Figure 5.59. EDX spectra of different regions in the corrosion layer of ZBLA glass, corroded in D.I. water flow at 67°C for 6 hrs. without stirring.

(a)

(b)

Figure 5.60. Corrosion layer of ZBLA glass formed in unstirred flow at 67°C for 6 hours, (a) before polishing; (b) after polishing; (c) X-ray line scan spectra.
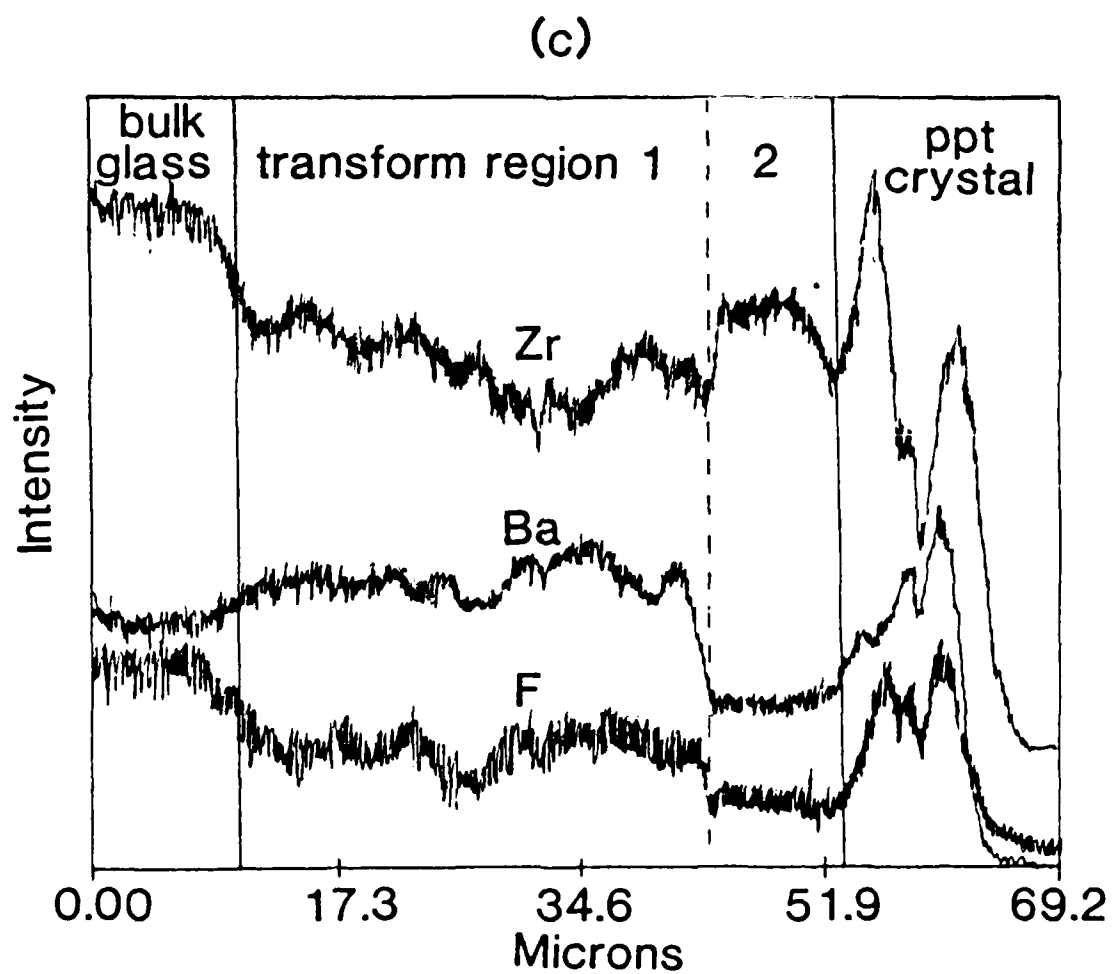
Figure 5.60. (continued)

be confirmed by the observed higher Ba leach rate in the high temperature flow tests as shown in Figure 5.48. The high leach rate combined with higher diffusion rate of corrosion species which normally occur with rising temperatures can cause a rapid increase in the overall corrosion rate which is indicated by a thickening transform layer. Moreover, the composition of the layer can also be temperature dependent due to changes in the dissolution rate or solubility of the glass components. Another important factor which needs to be considered is the solution pH which can be dramatically altered with the enhanced leach rate of Zr species.

The precipitation of fine colloids can occur in the transform layer owing to its thickness and the enhanced dissolution. The larger and heavier Barium (Ba) species will diffuse more slowly than the zirconium species (Zr), thus forming a high Ba/Zr ratio precipitate inside the layer as the corrosion products encounter a raised pH value due to the solution pH gradient in the pore solution. The precipitation process occurs similarly to flow conditions at room temperature. The transform region 2 is closer to the glass surface, thus Ba species are relatively depleted while the majority of the $ZrF_4 \cdot H_2O$ crystals and the metal-hydroxyl groups can form in this region instead of the high Ba/Zr ratio precipitates. Similarly, a forced supersaturation process by solution pH gradient plus an enhanced saturation

of the neighboring solution by the eletrokinetic effect of the glass surface charge can cause rapid crystal precipitation to occur on the glass surface if the transport processes cannot disperse the dissolved species into the bulk solution. The growth rate of the transform layer seems to slow down at higher temperatures, i.e. 80°C, see Figure 5.53, which could be due to an interference of the thickness of the precipitate-enriched transform layer with the interdiffusion processes of water and corrosion products. However, a very thick corrosion layer is formed before the growth rate drops.

5.7. Hydration/Dehydration Study

Infared spertroscopy has been a commonly used technique to study the corrosion processes of fluorozirconate glasses by measuring the peak change of the OH stretching (2.9 μm or 3440 cm^{-1}) and HOH bending (6.1 μm or 1630 cm^{-1}) vibration modes.

Two series of the tests were conducted for this study: room temperature flow and high temperature flow. Both hydration and dehydration measurements were made with a Fourier-Transform Infrared Spectrometer (FTIR). The change of concentration of absorbing species was measured by calculating integrated areas instead of peak heights, because the peaks broaden with time in addition to increasing in intensity, as has been pointed out by Simmons et

al..[18]

5.7.1 Static vs. Flow Condition

To investigate the extent of hydrolysis of fluorozirco-
nate glasses corroded under different conditions, ZBLA-F
glass was corroded in both static and flow conditions. FTIR
transmission spectra were taken on rinsed coroded sample and
corosion layer formation was observed under SEM. Figure
5.61 shows the corrosion layer formed. The water penetra-
tion depths for both samples are nearly equal around 2.4 μm,
and a smooth transform layer is formed in the flow sample
due to selective leaching while a relatively rough transform
layer is formed in the staticly corroded sample also due to
selective dissolution, with large ZrF_4 crystals. The
infrared transmition spectra are shown in Figure 5.62.
Interestingly, although the OH/HOH ratio appears relatively
close, peak areas are very different and the flow sample
contains more molecular water and hydroxyl groups than the
staticly corroded sample. This result at first seems
unexpected if compared with the longer time test result,
e.g. 6 hours test in Figure 5.35. However it agrees with
the SIMS results for an one hour corroded sample reported by
Houser et al..[22] These authors found that the rotated
sample has a deeper H profile than an unrotated sample. Two
conclusions can be drawn from this result, (1) The formation
of the transform layer in static corrosion is mainly

(a)

(b)

Figure 5.61. Corrosion layer of ZBLA glass formed at room temperature in D.I. water for 3 hours. (a) in stirred flow condition; (b) in static, S/V=2, condition.
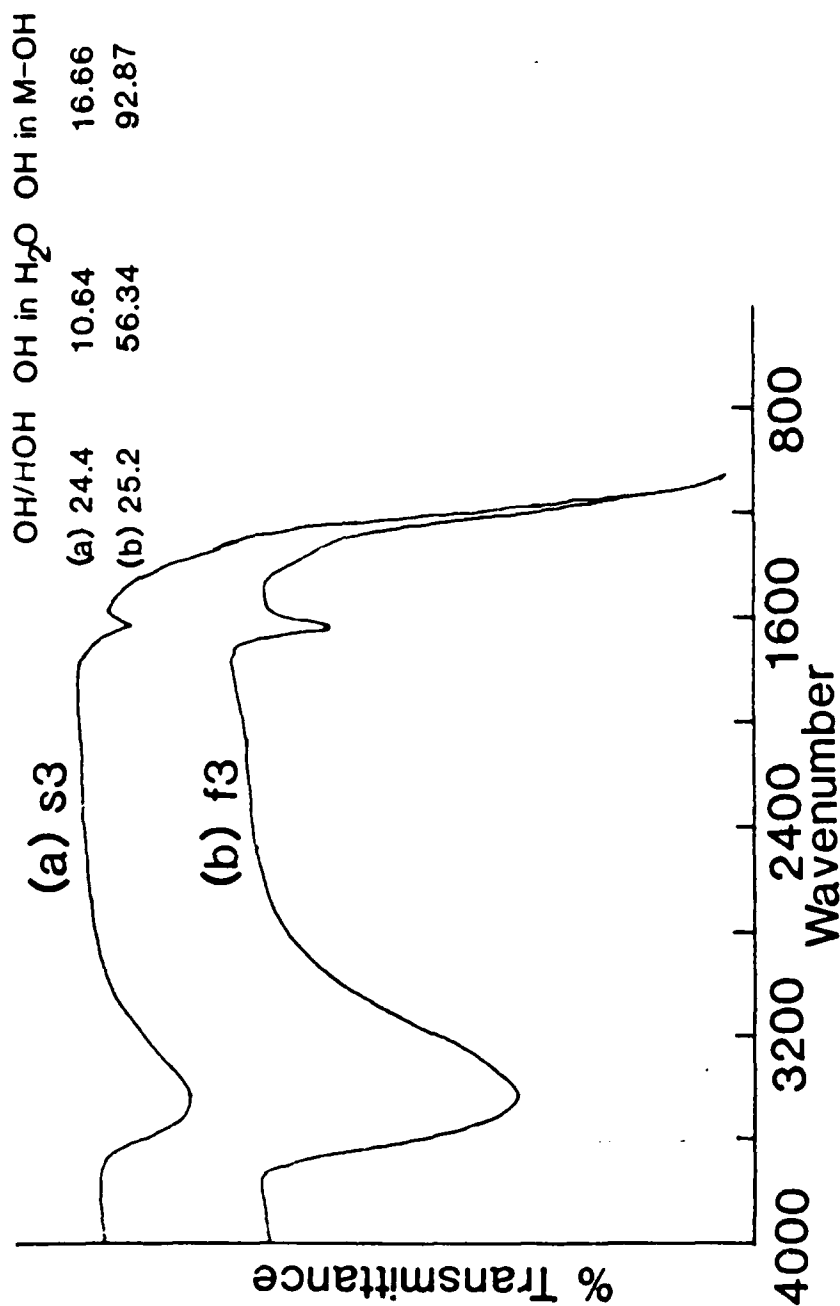
Figure 5.62. FTIR transmission spectra of (a) S/V=2 staticly corroded ZBLA-F glass; (b) stirred flow corroded ZBLA-F glass.

affected by the accumulation of corrosion products with time which causes the near surface pH to drop thus accelerating the selective dissolution processes. This accelerated dissolution process will increase as the transform layer becomes thicker, because of larger S/V ratios within this layer. For short time static corrosion, the effect of accelerated dissolution by pH drift is still not very severe. In the early stage, the transform layer is still thin and the corrosion products diffuse out easily. (2) In flow tests, the large amount of solution used plus the high stirring speed cause a replenishment of the solution both near and within the transform layer, thus the region close to the glass surface has greater difficulty reaching the solubility limit of corrosion products if the solution replenishing rate is high enough. However, owing to the high solubility of BaF_2 and ZrF_4 the dissolution rate is more limited by transport processess, i.e. solubility limit, rather than surface reaction control[46] and thus the dissolution rate of the glass components will increase as their concentration in solution decreases below the saturation level. Hence, in stirred flow condition the selective leaching of soluble species, e.g. Ba, is actually increased, if the complicated effect of solution pH excursion which occurs in static condition is avoided. The increase of selective dissolution rate of soluble species can be supported by the fact that even though the average

water penetration depth is about the same, the transform layer of the flow sample contains much more molecular water than that of the staticly corroded one, because the former has more micropores formed by selective leaching in which to hold the penetrating water.

The FTIR transmission spectra of pure D.I. water, see Figure 5.63 show an OH/HOH integrated area ratio is 9.5. By using this ratio as a standard, the separation of the contributions due to molecular water and that due to metal-hydroxyl groups in the hydroxyl vibration peak can be achieved. With this in mind, from Figure 5.62, we can tell that the transform layer of the flow sample has much more molecular water than that of the staticly corroded sample. Moreover, it also contains much more metal-hydroxyls than the staticly corroded sample. The possible metal-hydroxyl groups formed has been proposed as $ZrF_x(OH)_y$ and $LaF_x(OH)_y$ in section 5.6.1, $Zr(OH)_4$ and $La(OH)_3$ are possible to form due to their low solubility in cold water and the inter-mediate pH range,[51-3,4] while barium hydroxide is very soluble and Al is mostly leached. And these hydroxides have been experimentally proved to exist in the flow samples.[61] The hydroxides are expected in the gel layer near the glass-water interface. The result that the static corrosion sample has fewer metal hydroxides in the transform layer can be understood by knowing that both zirconium hydroxide and lanthanum hydroxide are more soluble in more acidic
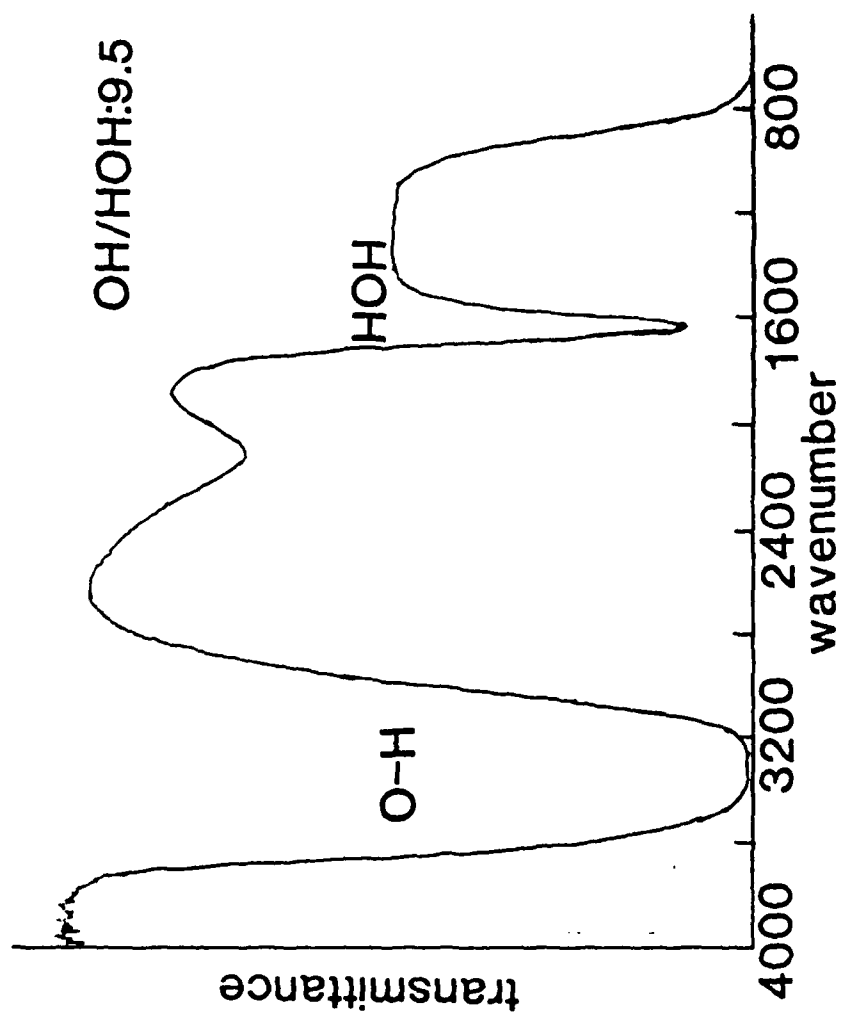
Figure 5.63. FTIR transmission spectrum of pure D.I. water.

environments[51-3,4] and that is the case in static
conditions.

5.7.2 Temperature Effect

A series of FTIR transmission spectra of leached ZBLA-F
samples was acquired. The samples were corroded for
different times of soaking in flowing D.I. water. The room
temperature hydration tests were conducted by using the same
piece of glass. After polishing, the sample was soaked in
the solution for 0.5 hr., after the removal for the measure-
ment sample was put in solution again for another 8.5 hours .
before being removed for next spectrum. After two measure-
ments, the sample was polished again to remove the corrosion
layer and then was used for 1.5 and 3 hours measurements
with the same procedure described above. The result is
shown in Figure 5.64. By using the OH/HOH ratio of pure
water to separate the contribution of molecular water and
contribution of metal hydroxide to the hydroxyl stretching
band. The amount of penetration of water and the formation
of hydroxide as a function of $t^{\frac{1}{2}}$ are plotted in Figure 5.65.
The existence of hydroxide in the transform layer indicates
an ion exchange process between solution OH^- groups and F^-
in the transform layer of the glass. Suprisingly, it
contributes more to the OH band than molecular water does.
Moreover, the rate of hydroxyl groups formation increases
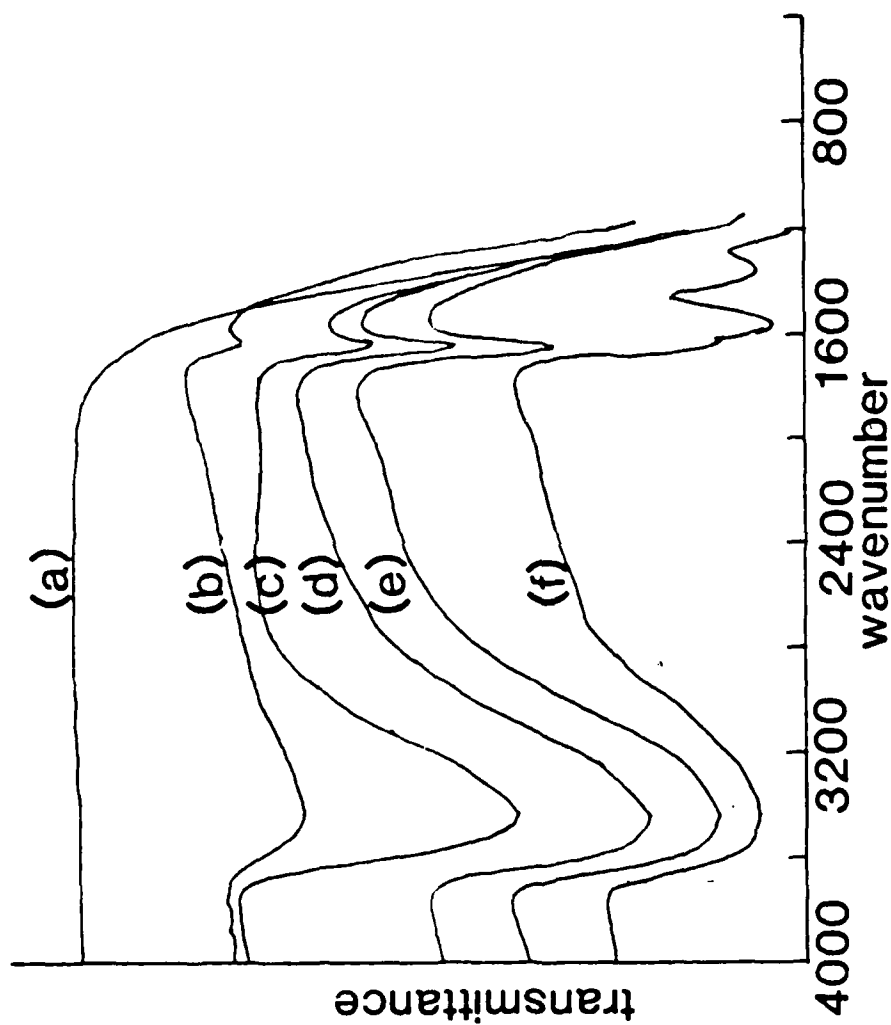rapidly at the beginning and then levels off for the longer

Figure 5.64. The FTIR transmission spectra of ZBLA-F glass corroded in stirred D.I. water flow at room temperature for different periods of time. (a) uncorroded; (b) 1/2 hr.; (c) 1.5 hr.; (d) 3 hr.; (e) 9 hr.; (f) 9.5 days.
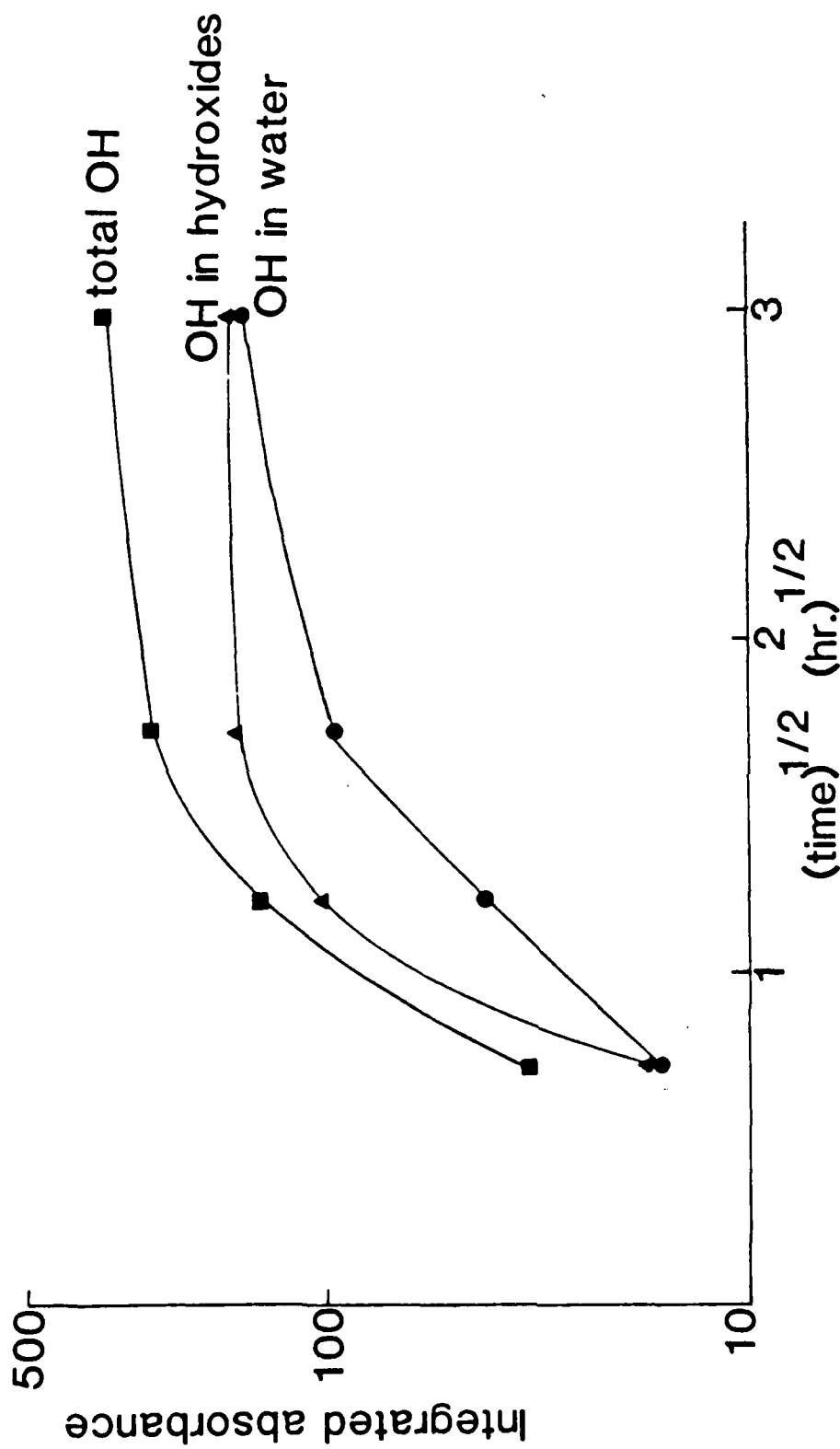
Figure 5.65. Time-dependence of the extent of hydration of ZBLA-F glass corroded at room temperature in stirred D.I. water flow.

times. This can be explained as a reduction of the solution pH in the layer as it thickens thus making hydroxide formation more difficult. Another possibility could be an interference from the increased F^- concentration in the transform layer. The penetration of water into the glass shows a linear dependance on $t^{\frac{1}{2}}$ at the early stage, and then decreases in slope, which could suggest that the rate of molecular water penetration into the glass in the early stages is a diffusion controlled process, while the slow down at longer times could be due to a precipitation process occurring inside the layer, which can partly block the diffusion paths and begin to interfere with the leaching processes. The same glass has been corroded at room temperature for a long time, see spectrum (f) in Figure 5.64, shows two new peaks at $1351.4cm^{-1}$ and $1562.8cm^{-1}$. This may be due to the formation of metal-hydroxyl groups. However, futher deconvolution work needs to be done to identify them.

Similar tests have been conducted at a higher temperature, i.e. 56°C. The FTIR transmission spectra are shown in Figure 5.66. Hydroxide formation was also found under this condition, see Figure 5.67, and occured much faster than at room temperature at the very beginning of corrosion. However, the rate of formation levels off rapidly and may even decrease a little for after 3 hours. The rapid decrease in the formation of hydroxides could be
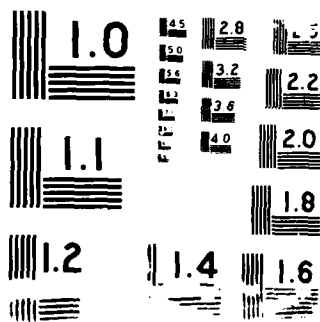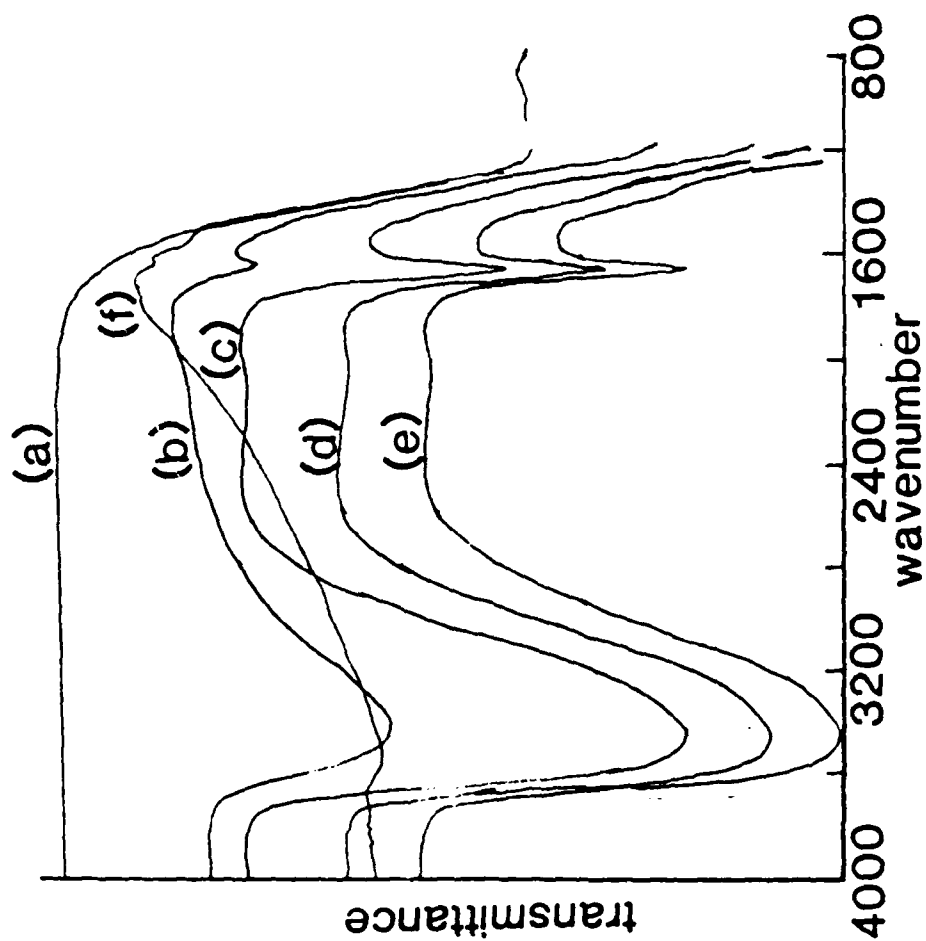
Figure 5.66. FTIR transmission spectra of ZBLA-F glass corroded in stirred D.I. water flow at 56°C for different periods of time. (a) uncorroded; (b) 1/2 hr.; (c) 1 hr. (d) 2 hr.; (e) 3 hr. (f) spectra of sample dehydrated up to 200°C, which was corroded at 65°C flow for 3 hours.
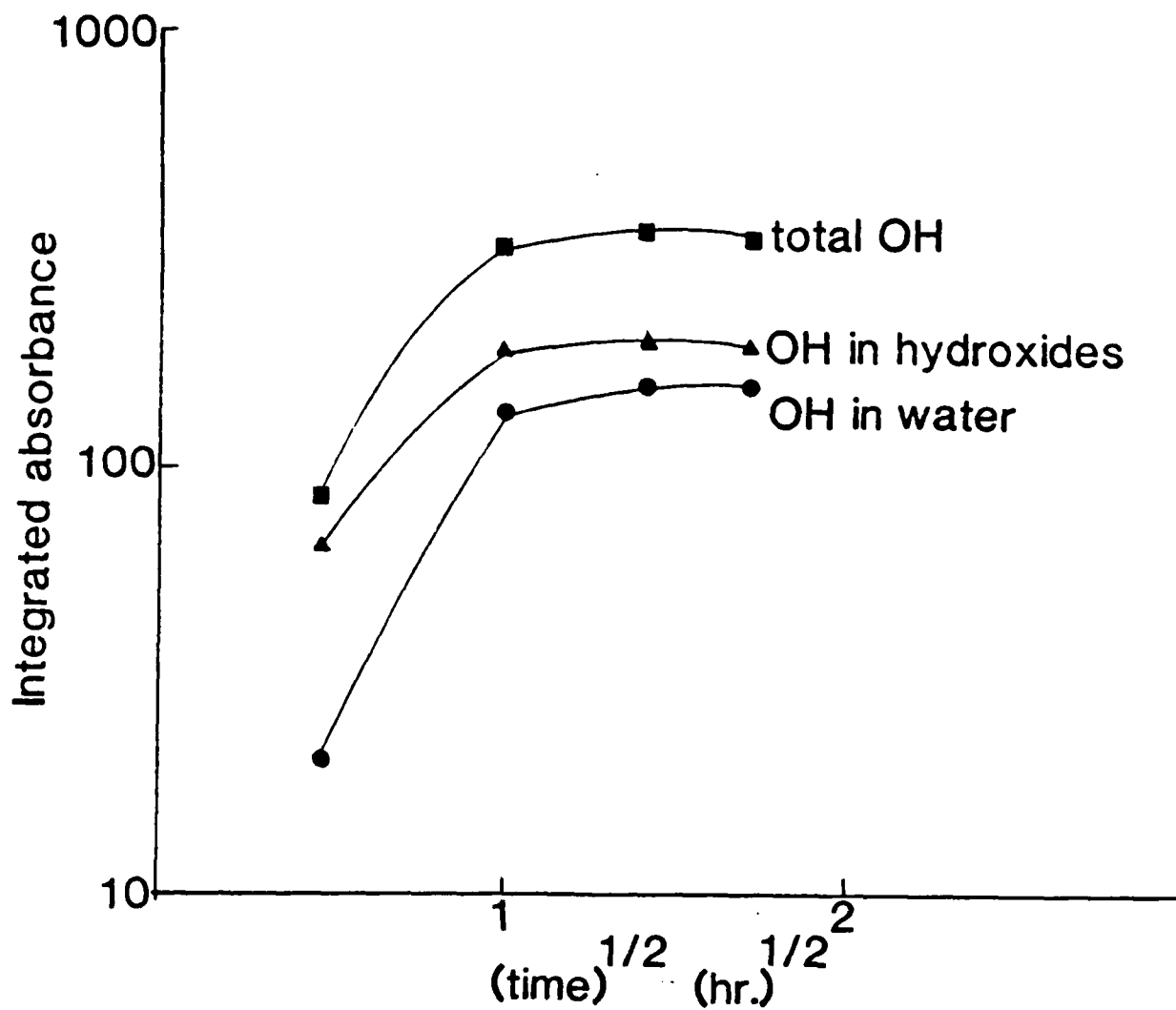
Figure 5.67.   Time-dependence of the extent of hydration of ZBLA-F glass corroded at 56°C in stirred water flow.

attributed to the enhanced leaching of glass components and the thick layer formed added to a larger pH drift which in turn decreases the formation rate of hydroxides. The decrease of hydroxides in the 3 hour test could also be due to the spalling of the corrosion layer during the experiment. Because $ZrF_4 \cdot H_2O$ crystals formed within the transform layer and the layer is thick, it could have more H_2O group than for the room temperature test. However, the rate of H_2O penetration into the layer also levels off rapidly which could be due to the large amount of precipitates formed within the transform layer, slowing down the diffusion processes.

After dehydration of the high temperature flow sample, a new peak appeared at $1548.7 cm^{-1}$, see Figure 5.66(f), which could be due to either oxide or hydroxide formation during drying at high temperatures, i.e. up to 200°C, however, the possibility of formation of ZrO_2 should be eliminated because $Zr(OH)_4$ will not dehydrate until heated above 500°C. More work still needs to be done to identify this peak.

CHAPTER VII

CONCLUSIONS

In conclusion, the dominant factor controlling the corrosion processes of the fluorozirconate glasses in water is the solubility of the individual glass components, especially that of ZrF_4. Since zirconium fluoride (ZrF_4) is the major network former of fluorozirconate glasses, the variation in solubility of ZrF_4 in different solutions essentially results in the same variation in durability of the whole glass. Because of the high solubility of the two main components of fluorozirconate glasses, i.e. BaF_2 and ZrF_4, in water, these glasses are much less durable than silicate glasses.

As found in raw material studies, the solubilities of the glass components, i.e. ZrF_4, BaF_2, LaF_3 and AlF_3, are a strong function of solution pH and exhibit a sharp increase in the acidic range. This is the cause of the relatively low durability exhibited by fluorozirconate glasses in acidic solutions. In a solution having pH values higher than 4.0, zirconium hydroxide tends to form in the solution during the dissolution of ZrF_4. Among the chemical components of ZBLA glass ZrF_4 causes the majority of the observed pH drop during leaching due to the hydrolysis of

189

its dissolved species. When ZrF_4 and BaF_2 compounds are mixed in solution according to the composition of ZBLA glass, a Zr/Ba containing precipitate can form.

The glass begins to dissolve as soon as it comes into contact with the water. After a short period of immersion, the solution pH experiences a drop toward the acidic range because of the hydrolysis of the dissolved ZrF_4 species and ion-exchange processes which occur between hydroxyl groups (OH^-) in solution and the fluorine ions (F^-) in the glass to form metal-hydroxyl (M-OH) groups in the glass. The leach rate of the glass components increases when the solution pH decreases due to the higher solubility of all the components in acidic environments. $Zr(OH)_4$ and $La(OH)_3$ may form in the early stages of corrosion, owing to their relatively low solubility in water, when sufficient hydroxyl groups exist in the solution. However, the rate of formation of these metal-hydroxyls in the transform layer of the leached glass is reduced as the solution pH drifts down.

The degree of the solution pH excursion will dramaticly affect the leaching process of the glass. Therefore, the glass surface area to solution volume ratio (S/V) has to be considered because the higher the S/V ratio the more rapid will be the solution pH drop. In pH2 solution, the glass will experience severe matrix dissolution leaving broad and extensive grooves on the glass surface, and the saturation/ reprecipitation processes are accelerated. In pH4, 6 and 8

solutions, selective leaching of the more soluble species in the glass cause the formation of a transform layer on the glass surface. The rate of formation of this transform layer is much higher in pH4 than in solutions of higher pH. In pH10 solution, no transform layer is found. The only visible corrosion is in the form of pits on the surface due to selected matrix dissolution.

In stagnant conditions, the accumulation of the corrosion products in the solution and ion exchange process at the glass surface cause a rapid, marked solution pH drop. Surface pH measurements show two plateaus in the curves of solution pH drift vs. time. The first one, occured between pH4-3.45, and is due to the buffering effect of HF which can be shown as follows:

$$H^+ + F^- \rightleftarrows HF \qquad pK = 3.45$$

The second plateau, occured between pH2-1.6, is attributed to the buffering effect of the dissociation of hydroxyl groups from the hydrolyzed species which can be shown as follows:

$$ZrF(OH)_2^+ \rightleftarrows ZrF(OH)^{+2} + OH^-$$

$$ZrF_2(OH)_2 \rightleftarrows ZrF_2(OH)^+ + OH^-$$

$$ZrF_2(OH)_2 \rightleftarrows ZrF_2^{+2} + 2OH^-$$
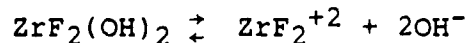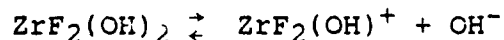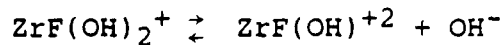
In stagnant conditions of intermediate S/V ratio, the
glass begins to dissolve as soon as it contacts water,
preferentially at the concave regions in the surface. Water
penetrates into the channels formed by selective dissolution
to further react with the glass and also to form a locally
high effective S/V ratio inside these pores which can
further enhance the leaching process. The adjacent solution
can reach saturation rapidly and crystals will reprecipitate
from the solution on the glass surface. The type of crystal
precipitated depend upon the composition of the solution and
the relative degree of supersaturation. Different crystals
precipitate in sequence instead of simultaneously. Three
types of crystals have been identified to be ZrF_4, $\alpha\text{-}BaZrF_6$
and BaF_2 crystals existing in the precipitation layer. ZrF_4
crystal precipitation usually precedes the others.

The precipitation layer thickens with corrosion time.
The electrostatic attraction forces, resulting from the
surface charge, between the leached glass and precipitated
crystals and/or between the different types of precipitated
crystals, cause the formation of multiple layers of
precipitates on the glass surface rather than in the
solution. The structure of the precipitation layer is so
porous that it plays only a minor role as a diffusion
barrier against further leaching.

The transform layer, produced by selective dissolution
of the soluble species from the glass, thickens with

corrosion time rapidly in the early stage of corrosion and slows down for the longer times. No steady state was reached within the experimental time. The microporosity formed in this layer creates a high effective S/V ratio condition for the solution in the pores, and thus accelerates the dissolution process. The thick transform layer can act as a diffusion barrier for the dissolved species causing supersaturation/reprecipitation processes to occur within this layer and slow down the leaching process. This layer contains higher Ba/Zr ratio than the bulk glass due to the precipitates inside the transform layer. However, the region next to the glass surface is relatively depleted of Ba because of the shorter diffusion path to transport the corrosion products through the porous precipitation layer into the bulk solution.

Under very low dilution conditions, the glass behaves similarly to corrosion in a highly acidic environment, where very severe matrix dissolution will occur. Only α-BaZrF$_6$ crystals was observed in this case.

In dynamic flow conditions, the transport processes are enhanced by solution flow. Therefore, the extraction rates of soluble species from the glass are higher than those in static conditions. The stirring speed and the flow rate determine the rate of removal of the corrosion products from the glass through the pore channels in the transform layer. When the stirring speed is high enough, very few colloidal

precipitates will form in the transform layer and the
solution pH does not experience a large drop, thus the leach
rate of the glass components remain relatively unchanged and
the average thickness of the transform layer grows nearly
linearly with time. If the stirring speed is not high
enough, amorphous colloids, which have a composition of
higher Ba/Zr ratio than the bulk glass, will precipitate in
the transform layer. The average size of the colloids
varies with stirring speed. Moreover, there is a size
distribution of the colloids in the layer with the region
closer to the glass surface having smaller colloids. The
glass solubility gradient, resulting from a solution pH
gradient, thus causes the precipitation of the colloids
inside the transform layer. Furthermore, crystalline
precipitates, such as ZrF_4, can form on the glass surface,
if the stirring speed is slow, by a supersaturation/
reprecipitation process due to additional concentration
gradients in the solution adjacent to the glass surface.
The electrokinetic influence, resulting from the zeta
potential at the leached glass surface, can help to maintain
the corrosion products near the surface and enhance
supersaturation conditions and thus facilitate
precipitation processes on the glass surface.

The Zr and La enriched gel layer, formed at the top
portion of the transform layer, contains large amounts of
metal-hydroxyl groups (M-OH), due to an OH/F ion-exchange

process. In this layer Ba, Al and F are depleted. Below the transform layer, numerous pits can be found. These can be produced by a localized accumulation of corrosion products together with the stress existing in the transform layer. The formation of the porous transform layer leads to severe cracking due to the large shrinkage of the layer after drying.

In room temperature flow conditions, the rate of formation of M-OH groups increases rapidly at the early stage of corrosion and then levels off for the longer times, which could be explained by the reduction of the solution pH in the transform layer as it thickens. The penetration of water into the glass, in the early stage, is a diffusion controlled process, while the precipitation process occurring, at longer times, inside the transform layer, is much slower due to partial blocking effects. The FTIR transmission spectrum of a sample corroded in flow at room temperature for 9.5 days, two new peaks at 1351.4 cm^{-1} and 1562.8 cm^{-1} were found, which could be due to the metal-hydroxyl groups formation in the thick transform layer during long corrosion time.

The corrosion under high temperature flow conditions occurs much faster than at room temperature, owing to the increased solubilities of the glass components and the higher diffusion rates. A thick transform layer forms. The top portion of this layer contains $ZrF_4 \cdot H_2O$ crystals and the

majority of the metal-hydroxyl groups, while the remainder of the layer has a composition of higher Ba/Zr ratio than the bulk glass due to precipitation inside the layer. The solution pH gradient between the pore solution and the bulk solution has the similar effect of enhancing supersaturation/reprecipitation processes as observed under room temperature flow conditions.

The formation of M-OH groups in the transform layer occurs much faster than at room temperature during the early stages of corrosion. The rate then levels off rapidly for the longer times. This rapid decrease in the formation rate could be due either to the formation of a thick layer or to the enhanced leaching which may cause a more rapid decrease in solution pH.

A new peak appears around 1548.7 cm^{-1} in the FTIR transmission spectrum of a dehydrated high temperature flow sample, which could be due to the M-OH groups formed during dehydration.

REFERENCES

1. M. G. Drexhage, C. T. Moynihan, M. S. Boules, and K. P. Quinlan, Advances in Ceramics, Vol.II, Physics of Fiber Optics, B. Bendow and S. Mitra ed., Am. Ceram. Soc., Columbus, Ohio, p.57, 1981.

2. V. G. Tsoukala, J. Schroeder, G. A. Floudas, and D. A. Thomoson, "Intrinsic Rayleigh Scattering in Fluoride Glasses," Proc. of 4th Intern. Symp. on Halide Glasses, p.295, 1987.

3. M. G. Drexhage, B. Bendow, and C. T. Moynihan, "IR Transmitting Fluoride Glasses," Laser Focus, Vol. 10, p.62-65, 1980.

4. P. W. France, S. F. Carter, M. W. Moore, and J. R. Williams "Optical Loss Mechanisms in ZrF_4 Glasses & Fibres," Proc. of 4th Intern. Symp. on Halide Glasses, p.290. 1987.

5. J. H. Simmons, R. Faith, and G. O Rear, "Molecular Dynamics Simulations of Fluoride Glass Structures," Proc. of 4th Intern. Symp. on Halide Glasses, p.101, 1987.

6. A. Lecoq, M. Poulain, "Fluoride Glasses in the ZrF_4-BaF_2-YF_3-AlF_3 Quaternary System," J. Non-crystalline Solids, Vol. 41, p.209, 1980.

7. J. Lucas and M. Poulain, "Vitreous rare earth fluorozirconates" from The Rare Earths in Modern Science and Technology, G. J. McCarthy and J. J. Rhynes ed., Plenum Pub. Co., New York, 1978.

8. B. F. Zhu, "Nuclear Waste Glass Leaching in a Simulated Granite Repository," Ph.D. Dissertation, Univ. of Florida, 1987.

9. B. Grambow, " The role of metal ion solubility in leaching of nuclear waste glasses," in Scientific Basis for Radioactive Waste Management, vol. 6, W. Lutze ed., Elsevier, New York, p.93, 1982.

10. A. Barkatt, J. H.Simmons, and P. B. Macedo," Evaluation of chemical stability of vitrifiction media form radioactive waste products," Phys. and Chem. of Glasses. Vol. 22, No.4, p.73, 1981.

11. P. B. Macedo, A. Barkatt, and J. H. Simmons, " A Flow Model for the kinetics of dissolution of nuclear waste glasses," Nuclear and Chemical Waste Management, Vol. 3, p.13-21, 1982.

12. R, B, Adiga, E, P, Akomer, and D, E, Clark, " Effects of flow parameters on the leaching of nuclear waste glass," Mat, Res. Soc, Symp. Proc. Vol. 44. p.45, 1985.

13. C. J. Simmons, and J. H. Simmons, "Investigation of Chemical Durability Mechanisms in Fluoride Glasses," Annual Report to ONR, 1984.

14. C. J. Simmons, H. Sutter, J. H. Simmons. and D. C. Tran "Dissolution of Fluorozirconate Glasses," Mat. Res. Bull. Vol. 17, p.1203, 1982.

15. T. A. McCarthy, and C. G. Pantano, "Dissolution of Fluorozirconate Glasses," Proc. of 2nd Intern. Symp.on Halide Glasses, 1983.

16. R. H. Doremus, D. Murpny, N. P. Bansal, W. A. Lanford, and C. Burman, "Reaction of Zirconium Fluoride Glass with Water: Kinetics of Dissolution," J. Materials Sci., Vol. 20, p.4445, 1985.

17. S. R. Loehr, A. J. Bruce, R. Mossadegh, R. H. Doremus, and C. T. Moynihan, "IR Spectroscopy Studies of Attack of liquid Water on ZrF₄-Based Glasses," Proc. of the 3rd Intern. Symp. on Halide Glasses, 1985.

18. C. J. Simmons, J. H. Simmons, "Chemical Durability of Fluoride Glasses: I. Reaction of Fluorozirconate Glasses with Water," J. Am. Ceram. Soc.. Vol. 69, p.661, 1986.

19. D. Ravaine and G. Perera, "Corrosion Studies of Various Heavy Metal Fluoride Glasses in Liquid Water; Application to Fluoride-Ion-Selective Electrode," J. Am. Ceram. Soc., Vol. 12, p.852-57, 1986.

20. C J. Simmons, J. Guery. D. G. Chen and C. Jocoboni, "Leaching Behavior of Heavy Metal Fluoride Glasses," Proc. of the 3rd Intern. Symp. on Halide Glasses, Mat. Sci. Forum, Vol.6, Halide Glass Trans. Tech. Pub., Aedermannsdorf, Switzerland, 1985.

21. C. J. Simmons, "Chemical Duradility of Fluoride Glasses: III. The Effect of Solution PH," J. Am. Ceram. Soc., in press.

22. C. A. Houser, and C. G. Pantano, "Surface Studies of Fluorozirconate Glass," Proc. of the 2nd Intern. Symp. on Halide Glasses, 1983.

23. C. A. Houser, T. A. McCarthy, and C. G. Pantano, "Dissolution and Surface Layer Formation in Fluorozirconate Glass," 1986, unpublished work.

24. C. J. Simmons, S. Azali, and J. H. Simmons, "Chemical Durability Studies of Heavy Metal Fluoride Glasses," Proc. of 2nd Intern. Symp. on Halide Glasses, 1983.

25. C. J. Simmons "Chemical Durability of Fluoride Glasses: II. Reaction of Ba-Th-Based Glasses with Water.," J. Am. Ceram. Soc., Vol.70, No.4, p.295-300, 1987.

26. E. C. Ethridge, D. E. Clark, and L. L. Hench, "Effects of Glass Surface Area to Solution Volume Ratio on Glass Corrosion," Phys. and Chem. of Glasses, Vol.20, No.2, p.35, 1979.

27. A. Paul "Chemical Durability of Glasses: A Thermodynamic Approach," J. Mat. Sci., Vol. 42, p.2246 1977.

28. R. H. Doremus, N. P. Bansal, T. Bradner and D. Murphy, "Zirconium Fluoride Glass: Surface Crystal Formed by Reaction with Water" J. of Mat. Sci. Lett., Vol. 3, p.484, 1984.

29 A. J. Bruce, S. R. Loehr and N. P. Bansal, "IR measurement of the Rate of Surface Layer Development on ZrF_4-BaF_2-LaF_3 Glass in Aqueous Solution," Proc. of the 2nd Intern. Symp.on Halide Glasses, 1983.

30. D. E. Clark, C. G. Patano, and L. L. Hench, Corrosion of Glass, Glass Industry, Books for Industry, New York 1979.

31. S. Mitachi, "Chemical Durability of Fluoride Glasses in the BeF_2-GdF_3-ZrF_4 System," Phys. and Chem. of Glasses, Vol.24, No.6, p.146, 1983.

32. C. G. Pantano, "Surface Chemistry and Fracture of Fluoride Glasses," Proc. of the 3rd Intern. Symp. on Halide Glasses, 1985.

33. C. L. Strecker, "Determination of the Heat of Adsorption for Water Vapor on Clean Calcium Fluoride Surfaces by ISS," Ph.D. Dissertation, Univ. of Dayton, April 1985.

34. M. Robinson, and M. G. Drexhage, "A Phenomenological Comparison of Some Heavy Metal Fluoride Glasses in Water Environments.," Mat. Res. Bull., Vol.18, p.1101, 1983.

35. D. Tregoat, G. Fonteneau, C. T. Moynihan, and J. Lucas "Surface -OH Profile from Reaction of a Heavy Metal Fluoride Glass with Atmospheric Water," J. Am. Ceram. Soc., Vol.68, No.7, p.C-127, 1985.

36. D. Tregoat, G. Fonteneau, and J. Lucas, "Corrosion of HMFG by H_2O Vapor: Determination of ε_{OH} and Diffusion Profile," Proc. of the 3rd Intern. Symp. on Halide Glasses, 1985.

37. E. O. Gbogi, K. H. Chung, C. T. Moynihan, and M. G. Drexhage, "Surface and Bulk -OH Infrared Absorption in ZrF_4 and HfF_4-Based Glasses," Commun. of Am. Ceram. Soc., C-51, 1981.

38. G. H. Fritchat, and I. Overbeck, "Chemical Durability of Fluorozirconate Glasses," Commun. of Am. Ceram. Soc., p.C-238, 1984.

39. G. H. Frischat, and I. Overbeck, "Chemical Durability of Fluorozirconate Glasses against Aqueous Solutions," Proc. of the 3rd Intern. Symp. on Halide Glasses, 1985.

40. D. Trgoat, G. Fonteneau, and J. Lucas, "Aqueous Corrosion of a HMFG," Proc. of the 3rd Intern. Symp. on Halide Glasses, 1985.

41. R. H. Doremus, N. P. Bansal, and D. Murphy, "Kinectics of the Reaction of Fluorozirconate Glasses with Water," Am. Ceram. Soc. Bull., Vol. 64, No. 3, p.475, 1985. (Paper No. 100-G.085).

42. D. J. Shaw, Introduction to Colloid and Surface chemistry, 3 ed. p.172, Butterworths, London, 1980.

43. R. N. Brown, B. Bendow, M. G. Drexhage, and C. T. Moynihan, "Ultraviolet Absorption Edge Studies of Fluorozirconateand Fluorohafnate Glass," Appl. Opt., Vol. 21, p.361-63, 1982.

44. M. Robinson, R. C. Paster, R. R. Turk, D. P. Devor, and M. Braunstein, "Infrared-Transparent Glasses Derived from the Fluorides of Zirconium, Thorium and Barium," Mat. Res. Bull., Vol. 15, p.735-42, 1980.

45. M. G. Drexhage, C. T. Moynihan, B. Bendow, E. Gboji, K. H. Chung, and M. Boulos, "Influence of Processing Conditions on IR Edge Absorption in Fluorohafnate and Fluorozirconate Glasses," Mater. Res. Bull., Vol. 16, p.943-47, 1981.

46. R. A. Berner, "Rate Control of Mineral Dissolution under Earth Conditions," Am. J. Sci., Vol. 278, p.1235-52, 1978.

47. D. M. Strachan, K. M. Krupka, and B. Grambow, "Solubility Interpretations of Leach Tests on Nuclear Waste Glass," Nuclear & Chemical Waste Management, Vol. 5, p.37, 1984.

48. J. F. Kerrisk, "Solubility Limits on Radionuclide Dissolution," Mat. Res. Soc. Symp., Vol. 44, p.237, 1985.

49. D. M. Strachan, "Results from a 1-year Leach Test: Long-Term use of MCC-1," Scientific Basis for Nuclear Waste Management, Vol. 5, W. Lutze ed., p.181, Elsevier New York, 1982.

50. J. H. Simmons, A. Barkatt, P. B. Macedo "Mechanisms which Control Aqueous Leaching of Nuclear Waste Glass," Nucl. Technol. (U.S.A.), Vol. 56, No. 2, p.265, 1982.

51. CRC Handbook of Chemistry & Physics, 66th ed., CRC Press. Boca Raton, Florida, 1985.
    51-1. p.D-163
    51-2. p.B-76
    51-3. p.B-105
    51-4. p.B-160

52. C. F. Baes, J., and R. E. Meomer, The Hydrolysis of Cations, p.159, John Wiley & Sons, New York, 1976.

53. N. P. Bansal, R. H. Doremus, A. J. Bruce, and C. T. Moynihan, "Crystallization of Fluorozirconate Glasses," Mat. Res. Bull., Vol. 19, p. 577-590, 1984.

54. G. L. McVay, and C. Q. Buckwalter "Effect of Iron on Waste Glass Leaching," J. Am. Ceram. Soc., Vol. 66, p.170, 1983.
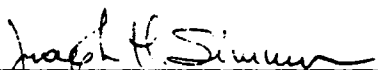
55. J. Jednacak, V. Pravdic, and W. Haller, "The
     Electrokinetic Potential of Glasses in Aqueous
     Electrolyte Solutions," J. Colloid and Interface Sci.,
     Vol.49, No.1, Oct. p.16, 1974.

56. J. M. Horn, J., and Y. Onoda, J., "Surface Charge of
     Vitreous Silica and Silicate Glasses in Aqueous
     Electrolyte Solutions," J. Am. Ceram. Soc., Vol 61,
     No.11-12, p.524, 1978.

57. W. M. Mularie, W. F. Furth, and A. R. C. Westwood,
     "Influence of Surface Potential on the Kinetics of
     Glass Reactions with Aqueous Solutions," J. Mat. Sci.,
     Vol. 14, p.2659-64, 1979.

58. C. T. Lee, and D. E. Clark, "Electrkinetics, Adsorption
     and Colloid Study of Simulated Nuclear Waste Leached in
     Aqueous Solutions," Mat. Res. Symp. Proc., Vol.44,
     p.221, 1985.

59. A. G. Metcalfe, M. E. Gulden, and G. K. Schmitz,
     "Spontaneous Cracking of Glass Filaments," Glass
     Technology, Vol.12, No.1, Feb. p.15, 1971.

60. A. G. Metcalfe, and G. K. Schmitz, "Mechanisms of
     Stress Corrosion in E Glass Filaments," Glass
     Technology, Vol.13, No.1, Feb. p.5, 1972.

61. M. Le Toullec, C. J. Simmons, and J. H. Simmons,
     "Infrared Spectroscopy Studies of Hydrolysis Reactions
     During Leaching of Heavy Metal Fluoride Glasses,"
     unpublished manuscript.

BIOGRAPHICAL SKETCH

Din-Guo Chen was born on January 11, 1959 in Taipei, Taiwan, Republic of China. He entered the National Cheng Kung University in Tainan, Taiwan, R.O.C., and received his Bachelor of Science in Metallurgical and Material Science Engineering in 1981.

After two years of military service, in the spring of 1985, he continued his education at the University of Florida to obtain his Master of Science.

I certify that I have read this study and that in my opinion it conforms to acceptable standards of scholarly presentation and is fully adequate, in scope and quality, as a thesis for the degree of Master of Science.

Dr. Joseph H. Simmons, Chairman
Professor of Materials Science
and Engineering

I certify that I have read this study and that in my opinion it conforms to acceptable standards of scholarly presentation and is fully adequate, in scope and quality, as a thesis for the degree of Master of Science.

Dr. Brij M. Moudgil
Professor of Materials Science
and Engineering

I certify that I have read this study and that in my opinion it conforms to acceptable standards of scholarly presentation and is fully adequate, in scope and quality, as a thesis for the degree of Master of Science.

Dr. John R. Ambrose
Associate Professor of Materials
Science and Engineering

This thesis was submitted to the Graduate Faculty of the College of Engineering and to the Graduate School and was accepted as partial fulfillment of the requirements for the degree of Master of Science.

August, 1987

_____
Dean, College of Engineering

_____
Dean, Graduate School

END
DATE
FILMED

8 - 88

DTIC